

University of Southampton Research Repository

Copyright © and Moral Rights for this thesis and, where applicable, any accompanying data are retained by the author and/or other copyright owners. A copy can be downloaded for personal non-commercial research or study, without prior permission or charge. This thesis and the accompanying data cannot be reproduced or quoted extensively from without first obtaining permission in writing from the copyright holder/s. The content of the thesis and accompanying research data (where applicable) must not be changed in any way or sold commercially in any format or medium without the formal permission of the copyright holder/s.

When referring to this thesis and any accompanying data, full bibliographic details must be given, e.g.

Thesis: Author (Year of Submission) "Full thesis title", University of Southampton, name of the University Faculty or School or Department, PhD Thesis, pagination.

Data: Author (Year) Title. URI [dataset]

University of Southampton

Faculty of Medicine

Clinical and Experimental Sciences

**Developing SERS-based point-of-care inflammatory monitoring for risk
identification of worsening progression of age-related disease**

by

Rachel Louise Kidd

ORCID ID 0000-0001-6337-1691

Thesis for the degree of Doctor of Philosophy

April 2022

University of Southampton

Abstract

Faculty of Medicine

Clinical and Experimental Sciences

Doctor of Philosophy

Developing SERS-based point-of-care inflammatory monitoring for risk identification of worsening progression of age-related disease

by

Rachel Louise Kidd

With an ageing population¹ we are seeing a rise in many age-related diseases which are having long-term health implications for patients and cost implications for our health services². Age-related hearing loss is the most common sensory deficit among older adults and can lead to decline in well-being and quality of life. A chronic state of raised inflammation in older people known as inflammaging^{3,4} has been linked to many age-related diseases³. Evidence from research suggests a link between inflammatory status and hearing thresholds in older people⁵⁻⁷.

Neopterin is a small inflammatory metabolite that can be monitored in either the blood or urine⁸⁻¹⁰. Neopterin levels reflect immune activation status as neopterin is released from monocyte-derived macrophages and dendritic cells following stimulation with the pro-inflammatory cytokine interferon- γ . Neopterin has been explored as a marker for chronic inflammation in several conditions^{11,12}. Most patients will happily give regular urine samples as they are non-invasive to collect. Urinary neopterin levels can be measured in a laboratory setting using gold-standard HPLC¹³ which can provide highly accurate quantitative results¹².

A 3-year longitudinal study measuring changes in hearing level and inflammatory profile of 45 adults (aged 65-75) has been carried out. Urine was collected monthly over 12 months for analysis of neopterin concentration. Individuals were stratified into groups depending on how often their biomarker was raised during the collection period. Pure Tone Audiometry was performed at baseline, after one year, and at the study end.

Results demonstrate a correlation between raised inflammatory state and greater change in hearing levels ($r = 0.334$, $p = 0.027$) and when stratified into groups, those with consistently raised (more than 50% of the time) inflammatory state, showed a greater deterioration in high-frequency hearing loss ($W(3.000, 19.60) = 9.164$, $p = 0.0005$). We also demonstrate that these individuals are more than twice as likely to have other co-morbidities.

However, for long-term regular monitoring of a patient's inflammatory state, HPLC is not cost or time effective. Therefore, there is a real need for a quick and cost-effective method of measuring urinary neopterin levels in patient urine samples long-term. Ideally, the method would enable point-of-care measurement that would give a real-time result within the patient consultation or at the patient's home. The technique wouldn't be required to compete with HPLC in terms of quantitative accuracy, but it would need to be sensitive enough to be used as a screening-like tool to identify those with consistently raised urinary neopterin levels compared to

normative values. The aim is to develop a point-of-care inflammatory monitoring device which would allow population screening, leading to identification of those 'at risk' of worsening age-related disease (including hearing loss). With this knowledge, an individual may seek earlier intervention or may wish to make lifestyle changes which may reduce their risk.

Such a technique has been explored utilising the technique of Surface-Enhanced Raman Spectroscopy. Raman spectroscopy utilises inelastic light scattering from a sample to identify the molecules present within it. By combining the sample with metallic nanostructures extremely large enhancement effects are seen which enable detection of molecular information as low as fM concentration¹⁴.

One of the difficulties with performing SERS on biofluids is the matrix effect. This research demonstrates the simple application of paper chromatography to urine samples, in order to achieve separation of the matrix prior to SERS acquisition to further eliminate the matrix effect. This research also demonstrates the use of a novel SERS substrate in urine. Colloidal SERS-sensors are formed using a layer-by-layer process where the metal nanoparticles are structurally spaced, giving control over the SERS enhancement. Results demonstrate improved reproducibility of these SERS sensors in comparison to colloidal metal nanoparticles.

Urine samples were analysed with both SERS and HPLC to validate, and the measured concentrations were generally in good agreement (R^2 of 0.936 and 0.990 for creatinine and neopterin) at physiologically relevant concentrations.

By having access to a technique that can provide fast but reliable urinary neopterin readings we can regularly monitor a cohort of older adults and identify those who are at increased risk of worsening age-related hearing loss so that they can be targeted for intervention.

Table of Contents

Table of Contents	i
Table of Tables	vii
Table of Figures	ix
Research Thesis: Declaration of Authorship	xiii
Acknowledgements	xv
Definitions and Abbreviations	xvii
Chapter 1 Introduction	1
1.1 Ageing, inflammation and immunity.....	1
1.1.1 Age-related disease burden	1
1.1.2 Ageing immune system	2
1.1.3 Biomarkers of ageing and inflammaging	3
1.1.4 Neopterin measurement.....	5
1.2 Age-related hearing loss.....	6
1.2.1 Burden of disease and management	6
1.2.2 The auditory system.....	7
1.2.3 Systemic inflammation in the inner ear	8
1.3 Surface-enhanced Raman spectroscopy (SERS).....	8
1.3.1 Raman theory and principles	8
1.3.2 Raman spectroscopy	9
1.3.3 Surface-enhanced Raman spectroscopy	11
1.3.4 Substrates for Surface-enhanced Raman spectroscopy	13
1.3.4.1 Metallic nanoparticle colloids	13
1.3.4.2 Nanoparticles on planar supports (bottom-up processing).....	15
1.3.4.3 Nanostructures fabricated using top-down techniques	15
1.3.5 SERS substrate enhancement factor	15
1.3.6 Quantitative analysis with SERS	16
1.3.7 Clinical and diagnostic SERS with urine.....	18
1.4 Paper chromatography	19
1.5 Thesis structure	20

Chapter 2	Determining an individual’s baseline systemic inflammation and subsequent risk of age-related conditions	22
2.1	Overview	22
2.2	Introduction	23
2.2.1	Goal to improve healthspan as well as lifespan	23
2.2.2	The ageing immune system	24
2.2.3	Low-grade chronic inflammation (inflammaging) and age-related disease....	25
2.2.4	Age-related hearing loss as an example age-related disease associated with inflammaging	25
2.2.5	Mechanism of hearing	26
2.2.6	Biological basis of hearing loss	27
2.2.7	How does systemic inflammation affect the inner ear	29
2.2.8	Current research on hearing loss and inflammaging.....	30
2.2.9	Research evidence for different measures of ageing and inflammaging.....	31
2.2.10	Potential prevention strategies for inflammaging.....	34
2.2.11	Research Gap	35
2.2.12	Hypotheses	37
2.2.13	Aims	38
2.3	Methods.....	38
2.3.1	Participants	38
2.3.2	Inclusion and exclusion criteria	39
2.3.3	Study design.....	39
2.3.4	Equipment and Procedure	40
2.3.4.1	Questionnaire	40
2.3.4.2	Hearing assessment	40
2.3.4.3	Blood sampling.....	41
2.3.4.4	Urine sampling	41
2.3.5	Measurement of inflammatory markers	42
2.3.5.1	White blood cell count.....	42
2.3.5.2	Serum cytokines.....	42
2.3.5.3	Urinary neopterin to creatinine ratio (UNCR).....	43

2.3.6	Ethical approval.....	43
2.3.7	Statistical analysis.....	44
2.4	Results	44
2.4.1	Subject Characteristics	44
2.4.2	Hearing changes from baseline to study end.....	48
2.4.2.1	Pure Tone Audiometry	48
2.4.2.2	Transient Otoacoustic Emissions (TEOAEs).....	50
2.4.3	Traditional Blood Markers.....	52
2.4.4	Monthly Urinary Neopterin to Creatinine Ratio (UNCR) for each subject.....	55
2.4.5	Stratification Process based on UNCR longitudinal data	59
2.4.6	Clinical characteristics of neopterin stratified groups	61
2.4.7	Inflammatory marker levels of stratified groups	64
2.4.8	Neopterin stratified groups and age-related disease/risk factors.....	66
2.4.9	Relationship between inflammatory profile and age-related hearing loss	67
2.4.10	Study attrition	71
2.5	Discussion.....	73
2.6	Conclusions and Future Work	79
Chapter 3	Development of a spectroscopy-based method for detecting and quantifying an inflammatory biomarker in urine	81
3.1	Overview.....	81
3.2	Introduction.....	81
3.2.1	Barriers to routine monitoring using standard analytical approaches	81
3.2.2	Surface-Enhanced Raman spectroscopy as a portable and sensitive analytical approach.....	82
3.2.2.1	Improving reproducibility of SERS substrates	82
3.2.3	Measuring urinary neopterin to creatinine ratio	83
3.2.4	Raman analysis of neopterin in biofluids: limited evidence of clinical application	84
3.2.5	Urinalysis with SERS is largely confined to classification of samples using multivariate analysis.....	84

Table of Contents

3.2.6	Considerations for developing a novel analytical sensor	85
3.2.7	Research Gap	86
3.2.8	Hypotheses	86
3.2.9	Aims	87
3.3	Methods.....	87
3.3.1	Layer-by-layer SERS Sensor Fabrication.....	87
3.3.2	Synthetic Urine Preparation	87
3.3.3	Human Urine Handling	88
3.3.4	Neopterin and Creatinine Standards	88
3.3.5	UV-Vis analysis of layer-by-layer SERS sensors.....	88
3.3.6	HPLC analysis	88
3.3.7	SERS analysis	89
3.3.8	Data Analysis.....	90
3.4	Results and Discussion	90
3.4.1	Development and Optimisation of Layer-by-layer SERS Sensors	90
3.4.2	Batch reproducibility and stability of SERS Sensors	92
3.4.3	Neopterin SERS verification	94
3.4.4	Validation with synthetic urine samples.....	96
3.4.5	Measurement of urinary neopterin to creatinine ratio (UNCR).....	98
3.4.6	Stratification of results into 'risk' categories/screening tool	101
3.5	Limitations.....	103
3.6	Conclusions	103
Chapter 4 Towards Point-of-Care testing: a paper-based lateral flow assay for SERS		
detection of inflammatory marker in urine.....105		
4.1	Overview	105
4.2	Introduction	105
4.2.1	The challenge of developing point-of-care testing.....	105
4.2.2	The need for point of care testing- a global pandemic driving force	107
4.2.3	Utilising intrinsic molecular characteristics of the target analyte-Raman spectroscopy for point-of-care testing	109
4.2.4	Using paper as an alternative cost-effective but reproducible substrate.....	110

4.2.5	Producing SERS active paper devices.....	111
4.2.6	Utilising paper substrates can allow sample separation	112
4.2.7	Employing paper-based SERS for healthcare.....	113
4.2.8	Research Gap.....	114
4.2.9	Hypotheses.....	115
4.2.10	Aims.....	115
4.3	Methods	115
4.3.1	Preparation of neopterin and creatinine samples.....	115
4.3.2	Preparation of layer-by-layer SERS sensors	116
4.3.3	Preparation of Whatman No.1 Paper devices with SERS sensors	116
4.3.4	Preparation of G1 devices with SERS sensors.....	117
4.3.5	Brightfield microscopy of SERS sensors within devices	117
4.3.6	Optimisation of run-time with paper-based devices.....	117
4.3.7	Single samples run on devices.....	118
4.3.8	Creatinine/neopterin mixture run on devices	118
4.3.9	SERS measurement of SERS sensors within paper device/spectra acquisition.....	118
4.3.10	Visualisation of analyte spots.....	120
4.3.11	Data analysis and statistics.....	120
4.4	Results and Discussion	120
4.4.1	Choosing a membrane for the device.....	120
4.4.2	Membrane and sensor background.....	124
4.4.2.1	Peak ratio.....	126
4.4.3	Optimising the run-length of the assay.....	128
4.4.4	Neopterin SERS measurement on paper-based devices.....	130
4.4.5	Using paper-based devices for separation of components	133
4.4.6	Paper-based devices for quantitative SERS measurement.....	137
4.5	Conclusions and Future Work	142
Chapter 5	General Discussion.....	143
5.1	Ageing and inflammation.....	143
5.1.1	Age-related hearing loss.....	144

Table of Contents

5.2	SERS-based neopterin measurement at point-of-care.....	149
5.3	Clinical Implications and Future Work.....	152
5.4	Conclusions	152
Appendix A InflammHear Subject Questionnaire.....		155
Appendix B InflammHear Subject Questionnaire Results Tables		159
Appendix C Assessing normality of InflammHear Data		161
C.1	Example Variable- Neopterin Mean	161
C.2	Example Variables- PTA Average, High Frequency Average and Low Frequency Average	162
Appendix D Example of SERS spectra pre-processing.....		165
Appendix E Example of curve fitting SERS spectra.....		167
Appendix F Batch to batch reproducibility SERS spectra.....		171
Appendix G Neopterin and Creatinine standard curves		175
Appendix H Synthetic Urine spectra and chromatograms		181
Appendix I Real Urine spectra and chromatograms.....		189
List of References		207

Table of Tables

Table 2.1	Reference values of neopterin in urine ($\mu\text{mol}/\text{mol}$ creatinine) ⁴⁷	33
Table 2.2	Table of subject demographics and clinical characteristics from beginning to end of study	45
Table 2.3	Number of subjects within each classification of hearing loss at baseline and year 3 (study end).....	48
Table 2.4	Percentage of ears with positive OAE responses meeting criteria (1, 1.4, 2, 3, 4 kHz, baseline and year3).....	51
Table 2.5	Characteristic data from the four stratified groups, never raised, occasionally raised, often raised and considerably raised.....	62
Table 2.6	Correlation Matrix of inflammatory markers and degree of hearing loss (Puretone average at start and end of study).	68
Table 3.1	Summary of results for human urine samples: HPLC, SERS and the associated percentage difference (RSD) between the two analytical approaches for neopterin(μM), creatinine(M) and UNCR($\mu\text{mol}/\text{mol}$).	99
Table 3.2	Measured concentrations of Creatinine (M) and Neopterin (μM) in urine samples, measured in triplicate with SERS using Lbl sensors.....	100
Table 3.3	UNCR($\mu\text{mol}/\text{mol}$) values obtained for urine samples via HPLC and SERS and agreement of risk stratification between two methods (presuming HPLC correct as gold standard).	102
Table 4.1	Run times and R_f values for the three different paper devices used. R_f values for both neopterin in water and synthetic urine.	123
Table 4.2	Quantitative measurements of neopterin in prepared samples using paper devices with SERS sensors.	138

Table of Figures

Figure 1.1	Biosynthetic pathway of neopterin and chemical structure of neopterin.	4
Figure 1.2	Jablonski energy level diagram illustrating the process of Rayleigh and Raman scattering and fluorescence emission from a molecule.	9
Figure 1.3	Demonstration of excitation of localised surface plasmon resonance (LSPR) and ‘hotspot’ formation.	12
Figure 1.4	Schematic of a layer-by-layer synthesised sensor and randomly aggregated nanoparticles.	14
Figure 2.1	Diagrammatic representation of the philosophy behind chapter 2.	37
Figure 2.2	Experimental design for InflammHear study.	39
Figure 2.3	Infographic depicting InflammHear questionnaire responses: demographics, risk factors and age-related conditions.	47
Figure 2.4	Average pure-tone audiometric thresholds for all subjects.	49
Figure 2.5	TEOAE responses.	52
Figure 2.6	Measurements of blood markers.	53
Figure 2.7	Baseline cytokine concentrations.	54
Figure 2.8	Variations in monthly UNCR measurement for participants 1-15 of study.	56
Figure 2.9	Variations in monthly UNCR measurement for participants 16-30 of study.	57
Figure 2.10	Variations in monthly UNCR measurement for participants 31-45 of study.	58
Figure 2.11	Histogram of neopterin volatility distribution.	60
Figure 2.12	Neopterin volatility groups, clinical characteristics and age-related risk factors.	63
Figure 2.13	Characteristics of the neopterin volatility stratified groups.	65
Figure 2.14	Audiometric thresholds, averages and change for subjects in neopterin volatility groups (n=45).	70
Figure 2.15	Change in TEOAE responses for subjects in neopterin volatility groups.	71

Table of Figures

Figure 2.16	Analysis of the 16 participants who did not continue in the study to completion.	72
Figure 3.1	Procedure for preparation of layer-by-layer (LbL) SERS sensors involving iterative steps of applying polyelectrolyte layers and 40nm gold nanoparticles (AuNPs) to a silica microparticle.....	87
Figure 3.2	Schematic of a SERS sensor.....	90
Figure 3.3	Results for optimisation testing of the SERS sensors.....	92
Figure 3.4	Verification of batch-to-batch reproducibility of the SERS sensors and improved enhancement over colloidal AuNPs.	93
Figure 3.5	Verification of neopterin SERS measurement in a complex matrix of urine. .	95
Figure 3.6	Results of expected vs measured synthetic urine samples.....	97
Figure 3.7	Summary of results for the triplicate analysis of urine samples.....	101
Figure 4.1	Methods of depositing gold nanoparticles onto paper substrates to make SERS active paper devices.....	112
Figure 4.2	Paper chromatography, before, during and after development and visualisation.	113
Figure 4.3	Images depicting the process of running a sample on a device and obtaining SERS measurement.	119
Figure 4.4	Brightfield microscope images of SERS sensors (example identified by a red arrow) on paper device membranes and SERS spectra of neopterin on devices.	122
Figure 4.5	SERS background signal from SERS sensors at 500-1000 cm^{-1} and 1500-2000 cm^{-1} , as well as the spectra for the contributing components and cellulose.	125
Figure 4.6	Using peak height ratio gives useable data.....	128
Figure 4.7	Optimising assay run time for neopterin.	129
Figure 4.8	SERS measurement of neopterin on paper devices.....	133
Figure 4.9	SERS spectra for neopterin (500-1000 cm^{-1})	134

Figure 4.10	Paper chromatography separation of creatinine and neopterin.	135
Figure 4.11	SERS spectra of creatinine and neopterin measured after paper chromatography separation.	136
Figure 4.12	Validation plots for paper SERS of neopterin	140

Research Thesis: Declaration of Authorship

Print name: Rachel Louise Kidd

Title of thesis: Developing SERS-based point-of-care inflammatory monitoring for risk identification of worsening progression of age-related disease.

I declare that this thesis and the work presented in it are my own and has been generated by me as the result of my own original research.

I confirm that:

1. This work was done wholly or mainly while in candidature for a research degree at this University;
2. Where any part of this thesis has previously been submitted for a degree or any other qualification at this University or any other institution, this has been clearly stated;
3. Where I have consulted the published work of others, this is always clearly attributed;
4. Where I have quoted from the work of others, the source is always given. With the exception of such quotations, this thesis is entirely my own work;
5. I have acknowledged all main sources of help;
6. Where the thesis is based on work done by myself jointly with others, I have made clear exactly what was done by others and what I have contributed myself;
7. None of this work has been published before submission

Signature: *R Kidd*..... Date: *12.5.22*.....

Acknowledgements

I have received immense help and support over the last 5 years, enabling me to complete this PhD and thesis.

First and foremost, I thank my family for their unwavering love and support through what has been a tough, challenging, and long 5 years. My husband Chris has been a pillar of strength when I have needed it, and sacrificed a lot in order to help me achieve my dreams, I feel I will be eternally indebted to him. Having become a parent whilst completing this PhD, I am thankful for my sons for giving me the motivation to see this through, although family time has suffered as a consequence, I hope they will be proud of my achievement and inspired for their own futures.

My profound gratitude also goes to my supervisors- Dr Tracey Newman and Prof Sumeet Mahajan; I have not given them an easy time, but they have continued to support me. Dr Newman in particular has offered guidance and support above and beyond her academic duty and kept me on track when I have needed it.

I have been lucky to be a member of two great research groups at the University of Southampton, and thank all members past and present who have supported and guided me on my journey. Particular thanks are extended to Dr Alan Sanderson and Dr Akosua Agyemang- Prempeh, who have contributed to work presented in chapter 2 of this thesis. My sincere thanks also extends to Charlotte Stuart who provided UPLC-MS measurements of urine samples for the work in chapter 2 and Dr Josh Prince for his HPLC knowledge and support.

I must also thank my NHS work colleagues, particularly the department of Audiology and Hearing Therapy, University Hospitals Southampton NHS Trust. For the past 18 months, they have supported me to write my thesis whilst working, even in the midst of a global pandemic!

Finally, I offer my appreciation and thanks to the participants who consented to take part in the study, this project would not have been possible without you.

Definitions and Abbreviations

ARHL.....	Age-related hearing loss
BLB	Blood-labyrinthine-barrier
CRP	C-reactive protein
CV	Coefficient of variation
EF.....	Enhancement factor
ELISA.....	Enzyme-linked immunosorbent assay
GCH-1	GTP-cyclohydrolase I
GTP.....	Guanosine triphosphate
HFA.....	High-frequency average
HGS.....	Hand- grip strength
HPLC.....	High-performance liquid chromatography
IHC.....	Inner hair cell
IL-1 β	Interleukin 1 beta
IL-6.....	Interleukin-6
LBL.....	Layer-by-layer
LFA.....	Low-frequency average
LFA.....	Lateral flow assay
LOD.....	Limit of detection
LOQ	Limit of quantification
LSPR.....	Localised surface plasmon resonance
NPs	Nanoparticles
OAE.....	Otoacoustic emission
OHC	Outer hair cell
POC.....	Point-of-care
POCT.....	Point-of-care testing

Definitions and Abbreviations

PTA.....	Pure-tone audiometry
PTAv.....	Pure-tone average
ROS	Reactive oxygen species
RSD.....	Relative standard deviation
SAM.....	Standard addition method
SERS	Surface-enhanced Raman spectroscopy
SNR.....	Signal-to-noise ratio
TEOAE	Transient otoacoustic emission
TNF- α	Tumour necrosis factor- alpha
UNCR.....	Urinary neopterin-to-creatinine ratio
WBC	White blood cell
WN1.....	Whatman No.1

Chapter 1 Introduction

1.1 Ageing, inflammation and immunity

1.1.1 Age-related disease burden

The population of the world is ageing. In many respects, this is a triumph for medical, social and economic advances, but it also brings with it medical, social and economic challenges. In 2018, globally for the first time, the number of people aged over 65 years outnumbered the number of children under five years¹⁵. At a global level in 2019, approximately 9% of the population are aged over 65 years, and this is expected to rise to 12% in 2030, and projected to reach 16% by 2050¹⁵. It is expected that by 2050, there will be 1.5 billion people aged over 65 years worldwide¹⁵. The number of people aged over 80 years is growing even faster. In 1990, there were just 54 million people in the world aged 80 years or over. By 2019, this number had risen to 143 million and is projected to reach 426 million in 2050¹⁵. Whilst individuals are living longer due to increased lifespan, most are living many of these years in poor health, as healthspan has not increased to the same extent, i.e., the period of life free from serious chronic disease and disability. Therefore, population ageing leads to many socioeconomic and public health challenges, particularly the increased cost burden of health and social care.

The prevalence of age-related diseases in older adults is significant. Around 25% of those aged over 85 years will have a severe form of visual impairment¹⁶, sarcopenia affects around 20% of this age group¹⁷, and one study showed 52% of 85-year-olds had a diagnosis of osteoarthritis¹⁸. Sixty-two percent of Americans over 65 years have more than one chronic condition¹⁹ and prevalence of multiple chronic conditions is rising, and accounts for a large percentage of healthcare spending.

As well as the economic and societal impact, living longer but in poorer health, has personal implications too. Older adults are more susceptible to infectious diseases, with an increased incidence of urinary tract infections²⁰, influenza²¹, and community-acquired pneumonia²². The severity of infection is usually greater with significantly increased infection-related morbidity and mortality rates^{23,24}. Age-associated changes in immune function, termed immunosenescence, are thought to underlie this increased incidence and severity of infection²⁵. Inflammaging is a chronic low-grade inflammatory state observed in older people and is a consequence of immunosenescence although lifestyle factors such as reduced physical activity and increased adiposity also play a major role²⁶. Increased systemic inflammation has been associated with

Chapter 1

greater risk of most age-related conditions²⁷⁻²⁹, and in poor health, older people accumulate diseases, described as multimorbidity. Multimorbidity puts some individuals at greater risk of disability and death, as well as depression and social isolation³⁰. This increased vulnerability is described as frailty and is believed to be a clinical manifestation of immunosenescence³¹. Inflammaging and measures of inflammaging have been shown to be predictors of frailty³².

This thesis aims to demonstrate a novel, simple, easy to use point-of-care test that would allow individuals who are at greater risk of age-related conditions, due to increased systemic inflammation, to be identified. The technique being proposed would enable high-repeat (multiple tests of the same patient) testing with low burden to the patient, using urine as a sample rather than blood.

1.1.2 Ageing immune system

The immune system consists of two components, the innate and the adaptive immune systems. The innate immune system is often considered the “first line of defence”. It is triggered to react to injury and infection. The innate response includes physical cellular barriers and the participation of circulating and tissue-resident cells including macrophages, neutrophils, dendritic cells, natural killer (NK) cells, and microbicidal molecules, such as nitric oxide and superoxide anion. The adaptive immune system mounts a slower response but offers longer-lasting, specific protection, due to keeping a memory of each pathogen it has encountered and mounting a specific response to each. The adaptive immune response mainly involves T and B lymphocytes (which mature in the thymus and bone marrow) and their products, cytokines and antibodies, respectively. Ageing is known to have a degrading effect on both systems, although the effect of ageing on the adaptive system is much better characterised.

For the innate immune system, the decline seen with age is not universal, with some elements seemingly unaffected. Although neutrophil numbers may be increased, there is a significant reduction in bactericidal and phagocytic function. This is partly explained by reduced expression of CD16 receptors to bind the antibody coating bacterial pathogens³³. Ageing also modifies macrophage function, including reduced phagocytosis and superoxide function, but the enhanced secretion of IL-6 and IL-8 in response to mitogens and lipopolysaccharide. NK cell numbers do not alter, but their cytotoxic capacity is reduced. Age-related changes to NK cell function are associated with mortality in older adults over 75 years³⁴.

In the adaptive immune system, fewer naïve T cells are produced by the thymus, meaning the proportion of memory T cells increases, as the pool of T cells is maintained at a constant level. This means the immune system is less able to deal with new pathogens as it ages. There is also a

decrease in the number and proliferative capacity of Th1 cells and increase in memory Th2 cells. Increased Th2 cells lead to increased production of IL-10, further suppressing the function of Th1 cells. The production of antibodies from B cells declines with age; for example, older people produce a lower antibody titre in response to vaccination than younger individuals, and the antibodies that are produced are usually of lower affinity. This is widely thought to be due to a decline in T cell help for B cells, and a reduced vaccination response has been shown to correlate with a low clonal expansion of CD4 Th cells in older adults.

1.1.3 Biomarkers of ageing and inflammaging

Ageing has an effect on all cells, tissues and organs within the body, and is usually characterised by loss of function. There is no current standard for biomarkers of ageing, which makes it difficult to compare results between studies on ageing as there is no consensus on biomarkers to be used. In recent years, collaborative approaches to produce recommendations of biomarkers have begun³⁵. A proposed panel of biomarkers was selected from those which are well established with robust supporting evidence for strong associations with ageing phenotypes, and which are likely to be practical and cost-effective for use in large-scale studies³⁵.

Biomarkers of physical capability, such as handgrip strength, gait speed, chair rise time and standing balance, are useful markers of current and future health³⁶. Poor performance in such tests is associated with higher mortality rates^{36,37} and are also associated with a higher risk of some age-related conditions³⁸.

Age-related disease and disability have also been associated with cortisol³⁹; abnormal levels have been associated with increased blood pressure, impaired glucose metabolism and increased incidence of cardiovascular disease and type 2 diabetes in men⁴⁰.

Biomarkers of age-related changes in immune function (immunosenescence) are not well characterised, as there are few longitudinal studies comparing measures of age-related immune function with mortality or age-related disease. The most commonly observed immune markers are T-cell phenotype and pro-inflammatory cytokine measurements, however, these do not consider innate immune factors. The most widely studied aspect of immunosenescence is the age-related increase in systemic inflammatory cytokines (inflammaging)⁴.

Research has shown that during the process of inflammaging some serological, cellular and genetic markers are elevated^{41,42}. One of the hallmarks of inflammaging is the upregulation of pro-inflammatory cytokines, and many studies have opted to determine levels of cytokines including CRP, TNF- α , IL-1 β , and IL-6^{27,42-44}. Higher plasma concentrations of IL-6 and TNF- α are associated

Chapter 1

with altered measures of physical capability, such as lower grip strength and gait speed in older adults⁴⁵.

Cytokines are produced predominantly by immune cells but also by epithelial cells and fibroblasts. Monitoring the upregulation of cytokines as a determinant of immune activation has a few drawbacks. Cytokines may exert their action locally and may not be available to be assayed in circulation⁴⁶. Secondly, cytokines are biologically labile and liable to rapidly bind to ligands on target cells which may render them immeasurable⁴⁶. Finally, binding of cytokines to target cells and membrane receptors, and their interaction with other cytokines may modify their effect⁴⁶. Fuchs et al. have suggested that an alternative is to monitor levels of stable inflammatory metabolites produced or induced by cytokines, neopterin is an example⁴⁶.

Neopterin is a metabolite of guanosine triphosphate (GTP). The biosynthetic pathway of neopterin is shown in figure 1.1. The enzyme GTP-cyclohydrolase I promotes the cleavage of GTP to form 7,8-dihydroneopterin triphosphate. In human epithelial cells, fibroblasts and lower animals, 7,8-dihydroneopterin is further broken down by 6-pyruvyl-tetrahydrobiopterin synthase to form 5,6,7,8-tetrahydrobiopterin (Biopterin). However, due to the deficiency of 6-pyruvyl-tetrahydrobiopterinsynthase in human monocytes/macrophages, the intermediate product 7,8-dihydroneopterin triphosphate is converted by phosphatases to 7,8-dihydroneopterin and oxidised to neopterin⁴⁷, making monocytes/macrophages the only true source of neopterin in humans.

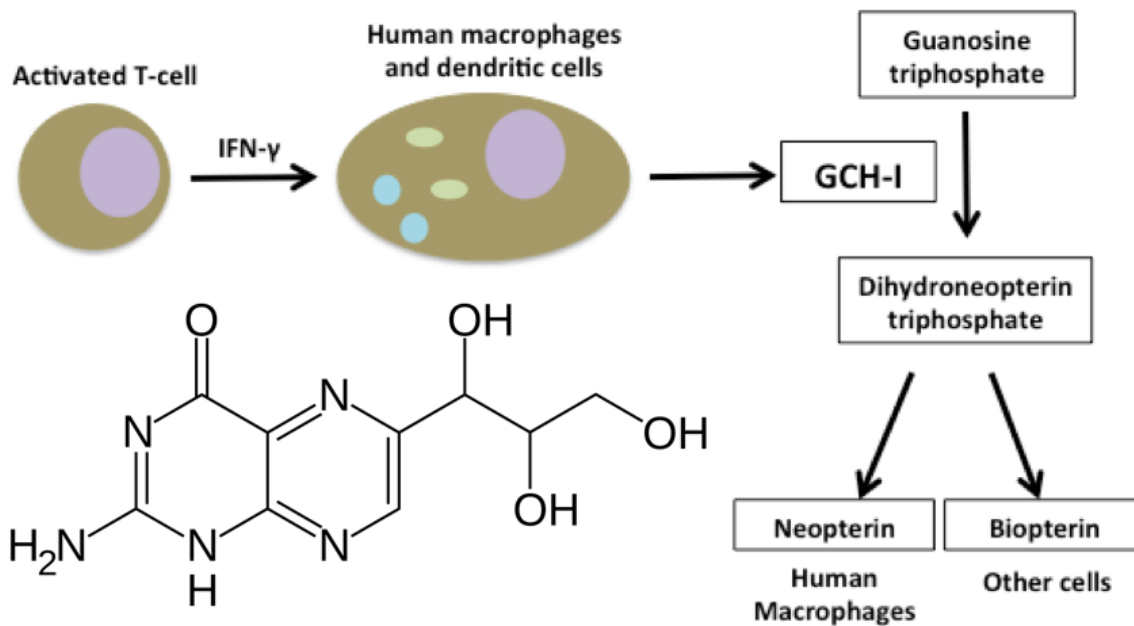


Figure 1.1 Biosynthetic pathway of neopterin and chemical structure of neopterin.

During cellular immune responses, activated T-cells release interferon-γ which in human macrophages and dendritic cells stimulates the enzyme GTP-cyclohydrolase

(GCH-I). GCH-I cleaves GTP to form 7,8-dihydroneopterin triphosphate. Because of a relative deficiency of the 6-pyruvoyltetrahydropterin synthase in human monocytes/macrophages, neopterin and 7,8-dihydroneopterin are formed after dephosphorylation and oxidation at the expense of biopterin derivatives.

Neopterin is released in large amounts from human monocyte-derived macrophages and dendritic cells preferentially following stimulation with the pro-inflammatory cytokine interferon- γ , thus reflecting the immune activation status. This process means that neopterin levels are influenced by both the innate and adaptive immune system, with both contributing to inflammaging^{48,49}. Neopterin levels in the urine have been found to correlate with serum levels, providing renal function is normal⁵⁰, since neopterin does not undergo breakdown before release in urine¹¹. Measuring neopterin in urine provides a non-invasive alternative to serum. Neopterin has been explored as a biological marker for inflammation in several conditions, such as Crohn's disease¹¹, systemic lupus erythematosus⁵¹, coronary artery disease⁵², transplant rejection monitoring⁵³, ovarian tumours⁵⁴, psoriasis⁵⁵, HIV-1 infection⁵⁶, pulmonary tuberculosis⁵⁷ and periodontitis⁵⁸. Studies assessing a cross-sectional population have found raised neopterin levels in older people^{13,46,59}. However, these studies are assessing the neopterin level at a single time point; only a few studies have assessed neopterin in the elderly and how inflammaging and age-related diseases are reflected by neopterin production^{60,61}.

1.1.4 Neopterin measurement

Neopterin levels can be assayed using validated methodologies in serum, plasma, urine and cerebrospinal fluid⁵⁰. The amount of neopterin in urine is measured as a ratio to the amount of creatinine (urinary neopterin to creatinine ratio (UNCR)). Two percent of the body's creatine is converted to creatinine, resulting in excretion of constant amounts. This property of creatinine makes it a useful marker to standardise the concentration of other molecules against allowing for state of hydration or physiological variations in urine concentration^{50,59}. Urine creatinine levels should remain constant unless there is advanced renal failure affecting more than 50% of nephrons. In the case of advanced renal failure, the urinary creatinine levels will decrease, resulting in an overestimation of urinary neopterin⁶².

High-Performance Liquid Chromatography (HPLC) is the gold-standard method for measuring urinary neopterin. In HPLC, a sample is passed through a stationary column, and the individual components are separated based on a physical or chemical interaction between the molecules and the column. A detector measures the amount of each separated component based on their

individual emission wavelengths. Neopterin has an emission wavelength of 438nm and creatinine 235nm, so therefore both molecules can be separated using the same experimental set-up^{46,59}. Using a well-known protocol for quantification of neopterin, the limit of detection was found to be 40nmol/L¹³. Intra- and inter-assay coefficients of variance (CV) for the neopterin/creatinine ratio were 4.7% and 5.8% respectively⁵⁹. To run a single sample through HPLC to get a measurement of both neopterin and creatinine (including disinfection/cleaning of the column between samples) would take more than one hour¹² and at a cost of ~ \$10 per sample⁶³. This would be expensive in time and money to measure multiple samples, multiple times, for long-term monitoring and therefore, despite the accuracy and quantitative ability, it is not a viable option to use.

Enzyme-Linked Immunosorbent Assay (ELISA), enables measurement of the target antigen in the sample competing with a known amount of antigen for binding sites of a known enzyme-linked antibody, producing a colourimetric colour change. A spectrophotometer is used to measure the optical density of the coloured solution, and the concentration of neopterin is determined using a standard curve derived from known target, neopterin, concentration^{46,59}.

HPLC and ELISA are time-consuming techniques, can require complex sample preparation, incur the cost of expensive reagents and/or involve high instrumental costs. Besides this, these techniques also require a trained person with considerable knowledge and expertise to perform the tests and evaluate the results. There is a great need for the optimisation and development of a novel analytical method for rapid, inexpensive, and on-site detection and monitoring of biomolecules in biological fluids⁶⁴.

1.2 Age-related hearing loss

1.2.1 Burden of disease and management

Age-related hearing loss (ARHL) is a rapidly growing problem in the UK as the population ages. By 2030 hearing loss will affect 1 in 5 people in the UK and be in the top 10 disease burdens, above type 2 diabetes and cataracts⁶⁵. People with hearing loss are twice as likely to develop depression and are at increased risk of anxiety and other mental health problems⁶⁶. There is evidence of a strong link between hearing loss and the risk of developing dementia⁶⁷⁻⁷⁰. There are known associations between hearing loss and diabetes, cardiovascular disease, stroke and obesity⁷¹⁻⁷⁵. Vascular changes that occur with diabetes, cardiovascular disease or obesity may be the link for increased risk of ARHL⁷⁶.

Hearing function is assessed clinically by pure-tone audiometry (PTA). PTA is a measure of the quietest sound level an individual can hear at octave frequencies ranging from 250-8000 Hz. Hearing level, based on a pure-tone average threshold, is usually described as normal, mild, moderate, severe, or profound. Age-related hearing loss typically presents as a bilateral, high-frequency, sloping, sensorineural loss on an audiogram, and over time extends to include loss at lower frequencies. Sensorineural means both the sensory and neural elements of the auditory pathway are affected, and presents on the audiogram with little to no threshold difference, between air-conducted thresholds and bone-conducted thresholds.

Currently, there is no way of restoring hearing or slowing down the progression of ARHL. Current management for hearing loss is using a hearing aid to improve audibility for the user. However, there is a major lack of uptake of, and compliance with the use of, hearing aids in the general population⁷⁷ with current use estimated at lower than 40% of those likely to benefit. A better understanding of the biological mechanisms involved in hearing loss may aid development of a disease-altering treatment. Equally, being identified as at risk of developing disease would provide individuals with opportunity to make lifestyle changes which have been shown to reduce inflammaging, and therefore may slow or prevent progression of disease.

1.2.2 The auditory system

The auditory system consists of both the peripheral and central auditory systems. The peripheral system is comprised of the outer, middle and inner ear. The outer ear consists of the pinna and external auditory canal, which acts as a resonator and enhances sound transmission. The middle ear comprises the tympanic membrane and ossicles and transforms air vibrations into the fluid-filled inner ear. The inner ear consists of the cochlea, vestibular system, and the auditory nerve. The majority of age-related changes in the auditory system occur in the inner ear and neural pathways, which lead to the characteristic sensorineural hearing loss.

Although hearing loss is incredibly common in the older population, about one-third of older individuals do not have a hearing loss⁷⁸. Therefore, ARHL is not an inevitability, and the occurrence and progression are variable⁷⁹. Contributory risk factors for ARHL are thought to be physiological degeneration, genetic makeup and environmental insult on the auditory system⁸⁰. Some of the environmental factors contributing to auditory insult are noise exposure, use of ototoxic medications, and lifestyle choices such as smoking⁸⁰. However, there is also a body of evidence to suggest the underlying biological mechanisms underpin the variability seen between individuals. A better understanding of the biological cause of hearing loss will significantly improve diagnosis and treatment options for older adults with hearing loss. Furthermore, an

improved understanding of the contributing factors, the effect of these on the auditory system, and the biological processes involved need to be better understood.

1.2.3 Systemic inflammation in the inner ear

There is evidence that inflammatory processes in the inner ear are responsible for the degeneration in function. For example, murine studies into the damage associated with noise exposure demonstrate that the induced cochlear damage and hearing loss is due to inflammatory processes^{81,82}. Both acute and chronic noise exposure have been found to cause a change in expression levels of proinflammatory cytokine TNF- α and IL-1 β ⁸¹. Additionally, blockade of the cytokine IL-6 pathway after noise exposure has been shown to protect against noise induced hearing loss and is a potential therapeutic target for various kinds of hearing loss⁸³. The link between inflammatory processes being involved in cochlear damage would make the monitoring of inflammatory mediators an interesting target for progression of age-related hearing loss.

As discussed, for long-term monitoring of inflammatory biomarkers, there is a need for an extremely low-cost technique that is suitable for repeated point-of-care measurement. Currently, a developed technique for monitoring urine samples in this way does not exist, however, there is great potential in the technique of Raman spectroscopy.

1.3 Surface-enhanced Raman spectroscopy (SERS)

1.3.1 Raman theory and principles

Raman spectroscopy is a vibrational spectroscopic technique based on the inelastic scattering process that occurs when light interacts with a molecule. As a vibrational spectroscopy technique, it is complementary to the also well-established infrared spectroscopy and offers non-invasive, non-destructive and chemically selective detection for biomedical and diagnostic applications.

When light is incident on a molecule, it can be absorbed, scattered, or have no interaction with the molecule at all. For absorption to occur, the energy of the photons in the incident light must closely match the energy gaps between molecular levels in the molecule. When this occurs, a photon can be absorbed, and the molecules pass into a higher excited energy level. An emission process involves both absorption of a photon and later emittance of a photon after some time, depending on the lifetime (τ) of the excited state. This corresponds to the radiative excitation energy decay of the molecule, which returns back to the ground state (fluorescence). While UV-Vis absorption and fluorescence belong to electronic spectroscopies, IR absorption and Raman scattering, involve nuclear vibrations and are vibrational spectroscopic methods.

1.3.2 Raman spectroscopy

Raman spectroscopy relies on inelastic scattering of monochromatic light, usually from a laser in the visible, near-infrared or near-ultraviolet range. The laser light interacts with molecular vibrations, phonons or other excitations in the system, resulting in the energy of the laser photons being shifted up or down. The energy shift gives information about the vibrational modes in the system. Infrared spectroscopy deals in the infrared region of the electromagnetic spectrum and is the result of absorption of light by vibrating molecules as compared to Raman, which is the scattering of light by vibrating molecules. The main difference between the two techniques lies in the nature of the molecular transitions taking place. For a transition to be Raman active, there must be a change in the polarizability of the molecule during the vibration. This means that the electron cloud of the molecule must undergo positional change. On the other hand, for infrared detectable transition, the molecules must undergo dipole moment change during vibration. So, when a molecule is symmetrical, e.g. O₂, no Infrared absorption lines are seen as the molecule cannot change its dipole moment.

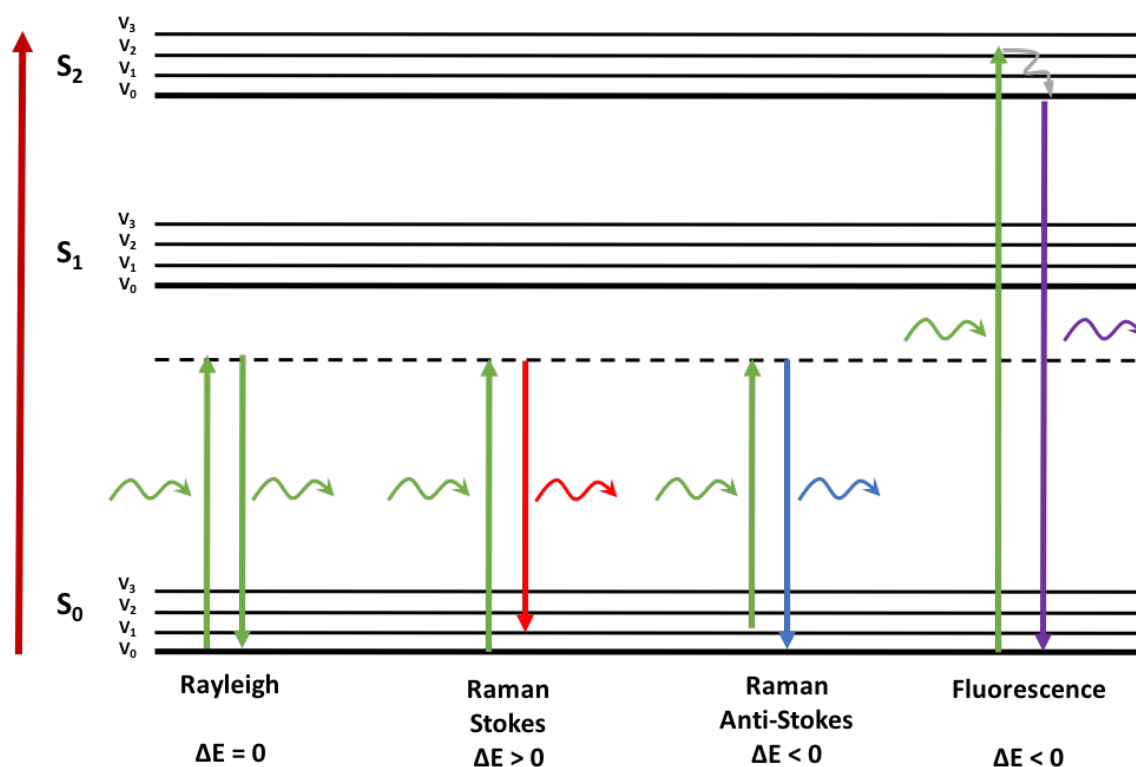


Figure 1.2 Jablonski energy level diagram illustrating the process of Rayleigh and Raman scattering and fluorescence emission from a molecule.

In the scattering processes, an incident photon causes excitation from a vibrational energy level to a virtual state. For Rayleigh scattering, the scattered photon is the same energy as the incident photon. For Stokes Raman scattering the scattered

Chapter 1

photon is lower in energy than the incident photon. For Anti-Stokes Raman scattering the scattered photon is higher in energy than the incident photon. In an absorption process, a molecule is excited to a higher electronic state before an emission process occurs, e.g. fluorescence.

During Raman scattering processes, a photon causes excitation of a molecule into a “virtual” state, followed by an almost instantaneous scattering of the photon with either the same energy (elastic Rayleigh scattering) or with slightly different energy (inelastic Raman scattering), where some energy is either lost or gained from the molecule, as shown in Figure 1.2. The energy difference is equal to that between the initial and final state of the molecule. If the final state is higher in energy than the initial state (energy lost to the molecule), the scattered photon will be shifted to a lower energy (Stokes Raman scattering). If the final state is lower in energy than the initial state (energy gained from the molecule), then the scattered photon will be shifted to higher energy (anti-Stokes Raman scattering). At room temperature, most molecules are in their ground vibrational state ($v=0$) with a much lower population in the first vibrationally excited state ($v=1$). Since there is a much higher probability (given by the Boltzmann distribution) that the molecule is in the ground vibrational state, Stokes Raman scattering is much more likely to occur than Anti-Stokes Raman scattering. In vibrational spectroscopy, it is common to measure frequencies in wavenumber units (waves per unit length) which are reciprocal to wavelength. The energy lost by the photons in the scattering events is called the Raman shift and is expressed in wavenumbers (cm^{-1}). It corresponds to the wavenumber of the vibrational mode that is involved in the scattering event. The position of Raman peaks is a property of the electronic ground state and independent of excitation wavelength. In normal Raman scattering, the Raman intensity is directly proportional to the concentration of the molecule.

For a nonlinear molecule composed of N atoms, there exists a maximum $3N-6$ internal modes of vibration, after subtracting 3 degrees of freedom for translation and 3 for rotation. Each normal vibrational mode has its own excitation energy, giving each molecule a unique set of Raman shifts or its characteristic Raman spectrum. By analysing the spectrum of scattered light for its characteristic shifts, it is possible to identify the scattering molecule. The Raman spectrum measured from a bulk material is the sum of Raman scattered photons from all molecules present. Therefore, the intensity of the Raman peaks corresponds directly to its concentration, enabling the quantification of the scattering molecules.

The main benefits and drawback of Raman spectroscopy for biomolecular applications have been summarised^{84,85}. A big advantage of Raman is that it can be used with solids, liquids and gases,

including obtaining Raman spectra of aqueous solutions because H₂O is weakly Raman active and does not cause interference. This makes Raman spectroscopy very suitable for biological samples in their native state. Another advantage is that no sample preparation is needed for Raman, whereas infrared sample preparation can be quite laborious. Finally, Raman is considered a non-destructive technique, which again highlights its suitability for dealing with biological samples. Raman spectroscopy, in comparison to other analytical techniques, can give molecularly-specific information on a sample in a matter of seconds.

Disadvantages of Raman spectroscopy include sample heating through the intense laser radiation, which can destroy a sample or mask the Raman spectrum. Also, serious problems in Raman occur when large background signals from fluorescence from impurities or the sample itself arise. However, the biggest disadvantage of Raman spectroscopy is that the Raman effect is inherently weak, making it difficult to measure substances present in low concentration. Care must also be taken when measuring and differentiating molecules of similar structures. Therefore, when dealing with molecules that are weakly Raman active or mixtures of molecules, an enhancement process is necessary along with robust validation and verification.

1.3.3 Surface-enhanced Raman spectroscopy

Surface-enhanced Raman spectroscopy (SERS) is based on the enormous enhancement of Raman scattering of molecules adsorbed on suitable metallic (mainly silver or gold) nanostructures. SERS was first reported by Fleischmann et al. in 1974, who observed a 10⁶ enhancement factor of Raman signals⁸⁶. SERS has been shown to provide between 10²-10¹⁴ enhancement in Raman signal intensity⁸⁷.

There are two different mechanisms that contribute to the total enhancement; an electromagnetic one, based on resonance excitations of surface plasmon in the metal, and a chemical (or molecular) one, increasing the polarizability of the molecule⁸⁸.

The electromagnetic mechanism is largely considered to be the dominant enhancement factor. It occurs due to the unique ability of metallic or plasmonic structures to interact with light and cause an excitation of their localised surface plasmon resonance (LSPR) demonstrated in Figure 1.3. Light interacts with metal nanoparticles, causing their free conduction electron cloud to oscillate and excite the surface plasmons inducing a strong evanescent field on the metal surface. In aggregated systems, "hot spots" form when two neighbouring nanoparticles are in close enough proximity that their LSPRs couple. "Hot spot" formation is heavily dependent on the size and shape of the nanoparticle as well as the inter-particle distance and the aggregation of the nanoparticles needs to be controlled to ensure reproducible enhancement.

Chapter 1

The chemical enhancement can be attributed to a charge-transfer between the metal surface and the adsorbed molecule, causing a change in the molecule's polarisability. When a molecule becomes adsorbed onto a metal surface, an adsorbate-metal complex is formed, and its highest occupied molecular orbital (HOMO) and lowest unoccupied molecular orbital (LUMO) are generally positioned symmetrically about the metal's Fermi level. This arrangement allows for electron transfer between the molecule and the metal to occur at much lower energies than that required for the excitation of the molecule itself.

Overall, at a given wavelength, a SERS spectrum is similar to the standard Raman spectrum, although some differences may arise from the wavelength-dependence of the plasmon resonance. Due to molecules being adsorbed onto the metallic surface some differences may also be seen due to the orientation of the molecules on the surface, the angle of the molecule in respect to the surface, the degree of packing and interaction with neighbouring molecules. Therefore, it can be difficult to assign bands in a SERS spectrum as the symmetry of the molecule may cause a shift in the Raman bands and relative intensities, as well as the appearance of new bands.

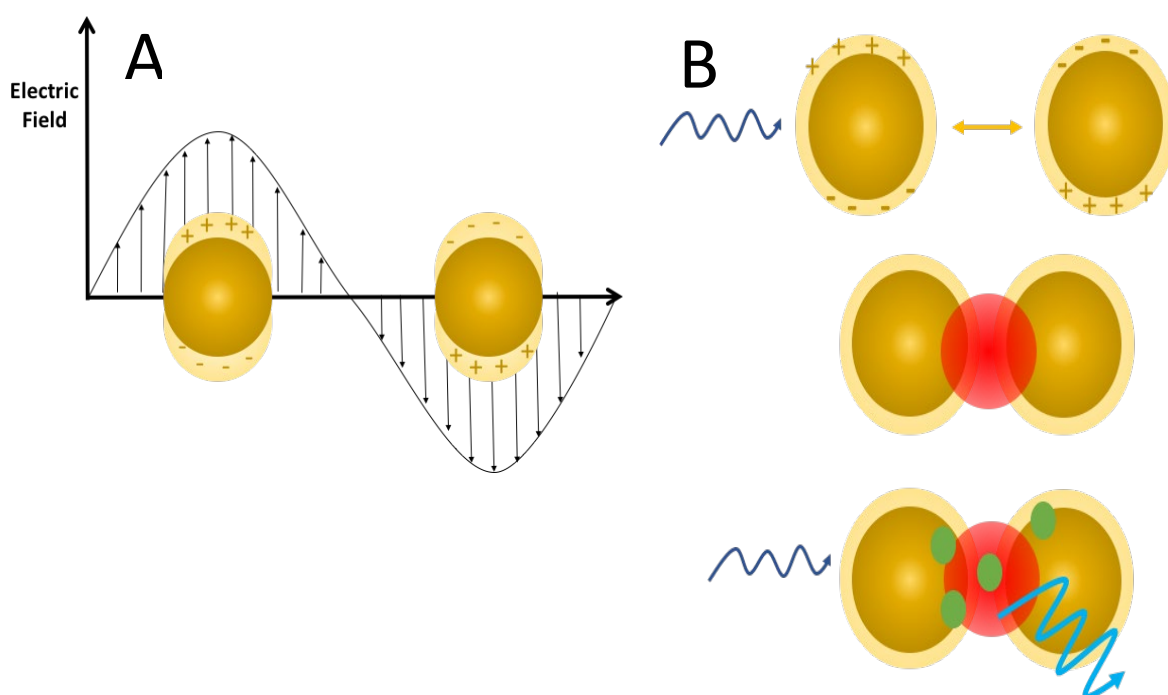


Figure 1.3 Demonstration of excitation of localised surface plasmon resonance (LSPR) and 'hotspot' formation.

Interaction of light with a metal (nanoparticle) causes free electrons at the metal surface to oscillate collectively and excite the surface plasmons inducing a strong evanescent field at the surface – LSPR. When nanoparticles aggregate in close enough proximity, their LSPRs couple to form a 'hotspot' of enhancement.

1.3.4 Substrates for Surface-enhanced Raman spectroscopy

1.3.4.1 Metallic nanoparticle colloids

For SERS enhancement, the simplest substrates are colloidal metal nanoparticles (usually Ag or Au) which are formed by the suspension of metallic nanoparticles (NPs) in various shapes and diameters. Such Ag or Au colloids can be prepared simply and inexpensively using “wet chemistry”, for example, reduction of AgNO_3 or HAuCl_4 with an appropriate reducing agent such as trisodium citrate⁸⁹.

UV-Vis absorption spectroscopy is a useful tool for determining morphological and optical properties of metallic NPs in colloid suspension. The Surface Plasmon Enhancement (SPE) maxima range from 380 to 440nm and 510 to 540nm for Ag and Au colloids respectively, showing different LSPR properties for both metals. Electron microscopy of dried colloid drops on carbon-coated Cu grids can also give useful information⁹⁰.

Nanoshells are hybrid NPs consisting of a dielectric core (such as silica) and a metallic shell⁹¹. The LSPR behaviour of nanoshells is sensitive to the inner and outer dimensions of the metallic shell layer. A redshift is achieved by increasing the size of the silica cores while simultaneously reducing the thickness of the metallic shell⁹². Moreover, the hybrid resonance response can be tuned by an interaction between the LSPR supported by the inner and the outer surfaces of the metallic shell layer⁹³. The tuneable plasmon wavelength range of Au nanoshells is from 600nm to 2.2 μm , which makes these substrates ideal for use in the biological environment as IR excitation reduces problems associated with autofluorescence of biological media.

Shell-isolated NPs (SHINs) are prepared using either a Ag or Au core which is then protected by an ultrathin shell of SiO_2 , Al_2O_3 , MnO_2 or Ag_2S to meet the demand of various chemical environments⁹⁴. The shell must be less than 5nm thick to ensure sufficient electromagnetic enhancement. Li et al. have developed SHINs for use as SERS specific probes with the advantage that they offer better stability than bare NPs⁹⁵. Also, the shell isolates the metal surface from the probed molecules and therefore prevents a potential disturbing interaction.

Freshly prepared colloids consist of NPs isolated due to the Columbic repulsive barrier resulting from the double layer of charged ions on the NP surface⁹⁰. Interaction of an adsorbate with the colloid surface causes the NPs to stick together, forming aggregates of different size and shape (Figure 1.4b). Aggregation of metallic colloids is known to be influenced by various parameters including the surface potential of the colloid, the chemical nature and concentration of the adsorbate, and the temperature and the presence of a particular pre-aggregating agent such as chloride anions. Aggregation of NPs has a significant influence on a SERS experiment. Whereas the

single NP resonates at a particular frequency, its random aggregate could resonate at a different wavelength within broad spectral regions and therefore, the aggregation shifts the SPE to red with respect to the SPE of isolated NPs. Another important impact of aggregation is the interparticle coupling of LSPR of NPs being close to or touching each other. This effect leads to much higher SERS enhancement in comparison to individual NPs. Certain LSPRs generated in the nanosized gaps between NPs (“hot spots”) are the source of extremely high enhancement. The big disadvantage is that the aggregation process is time-dependent as some big macroscopic aggregates tend to precipitate from the solution. Moreover, the distribution of LSPR of NP aggregates of different sizes and shapes is strongly inhomogeneous, which causes poor reproducibility of SERS enhancements⁹⁶.

One way of achieving the benefits of aggregated NPs whilst reducing the disadvantages associated with uncontrolled aggregation is to use a layer-by-layer synthesis of colloidal NPs⁹⁷. By applying layers of NPs around a core with ionic spacer layers (see Figure 1.4a), two (or more) layers of nanoparticles can be brought together so that they are in close enough proximity to form “hot spots” between layers but fixed enough in space so that uncontrolled aggregation is limited⁹⁸.

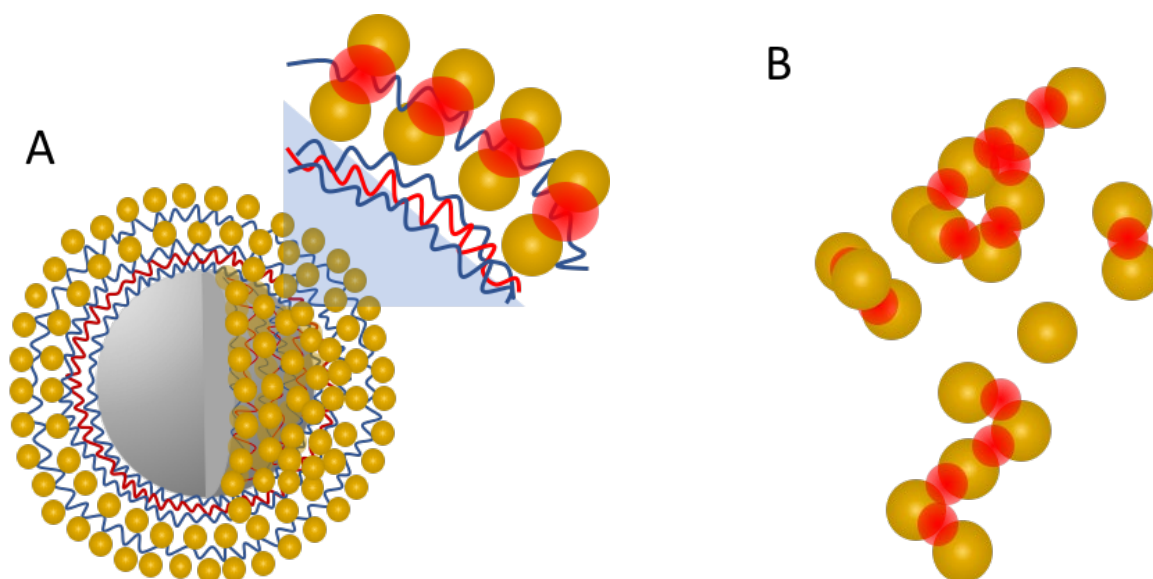


Figure 1.4 Schematic of a layer-by-layer synthesised sensor and randomly aggregated nanoparticles.

- A) An iterative process of applying ionic spacer layers and NPs forms a nanostructured particle with 2 layers of NPs evenly distributed and fixed in space to allow coupling of LSPR between layers and ‘hot spot’ formation. Blue and red lines indicate polyelectrolyte spacer layers controlling the spacing between NPs
- B) Randomly aggregated NPs allow uncontrolled formation of ‘hot spot’ formation.

1.3.4.2 Nanoparticles on planar supports (bottom-up processing)

Stability and spectral reproducibility of metallic NPs can be significantly improved if rationally designed NPs are self-assembled or immobilized on planar solid supports using a bottom-up technique. Different techniques employed to assemble metallic NPs with various sizes and shapes have been reviewed^{99,100}. Preparation procedures include chemical attachment of NPs via small molecules or bifunctional polymers¹⁰¹, inverse micelle polymer film¹⁰², layer-by-layer assembly⁹⁷, solvent-induced evaporation¹⁰³, electrostatic interaction between NPs and surface¹⁰⁴. The average enhancement factors reported for assembled and immobilised NPs range from 10^5 to 10^7 ^{99,105,106}.

1.3.4.3 Nanostructures fabricated using top-down techniques

Highly ordered metallic nanostructures can be prepared using top-down techniques such as electron-beam lithography and chemical etching techniques. Using electron-beam lithography and ion-beam lithography, an array of highly ordered structures is produced by a focused electron or ion beam drawing patterns over a resist wafer in a serial manner with nanometre resolution¹⁰⁷. After removal of the photoresistor layer, the substrate will present a series of isolated NPs, separated by regions where bare substrate is exposed.

Electron-beam and ion-beam lithography methods suffer from high cost, long preparation times (several days) and a need for specialised equipment. A cheaper and faster technique is the use of templates to allow the deposition of metal with controlled geometry; nanosphere lithography is such a technique. Nanosphere lithography uses self-assemblies of polystyrene micro- or nanoparticles on solid surfaces as 2- or 3-dimensional masks for metal deposition^{108,109}. The size and shapes of the close-packed nanospheres and the holes between them, in addition to the metal deposition conditions, such as evaporation angle or specific deposition technique (e.g. sputtering, thermal deposition), influence the achieved metallic patterns.

1.3.5 SERS substrate enhancement factor

As there are a variety of different SERS substrates available to use, there is a need for a commonly accepted way to gauge their effectiveness. The enhancement factor is one of the key parameters that is currently used to compare and evaluate different substrates. The enhancement factor (EF) is essentially the enhancement in SERS signal that results from the presence of nano features compared to the pure Raman spectrum. Experimentally it can be calculated:

$$EF = \left(\frac{I_{SERS}}{I_{Raman}} \right) \times \left(\frac{N_{Raman}}{N_{SERS}} \right)$$

Chapter 1

Where I_{SERS} and I_{Raman} are the SERS and Raman intensities at a selected peak and N_{SERS} and N_{Raman} are the total number of analyte molecules responsible for generating the corresponding SERS and Raman intensities.

The two intensity measurements can easily be obtained from the output of the spectrometer; however, the total number of analyte molecules is much more difficult to calculate. In determining N_{SERS} , one must be careful to count only those molecules which are actually adsorbed onto the nanostructures and hence are responsible for the SERS, and not the molecules which are adsorbed onto any support material or in solution. In particular, the concentration of analyte used should be such that the surface coverage is significantly smaller than one monolayer. As SERS is highly distance-dependent, the existence of more than a single monolayer when performing SERS means that the scattering intensity is no longer proportional to the number of molecules. The enhancement factor is also dependent on the analyte used for testing, due to the difference in adsorption of molecules onto the surface of the nanostructure. Therefore, comparison of EF between different substrates is only valid if similar analyte-nanostructure interaction can be achieved, which is generally very difficult to do.

1.3.6 Quantitative analysis with SERS

Sensitivity and reproducibility are the major concerns when developing quantitative SERS methods^{110,111}. The main requirements for a SERS enhancing metallic substrate are⁸⁴:

- SERS sensitivity: The substrate should provide high SERS sensitivity, which is generally considered as SERS enhancement better than 10^5 .
- Spot-to-spot reproducibility: The substrate should be uniform so that the SERS signal shows variation less than 20% over a 10 mm^2 area.
- Substrate-to-substrate (batch-to-batch) reproducibility: The SERS signal variation for different batches of a substrate prepared by the same method should be less than 20%.
- Stability: The substrate should provide good stability even after a longer shelf time (signal variation less than 20% measured over one month). It particularly means that the substrate should be long-term stable without any destabilization or destruction by environmental conditions, like oxidation.
- The substrate should be clean enough so that it can be applied to study even weakly adsorbed analytes. It particularly means that the signals from the SERS substrate itself involving Raman spectrum of possible surface contaminants as well as background of the substrate such as autofluorescence of metal should be as low as possible. In practice, the

obtained SERS spectrum should be good enough to distinguish the Raman features of the analyte present in low concentrations from the background signal of the SERS substrate.

- Ease and low-cost preparations and use of the substrate.

There is a fine balance between achieving reproducibility and large SERS enhancement when dealing with SERS sensors as it tends to be the case that the higher the substrate reproducibility, the lower the enhancement factor that tends to be seen¹¹². For any form of quantitative analysis, reproducibility and uniformity of the substrate are crucial. In addition, for bioanalytical and clinical applications, a clean, highly enhancing and biocompatible substrate is needed (usually a gold-based substrate). The cost and ease of preparation and use are also incredibly important.

In the work of Mamián-López and Poppi, urinary nicotine was determined in the presence of its metabolite cotinine and the alkaloid on AuNPs¹¹³. The urine samples were spiked with known amounts of the analyte and added to a suspension of AuNPs for SERS analysis. SERS spectra were decomposed using the multivariate curve resolution-alternating least squares method and successfully measured concentrations of 0.10, 0.20 and 0.30 $\mu\text{g}/\text{ml}$ with a total variance of less than 10%. This demonstrates that you can use SERS to reproducibly detect an analyte of interest in the presence of other similarly structured metabolites, demonstrating the specificity of the technique.

Another very simple and low-cost analytical technique for SERS detection uses AgNPs printed onto paper by a commercial inkjet printer¹¹⁴. The ink was formed with standard citrate-reduced Ag NPs concentrated 100x by centrifugation and mixed with glycerol and ethanol to optimise the surface tension and viscosity for optimal printing. Reusable ink cartridges were used to hold the ink and print onto the desired regions of the paper. During the printing process, NPs in the ink aggregate and form clusters in the cellulose matrix. After printing, individual dipsticks were cut out of the sheet. The entire paper strip can be utilized for sample collection, while the end of the dipstick or swab containing the AgNPs acts as the SERS-active medium. For the dipstick experiments, 5 μl of a sample (heroin and cocaine dissolved in methanol) was added to the collection zone in a controlled approach to mimic the uptake of the analyte onto the paper. After the dipstick had dried, it was placed into a vial containing 2ml of methanol which is quickly wicked up into the dipstick toward the detection tip. After 20 minutes of run time, the dipstick was allowed to dry, and the detection zone was scanned to determine the strongest SERS signal. A portable spectrometer with a fibre optic Raman probe was used for SERS detection. By use of the lateral flow concentration, the authors achieved LOD as low as 15ng of cocaine and 9ng of heroin. Although these detection limits are already comparable to many rigid SERS substrates, their

approach is much simpler when compared to conventional SERS substrates and traditional microfluidic devices. These detection limits are also comparable to those from other techniques. A reported LOD for cocaine measured with LC-MS is 0.9 ng/ml¹¹⁵ and with a commercially-available ELISA kit 3.3nM.

1.3.7 Clinical and diagnostic SERS with urine

Generally, SERS detection of biomolecules can be accomplished by two methods: (i) direct-intrinsic- (often called label-free) and (ii) indirect-extrinsic-using labels.

Direct detection SERS is also known as a “label-free” approach and aims to directly acquire a SERS spectrum of an analyte without the need for a label, such as a dye or Raman reporter molecule.

Indirect SERS requires some form of labelling so that the spectra obtained comes from the label rather than the analyte itself. SERS labels are usually chemical species (often dyes) that have a well characterised, intense and stable SERS spectrum that can be used to signal the presence and concentration of the analyte of interest. Indirect SERS protocols have emerged as a highly sensitive detection technique. SERS labels are usually covalently bonded to metal nanoprobe, accompanied by biomolecular ligands and are used to detect target analytes by biomolecule-ligand recognition¹¹⁶. One indirect method that has gained increasing popularity for biofluid diagnostics is SERS immunoassays, which can be qualitative or quantitative tests to detect specific biomarkers using antibodies and have been shown to have incredibly good sensitivity¹¹⁷⁻¹¹⁹.

Direct, label-free detection would be the method of choice where possible because it is reliable and convenient; however, it can be difficult to employ as it has limited sensitivity to analytes at low concentrations making them difficult to detect, and it exhibits poor selectivity in complex mixtures because of the overlapping of Raman bands making identification complicated. Novel label-free detection methods are constantly emerging, for example, with the development of SERS-active substrates and sample-pre-treatment methods.

Most diagnostic applications of Raman and SERS with urine have been limited to solid tumour biology, including prostate¹²⁰, oral¹²¹, breast¹²², esophageal^{123,124}, lung¹²⁵ and bladder¹²⁶ cancer. However, additional pathologies that have been looked at are kidney disease¹²⁷⁻¹²⁹, risk of kidney transplant rejection or renal failure¹³⁰, renal complications in patients with diabetes and hypertension^{131,132} and preeclampsia^{128,133}.

In the majority of studies, SERS spectra are generated for samples collected from a group of patients diagnosed with a specific form of cancer with healthy subjects acting as a control^{120-124,126}. Through pre-processing of data and principal component analysis (PCA) to reduce the number of

variables, investigators have been able to build predictive classification models using linear discriminant analysis (LDA) or in some cases support vector machine (SVM) algorithms. The diagnostic performance of the models can be evaluated by calculating sensitivity, specificity and diagnostic accuracy. Using such statistical differentiation methods, excellent sensitivity, specificity, and diagnostic accuracy have been reported. Elumalai et al. have reported a model with 98.6% sensitivity, 87.1 % specificity and 93.7% diagnostic accuracy for identifying those with oral cancer from those without¹²¹. This particular study by Elumalai et al. shows very promising results and a reasonably sized cohort was used (93 oral cancer patients and 74 healthy controls). However, other studies report results from much smaller sample sizes, which still show promise for the technique, but would need a larger study to truly show the diagnostic capability of the test^{120,122}. Work by Beleites et al. discussed the requirements for adequate sample size when using classification models to get statistically relevant results and reported that 75-100 subjects are needed in each class¹³⁴. However, the mass majority of SERS-based diagnostic studies have been performed on much smaller numbers of subjects.

1.4 Paper chromatography

Paper chromatography is an exceptionally simple method of separating mixtures, using a solvent and filter paper. A pencil line is drawn on the chromatography paper, and a spot of mixture deposited onto it. In ascending chromatography, the paper is suspended in a container with a shallow layer of solvent below the pencil line. As the solvent travels up the paper, the different components of the mixture travel at different rates and the mixtures are separated into different spots. The distance travelled by each compound relative to the solvent is a constant as long as you keep everything else constant- the type of paper, the composition of the solvent etc. The retention factor (R_f) is the relative ratio of the distance travelled by the compound, to the distance travelled by the solvent. If the compounds are colourless, development agents (e.g. I_2 , ninhydrin) or UV can be used to visualise them, depending on what the compound is.

The separation of compounds on the stationary phase is due to the ability of the different molecules to bond with the surface. For instance, in Thin Layer Chromatography (TLC), silica gel is commonly used as the stationary phase. Silica is a covalent structure with Si-O-Si bonds, however at the surface of the silica gel you get Si-O-H bonds making the surface very polar, because of the -OH groups, hydrogen bonds can form with suitable compounds around it as well as van der Waals dispersion forces and dipole-dipole attractions. Paper is made of cellulose fibres, the polymer chains in cellulose also have -OH groups sticking out all around them, but cellulose fibres also attract water vapour from the atmosphere as well as any water that was present when the paper was made. Therefore, paper is cellulose fibres with a thin layer of water molecules attached to its

Chapter 1

surface. During paper chromatography, it is the interaction with this water on the surface which has the most important effect.

When the solvent moves up the plate, it dissolves the compounds in the sample spot and carries them with it. The speed the compounds move at depends on how soluble they are in the solvent (the attraction between the compound molecules and those of the solvent), and how much attraction there is between the molecules of the compounds attached to the stationary phase (the attraction between the compound molecules and the stationary phase). If a compound can form hydrogen bonds, and another can only for van der Waals interactions, the one which can hydrogen bond will be adsorbed to surface more strongly. Adsorption is not permanent, and there is a constant movement of the molecules between being adsorbed and going back into solution in the solvent. The compound can only travel up the surface whilst it is dissolved in the solvent, whilst adsorbed to the surface, it is temporarily stopped and the solvent moves without it. Therefore, the stronger the adsorption of the compound, the less distance it will travel up the plate. The attractions between the compound and the solvent are also important and will affect how easily a compound is pulled back into solution. This is why changing the solvent may help separate out the components, including changing the pH of the solvent.

Paper chromatography, combined with SERS, has been demonstrated in the literature. Paper-based SERS strips possess several advantageous features in terms of simplicity, cost-effectiveness, and on-site detection. Moreover, paper strips could separate the mixtures with their inherent ability of fluidic capillary-action. Recent work by Zhang et al. has coupled shell-isolated nanoparticle-enhanced Raman spectroscopy with paper chromatography for simultaneous separation and optical detection of multiple components of a sample¹³⁵. Yu and White have used a paper substrate for chromatographic separation and detection of an analyte from a complex sample¹³⁶. A drop of sample is pipetted onto a paper SERS substrate that has been printed with nanoparticles and allowed to dry. The substrate is then placed upright in a sealed jar that has been pre-saturated with the mobile phase that is chosen depending on the sample and target components being separated. As the solvent is wicked up the substrate, the components of the sample are separated. The combination of SERS with paper chromatography allows analyte detection of the chromatogram without any chemical modifications and also allows concentration and quantification of analytes without the need for extraction¹³⁶.

1.5 Thesis structure

The overall aim of this thesis is to demonstrate the potential of a SERS-based point-of-care device for repeated measures of an inflammatory marker in urine samples. The goal of such a device

would be to monitor individuals' systemic inflammation and identify those who are inflamed or heading towards, and therefore at greatest risk of, and worsening progression of, age-related diseases. This thesis consists of three experimental chapters. The first chapter (chapter 2) provides the evidence for the need of longitudinal monitoring of an inflammatory marker (neopterin) in urine. It demonstrates the relationship between consistently elevated systemic inflammation, with worsening age-related disease (age-related hearing loss). Chapter 3 demonstrates that SERS can be used to accurately measure this inflammatory marker in samples of urine, with results validated against the gold-standard analytical technique, HPLC. Chapter 4 moves on to show how a potential point-of-care device made with a paper substrate could operate, incorporating separation of a mixture (urine) by paper chromatography, with detection of the analyte of interest via SERS.

Chapter 2 Determining an individual's baseline systemic inflammation and subsequent risk of age-related conditions

2.1 Overview

This chapter demonstrates how long-term inflammatory monitoring can develop a unique inflammatory profile of an individual, with potential diagnostic or screening implications. Low-grade chronic inflammation, also known as inflammaging, is associated with diagnosis and progression of many age-related conditions. This longitudinal cohort study monitored neopterin, a small inflammatory metabolite, in monthly urine samples of 45 older adults (aged 65-75 years). Neopterin volatility was used to establish an individual's baseline systemic inflammation for this targeted healthy, independent, community-dwelling population. This allowed stratification of the cohort into risk categories based on how often in a 12-month period their urinary neopterin level was raised. Using age-related hearing loss as an example of a condition that causes disability affected life-years, the evidence demonstrates that those with high inflammatory baseline see greater progression in disease over a 4-year period. The evidence is that those who are the most inflamed are more likely to be suffering from multiple age-related conditions. Such monitoring and screening of individuals has huge potential in the clinical setting. Identifying and effectively managing these individuals offers improvement for their wider psychological wellbeing, as well as the economic benefits of individuals staying healthier for longer. The results demonstrate the variability of inflammatory load in the elderly and the need for a stratified approach in the treatment/delay of age-related conditions via targeting inflammaging. By highlighting people's risk status early enough, those individuals can adopt lifestyle changes or therapeutic intervention which may reduce their risk of inflammaging and in turn, age-related disease.

It should be made clear that the contribution to this work is not solely the author's. All data from baseline until month 13 (year 1) were collected and analysed by Dr Akosua Agyemang-Prempeh. The urine samples were then re-analysed by the author using surface-enhanced Raman spectroscopy and Charlotte Stuart using Mass Spectrometry. The analysed data contained in this chapter is mass spectrometry data for urinary neopterin to creatinine ratio (UNCR). The author and Dr Alan Sanderson carried out the Year 3 face-to-face questionnaires, pure-tone audiograms

and otoacoustic emissions. Data compilation, analysis and interpretation, is the sole work of the author.

2.2 Introduction

2.2.1 Goal to improve healthspan as well as lifespan

Ageing is an inevitable time-dependent biological process that is characterised by progressive loss of cell functions and tissue regeneration, leading to physical deterioration. Many factors contribute to the complex, heterogeneous and dynamic mechanisms of ageing¹³⁷. Ageing is a major risk factor for common diseases such as cardiovascular disease¹³⁸, diabetes¹³⁸, osteoarthritis¹³⁹ and neurodegenerative diseases^{140,141}. The rate of ageing varies both between and within a species and within the different tissues of an individual.

Across the world, as life expectancy continues to rise, the consequences of age and physiological demise increase. Advancements in medical care, improvements in environment, and nutrition have extended life expectancy for humans; however, there is little evidence that the rate of ageing has slowed¹⁴². In some areas of the world, known as blue zones, the elderly consistently live beyond the age of 100 years, and largely without chronic disease, however, these areas are exceptional. In nearly every developed nation in the world, there is growth in the number of elderly, but although they are living longer, they are living with multiple age-associated disorders¹⁴³ which in turn has dramatic social and economic consequences.

A new perspective is that most age-related conditions share a common underlying biology. Therefore interventions targeting the molecular processes of ageing can simultaneously delay the onset, and progression of, most age-related conditions^{144,145}. If age-related research focused on delaying age-related morbidity and compressing the majority of lifetime illness into a shorter period, nearer the end of life, this would allow individuals to live free from disability and illness for longer. In turn, this allows greater numbers to retain functionality and productivity for a larger part of their life¹⁴⁶, benefiting both the individual and society.

Centenarians are a subset of humans whereby many have achieved longevity and maximal healthspan. Studies have shown that they display cytokine profiles in keeping with younger adults and do not develop inflammaging¹⁴⁷⁻¹⁵⁰. Additionally, their offspring also display cellular modification of T and B cell compartments which share characteristics with younger people rather than their age-matched equivalents^{151,152}. A better understanding of the biological mechanisms contributing to the shared underlying biology between centenarians and younger adults is needed.

Chapter 2

The World Health Organisation defines healthy ageing as ‘the process of developing and maintaining the functional ability that enables wellbeing in older age’ with an extension of ‘intrinsic capacity’, which comprises all the mental and physical capacities that a person can draw on, including their ability to walk, think, see, hear and remember¹⁵³. This really helps to understand the concept of healthy ageing as broad and holistic, encompassing mental, physiological and sensory components.

2.2.2 The ageing immune system

In the last 20 years, enormous steps have been taken to better understand the involvement of the immune system in ageing^{3,4,43,154-156}. The immunological theory of ageing has followed, encompassing the intricate involvement of both the innate and adaptive immune systems¹⁵⁷.

Metchnikoff first described a decline in the innate immune system as one of the pillars of ageing, and in 2000, Franceschi developed the concept of inflammaging⁴. Inflammaging describes the systemic and sterile (absence of infection) low-grade chronic inflammation that is now largely considered a central biological pillar in the ageing process^{3,4,158}. Inflammaging is a predictor of frailty^{32,159} and chronic low-grade inflammation is now accepted as a key pathogenic factor in the development of many different age-related conditions, including cancer²⁶, cardiovascular disease¹⁶⁰, type 2 diabetes¹⁶¹ and hearing loss^{5-7,162,163}. It manifests as elevated levels of pro-inflammatory cytokines such as interleukin 6 (IL-6) and Tumour necrosis factor-alpha (TNF α) and acute-phase proteins such as C-reactive protein (CRP)⁴. Additionally, the levels of cytokines that resolve inflammation, such as interleukin 10 (IL-10), are reduced with age¹⁶⁴, leading to the idea that inflammaging is caused by disequilibrium between the innate and adaptive immune systems. The innate system remains well preserved in the elderly in comparison to the deterioration in function of the adaptive immune system⁴.

Inflammaging is, therefore, a consequence of an ageing immune system known as immunosenescence. However, the two share the same underlying causative phenomenon of chronic, repetitive, lifelong exposure to inflammatory stimuli and antigens, to which an individual has been exposed during their lifetime known as “immunobiography”^{154,165}. Every individual will have a different immune history, so, therefore, will have differing outcomes ranging from healthy, successful ageing, to pathological ageing (ageing associated with multiple age-related conditions).

Age-related inflammation results from the complex interplay between immunosenescence, cellular senescence, self-debris, obesity, gut microbiota and dietary patterns. All of these factors are thought to contribute to the systemic inflammatory state, through the imbalance of pro-inflammatory and/or anti-inflammatory mediators^{166,167}.

2.2.3 Low-grade chronic inflammation (inflammaging) and age-related disease

The presence of a chronic inflammatory state drives damage to tissues. Inflammation has become a key area of interest in the research of many age-related conditions. Chronic inflammation has been linked to both incidence and progression of many diseases such as, cardiovascular disease¹⁶⁸⁻¹⁷¹, cancer^{26,172-175}, diabetes^{138,176-178}, neurodegenerative diseases (Alzheimer's disease, Parkinson's disease, multiple sclerosis etc.)^{48,179,180}, sarcopenia¹⁸¹, macular degeneration¹⁸², depression¹⁸³, frailty^{32,41,159,184-188}, hearing loss^{5,7,162,163,189,190}, arthritis^{139,191} and osteoporosis¹⁹². Many of these conditions are known risk factors for each other, and it is not uncommon for an older individual to experience two or more, highlighting the key common factor of inflammation in all these conditions.

2.2.4 Age-related hearing loss as an example age-related disease associated with inflammaging

Sensory impairment is common in older adults, with loss of hearing and vision being the most prominent¹⁹³. Sensory impairments can significantly reduce the ability to undertake daily activities, maintain social interactions and independence. Despite the abundance of evidence for the effect of inflammaging on other disease models, there is a significant lack of research of inflammaging on ageing sensory systems.

The National Institutes of Health (NIH) Toolbox[®] has included measures of sensory function in its resource for monitoring neurological and behavioural function¹⁹⁴. The sensory measures include measurements of audition, vision, olfaction, gustation, vestibular function and pain. Most of these functions (except pain) decrease across the lifespan and sensory changes may overlap with changes in cognitive and motor functions. For example, olfactory dysfunction is one of the earliest 'preclinical' symptoms of neurodegenerative diseases¹⁹⁵ and is associated with mortality in the National Social Life, Health and Aging Project¹⁹⁶. In a commentary on the evidence for whether inflammaging plays a part in age-related macular degeneration, Gallenga et al. concluded unequivocal evidence for the involvement of inflammation and immune-mediated processes in the pathogenesis of age-related macular degeneration¹⁹⁷.

As an example of an age-related condition, this research focusses on age-related hearing loss (ARHL) as a model sensory system. Acute inflammation and early-phase inflammatory responses have been implicated in noise-induced hearing loss⁸² and idiopathic sudden sensorineural hearing loss models^{198,199}. These parallels in other hearing loss models suggest the likeliness of inflammation being involved in ARHL.

Chapter 2

Age-related hearing loss is one of the most prevalent conditions among elderly individuals, with around 10 percent of the world's population being affected. By 2030 it is reported that hearing loss will be in the top 10 disease burdens, above diabetes and cataracts²⁰⁰. Those living with hearing loss, generally have difficulty communicating with colleagues and loved ones, which can affect quality of life²⁰¹. They are also twice as likely to develop depression and are at increased risk of anxiety and other mental health problems⁶⁶. However, no two individuals will experience the same ARHL, onset and progression of disease varies from person to person.

ARHL is a multifactorial condition with multiple pathways and underlying conditions contributing to the biological mechanisms²⁰². Unlike other chronic conditions with similar prevalence, ARHL lacks any biomedical treatment or preventative measures that reduce risk. Currently, the most common intervention for managing hearing loss is amplification (in the form of a hearing aid or cochlear implant) to improve audibility for the user. However, there is a major lack of uptake of and compliance with the use of hearing aids in the general population⁷⁷. A better understanding of the biological mechanisms involved in hearing loss may aid development of a disease-altering treatment. Equally, being identified as at risk of developing disease would provide individuals with opportunity to make lifestyle changes which have been shown to reduce inflammation, and therefore may slow or prevent progression of disease.

2.2.5 Mechanism of hearing

When a sound wave enters the outer ear, it comes into contact with the tympanic membrane of the middle ear causing it to vibrate, which in turn moves the ossicles (middle ear bones) with the same frequency of vibration. The stapes footplate rests on the oval window of the cochlea, and transforms the air vibration into the fluid-filled cochlea. The fluid-filled cochlea is located in the temporal bone and is formed of bony labyrinth enclosing a membranous labyrinth and is a coiled, shell-like structure about 35mm in length. There are three fluid-filled compartments: the scala tympani, the scala vestibuli, and the scala media. The scala tympani and vestibuli contain perilymph, which has a high sodium concentration. The scala media contains endolymph, which has a high potassium concentration. The scala media is separated from the scala vestibuli by the Reissner's membrane, and the scala media is separated from the scala tympani by the basilar membrane. A direct current resting potential, known as the endolymphatic potential, of 80-90 mV is measurable in the scala media. The endolymphatic potential arises from Na⁺ K⁺ ATPase pumps in the stria vascularis which is located on the lateral wall of the cochlea.

The organ of Corti is the auditory transducer and contains sensory cells; three rows of outer hair cells (OHC) and one row of inner hair cells (IHC). A travelling wave along the basilar membrane is

produced by the movement of the stapes in the middle ear, against the oval window of the cochlea. The travelling wave moves from the base (high-frequency) towards the apex (low-frequency) of the cochlea. The travelling wave causes deflection of stereocilia on the hair cells, opening and closing ion channels, resulting in a current flow of potassium ions into the hair cell. The depolarisation of the hair cells causes an enzyme cascade, releasing chemical transmitters and activating afferent nerve fibres.

2.2.6 Biological basis of hearing loss

Original research into the biological mechanisms of hearing loss was by Schuknecht^{203,204}, who described four structures important for cochlear function; the organ of Corti, the stria vascularis, the auditory nerve and the basilar membrane. Age-related degenerative changes to these structures led to the classification of three main pathological types of ARHL, sensory (degeneration of the organ of Corti), metabolic (degeneration of the stria vascularis) and neural (degeneration of the spiral ganglion cells of the auditory nerve).

The organ of Corti comprises the inner hair cells (IHC), the outer hair cells (OHC) and their supporting cells to make up the sensory region of the cochlea. Degeneration of the sensory and supporting cells affects sound transduction and may also result in degenerative changes in the auditory nerve²⁰⁵. Sensory ARHL is most strongly associated with the basal portion of the cochlea corresponding to the transduction of high-frequency sounds and presents on the audiogram as a steep sloping high-frequency hearing loss²⁰³. Noxious agents including exposure to noise and ototoxic medication generate reactive oxygen species (ROS) in the organ of Corti, which contributes to the degeneration of the hair cells²⁰⁶ by causing damage to proteins including prestin, an important constituent of OHC plasma membrane²⁰⁷. Ageing is also associated with increased generation of ROS; however, some researchers suggest sensory ARHL is due to a lifetime accumulation of environmental noise and does not truly reflect ageing^{202,208}. Aged laboratory animals without a genetic predisposition to hair cell loss that have been raised in a quiet environment have been found to have intact hair cells^{202,208}. This has led to the conclusion that a combination of genetic predisposition and noise are the cause of sensory ARHL.

According to Schuknecht, neural ARHL was characterised by loss of spiral ganglion cells and auditory nerve fibres. Neural ARHL is believed to be influenced by genetic factors, which may also affect neurons in other areas of the central nervous system²⁰⁴. The hearing loss becomes apparent in later life when more than 50% of spiral ganglion cells have undergone degeneration. It is characterised by a speech discrimination score that is worse compared to the associated audiogram. Degeneration of spiral ganglion cells was previously believed to be a consequence of

Chapter 2

retrograde hair cell loss²⁰⁹. However, there is now evidence that neurodegeneration of auditory nerve fibres can occur long before there is a frank loss of hair cells or cell bodies of the spiral ganglion cells^{210,211}.

Metabolic ARHL occurs as a result of degeneration of the stria vascularis, which is the part of the cochlea that generates the endolymphatic potential. Degeneration of the stria vascularis affects the cochlear amplifier²⁰⁸ and results in an audiogram that is flat at the low frequencies and gradually sloping at the high frequencies²⁰⁸. The high metabolic activities of the stria vascularis in maintaining the endocochlear potential renders it susceptible to age-related changes²¹². In addition, ageing itself is associated with chronic vascular diseases such as atherosclerosis and type 2 diabetes that potentially can affect vessels in the stria. This may be a mechanism by which vascular and inflammatory diseases are associated with ARHL.

A fourth type of ARHL needs to be considered, and that is central ARHL, which refers to age-related changes that occur in the central auditory pathway that results in a decline of auditory perception or speech intelligibility²¹³. Neurodegeneration that can occur in ARHL can be as a result of secondary degeneration from the peripheral pathway or can occur independently to peripheral changes²¹³. There is evidence of age-associated primary degeneration in the structure and function of the central auditory system²¹⁴. Some studies have suggested that neurodegeneration in the central auditory pathway is in response to a loss of peripheral inputs^{215,216}. Assessing central auditory deficits is difficult as the routine audiogram does not depict this. Speech tests can be used to assess central auditory difficulties; however, poor speech understanding cannot be wholly attributed to central auditory deficits as other peripheral deficits, and cognitive decline can also contribute²¹³.

Evidence from both the visual and auditory systems, suggest a loss of sensory stimulation adversely affects the morphology and function of microglia, and it has been suggested that some of the early changes that occur in ARHL, take place at synaptic level²¹⁷. Murine studies demonstrate loss of presynaptic IHC ribbons and postsynaptic glutamate receptors of the peripheral axons of the spiral ganglion cells, long before hair cell loss or death of spiral ganglion cells occurs²¹¹. Microglia are constantly surveying their environment through specialised cytoplasmic processes, making contact with synapses and responding to changes in the brain. Microglial processes in the visual system make around five independent contacts with a synapse every hour, and these contacts are diminished during sensory loss²¹⁸. Any changes that occur to the synapses will result in changes in neurological information which can activate receptors for neurotransmitters and neuromodulators on the microglia, resulting in the removal of the synapse, known as synaptic stripping²¹⁹. As a result of sensory loss, changes in the synapse can result in

reduced regulation of microglia, and is possible they may inadvertently phagocytise normal synapses.

2.2.7 How does systemic inflammation affect the inner ear

The human cochlea is not an “immune-privileged” organ despite the presence of the blood-labyrinth barrier (BLB)²²⁰⁻²²². Resident macrophages are present in the lateral wall of the cochlea, the spiral limbus and the scala tympani side of the basilar membrane²²³. Insults, such as loud or persistent exposure to noise, ischemia and surgical trauma, have been demonstrated to activate these macrophages²²⁴⁻²²⁶. Inflammatory cytokines released by the macrophages, regulate the permeability of the BLB^{225,226} and this inflammation would increase BLB permeability to drugs²²⁷ some of which are ototoxic.

Murine studies identify that environmental exposure to noise induces cochlear damage and hearing loss via inflammatory processes^{81,82}. Another hearing loss model associated with inflammation is noise-induced hearing loss (NIHL) that has similar mechanisms to chronic exposure to noise but on a more acute timeline²²⁸. Measurement of pro-inflammatory cytokines in the cochlea following noise-injury and identified that IL-6 expression is increased at 3 and 6 hours after noise exposure and that a key area for inflammation is the non-sensory areas of the cochlea, particularly the lateral wall⁸². Acute and chronic noise exposure have been found to cause a change in expression levels of proinflammatory cytokine TNF- α and IL-1 β ⁸¹. Additionally, blockade of the cytokine IL-6 pathway after noise exposure has been shown to protect against noise induced hearing loss and is a potential therapeutic target for various kinds of hearing loss⁸³.

However, this association has not been shown to be consistent for all these mediators²²⁹. A study by Morrisette-Thomas et al. investigated 19 biomarkers including pro- and anti-inflammatory cytokines, cytokine receptors, chemokines and C-reactive protein (CRP) in a cohort of different ages, and observed that 10 of the biomarkers showed a significant age association. The results of this study also indicated that inflammaging does not simply reflect an increase of pro-inflammatory markers but an overall activation of inflammatory systems that probably also promotes a concomitant rise in the levels of anti-inflammatory mediators²²⁹. This process may result in different outcomes depending on the nature of the stimulation, the pre-existing physiological reserve, the immune background and exposure to infections²²⁹ hence the term “immunobiography” suggesting a lifelong exposure to antigens and inflammatory stimuli²³⁰.

In sterile inflammation, the resolution phase is initiated by apoptosis and clearance of damaged cells²³¹. Damage-associated molecular patterns (DAMPs)- the pathogens and by-products of cellular damage, stimulate pattern recognition receptors (PRRs). Activation of PRR in the cochlea

leads to the resident macrophages becoming activated and releasing pro-inflammatory cytokines and production of reactive oxygen species (ROS), which in turn leads to apoptosis of damaged cells and infiltration of immune cells into the scala vestibuli and scala tympani²³². The infiltrating immune cells transform and activated macrophages further express pro-inflammatory proteins²³³.

2.2.8 Current research on hearing loss and inflammaging

When searching the ARHL literature, it becomes clearly apparent that there are known associations between hearing loss and many conditions also linked to inflammaging, including diabetes^{71,234,235}, cardiovascular disease^{72,75}, dementia²³⁶⁻²³⁸, stroke^{73,74}, and obesity^{75,239-242}. Therefore, it is plausible that inflammation also plays a role in ARHL and may be a contributing factor to the variability in occurrence and progression observed. Chronic inflammation could lead to hearing loss via vascular damage, compromised blood supply to the cochlea and the tissue of the central auditory pathway^{5,243} and a direct effect on the cochlear hair cells by inducing apoptosis and potentiating ototoxic drugs²³². A population-based cohort study that compared healthy adults, to those with rheumatoid arthritis (characterised by chronic inflammation) showed twice the risk of hearing loss, after adjusting for age, sex and comorbidities²⁴⁴. There have been a few studies in the last 6 years that have investigated the role of inflammation in ARHL and generally these have found an association between elevated inflammatory biomarkers and poorer ARHL^{5-7,162,189,190,245}.

Verschuur et al. have investigated the association between inflammatory markers and hearing in two cohort studies, The Hertfordshire Aging Study (HAS)⁷ and the MRC national study on hearing⁶. In the HAS, the association between inflammatory markers and hearing threshold were investigated in a group of 611 (63-74 years) residents of Hertfordshire. Results identified an association between hearing threshold and inflammatory markers including white blood cell count (WBC), neutrophil count, IL-6 and CRP, independent of age, positive history of noise exposure, smoking and male gender. However, in this study, audiometric data was only collected between 0.5 and 4 kHz, limiting the investigation to the effect of inflammation on the mid-frequency speech range. Therefore, the effect of inflammation at the extreme speech frequencies could not be investigated. Also, only air conduction thresholds were measured, which meant the origin of the hearing loss could not be determined, which is important because a conductive hearing loss is not a feature of ARHL. In the MRC study, 320 individuals (aged 60-89 years) had audiometric data collected (0.25-8kHz) and a white blood cell count (WBC). WBC was found to affect both the pure-tone average threshold and low-frequency average, suggesting inflammation may act on the stria vascularis, which is evidenced to affect low-frequency hearing²¹². The study

also demonstrated that the association between WBC and hearing threshold was greater in the very old subgroup (aged 75-89 years) compared to the younger subgroup (60-74 years)⁶.

In a longitudinal study, Nash et al. have also shown that consistently elevated CRP levels were associated with a higher risk of developing ARHL over the next ten years⁵, but only for individuals <60 years of age. Simpson et al. have also studied the relationship between CRP and pure-tone audiometry (PTA) over-time in a large study of 837 older adults but found when controlling for age and sex, there was no statistically significant association between PTA and CRP¹⁹⁰. A recent study on female nurses in two cohorts (aged 42-69 year and 32-53 years) has also found no relationship between inflammatory markers (CRP, IL-6, TNFR-2) and risk of hearing loss; however, this study used a self-report measurement of hearing rather than a stringent and widely accepted measurement such as PTA²⁴⁵. These findings would suggest that not all biomarkers of inflammation, particularly CRP, show a relationship with ARHL and that the design of the study and measurements used are essential to tap into the sensitive nuances.

Chronic inflammation can go unnoticed for a prolonged period of time and develops subtly and slowly, which echoes the development of ARHL. It is impossible to know, therefore if hearing loss is a later-life comorbidity of inflammation or whether the two co-develop throughout life. A recent cross-sectional study sampling younger adults has investigated a novel biomarker of chronic inflammation, glycoprotein A (GlycA). Results showed that as early as mid-childhood, higher values of GlycA are associated with poorer hearing, suggesting that hearing loss associated with inflammatory antecedents is a life-course condition¹⁶².

These findings are consistent with the hypothesis that inflammation contributes to ARHL and that raised inflammatory status, demonstrated by raised inflammatory markers is detrimental to hearing function. However, to date, no ARHL study has monitored a biomarker over time to build an inflammatory baseline profile for an individual. The benefit of longitudinal monitoring rather than one-off measurement is that levels of inflammatory markers in circulation can vary extensively from day to day²⁴⁶⁻²⁴⁸, due to acute infection or inflammatory insult, therefore, to get a true picture of an individual's inflammatory profile, multiple measures should be taken over a period of time.

2.2.9 Research evidence for different measures of ageing and inflammaging

To allow early identification of individuals at high age-related risk throughout life, appropriate measures and biomarkers of ageing are needed as well as the associated clinical health outcomes. Improved knowledge of key biomarkers will pave the way for future biomedical interventions²⁴⁹ as well as give new insights into the pathology of progressive disease.

Chapter 2

Frailty describes individuals who are in a state of increased risk of vulnerability to disease, disability and death, compared to others of the same age²⁵⁰. Connecting the clinical state of age-related frailty with underlying biological age, as measured by biomarkers, is a goal. Frailty can be evaluated, and health status quantified, by the number of health deficits that individuals accumulate. Specifically, the frailty index (FI) is the ratio of the deficits present in a person, to the total number of potential deficits evaluated²⁵¹. The FI has been used in many epidemiological and clinical studies to grade the degree of risk of several adverse outcomes, including mortality, health service use, hospital-acquired complications, worsening health, and loss of independence²⁵²⁻²⁵⁴, as well as conditions such as cognitive impairment²⁵⁵, heart disease²⁵⁶ and osteoporosis²⁵⁷. Another functional indicator of frailty is hand-grip strength(HGS) which is also associated with inflammatory biomarkers²⁵⁸.

Most age-related conditions involving inflammatory processes consist of similar proteins and molecular mechanisms²⁵⁹. The 2- to 4-fold increase in serum levels of several inflammatory mediators in the elderly has been well described⁴², and there is a body of evidence that circulating concentrations of many markers and mediators of inflammation are higher in older adults^{27,44,147,260-263}. Many studies have chosen to measure the upregulation of circulating pro-inflammatory cytokines such as CRP, TNF- α , IL-1 β and IL-6^{27,42-44,166}. However, monitoring cytokines has a few drawbacks. Cytokines may exert their action locally and may not be available to be assayed in the circulation⁴⁶. Cytokines are biologically labile and liable to rapidly bind to ligands on target cells which may render them immeasurable⁴⁶. Finally, binding of cytokines to target cells and membrane receptors, and their interaction with other cytokines may modify their effect⁴⁶. For example, cytokines that have been implicated in ageing, including IL-6, and TNF- α , have been shown to bind to circulating proteins such as α 2-macroglobulin, the concentration of which is affected by ageing and inflammation²⁶⁴. Changes in α 2-macroglobulin concentrations will influence the number of cytokines available for detection, which may be different from the true levels of the cytokine. Such properties and interactions of cytokines modify the levels of detectable cytokines and limit their use as markers in monitoring immune activation. Previous studies have shown inconsistent findings for acute-phase reactants, including CRP, IL-6 and WBC^{5-7,190}.

An alternative is to monitor levels of stable inflammatory metabolites produced or induced by cytokines, neopterin is an example⁴⁶. Neopterin is released in readily detectable amounts from human monocyte-derived macrophages and dendritic cells preferentially, following stimulation with the pro-inflammatory cytokine interferon- γ , thus reflecting the immune activation status. This process means that neopterin levels are influenced by both the innate and adaptive immune system, with both contributing to inflammaging^{48,49}. Neopterin levels in urine correlate with

serum levels, providing renal function is normal⁵⁰, since neopterin does not undergo breakdown before release in urine¹¹. Measuring neopterin in urine provides a non-invasive alternative to measures in serum.

Recent reviews of neopterin as a biomarker for inflammatory diseases have reported that in most of the diseases in which the cellular immune system is involved, neopterin concentrations are usually high¹² and its clinical usefulness discussed⁹. Studies assessing a cross-sectional population have found raised neopterin levels in older people^{13,46,59}. Neopterin has been explored as a biological marker for inflammation in several conditions, including Alzheimer's disease^{60,265,266} and urine neopterin levels have also been shown to correlate with cognitive performance²⁶⁷. Increased neopterin has also been reported in individuals with malignant and benign tumours compared to healthy individuals^{54,268,269}. Neopterin's benefits as a prognostic marker have also been demonstrated in patients with chronic heart failure²⁷⁰, and it has been used as a diagnostic marker in pulmonary tuberculosis⁵⁷ as well as a tool for monitoring Crohn's disease¹¹. In a study of immune biomarkers in older adults, higher serum neopterin levels were found in subjects with reduced physical activity²⁷¹.

Table 2.1 Reference values of neopterin in urine ($\mu\text{mol}/\text{mol}$ creatinine)⁴⁷

Age (years)	Men		Women	
	Mean \pm SD	97.5th percentile	Mean \pm SD	97.5th percentile
19-25	123 \pm 30	195	128 \pm 33	208
26-35	101 \pm 33	182	124 \pm 33	209
36-45	109 \pm 28	176	140 \pm 39	239
46-55	105 \pm 36	197	147 \pm 32	229
56-65	119 \pm 39	218	156 \pm 35	249
>65	133 \pm 38	229	151 \pm 40	251

Urinary neopterin is measured as a ratio to creatinine, the urinary neopterin-to-creatinine ratio (UNCR). Stuart et al. have demonstrated longitudinal monitoring of UNCR is important to capture a more representative estimate of an individual's inflammatory state, rather than a 'snap-shot' single time point²⁷². Reference values of neopterin in urine of healthy individuals are shown in table 2.1. Examples of raised neopterin levels in diseased individuals can be found in the literature. Stuart et al. measured a median of 316.23 $\mu\text{mol}/\text{mol}$ creatinine in individuals with multiple

sclerosis (n=11, 8 females, 3 males with mean age of 43.3)²⁷². In patients with psoriasis a mean neopterin level of 198.3 $\mu\text{mol/mol}$ creatinine was shown (n =22, 4 females, 18 males, with mean age of 27.5)⁵⁵.

2.2.10 Potential prevention strategies for inflammaging

Ageing is a malleable process with the ageing trajectory showing a high degree of plasticity. Ageing in humans is affected in large part by lifestyle choices, disease and environmental factors. Various biomarkers of ageing appear to be accelerated with poor lifestyle, including increased senescent cells with obesity²⁷³ and raised systemic inflammation with obesity and inactivity²⁷⁴. Sedentary living and physical inactivity are highly prevalent and strongly related to old age²⁷⁵, and as accelerants of the biological ageing process, they predispose for chronic disease²⁷⁶.

Physical activity can preserve the function of major body systems, including the musculoskeletal²⁷⁷ and immune systems²⁷⁸ and protects against many age-related conditions such as cardiovascular disease, cancers and neurodegenerative disorders²⁷⁸⁻²⁸¹, specifically aerobic exercise delays the onset of morbidity and enhances both health and lifespan²⁸²⁻²⁸⁴. The WHO's 2010 Global Recommendations on Physical Activity for Health are for 150 minutes or more a week to have substantial health benefits²⁸⁵. However, epidemiological evidence suggests that as little as 10 to 20 minutes of leisure physical activity per day is sufficient to extend life expectancy²⁸⁶. Physical activity improves physical capability and aerobic power due to adaptations of physiological systems, most notably within the neuromuscular and cardiopulmonary systems and metabolic processes, modifying the trajectory towards frailty²⁸⁷.

Dietary restriction has been shown to positively affect lifespan and healthspan^{288,289}, reducing both inflammation and the accumulation of senescent cells^{290,291}. Diets that favour longevity and healthspan are generally characterised by minimally processed foods, being predominantly plant-based, low alcohol consumption and a lack of overeating. There is already evidence that ageing biomarkers can be modified by interventions that target ageing, such as the CALERIE study of calorie restriction in humans²⁹².

The malleability of longevity has also been demonstrated using compounds such as rapamycin, aspirin and metformin, which target the core ageing processes directly to extend lifespan in mice and other model organisms²⁹³⁻²⁹⁵. Some of these drugs also improve healthspan measures in some tissues in animal models²⁹⁶⁻²⁹⁸.

Metformin has been found to target several molecular mechanisms of ageing²⁹⁹. A large retrospective observational study of patients with diabetes who received metformin showed

increased lifespan in comparison to even individuals without diabetes³⁰⁰. In randomised controlled trials, metformin prevented the onset of diabetes, improved cardiovascular risk factors and reduced mortality^{301,302}. Epidemiological studies have suggested that metformin use might also reduce the incidence of cancer and neurodegenerative disease²⁹⁹.

The beneficial effect of statins in the prevention of cardiovascular events by blocking cholesterol synthesis is well established. Recent studies have shown that statins also possess anti-inflammatory properties and can reduce inflammatory markers, especially IL-6 and CRP, both during chronic inflammatory conditions³⁰³ and also in healthy older individuals³⁰⁴.

The ASPREE-HEARING study is investigating the potential therapeutic benefits of low-dose aspirin, a weak anti-inflammatory agent on ARHL. The investigation aims to determine whether this basic therapy will lessen the progression of the disease in elderly individuals. This large Australian-based clinical trial is targeting 1262 individuals age 70 years old or older but is still currently in progress³⁰⁵. This trial provides large potential for an incredibly inexpensive yet feasible treatment option for preventing or reducing ARHL.

2.2.11 Research Gap

Figure 2.1 pictorially represents the philosophy of this chapter. The underlying pillars are the effects of ageing, the cause/effect factors of inflammaging, the effect on the microenvironment and the consequential pathological processes that occur. From the core of that then comes the clinical effects observed by an individual, the related measurements and biomarkers that identify these, and possible interventions that may reduce or eliminate these central effects.

A clear association exists between low-grade chronic inflammation (inflammaging) and the increased risk of age-related disease, however sensory deficits of ageing such as age-related hearing loss (ARHL) have been minimally studied. Furthermore, studies have measured increased inflammatory markers to show immune activation in association with ageing and disease at single time points. However, there is limited published work that has used multiple serial measurements to build an inflammatory profile of an individual over time. Inflammatory markers can fluctuate with acute illnesses, or inflammatory episodes such as during a surgical procedure, so a single time point measurement would not be a true reflection of an individual's general inflammatory baseline. For the purpose of serial measurements over time and use as a screening tool, a biomarker present in urine, which is non-invasive to collect, would be a far more suitable marker than those in blood. Therefore, neopterin, along with its other benefits of being a stable inflammatory metabolite, is a preferable biomarker to use.

Chapter 2

As a clinical tool to identify individuals with increased low-grade inflammation and therefore at risk of age-related disease, the monitoring needs to be sensitive to such changes in a cohort at an age, and with a low burden of disease, who would have the years in life remaining to make significant disease-averse changes. The measures and markers used must be reliable and validated, for example, using Pure-Tone Audiometry and Otoacoustic Emissions as measures of hearing loss rather than subjective self-report.

Addressing this knowledge gap requires a population-based study that combines valid audiometric data with a biomarker for underlying inflammation suitable for long-term monitoring. Therefore, this study undertook serial neopterin measurement in a cohort of healthy, independent, community dwellers aged 65-75 years and measured changes to hearing over time. The longitudinal data allowed changes in neopterin levels over time to be reliably quantified to allow for inflammation resolution. The study intended to identify those individuals who were poor resolvers of inflammation and potentially at risk of developing, or of rapidly progressing, age-related conditions.

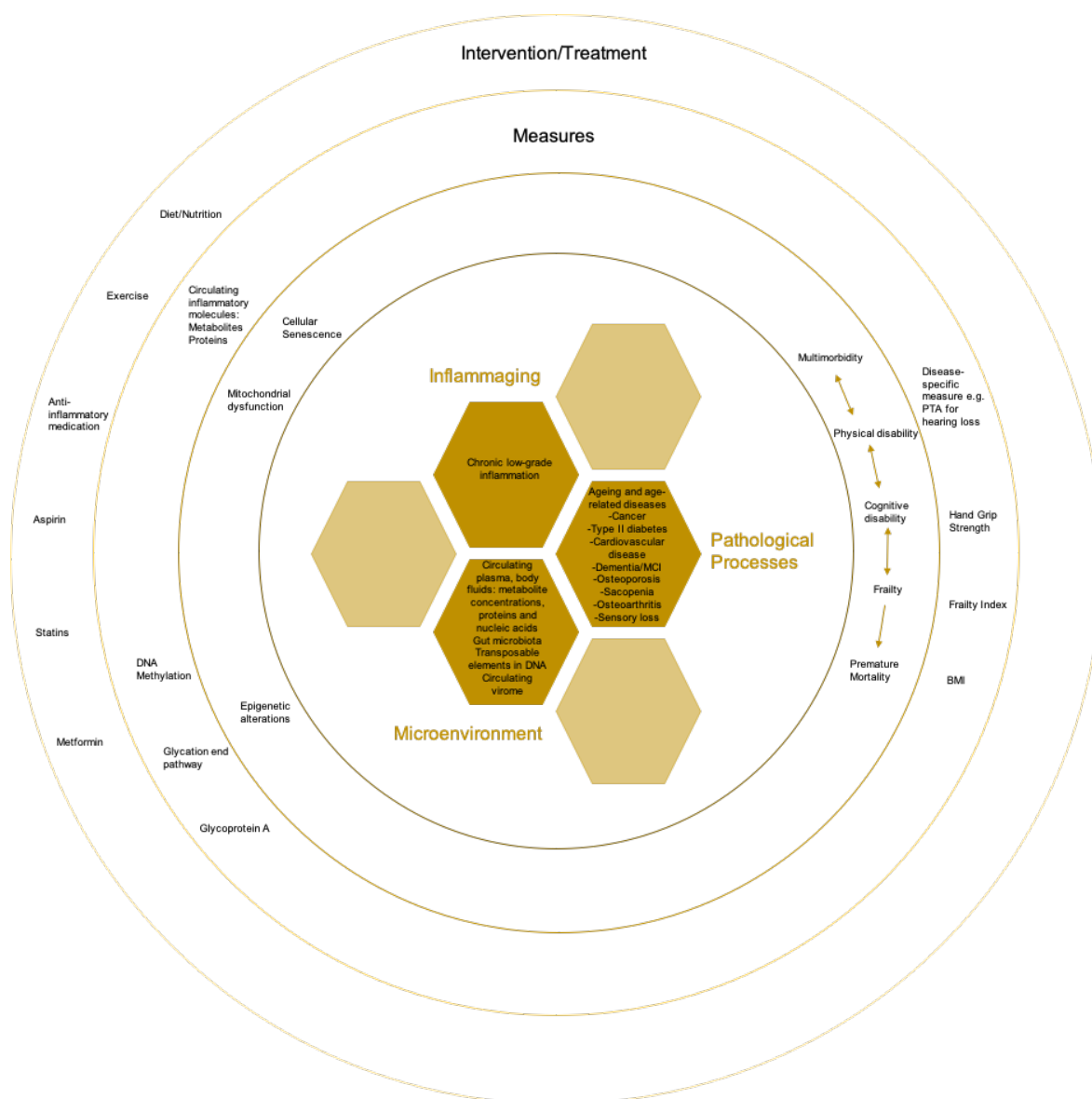


Figure 2.1 Diagrammatic representation of the philosophy behind chapter 2.

The central effects of ageing, the cause/effect factors of inflammaging, microenvironment and subsequent age-related pathological processes. The resulting effects observed in the individual. Potential biomarker and measures associated with the central effects and potential interventions.

2.2.12 Hypotheses

1. Serial measurements of urinary neopterin will identify those with chronic systemic inflammation (inflammaging)
2. High neopterin volatility (volatility is percentage of months neopterin raised above normal limit) is associated with having multiple age-associated conditions/co-morbidities
3. Smokers are at greater risk of chronic inflammation and will have increased neopterin volatility

4. High neopterin volatility is associated with a greater decline in age-related hearing loss.

2.2.13 Aims

1. To measure serial levels of urinary neopterin in a cohort of healthy community-dwelling older adults
2. To compare urinary neopterin measurements to serum biomarkers of inflammation
3. To compare neopterin volatility with prevalence and progression of age-related hearing loss by measuring hearing thresholds over 4 years using pure-tone audiometry and otoacoustic emissions.

2.3 Methods

A four-year longitudinal study investigating the association between urinary inflammatory markers and age-related hearing loss was conducted. It is hypothesised that inflammaging is key in the progression of age-related conditions including ARHL. Assessing inflammatory mediators and building an individual's inflammatory profile, could help in determining those at risk of ARHL and other age-related conditions.

2.3.1 Participants

Convenience sampling was used to recruit a sample of community-dwelling older adults. The study was promoted via interest groups likely to contain a sample of older adults, including the University of the Third Age (U3A) in Southampton, Winchester, Eastleigh and Lymington, and an over 50's group in Southampton, UK. These groups were targeted as their ethos promotes active participation and engagement, potentially indicative of low burden of disease. Recruitment was geographically targeted at locations within the South coast of England due to the number of study visits required, and the higher-than-average population of older adults resident in this region.

Interested participants received a copy of the patient information sheet and given the opportunity to ask questions. Written informed consent was obtained from those willing to participate.

A total of sixty-one individuals (aged 65- 75 years) consented to take part. During the study sixteen individuals withdrew for reasons un-related to the study. Any previous collected data from the withdrawn participants was removed from analysis. A total of forty-five individuals completed all time points of the study.

2.3.2 Inclusion and exclusion criteria

The main criterion for inclusion was age, subjects recruited ranged from 65 to 75 years. According to the inflammaging hypothesis by Franceschi et al., the period in which unsuccessful ageing occurs is maximal between the ages of 60 and 80 years⁴, therefore the age-range was selected to capture a cohort in whom inflammaging had potentially begun to occur. Secondly, since the aim was also to measure change in hearing threshold, which is known to progress with age, a relatively younger cohort was chosen, whose hearing is unlikely to go beyond the limit of testing via pure-tone audiometry. Lastly, a narrow age range was chosen to limit variations that would occur with a wide age range.

Exclusion criteria were i) hearing loss that is severe or profound in severity (as thresholds may exceed audiometric limit), ii) hearing loss caused by known otological pathology other than age-related hearing loss, iii) inability to provide informed consent due to psychological condition e.g., dementia, and iv) individuals with cancer, auto-immune diseases, or use of immunosuppressive medication, as all may inflate neopterin levels.

2.3.3 Study design

Participants attended 3 face-to-face visits at the Hearing and Balance Centre (HaBC) at the University of Southampton. These were at baseline, end of year 1 and end of year 3. Hearing measurements were collected at all 3 face-to-face sessions, while inflammatory measures were only collected at baseline and year 1. Urine samples were also collected for the months in between baseline and year 1, which the participants collected at home and posted in. The study design is depicted in figure 2.2.

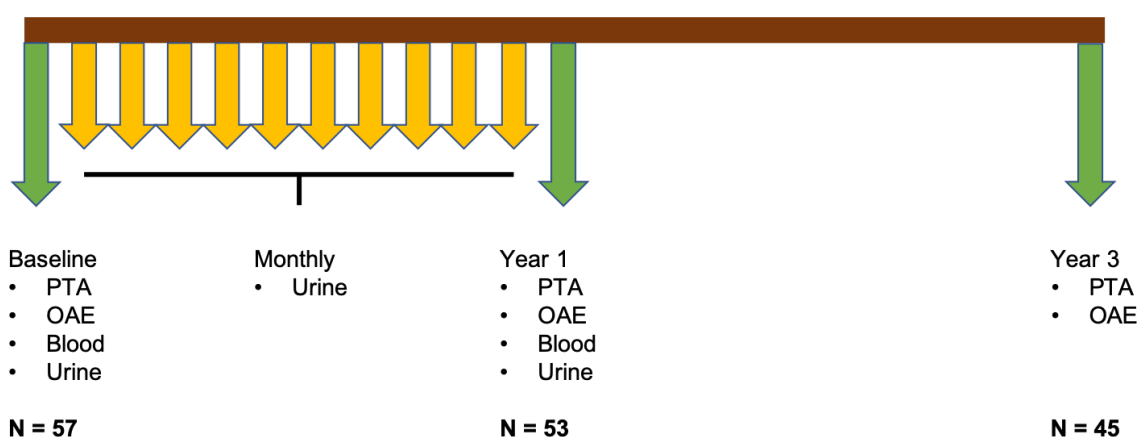


Figure 2.2 Experimental design for InflammHear study.

Hearing (PTA and OAE) measurements collected at baseline, year 1 and year 3 of the study. Inflammatory (WBC, urine and serum neopterin and cytokines IL-1 β , IL-6, TNF-

α , IFN- γ) measures collected at baseline and year 1 of the study. Urine was collected monthly within the first year of the study for neopterin analysis.

2.3.4 Equipment and Procedure

2.3.4.1 Questionnaire

Testing took place at the Hearing and Balance Centre (HaBC) of the University of Southampton by A A-P, A S and R K. Participants were given a questionnaire to fill in (Appendix A) at baseline and year 3 visit. The questionnaire was split in four sections:

1. **Demographics:** demographic characteristics including age, gender and occupations, which are known to impact on hearing.
2. **Hearing:** this section explored individual hearing difficulties, if any. Questions included history of childhood ear infections, family history of hearing loss and noise exposure.
3. **Lifestyle:** lifestyle factors that influence hearing such as smoking were enquired about.
4. **Medical History:** this section enquired if subjects had common chronic diseases that are associated with greater hearing loss including diabetes and cardiovascular diseases.

As the questionnaire was only completed at 2 time points (baseline and year 3 visit), there was no attempt to document individual information on infections or illness during the study, but this is something that could be considered for future work.

2.3.4.2 Hearing assessment

Hearing was assessed using pure-tone audiometry (PTA) and transient otoacoustic emissions (TEOAE). Hearing measurements took place in a soundproof booth. The ambient noise in the booth, measured with a sound level meter was always below 35 dB(A), therefore in keeping with the relevant ISO requirements. Otoscopy was performed on each participant to exclude the presence of wax, and other ear abnormalities, including perforated tympanic membrane and middle ear infections, which could alter their audiometric thresholds. Subjects with occluding wax were requested to have it removed via their GP before testing, to eliminate any temporary conductive hearing loss caused by the occlusion.

Pure-tone audiometry testing was performed using a GSI G1 Clinical Audiometer, calibrated according to ISO-389-1: 2000 Standards. Tones of frequencies 0.5-8 kHz were presented through TDH-39 supra-aural earphones. A RadioEar B71 bone vibrator was used for measuring bone conduction thresholds. PTA was performed according to the British Society of Audiology (BSA) recommended procedure (BSA)³⁰⁶. PTA air conduction thresholds were measured at 0.25, 0.5, 1,

2, 3, 4, 6, and 8 kHz for both ears. Thresholds for bone conduction were determined at 0.5, 1, 2, 3 and 4 kHz. Thresholds were measured in 5dB intervals. The limit of the audiometer was 110 dB HL, when threshold was beyond this limit, it was assigned a threshold of 120 dB HL. Masking was appropriately applied where there was an asymmetry between ears, or an air-bone gap, in accordance with the BSA procedure. Pure-tone average threshold was calculated for the frequencies 0.5, 1, 2, and 4 kHz for each ear. Low frequency average (0.25, 0.5 and 1kHz) and high frequency average (4, 6, 8 kHz) were also calculated for each ear.

Measurement of TEOAE was performed using Otodynamics ILO 292 equipment and EZ-Screen software (Otodynamics, ILO V6 Module) connected to a laptop computer. Stimuli were transmitted to the ear via a standard adult probe-microphone system. TEOAE recordings were made at 1, 1.5, 2, 3 and 4 kHz using Quickscreen mode. The stimulus was a conventional non-linear click presented as a set of four clicks at a rate of 50 clicks/s, each set comprising one at a maximum of 90 dB peSPL and three at 80 dB peSPL.

2.3.4.3 Blood sampling

Under sterile conditions and using a non-touch procedure, venesection was performed by A A-P. Blood was taken from the median cephalic vein in the cubital fossa. Prior to this, the vein was identified and the skin area cleaned with alcohol wipe. The skin was allowed to air dry, then a venous blood sample was taken. Blood samples were collected into vacutainer EDTA bottles and serum bottles. Blood in the EDTA bottle was used to measure white blood cell count (WBC) immediately. Blood in the serum bottle was allowed to stand for 30-60 minutes in order for a clot to form. Separation of the clot was performed by centrifuging the sample at 2000rpm at a temperature of 4°C for 10 minutes. The supernatant serum obtained was pipetted into 500µL aliquots and stored at -80°C to be used to measure serum neopterin, IFN- γ , IL-1 β , TNF- α and IL-6 levels. Blood samples were taken at two time points during the study; at the start of the study and at the end of the first year.

2.3.4.4 Urine sampling

Participants gave morning urine samples once a month for 12 months. At the months 1 and 12 when blood samples had to be collected as well, participants brought in their urine samples to the centre. During the remaining months, participants posted their urine samples by first class mail, using urine collection tubes and pre-paid envelopes that were supplied to them. Urine samples received were centrifuged at 2000rpm at a temperature of 4°C for 10 minutes and stored at -20°C for analysis of neopterin and creatinine levels.

Chapter 2

Neopterin stability in urine has been shown to be fairly consistent at different ambient temperatures, so time of year when the sample is taken and transported shouldn't affect the sample²⁴⁷. The length of time between the sample being taken to being processed and stored at 4°C may affect the neopterin in the sample, therefore the subjects in the study were requested to send their samples promptly and were provided with prepaid first-class mail. However, it is impossible to say if any samples were delayed >24 hours, and subjects were not asked to document time between sample collection and posting. In future, it may be worth assessing this and if deemed to be an issue, it may be worth considering some form of refrigerated transport.

2.3.5 Measurement of inflammatory markers

2.3.5.1 White blood cell count

The amount of WBC in the blood was measured using an automated machine, HemoCue WBC and differential analyser. About 100µL of blood that had been previously collected in EDTA tubes was placed onto a microcuvette and inserted in the HemoCue analyser to give an automated WBC and differential reading. The differential count included neutrophils, lymphocytes, monocytes, eosinophils and basophils.

2.3.5.2 Serum cytokines

Cytokine levels have been known for their association with inflammaging. Some of the implicated cytokines that were measured to further investigate their role in inflammaging were IFN- γ , TNF- α , IL-1 β and IL-6.

Cytokine concentrations were measured using 96-well MSD Multi-spot Pro-inflammatory panel-1 kit. Testing of cytokines was performed only at one time point, at the start of the study. Samples were blinded to the investigator by relabelling performed by a person unrelated to the study.

Each serum sample was thawed on ice, centrifuged at 2000G for 4 minutes, diluted 2-fold with MSD diluent, and pipetted into randomly selected two adjacent wells on the ELISA plate. Wells contained pre-fixed capture antibodies. Samples were tested in duplicates to ensure repeatability. After incubation and washing stages, MSD detection antibody and then read buffer were added to sample solution. Calibrators and controls for each cytokine were processed the same way as samples. The concentrations of measured cytokines were read on an MSD plate reader according to the curve obtained from the calibrators.

2.3.5.3 Urinary neopterin to creatinine ratio (UNCR)

For the analysis of the data in this chapter, urine neopterin and creatinine concentrations were measured via Ultra performance liquid chromatography -Mass spectrometry (UPLC-MS) by C S. The investigator was provided with the results for all the analysed urine samples as a urinary neopterin to creatinine ratio (UNCR). All measurements were undertaken using ACQUITY UPC interfaced with a Waters Xevo triple quadrupole (TQD) mass spectrometer equipped with an electrospray ionization probe, column oven, and autosampler (Waters, Elstree Herts, UK). All samples were kept in the dark at 5°C. Separation at 24°C was achieved using a UPLC Fluoro-phenyl (1.7 μ m, 2.1 \times 100 mm) column fitted with its equivalent guard column (1.7 μ m, 2.1 \times 5mm, VanGuard) (Waters, Elstree Herts, UK). The primary mobile phase (A) was 0.2% formic acid and the co-solvent (B) consisted of 0.2% formic acid in acetonitrile. Total run time was 8 minutes and included a 2.5 minute gradient from 99% (A) to 93.5% (A) followed by a 2 minute wash in 100% (B) and a 2.5 minute re-equilibration at 99%A. Injection volume was set at 10 μ l for neopterin analysis and 5 μ l for creatinine analysis.

After separation, the compounds were monitored in scheduled multiple-reaction monitoring (MRM) mode with positive electrospray ionization. Optimised flow injection parameters consisted of cone energy of 30V and collision energy of 20V. The MRM transitions for creatinine and creatinine-D3 were 114.1 > 44.1 and 117.1 > 47.1 respectively and for D-erythro-neopterin and D-erythro-neopterin-13C5 were 254.1 > 206.1 and 259.1 > 210.1 respectively.

Urine had been stored at -20°C, so prior to analysis the samples were thawed and then diluted 1:10 or 1:500 for neopterin and creatinine respectively. Each urine sample was measured in duplicate and the result averaged. Urinary creatinine and neopterin concentrations were determined based on the calibration curve with neopterin and creatinine expressed as μ g/L and mg/dL respectively. UNCR was calculated for each sample and expressed in μ mol/mol.

This UPLC-MS method has demonstrated LOD for neopterin of 0.3 μ g/L, an interassay coefficient of variation of 6.34% and intraassay coefficient of variation of 2.77%. For any future work it would be recommended to have a single standard reference sample that was measured by UPLC-MS and any other analytical methods, to ensure no variability in result.

2.3.6 Ethical approval

The study was ethically approved by the National Research Ethics Service (REC: 13/SC/0507) and the University of Southampton Ethics and Research Governance (reference number: 7923).

2.3.7 Statistical analysis

Data was compiled using Microsoft Excel. Statistical analysis was performed using GraphPad Prism 8 and IBM SPSS Statistics 26. Shapiro-Wilk's test of normality was applied to the data to assess normal distribution in deciding whether to utilise parametric or non-parametric statistics (see Appendix C). The data was sorted with pre-planned stratification process that was used prior to analysis, see section 2.4.5.

Analysis of variance (ANOVA) measures were used to compare groups with $p < 0.05$ being considered significant. A one-way ANOVA was used to compare the mean neopterin concentration of each neopterin stratified group, with a Tukey post-hoc multiple comparisons test. A one-way ANOVA was also used to compare WBC and WBC differentials between neopterin stratified groups, cytokine levels between neopterin stratified groups, and hearing averages (Pure tone average, low-frequency average, high-frequency average) between neopterin stratified groups. A Welch ANOVA was used to assess significance for change in hearing level from baseline to end of study for each of the hearing averages, with a post-hoc Dunnett T3 multiple comparisons test. A one-way repeated measures ANOVA was used to compare hearing averages at baseline, year 1 and year 3 (study end). Two-way repeat ANOVA was used with hearing frequency and time as within subject variables and TEOAE SNR level as dependent variable. Another was used with neopterin volatility groups as between subject variable, frequency as within subject variable and SNR as dependent variable. Pearson product-moment correlations were used to consider relationships between variables. Factoring for age, all variables of hearing loss and inflammation were compared.

Study power was calculated based an average change in hearing threshold of study group to be greater than $10\text{dbHL} \pm 5\text{ dBHL}$. Prior to the start of the study sample size was determined to be 42 for 90% power with an α of 0.05.

2.4 Results

2.4.1 Subject Characteristics

There were 45 adults who completed the study from baseline until year 3, aged 65-75 years at the start, and consisting of 11 males and 34 females, living in and around the Southampton area. Originally 61 adults were recruited into the study but there was 26% attrition throughout the duration. Some interesting demographics and clinical information are shown in Table 2.2.

Table 2.2 Table of subject demographics and clinical characteristics from beginning to end of study

Information from study questionnaire completed at baseline and end of study.

Determination of hearing loss is based on pure-tone average threshold calculated from pure tone audiogram.

Characteristic	Baseline	Study End
	Number (percentage)	Number (percentage)
General		
Age	68.98 years	72.49 years
Male	11 (24.4%)	11 (24.4%)
Female	34 (75.6%)	34 (75.6%)
Health		
Diabetes Dx	1 (2.2%)	2 (4.4%)
Stroke	0	1 (2.2%)
Hypertension Dx	17 (37.8%)	21 (46.7%)
Heart disease Dx	6 (13.3%)	7 (15.6%)
Statins Prescribed	16 (35.6%)	16 (35.6%)
One or more chronic disease Dx	18 (40.0%)	22 (48.9%)
Hearing		
Difficulty hearing speech in quiet	11 (24.4%)	15 (33.3%)
Difficulty hearing speech in noise	37 (82.2%)	37 (82.2%)
Prescribed a hearing aid	9 (20%)	13 (28.9%)
Number with normal hearing (≤ 20 dB HL)	11 (24.4%)	5 (11.1%)
Number with hearing loss (>21 - 40dB HL)	34 (75.6%)	40 (88.9%)

The infographic in Figure 2.3 depicts visually some of the subject characteristics established via the questionnaire, a table of results can be found in Appendix B. Seventeen subjects had been a

Chapter 2

smoker at some point in their lives, however eight of these had given up smoking by the age of 40 years. Four common age-related chronic diseases were enquired about in the questionnaire; diabetes, stroke and cardiovascular diseases (including hypertension and coronary artery disease). Hypertension was the most common chronic disease affecting 37.8% of the subjects, 13.3% had other cardiac disease, 2.2% had diabetes and none of the subjects had had a stroke. 35.6% of subjects were being prescribed statins.

The majority of subjects (75.6%) had no difficulty hearing speech in a quiet environment, however, as typically seen in sensorineural hearing loss, 82.2% had difficulty hearing speech in a noisy environment. Ten of the 45 subjects had a history of noise exposure, 9 had been prescribed hearing aids and 15 reported tinnitus. 62.2% of the subjects reported no history of repeated ear infections and one-third of the subjects had a positive family history of hearing loss before the age of 60 years.

The same questionnaire was repeated at the end of the study (year 3) and slightly different answers were recorded. Four individuals had been diagnosed with a co-occurring chronic disease since the baseline questionnaire was completed including hypertension, heart disease and diabetes. Since the baseline questionnaire, one individual had had a stroke.

By study end, the majority of subjects (64.4%) still reported having no difficulty hearing speech in quiet but there was an increase in the numbers having some difficulty. The report of difficulty hearing speech in noise remained the same. Four extra people had been prescribed a hearing aid but the number of individuals reporting tinnitus remained the same.

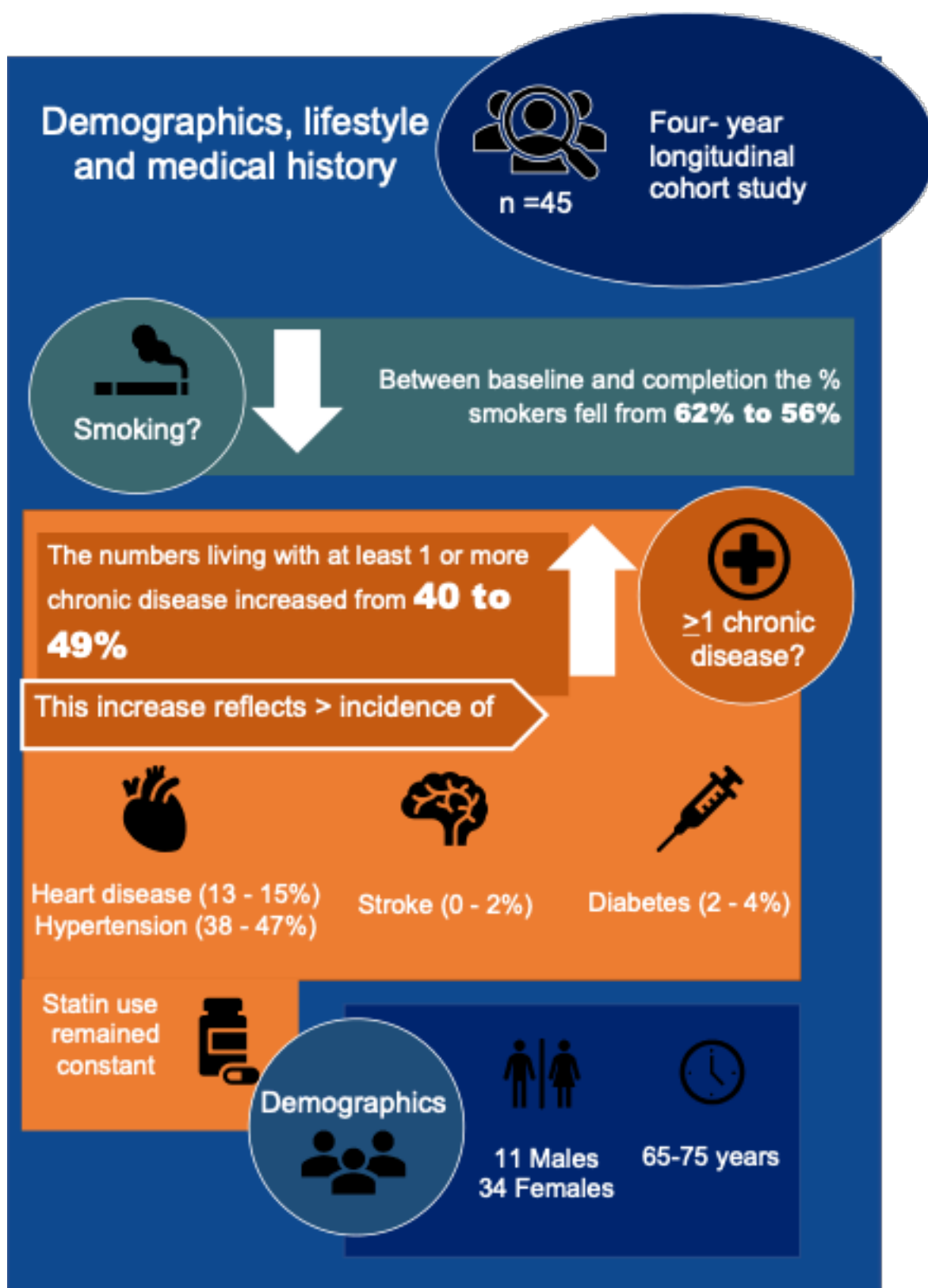


Figure 2.3 Infographic depicting InflammHear questionnaire responses: demographics, risk factors and age-related conditions.

Full table of questionnaire results can be found in appendix B.

2.4.2 Hearing changes from baseline to study end

2.4.2.1 Pure Tone Audiometry

Every subject had their hearing thresholds assessed using PTA at three time points, Baseline, Year 1 and Year 3 (Figure 2.4). The general trend of hearing loss is a bilateral high-frequency sloping, which is the expected presentation of hearing loss associated with ageing (presbycusis)^{80,202}. Conventionally, hearing thresholds ≤ 20 dB HL are said to be within normal limits³⁰⁶. The greatest change in hearing can be seen at the higher frequencies, which is again consistent with the deterioration expected with an age-related hearing loss.

From the beginning of the study to its end, the percentage of individuals with normal hearing dropped from 24.4% to 11.1%, with a 6.7% increase in the number of individuals with both mild and moderate losses (Table 2.3).

Table 2.3 Number of subjects within each classification of hearing loss at baseline and year 3 (study end).

Based on worst ear pure-tone average (0.25-8kHz) (N=45).

Degree of hearing loss	Baseline	Study End
	Number (Percentage %)	Number (Percentage %)
Normal Hearing (≤ 20 dB HL)	11 (24.4 %)	5 (11.1%)
Mild loss (21-40dB HL)	24 (53.3%)	27 (60.0%)
Moderate loss (41-70 dB HL)	10 (22.2%)	13 (28.9%)
Severe loss (71-90 dB HL)	0	0

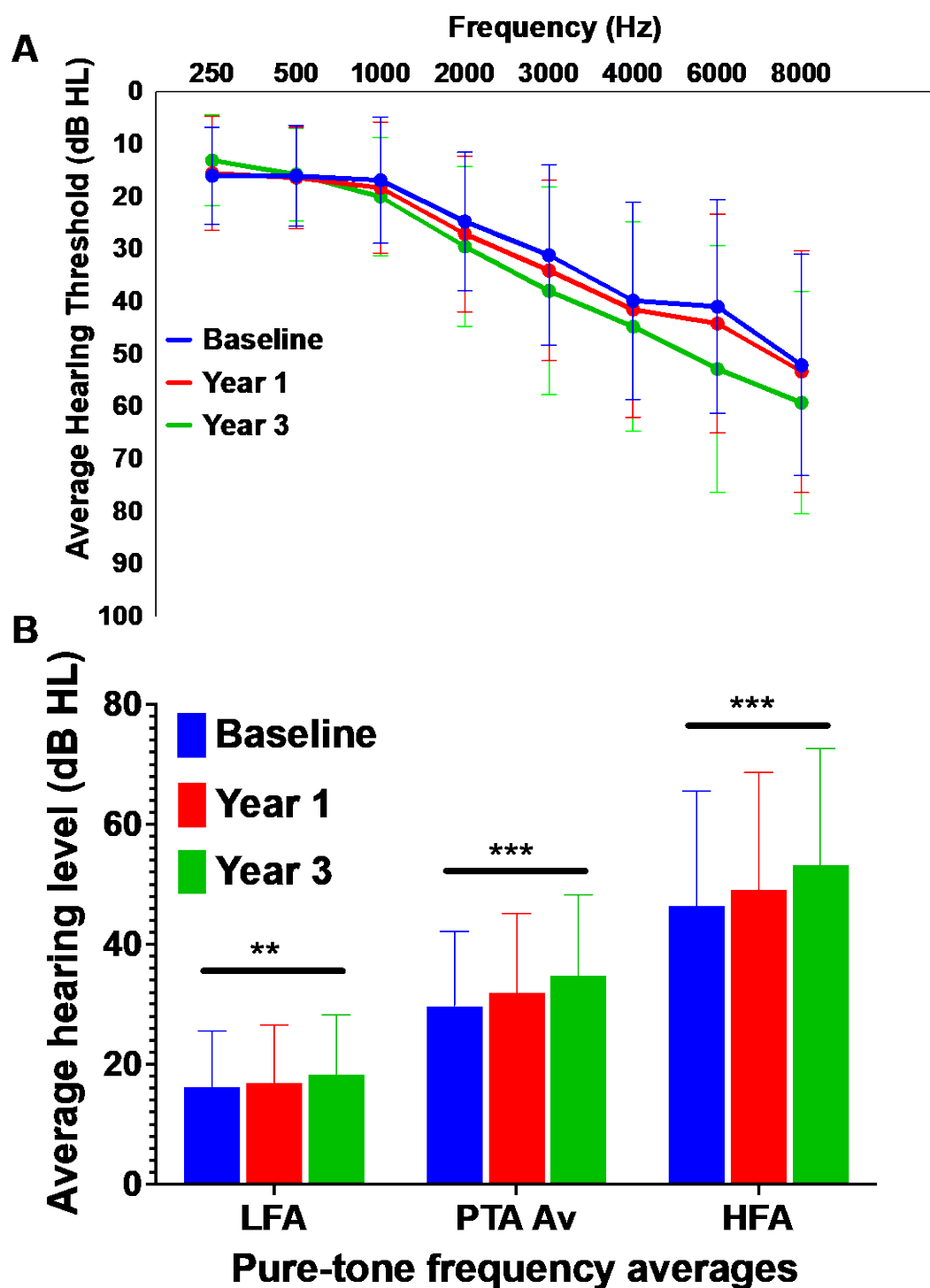


Figure 2.4 Average pure-tone audiometric thresholds for all subjects.

Blue is baseline, red is year 1 and green is year 3. Worst ear air conduction thresholds used (N=45). Error bars represent standard deviation. A) Thresholds from the worse hearing ear by air conduction across frequencies (0.25-8kHz) (N=45). Thresholds at baseline, end of year 1 and end of year 3 of the study. A deterioration in high-frequency hearing can be seen across the years. Error bars represent standard

deviation. B) Average audiometric thresholds for low frequency (LFA), pure-tone (PTA Av) and high frequency (HFA) averages.

There are three widely used audiometric averages used to describe PTA data. Pure-tone average threshold (average threshold across 0.5-4kHz), low-frequency average threshold (average threshold across 0.25-1kHz) and high-frequency average threshold (averaged threshold across 4-8kHz). These averages were calculated for the poorer hearing ear (determined by PTA Average) and used for analysis.

A one-way repeated measures ANOVA was conducted to compare the pure-tone average threshold at baseline, year 1 and year 3 (study end) (Figure 2.4B). There was a significant effect for time, Wilks' Lambda = 0.39, $F(2, 43) = 34.36$, $p < 0.001$, multivariate partial eta squared = 0.62 suggesting a very large effect size (Cohen 1988)³⁰⁷. This analysis was repeated for low-frequency average and there was a significant effect for time, Wilks' Lambda = 0.77, $F(2, 43) = 6.32$, $p = 0.004$, multivariate partial eta squared = 0.23. The same analysis for high-frequency average produced another significant time effect, Wilks' Lambda = 0.40, $F(2, 43) = 32.08$, $p < 0.001$, multivariate partial eta squared = 0.60.

Both age and sex are thought to be important variables for risk of hearing loss, with older males being the most likely to have poorer hearing. In this study, the relationship between age/sex and degree of hearing loss was investigated using Pearson product-moment correlation coefficient. No correlation was found between sex and pure-tone average threshold either at the start $r = -0.176$, $n = 45$, $p = 0.248$, or end of the study $r = -0.124$, $n = 45$, $p = 0.415$. When looking at the age of the subject at the start of the study, there was a strong, positive correlation between age and pure-tone average thresholds, $r = 0.533$, $n = 45$, $p < 0.001$.

2.4.2.2 Transient Otoacoustic Emissions (TEOAEs)

Otoacoustic emission (OAE) responses are measured against noise floor, therefore the response is a signal to noise ratio (SNR). There are recommended criteria to be met for a response to be accepted as a true one. Different studies have set-out different criteria for an acceptable SNR response, including $SNR \geq 6\text{dB}$ ³⁰⁸, 3dB ³⁰⁹ and 0dB ³¹⁰. The conservative approach would be to use a $SNR \geq 6\text{dB}$ for a true OAE response, however given the high proportion of hearing loss within the cohort, this stringent criterion would disqualify the majority of the responses and could even eliminate some true responses. On the other hand, accepting all responses as true responses could introduce a large number of false positive responses into the data and reduce the effect of the results. Therefore, a $SNR \geq 3\text{dB}$ was chosen for this study. This criterion has been found to be

robust in determining a true OAE response^{309,311}. In addition, when considering the reproducibility of a response, 75% was accepted, to ensure the response was repeatable. A TEOAE reproducibility range between 70% and 90% has been demonstrated in the literature^{308,312}.

Table 2.4 Percentage of ears with positive OAE responses meeting criteria (1, 1.4, 2, 3, 4 kHz, baseline and year3).

Criteria of response was $\text{SNR} \geq 3$ dB and reproducibility $\geq 75\%$.

Number (percentage) of ears with TEOAE responses					
Frequencies (kHz)	1	1.5	2	3	4
Baseline	53(58.8)	63(70)	61(61.7)	53(58.8)	38(42.2)
Year 1	38(42.2)	43(47.7)	44(48.8)	36(40.0)	29(32.2)
Year 3	31(34.4)	45(50.0)	50(55.5)	42(46.6)	32(35.5)

Table 2.4 shows for each frequency, the percentage of ears that had a response meeting the criteria of $\text{SNR} \geq 3$ dB and reproducibility $\geq 75\%$, at baseline, year 1 and year 3. However, with these criteria, just 29 ears had TEOAE responses for all frequencies at baseline, 24 ears at Year 1 and 11 ears at Year 3. High SNR levels of OAE indicate good outer-hair cell function. When TEOAE are used as a screening protocol, clear responses at 3 out of 5 frequencies is accepted as that ear having a response. When considering the data in this way, 45 ears had a response at baseline that remained at Year 3. Two-way repeat ANOVA was performed with frequency and time as within subject variables and TEOAE SNR level as dependent variable. Results from the ANOVA showed a significant difference between TEOAE levels at baseline and after three years, $F(1,440) = 54.51$, $p < 0.0001$ (Figure 2.5). A post-hoc Sidak test found significant differences at frequencies 1 kHz ($p < 0.0001$), 1.5 kHz ($p < 0.0001$), and 2 kHz ($p = 0.0482$). There was a significant difference between the frequencies $F(4,440) = 23.78$, $p < 0.0001$ and a significant interaction between frequency and time $F(4,440) = 3.199$, $p = 0.0132$.

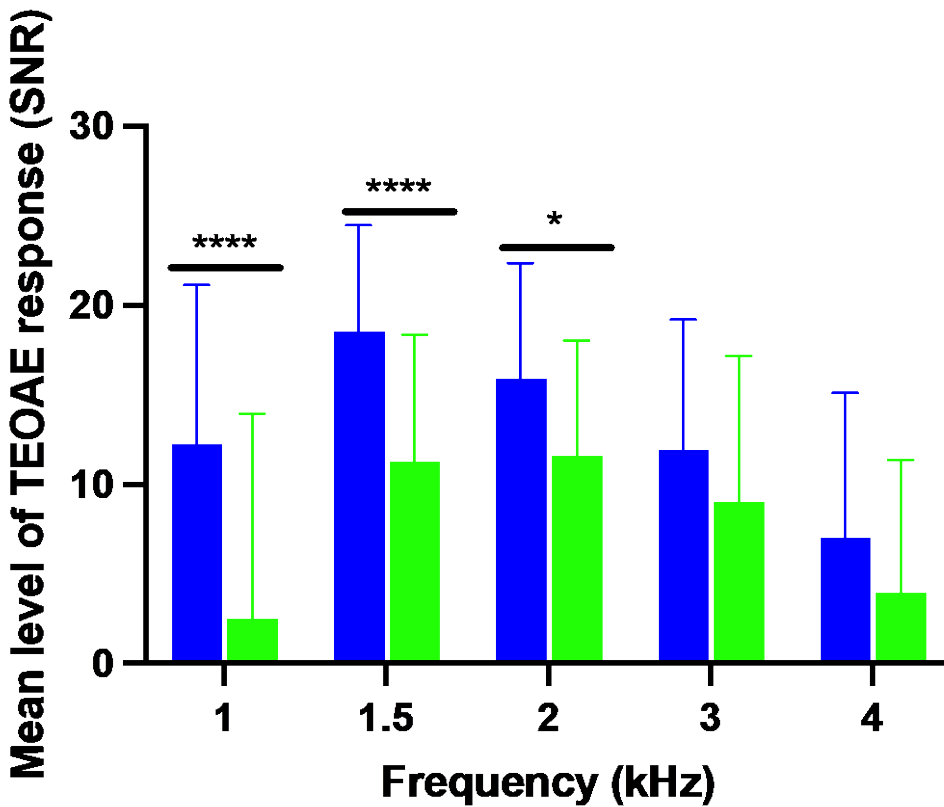


Figure 2.5 TEOAE responses.

TEOAE for ears that have passed a screening at baseline (blue) and year 3 (green) for frequencies 1-4kHz. Error bars represent SD. N= 45 ears.

2.4.3 Traditional Blood Markers

Blood samples were collected from individuals at two time points (Baseline and after 12 months) and traditional markers were measured, particularly those that have been used in other studies as determinators of inflammation. The measures included white blood cell count (WBC), monocyte, lymphocyte and neutrophil cell counts measured at baseline and after one year, as well as cytokine measures, TNF- α , IFN- γ , IL-6 and IL-1 β measured at baseline. Figure 2.6 shows that mean cell counts between the two time points are not significantly different, however, for some individuals a significant change in measure has occurred which could be due to an acute inflammatory event at either time-point, thus highlighting the need for longitudinal monitoring of individuals to negate false positive for inflammaging by taking single time points. Figure 2.7 depicts the cytokine measurements which were only measured at baseline. Variability in cytokine concentration can be seen, but this data would not be enough alone to conclude whether an increased concentration in a cytokine marker is due to inflammaging or an acute inflammatory event at the time of sampling.

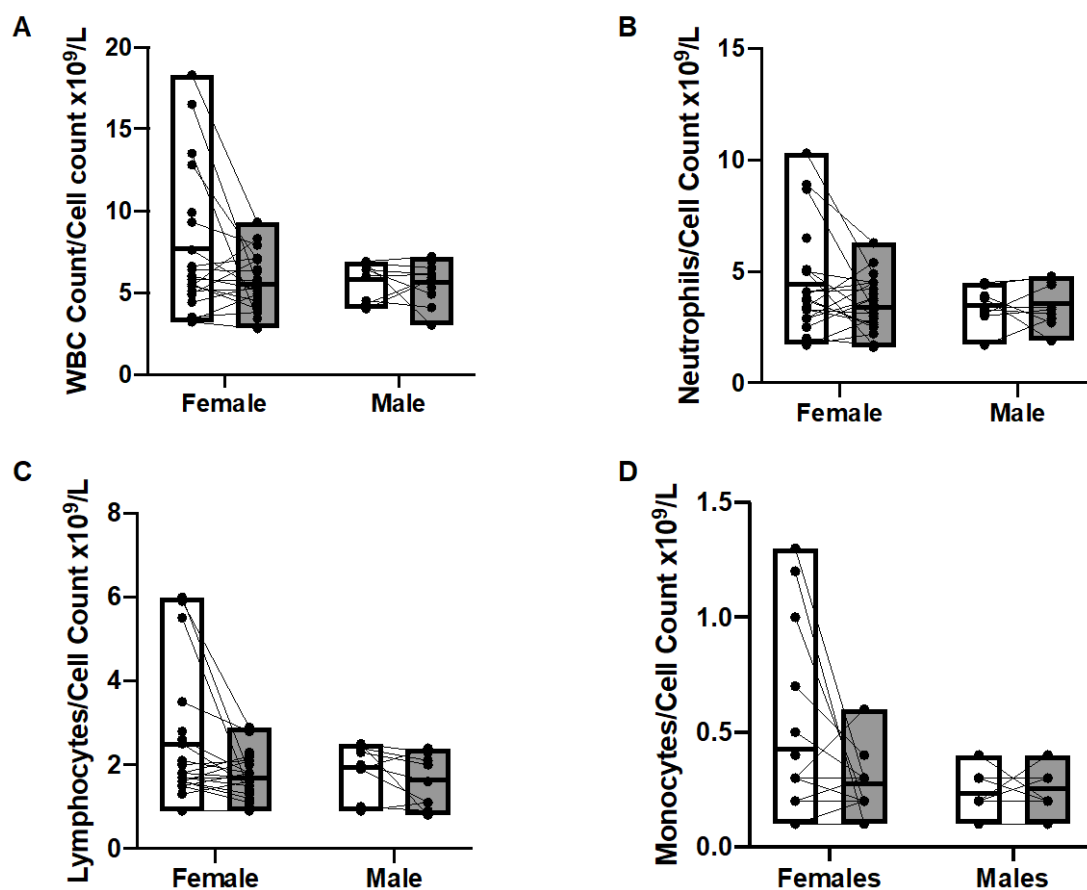


Figure 2.6 Measurements of blood markers.

White is baseline data and dark grey year 1 data. Data split by sex for each marker to demonstrate no significant effect on marker due to sex. Box plot depicts mean with upper and lower limit, and symbols are the individuals with lines to show an individual's change in measurement between the two time points. A) White blood cell count. B) Neutrophil count. C) Lymphocyte count. D) Monocyte count.

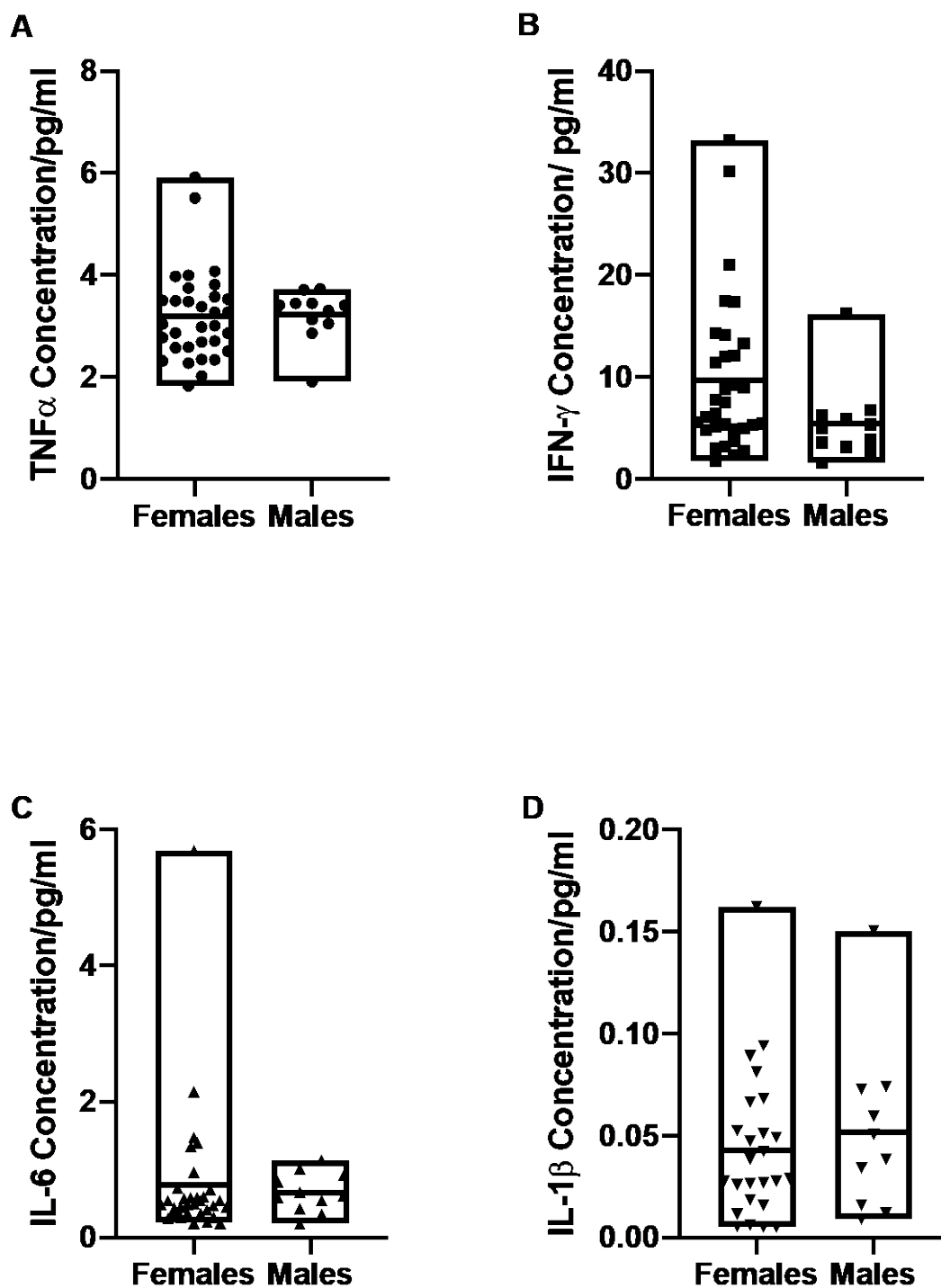


Figure 2.7 Baseline cytokine concentrations.

Data split by sex for each marker to demonstrate no significant sex effect. Box plot depicts mean with upper and lower limit, and symbols are the individual values. A) TNF α concentration. B) Interferon - γ concentration. C) Interleukin- 6 concentration. D) Interleukin- 1 β concentration.

2.4.4 Monthly Urinary Neopterin to Creatinine Ratio (UNCR) for each subject

Taking multiple measurements of neopterin for each individual over 12 months rather than measuring a marker at a single time point, gives rise to a variable that more accurately conveys an individual's variation in inflammatory state and therefore provides an inflammatory profile. We used an upper limit of normal of 251 $\mu\text{mol/mol}$ creatinine based on normative values in the literature^{46,47}. The month-by-month UNCR for each participant in the study are shown in figure 2.8-2.10, the fluctuation in concentration is clear to see. It is also apparent that some individuals spend a considerable time above the normal limit, whilst some others never fluctuate above it, and others are somewhere in between. These variations above and below a normal value that are evident in this longitudinal data, would be missed if measurement was only taken at a single timepoint. For that reason, this research focusses on longitudinal data collected monthly over 12 months, and uses a measure of how often individuals fluctuate above the normal value as a biomarker of immune activation.

Chapter 2

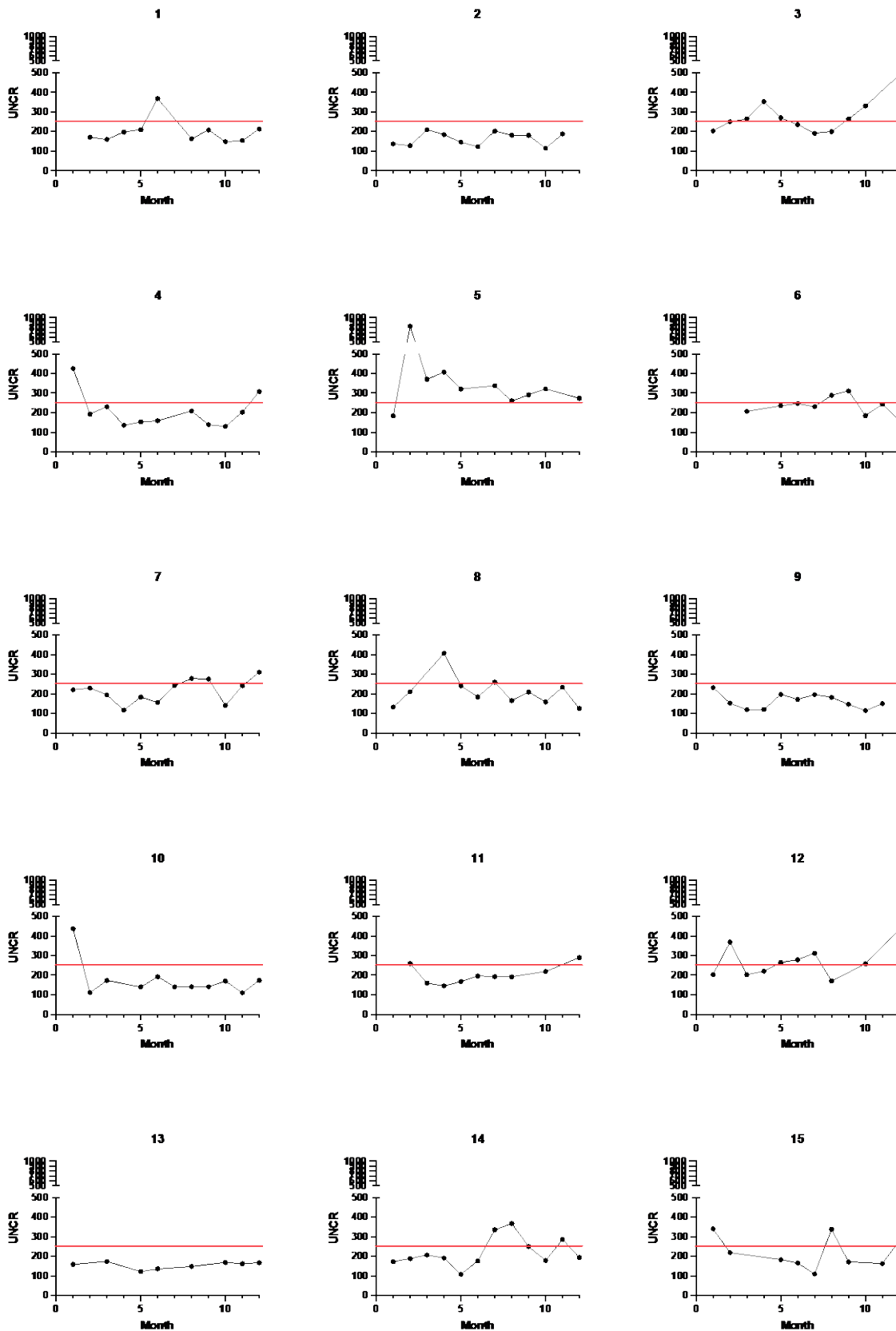


Figure 2.8 Variations in monthly UNCR measurement for participants 1-15 of study

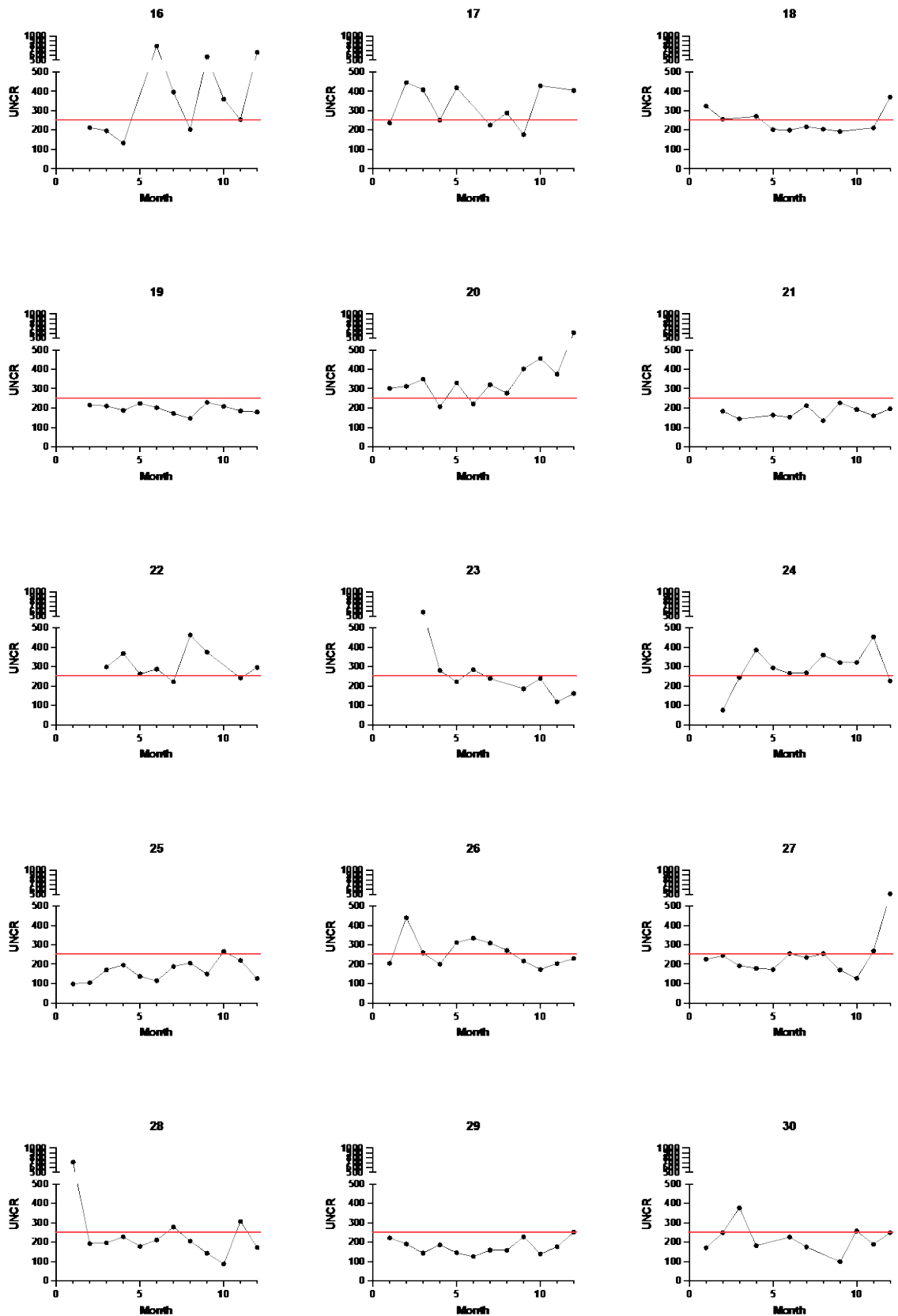


Figure 2.9 Variations in monthly UNCR measurement for participants 16-30 of study

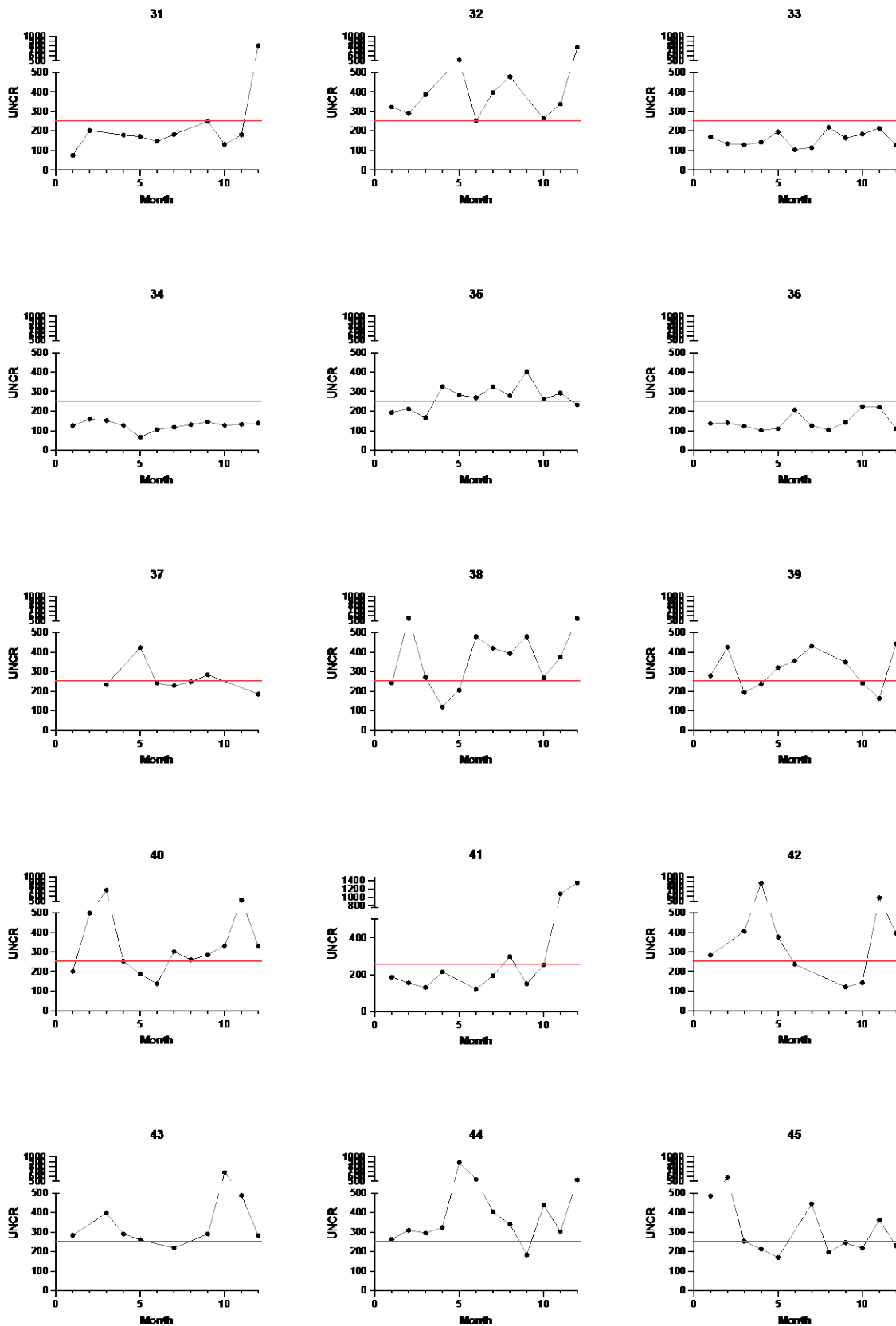


Figure 2.10 Variations in monthly UNCR measurement for participants 31-45 of study

2.4.5 Stratification Process based on UNCR longitudinal data

One of the unique and novel features of this study is the multiple measurements of neopterin for each individual over a 12-month period. Other studies that have measured at a single time point or several years apart⁵⁻⁷ have not needed a variable that encompasses multiple timepoints.

Therefore, rather than consider a mean or median value, neopterin volatility is a useful variable to encompass an individual's variation in inflammatory baseline and therefore report an overall inflammatory profile. Neopterin volatility is defined as a ratio of the number of months neopterin level exceeded normal limits, to the total number of months samples were obtained.

$$\text{Neopterin volatility} = \frac{\text{Number of months neopterin level exceeded normal limit}}{\text{Total number of months neopterin was measured}} \times 100$$

Neopterin levels rise prior to clinical symptoms of infection, therefore neopterin measurement is sensitive to subclinical infections and susceptibility to infection is a feature of inflammaging. As an example, some work looking at the risk and progression of Alzheimer's disease has shown that repeated inflammatory challenges, indicated by fluctuations in inflammatory markers, exacerbates progression of the disease³¹³ and therefore can be used as a measure of inflammaging.

The literature reports normative values for urine neopterin depending on age and sex^{13,46,47} and these values are shown in table 2.1. For men over 65 years, the mean is 133 $\mu\text{mol/mol}$ with an upper limit of normal (97.5th percentile) reported as 229 $\mu\text{mol/mol}$. For women, the mean is 151 $\mu\text{mol/mol}$ with an upper limit of normal (97.5th percentile) noted as 251 $\mu\text{mol/mol}$. Therefore, for this work a cut-off value was set at 251 $\mu\text{mol/mol}$ Creatinine as the most conservative upper limit of normal for our age group.

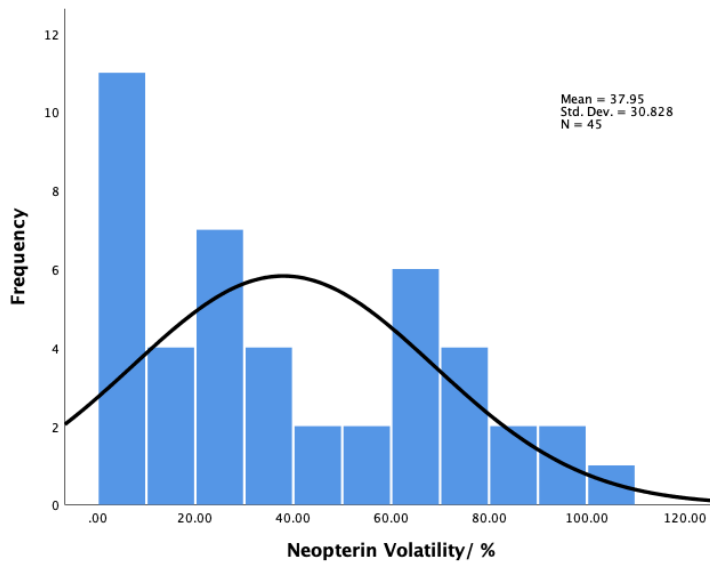


Figure 2.11 Histogram of neopterin volatility distribution.

Demonstrating the large proportion of subjects with 0% neopterin volatility and also a large proportion of subjects with a neopterin volatility over 50%.

Based on individual neopterin volatility levels, the cohort was stratified into groups. Stratifying the cohort into groups according to the percentage of time their neopterin was raised provides groups with the most clinical meaning.

Participants were assigned to groups according to:

1. neopterin levels are **never raised** above the limit ($251\mu\text{/mol}$ creatinine) (8)
2. neopterin levels **raised** $\leq 25\%$ of the time (13)
3. neopterin levels **raised 25-50%** of the time (8)
4. neopterin levels are **chronically raised i.e. >50%** of the time (16)

These groups were deemed clinically meaningful, because an individual who never had a raised level of neopterin, can be considered to be very 'healthy', whereas individuals whose neopterin was raised occasionally could be considered within the 'normal response range', those with raised levels often are perhaps leaning towards the 'unhealthy', and those individuals who had raised neopterin in more than half their samples, could be classified as chronically inflamed. Another study which has investigated the importance of longitudinal monitoring of UNCR over single time point measurement, has shown that UNCR is consistently higher in patients with relapsing-remitting multiple sclerosis, a well characterised inflammatory condition²⁷².

This stratification method results in subsets with uneven numbers in each group which is not ideal for making statistical comparisons between groups, however it considers and stratifies the cohort on the basis of the clinical variation between individuals which is the premise of the study. An alternate way of stratifying the cohort is to make groups with equal numbers of subjects, for example 3 groups (tertiles) as used in the MRC study of Verschuur et al.⁶. In this study, that would make the following groups: Low ($0 \leq 18.18$ % raised), moderate (18.19-54.55 % raised), and high (≥ 54.56 % raised). As seen in figure 2.11, a histogram of distribution of neopterin volatility scores, shows a multi-modal distribution, with a peak at 0% volatility, a second peak at 20% and then at 60-70%. There are a large proportion of subjects with a neopterin volatility of 0%, meaning their neopterin level was never raised above the cut-off value. At the other end of the scale, there are a few individuals whose neopterin volatility is considerably higher than the mean of 37.95%. Splitting across tertiles would lose the clinical nuances that this data is showing at the two extremes. For the purpose of this study, the clinical meaning of the results is of most interest, and equally due to the small sample size and power, statistical conclusions would be tentative anyway.

2.4.6 Clinical characteristics of neopterin stratified groups

With the individuals stratified into the 4 groups, some of the clinical characteristic data of each group have been detailed in table 2.5 and shown later in figure 2.12 and 2.13.

Chapter 2

Table 2.5 Characteristic data from the four stratified groups, never raised, occasionally raised, often raised and considerably raised.

Individuals were stratified into these groups by their neopterin volatility- the number of months out of 12 that their neopterin level was raised about a normal value of 251 μ mol/mol creatinine.

	Never Raised N=8	Occasionally Raised N=13	Often Raised N=8	Considerably Raised N=16
Age (Mean)	68.6	68.6	68.9	69.5
Female (% of group)	37.5	84.6	75	87.5
Neopterin (Mean)	160.8	208.1	271.0	336.6
Individuals with >1 comorbidity (% of group) at Baseline	2 (25%)	4 (31%)	3 (38%)	9 (56%)
Baseline Puretone average hearing level (mean)	31.2 dB(HL)	27.5 dB(HL)	31.8 dB(HL)	29.8 dB(HL)
Study End Puretone average hearing level (mean)	33.52 dB(HL)	32.28 dB(HL)	37.7 dB(HL)	35.9 dB(HL)

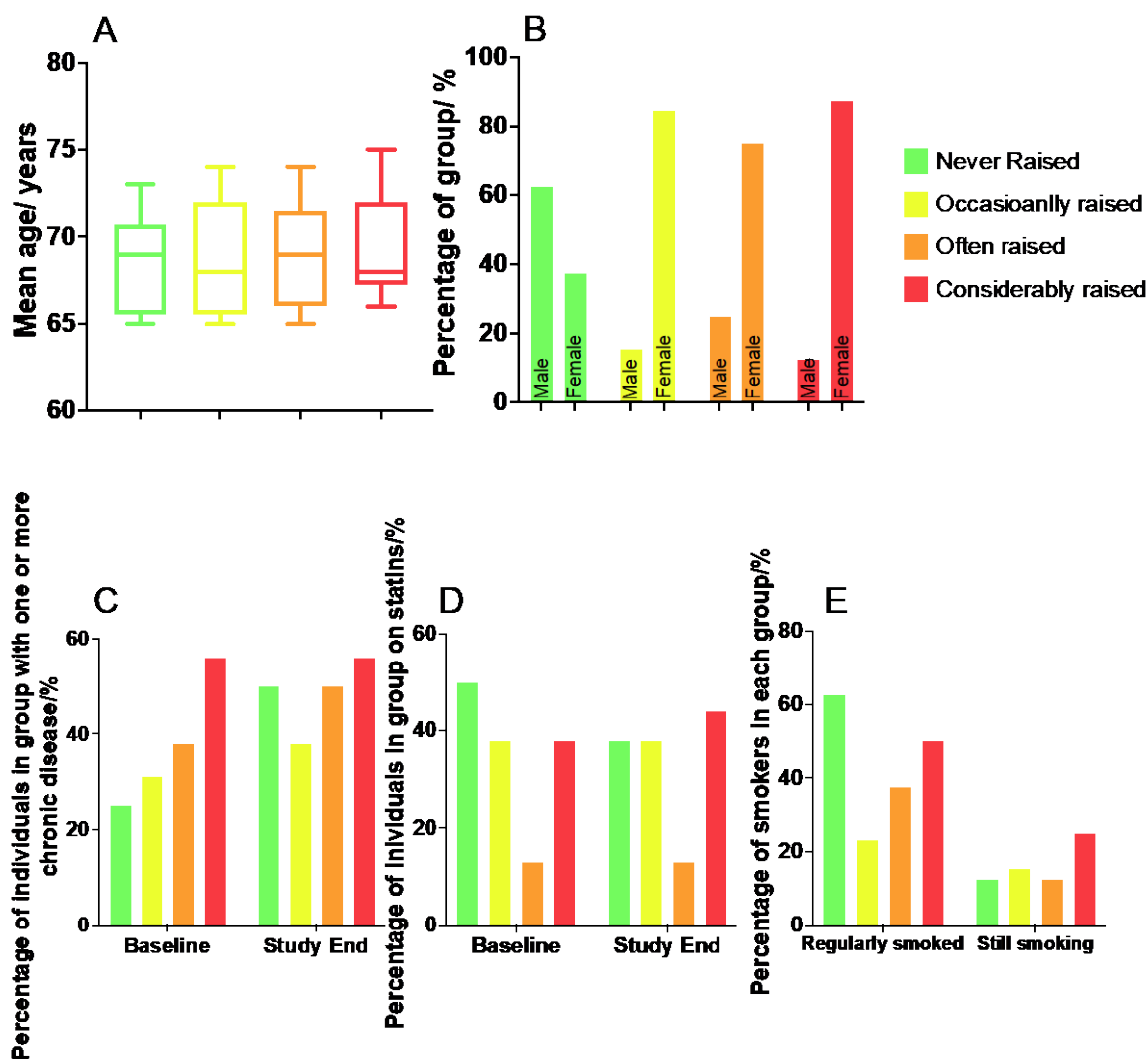


Figure 2.12 Neopterin volatility groups, clinical characteristics and age-related risk factors.

Green is never raised, yellow occasionally raised, orange often raised and red considerably raised. Only data for those who completed the whole study is included

A) Average age in years of participants in each of the neopterin volatility groups, there is no significant difference in age between the groups. B) Percentage of male/female within each neopterin volatility group, except the never raised group there are considerably more females in each group than males.

C) Percentage of individuals within each group who are diagnosed with one or more chronic disease (cardiovascular disease and type 2 diabetes), those in the considerably raised group have 2.2x greater risk of having a co-occurring age-related condition than those in the never raised group at the study start. By the end of the study, a general increase in diagnosis of co-occurring diseases across all groups is observed. D) Percentage of smokers in each of the neopterin volatility groups that reported having regularly smoked and those still smoking at the time of the study. 25% of those in the considerably raised group at the time of the study were smokers,

with smoking being a pro-inflammatory factor. E) Percentage of individuals within each neopterin volatility group who are prescribed statins. At baseline, 50% of the never raised group reported being prescribed statins which have anti-inflammatory properties, although this association is not consistent.

2.4.7 Inflammatory marker levels of stratified groups

Mean neopterin was calculated for each individual as an average (mean) of their monthly urinary neopterin to creatinine ratios. Those in the never-raised group had a mean urine neopterin level over 12 months of 160.8 $\mu\text{mol/mol}$ creatinine (SD = 20.47). Subjects within the occasionally-raised group had a mean neopterin level of 208.1 $\mu\text{mol/mol}$ creatinine (SD = 23.92). The individuals in the often-raised group had a mean neopterin concentration of 271 $\mu\text{mol/mol}$ creatinine (SD= 50.09). Subjects within the considerably raised group had a mean level of 336.6 $\mu\text{mol/mol}$ creatinine (SD = 43.98). A one-way ANOVA demonstrates a significant difference between the mean neopterin concentration for each group $F(3, 41) = 50.46, p < 0.0001$. The effect size, calculated using eta-squared, was 0.8 which suggests a very large effect size (Cohen 1988). A Tukey post-hoc, multiple comparisons test revealed a significant difference between the mean of each of the groups when compared to each other at the $p < 0.05$ level (Figure 2.13A). There is no significant difference between the mean age of individuals within each group, therefore the increase in mean neopterin concentration between groups is independent of increasing age (Figure 2.12A). When looking at the male/female ratio of each group, it is difficult to draw any firm conclusion as there were considerably more female subjects than males in the study, however results would suggest that the increase in mean neopterin concentration observed between groups is not due to sex (Figure 2.12B). Mean urine neopterin level for males was 214.78 $\mu\text{mol/mol}$ creatinine and for females was 261.86 $\mu\text{mol/mol}$ creatinine, however females are known to have higher neopterin levels than men and this is well documented in the literature⁴⁷.

A one-way ANOVA found no significant difference in WBC or WBC differentials, between stratified groups based on neopterin volatility (WBC $F(3, 41) = 0.4066, p = 0.7490$, Neutrophils $F(3, 41) = 0.3566, p = 0.7846$, lymphocytes $F(3, 41) = 0.4734, p = 0.7025$, monocytes $F(3, 41) = 0.7576, p = 0.5244$) (Figure 2.13B). Similarly, cytokine levels in the neopterin volatility stratified groups showed no between group significance (TNF- α $F(3, 39) = 0.2072, p = 0.8908$, IFN- γ $F(3, 39) = 0.2472, p = 0.8628$, IL-6 $F(3, 39) = 0.8566, p = 0.4717$, IL-1 β $F(3, 39) = 0.2269, p = 0.8771$) (Figure 2.13C). Cytokine measurements were not made for two subjects. As these markers were all measured at a single timepoint only, in a similar way to other research in the area, individual fluctuations are not taken into account and therefore it is no surprise that no significant trend is observed. The neopterin

data collected over a 12-month period however, does show a significant difference between groups.

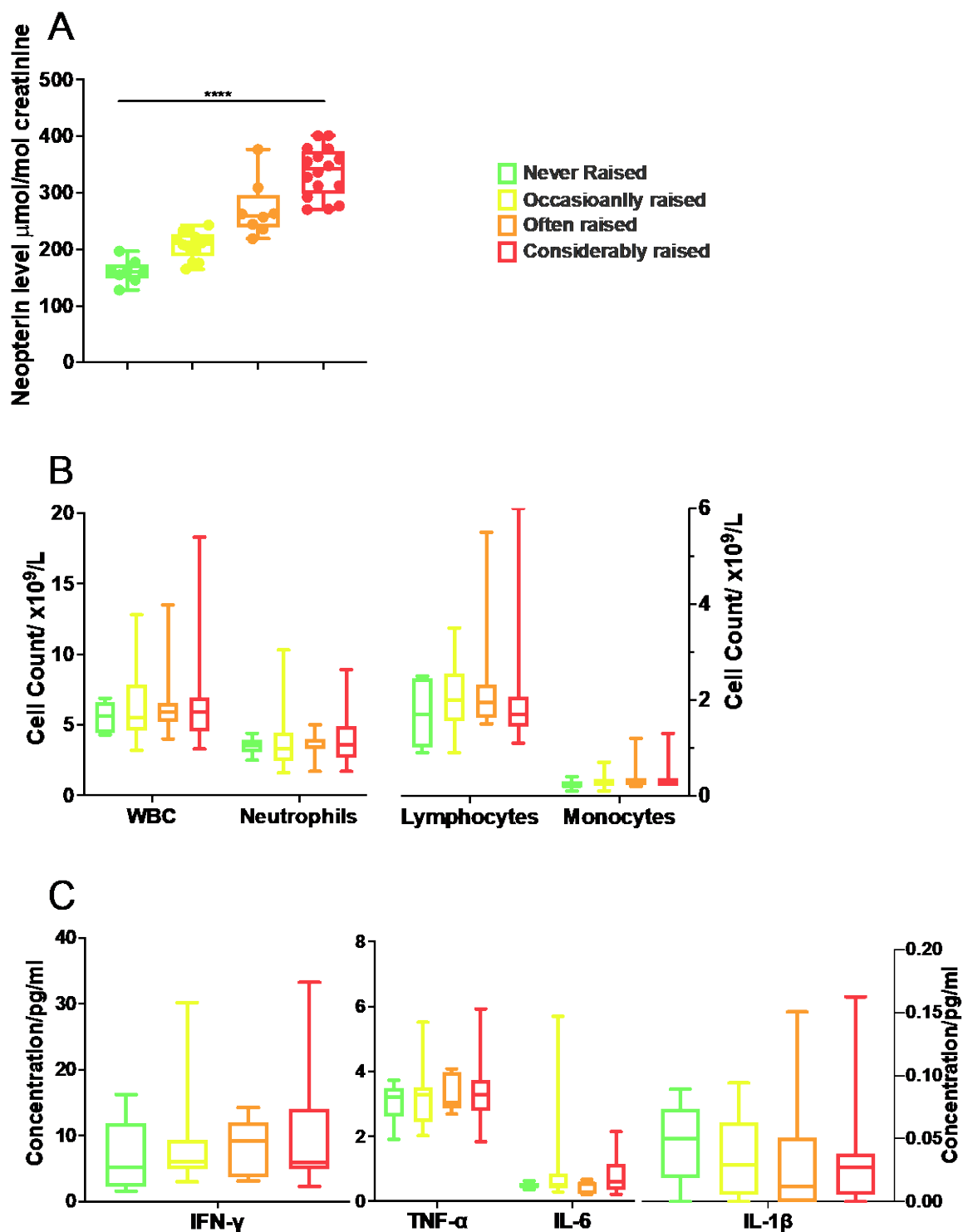


Figure 2.13 Characteristics of the neopterin volatility stratified groups.

Green is never raised, yellow occasionally raised, orange often raised and red considerably raised. A) Average urine neopterin level for each neopterin volatility group, the difference between groups is significant at the $p < 0.0001$ level. B) Average WBC, neutrophil count, lymphocyte count and monocyte count for each neopterin

volatility group, one-way ANOVA's showed no significant difference between groups for any of these markers. C) Average levels of cytokines TNF- α , IFN- γ , IL-6 and IL-1 β for each neopterin volatility group, one-way ANOVA's showed no significant difference between groups for any of these markers.

2.4.8 Neopterin stratified groups and age-related disease/risk factors

In the questionnaire, the cohort were asked about some co-occurring chronic diseases which are known risk factors for hearing loss and considered to be age-related conditions. These were cardiovascular disease (hypertension, valvular heart disease or coronary artery disease) and type 2 diabetes. It was beyond the scope of this questionnaire to take a full medical history and to highlight all co-occurring chronic diseases, but these are some of the most commonly observed. The percentage of individuals within each of the stratified groups with one or more of these chronic age-related conditions was determined. In the never-raised group, 25% subjects had at least one age-related condition, 31% of the occasionally raised group, 38% in the often raised group and 56% in the considerably raised group (Figure 2.12C). The relative risk of having a co-occurring age-related condition in the considerably raised group compared to the never raised group was 2.2, therefore an individual in that group is more than twice as likely to have a co-occurring age-related condition than those in the never raised group. After 3 years, at the end of the study, the subjects completed the questionnaire again and it can be noted that there was a general trend that more individuals had been diagnosed with a co-occurring chronic disease, as would be expected with an ageing community³¹⁴. An increase in percentage of the group with at least one age-related condition was seen for all groups except the considerably raised group which remained at 56%. Interestingly, the group with the least co-occurring chronic conditions became the occasionally-raised group (Figure 2.12C).

Smoking is an identified risk factor for age-related hearing loss and chronic inflammation. Participants of the study were asked if they had been regular smokers and whether they had given up before they age of 40 (Figure 2.12E). The group with the highest number of regular smokers was the never raised group, followed by the considerably raised group. However, when looking at the numbers still smoking in each group, 25% of the considerably raised group were still smoking when taking part in the study compared to just 12.5% in the never raised group. Therefore, there were twice as many individuals still smoking in the considerably raised neopterin volatility group than the never raised group.

Participants of the study were also asked if they had been prescribed statins (Figure 2.12D). Statins are cholesterol-lowering drugs that also have an anti-inflammatory effect. Therefore, it

might be expected that medicating with statins has an anti-inflammatory protective effect against inflammaging. On entering the study, 50% of the never raised group reported being prescribed statins, more than any of the other groups. However, by the end of the study this number had dropped to 38%. Other medications with known anti-inflammatory effects such as non-steroidal anti-inflammatory drugs (NSAIDs) and aspirin, were not asked about in the questionnaire, but should be included in any future work.

2.4.9 Relationship between inflammatory profile and age-related hearing loss

Pearson-product moment correlation coefficients have been used to look for relationships between variables of hearing loss and inflammation (factoring for age). There were no significant correlations between any of the measured markers of inflammation (neopterin, WBC differentials, cytokines) and degree of hearing loss (see table 2.6).

However, when looking at degree of change in an individual's hearing from the start of the study to the end, some clear relationships are seen. Neopterin volatility is positively correlated with change in high-frequency hearing (Worse ear HFA change), $r = 0.334$, $n = 45$, $p = 0.027$, with high neopterin volatility being associated with greater change in high-frequency hearing. When grouping individuals into four groups based on their neopterin volatility (never raised, occasionally raised, often raised, considerably raised), this association becomes even stronger, $r = 0.401$, $n = 45$, $p = 0.007$. WBC ($r = 0.398$, $n = 45$, $p = 0.0080$), lymphocyte concentration ($r = 0.485$, $n = 45$, $p = 0.001$) and monocyte concentration ($r = 0.488$, $n = 45$, $p = 0.001$) also show a positive correlation with change in high-frequency hearing. None of the cytokines demonstrate this relationship, although $IFN\gamma$ is negatively correlated with low-frequency change, $r = -0.470$, $n = 43$, $p = 0.002$), with high levels of $IFN\gamma$ being associated with stable low-frequency hearing.

One of the main aims of this study was to investigate the relationship between neopterin volatility as a marker of chronic inflammation and progression of hearing loss. The pure-tone audiometric thresholds of every individual (categorised into neopterin volatility groups) were measured at baseline, end of year 1 and end of year 3. Figure 2.14A displays the average thresholds for each group across the three time points and figure 2.14B shows the audiometric averages for each neopterin volatility group.

Chapter 2

Table 2.6 Correlation Matrix of inflammatory markers and degree of hearing loss (Puretone average at start and end of study).

Factoring for age, no significant correlations are found between a measure of hearing and an inflammatory marker. Table lists correlation coefficient, ** correlation is significant at $p < 0.01$, * correlation is significant at $p < 0.05$.

	PTAv Start/ dB HL	PTAv End/ dB HL	Neopterin Mean/ $\mu\text{mol/mol}$	Neovolatility/%	WBC	Neutrophils	Lymphocytes	Monocytes	TNF α	INF γ	IL6	IL-1 β
PTAv Start/dB HL		.940**	.026	-.006	-.078	-.113	-.022	-.128	.136	-.175	.128	.132
PTAv End/dB HL	.940**		.094	.075	.001	-.057	.069	-.033	.158	-.215	.107	.151
Neopterin Mean/ $\mu\text{mol/mol}$.026	.094		.912**	.078	.017	.094	.147	.195	.083	.190	-.053
Neovolatility/%	-.006	.075	.912**		.123	.088	.100	.192	.153	.082	.149	-.023
WBC	-.078	.001	.078	.123		.903**	.860**	.876**	-.005	-.018	-.055	.129
Neutrophils	-.113	-.057	.017	.088	.903**		.579**	.673**	-.024	.051	-.073	.197
Lymphocytes	-.022	.069	.094	.100	.860**	.579**		.885**	.002	-.136	-.031	.020
Monocytes	-.128	-.033	.147	.192	.876**	.673**	.885**		.024	.057	-.048	.005
TNF α	.136	.158	.195	.153	-.005	-.024	.002	.024		.454**	.122	.307*
INF γ	-.175	-.215	.083	.082	-.018	.051	-.136	.057	.454**		.190	-.007
IL6	.128	.107	.190	.149	-.055	-.073	-.031	-.048	.122	.190		.022
IL-1 β	.132	.151	-.053	-.023	.129	.197	.020	.005	.307*	-.007	.022	

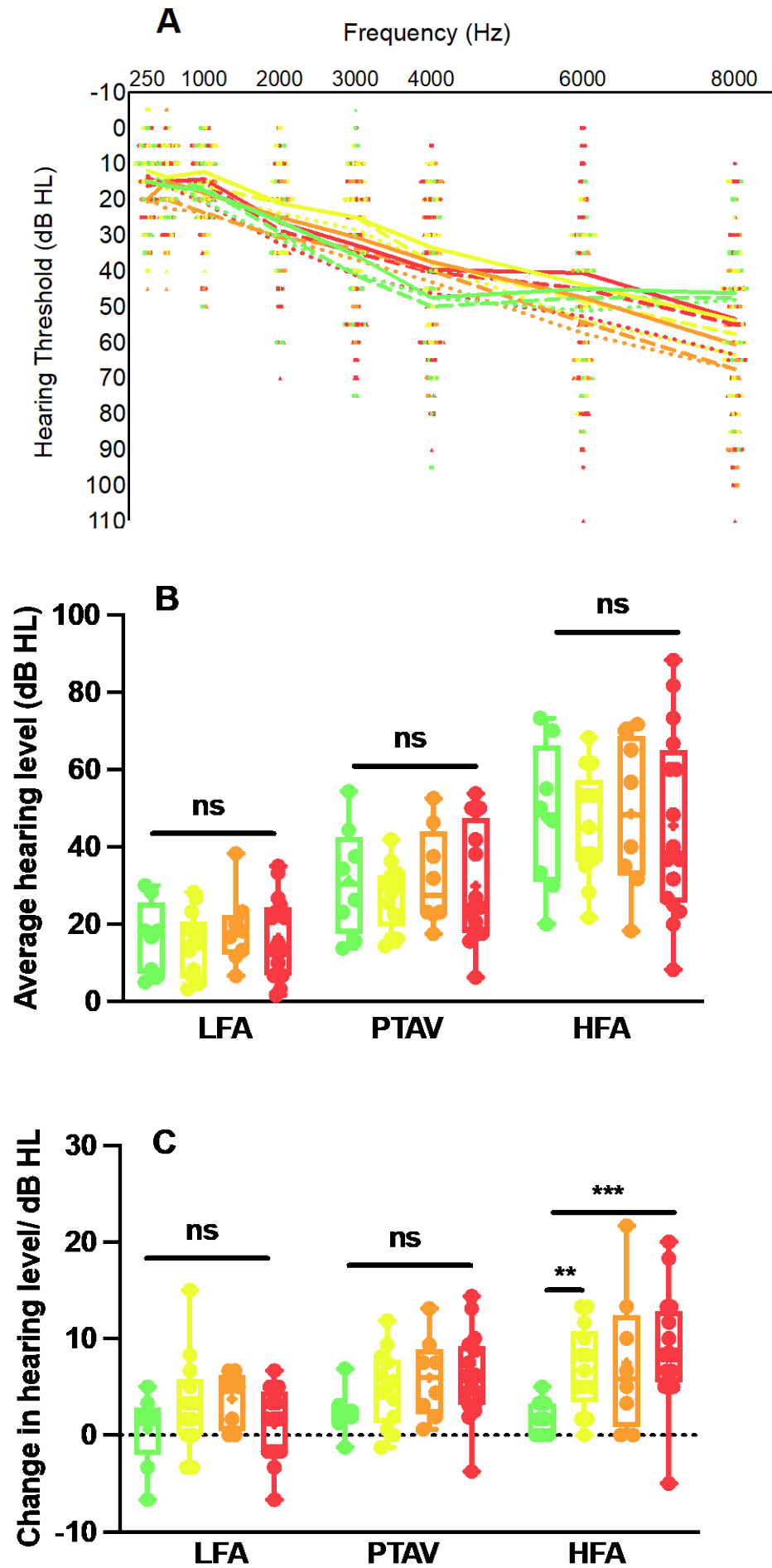


Figure 2.14 Audiometric thresholds, averages and change for subjects in neopterin volatility groups (n=45).

Green is never raised, yellow is occasionally raised, orange is often raised and red is considerably raised A) Average audiometric thresholds for subjects in each neopterin volatility group across baseline (solid line), year 1 (dashed line) and year 3 (dotted line). B) Mean baseline audiometric thresholds of Pure-tone average (PTA Av), low-frequency average (LFA) and high-frequency average (HFA) for neopterin volatility groups. Higher threshold represents poorer hearing. C) Mean change in audiometric threshold averages over the course of the study (Baseline to Year 3) for each neopterin volatility group.

A one-way ANOVA was performed for each audiometric average (PTA Av, LFA and HFA) between the neopterin volatility groups. For average hearing level, there was no significant difference between neopterin group for any of the three audiometric averages; Pure-tone average threshold $F(3, 41) = 0.2358$, $p = 0.8709$, low-frequency average $F(3,41) = 0.3247$, $p = 0.8075$, high-frequency average $F(3,41) = 0.05378$, $p = 0.9833$. For change in hearing level from baseline to end of study (year 3) a Welch ANOVA was also performed for each of the audiometric averages. There was no significant difference between neopterin volatility groups for PTA Av ($W(3.000, 20.28) = 3.043$, $p = 0.0523$) or LFA ($W(3.000,19.77) = 1.799$, $p = 0.1802$). The Welch's ANOVA for high-frequency average did show a significant difference between neopterin volatility groups $W(3.000, 19.60) = 9.164$, $p = 0.0005$. Post-hoc Dunnett T3 multiple comparisons test, showed the significant comparisons to be between the never raised and the occasionally raised groups ($p = 0.0110$) and the never raised and considerably raised groups ($p = 0.0016$).

Otoacoustic emission (OAE) responses were also measured at baseline and end of the study for each participant. To establish if there was a significant change in OAE response for baseline to year 3 for the members of the neopterin volatility groups, a repeat ANOVA was used, with neopterin volatility group as the between subject variable, frequency as the within subject variable and SNR as the dependent variable. A greater reduction in OAE SNR indicates worsening PTA thresholds. There was no significant difference in the change in OAE SNR between the neopterin volatility groups $F(3, 205) = 0.8420$, $p = 0.4723$ (see Figure 2.15).

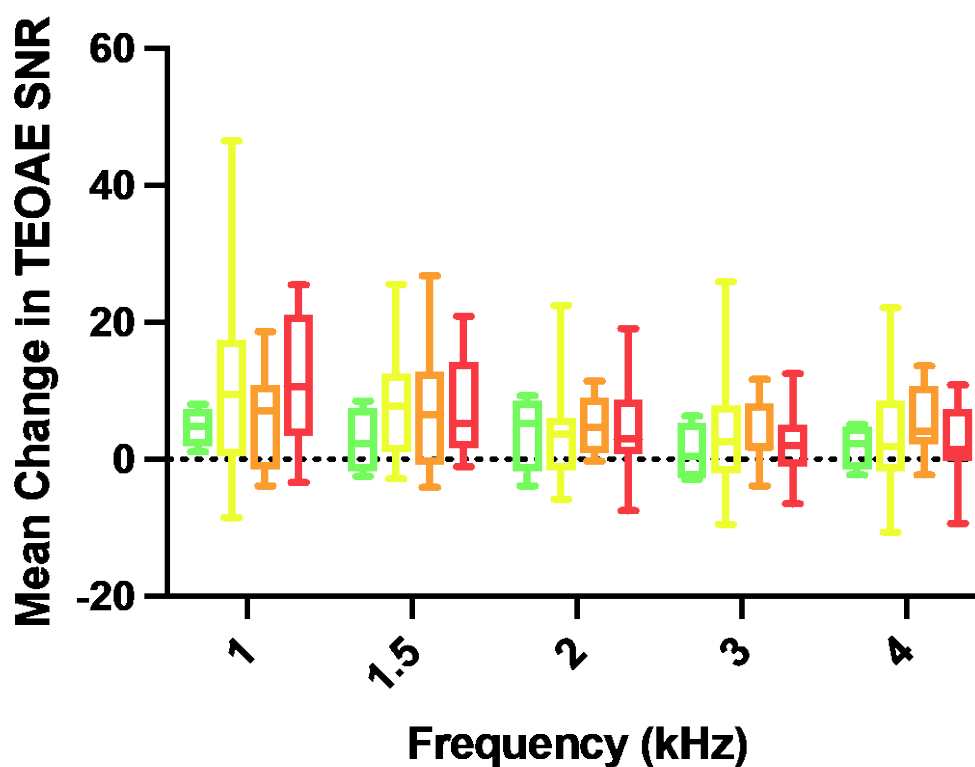


Figure 2.15 Change in TEOAE responses for subjects in neopterin volatility groups.

TEOAE responses at all frequencies for the ears that pass a screening at baseline and year 3 for the different neopterin volatility groups, green is never raised, yellow is occasionally raised, orange is often raised and red is considerably raised.

2.4.10 Study attrition

Sixteen participants did not continue in the study until its end. The data from these subjects has not been used in the analysis, however we sought to determine if there was any trend or stand-out factor that separated the dropouts from those who completed the study. Four variables were considered, neopterin volatility, age, average white blood cell count and PTA Av, there was no significant difference between the average of each of these variables in the dropouts compared to the participants (Figure 2.16A). The neopterin volatility stratified group to which each of the dropouts would have been assigned to showed no significant favour to any particular group, with an even spread of dropouts from all of the groups (Figure 2.16B).

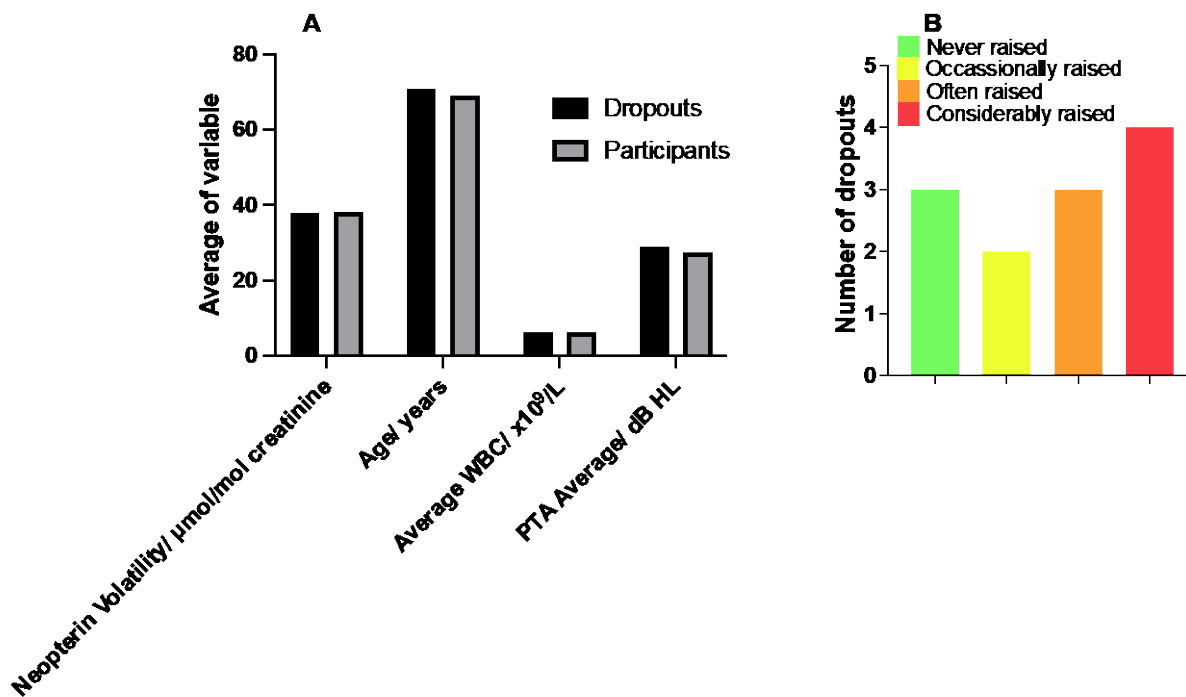


Figure 2.16 Analysis of the 16 participants who did not continue in the study to completion.

A) A selection of variables assessed for differences between those who withdrew from the study and those who didn't. There was no significant difference in any of the assessed variables between the two groups. B) The neopterin volatility groups to which the participants who withdrew would have been assigned, the spread of groups is even, so no bias to final results.

2.5 Discussion

In this study, we have established an individual's underlying (longitudinal) inflammatory state by taking serial monthly urine neopterin measurements across a 1 year period. This negates the effect of fluctuations in inflammatory state over time which may be seen in cross-sectional testing. The purpose of establishing this information was to investigate the relationship between chronically raised inflammation, and the incidence and susceptibility of age-related conditions in older adults. We further investigated the relationship, with a focus on age-related hearing loss, to assess if a high inflammatory state is associated with poorer hearing and greater progression of hearing loss. There is evidence that low-grade chronic inflammation associated with ageing, is a key driver in many age-related conditions^{3,4}. Control or reduction of inflammation may be a central target for therapeutic interventions in reducing the progression of age-related disease and increasing healthspan.

We have demonstrated the use of neopterin volatility as a measure of inflammatory load and an alternative to using mean neopterin or one-off time point measures. Inflammaging can be viewed as a spectrum, at one end will be the healthy adult with no age-related chronic disease and normal levels of inflammatory markers, and the other end, an unhealthy individual with multiple chronic diseases and chronically raised inflammatory markers. There were 8 individuals in this study who never had a raised neopterin level (0% neopterin volatility) during the 12 months of the study and 3 individuals who had greater than 90% neopterin volatility during the 12 months. As only a few subjects had chronically raised inflammatory markers, using the actual level of neopterin would not correctly categorise the subjects effectively, therefore using neopterin volatility to demonstrate the frequency of inflammatory responses, the number of times neopterin was elevated over 12 months, better indicates their level of immune activation. This is based on the premise that the more frequent the systemic challenge, the more tissue injury caused, which has been shown in Alzheimer's disease, where each infection or systemic challenge drives greater neuronal damage and greater decline in cognition^{3,13}. Therefore, this study effectively demonstrates the utility of measuring frequency of inflammatory response as a way of assessing inflammaging, especially in people who do not have chronically elevated inflammatory markers.

The use of urine instead of blood samples provides a non-invasive and easy way to obtain samples for monitoring purposes. Giving frequent urine samples for testing is preferable to individuals than regular blood sampling. Another benefit of using urine samples is that non-medical professionals or individuals themselves would be able to test urine neopterin without the need

Chapter 2

for an appropriately trained individual to take blood. Additionally, blood samples would require specific processing, transport to a laboratory, and storage that would come with an associated cost. Comparatively urine samples would require less cost and have greater potential to be processed and analysed at the point of collection.

Neopterin levels in the cohort were found to be associated with other markers of inflammation: blood markers and cytokines. When individuals were stratified into groups based on their neopterin volatility, a similar relationship between groups was seen for each marker, although none of these were found to be significant between-group, this is most likely due to the one-time point sampling of these markers.

Neopterin measurements have been used to monitor disease progression in a variety of conditions^{8,11,270,315-317}. Neopterin levels have been shown to correlate well with disease activity in autoimmune diseases such as Crohn's disease because these diseases are modulated by proliferation of T-lymphocyte activity, which induces the production of IFN- γ to activate the neopterin pathway¹¹. Neopterin levels have also been used to monitor the progression of certain malignancies and for their prognosis, as neopterin production may be induced in certain types of tumours^{10,268,269}. It has also successfully been used as a prognostic marker in patients with chronic heart failure²⁷⁰. These studies provide evidence that neopterin measurement can be used as a monitoring tool in diseases that cause immune activation⁴⁷.

The results of this study have demonstrated that serial measurements of urine neopterin can identify an individual's inflammatory baseline, and this is associated with prevalence of age-related diseases. Based on individual neopterin volatility, the cohort were stratified into categories, from neopterin never raised, to considerably raised (>50% of the time). Those in the considerably raised group, had the highest prevalence of age-related diseases with more than twice the risk of having an age-related disease including cardiovascular diseases and type 2 diabetes, than those in the never raised group. Other studies have shown associations between other inflammatory markers and age-related diseases, including frailty and age-related hearing loss^{5,32}. Studies that have used neopterin as a marker to draw associations about age-related disease include those that have found plasma neopterin levels to be higher in patients with Alzheimer's Disease^{60,266}, another study has shown high neopterin levels in those with frailty when measuring serum neopterin at a single time point³¹⁸. However, to date, to the best of the author's knowledge, no study has investigated the association between longitudinal measures of neopterin and the occurrence and progression of age-related diseases. Also, no other study has looked at urine neopterin as a marker of inflammation in relation to age-related hearing loss. Other studies that have demonstrated elevated immune markers in association with age-related hearing loss

are only measured at a single time point, for example, the two large cohort studies by Verschuur et al.^{6,7} In these large cohorts, the subjects were self-reportedly well with no acute illness. Therefore it could be assumed that their level of inflammatory marker was consistent with their usual baseline, additionally, because of the large sample size, the effect of a few people having acute inflammation would be negligible. However, to overcome the issue of individual fluctuating inflammation levels, repeated measurement of an immune marker over a period time is a more reliable technique to truly reflect an individual's immune status and therefore may be better associated with age-related chronic diseases. The fact that we have shown, in even a small cohort, that serial neopterin measures are associated with the prevalence of age-related chronic diseases strengthens the association between inflammaging/immune activation and age-related hearing loss.

The study has investigated factors that affect inflammatory state such as smoking and statin use. Smoking has a known pro-inflammatory effect due to activating immune cells and inducing secretion of pro-inflammatory cytokines and chemokines, including IFN- γ ³¹⁹. We have seen that although over 60% of the never raised group report having smoked regularly, the majority of them had given up before the age of 40. Similarly, in the occasionally raised and often raised groups, most had given up before the age of 40. However, 50% of the considerably raised group reported having been a regular smoker, and 25% were still smoking at the time of the study. Statins are cholesterol-lowering drugs that have anti-inflammatory properties; they are known to reduce the levels of pro-inflammatory cytokines, especially c-reactive protein³²⁰. When looking at statin use within the cohort, on entering the study, 50% of the never raised group reported being prescribed statins which was more than any of the other groups and suggested that those taking statins are experiencing an anti-inflammatory effect. However, by the end of the study, this relationship was no longer observed, and overall no conclusion can be drawn based on statin use affecting neopterin volatility. A limitation of this study was that individuals were asked via questionnaire if they had been prescribed statins rather than if they were actively taking prescribed statins, non-adherence with statin use is a known issue^{321,322}. Therefore, we can suggest that the report of statin prescription is a poor indicator of statin use. The effect of smoking and possibly statin use on inflammatory status that has been observed suggests that environmental factors such as these can alter an individual's inflammatory profile and control inflammation which identifies an opportunity for possible interventions to prevent or reduce the progression of age-related conditions.

The average audiogram of the individuals shows the typical configuration of hearing loss expected with ARHL- a bilateral high-frequency sloping loss^{80,202,204}. Other studies have found that males have poorer hearing than females³²³, but with considerably fewer males than females in the

Chapter 2

cohort, we cannot draw clear conclusions regarding gender-bias in the effect. Seventy-five percent of the cohort had a measurable hearing loss on testing at the start of the study compared to 89% by the end, which is typical of the prevalence of hearing loss expected in a cohort of this age^{79,323}, with more people having a mild or moderate loss by the end of the study. For all three audiometric averages (Pure-tone, low-frequency and high-frequency average), a significant difference in the average hearing level (dB HL) from baseline to end of the study was observed. The greatest change to the hearing throughout the study was in the high-frequency region, which is again where deterioration due to age is expected^{80,202,204}.

In this study, no significant correlation was found between any measured inflammatory marker and degree of hearing loss, however when looking at the degree of change in hearing from baseline to end of the study, significant correlations were seen for neopterin volatility, neopterin volatility stratified groups, lymphocyte and monocyte concentration. This identifies that assessing inflammatory profile via an inflammatory marker is not associated with an individual's level of hearing loss, but rather with the progression of hearing loss over time. This supports the idea that chronic inflammation drives progression of age-related disease rather than disease onset or severity.

When individuals were stratified into groups based on their neopterin volatility, a significant effect was seen in the degree of change to high-frequency hearing between groups over time. Particularly between the never raised group and the other groups. The mean change in high-frequency average for the never raised group was 2 dBHL and 9dBHL for the considerably raised group, a 350% increase. Despite this significant increase, further work with a study over a greater duration is needed to validate this result. This is because although age-related hearing loss is reported to progress at a rate of about 1dB per year, the test-retest reliability of pure-tone audiometry is 5dB^{324,325}, therefore at any one time, a difference in pure-tone threshold of 5dB would not be considered significant.

Otoacoustic emission response is identified as decreasing with ageing³²⁶⁻³²⁸. While the argument could be made that the decline in OAE response is associated with the hearing loss that comes with ageing, other researchers are of the view that the decline in OAE response occurs even with normal hearing^{327,329}. Only 11 ears, of the 90 tested in the cohort, had recordable TEOAE responses at all of the frequencies (1, 1.5, 2, 3 4 kHz) by the end of the study. Using a screening protocol that accepts 3 out of 5 frequencies being present, improved this to 45 ears. The results show a significant difference in the change of SNR between baseline and the end of the study for 1, 1.5 and 2kHz TEOAE. We expect to see the most change in high-frequency hearing but the lack of significant difference at 3 and 4kHz is most likely due to very few individuals actually having a

recordable TEOAE at these frequencies. When individuals were stratified into groups based on their neopterin volatility, there was no significant difference between groups for mean change in TEOAE SNR. A reason for this could be that inflammation has a greater influence on the stria and neural synapses which are rich in CNS immune cells and microglia, compared to the outer hair cells, which is the area responsible for OAE production. The lack of significant findings with TEOAE is also highly likely due to so few people having recordable OAEs within the study. Evidence in the literature suggests that anything more than a mild hearing loss is likely to lead to the TEOAE response being diminished^{330,331}. Therefore, TEOAE SNR as a measure of change in hearing, although sensitive is not a reliable measure in a cohort of older adults. Pure-tone audiometry, which is indicative of the functioning of the entire auditory system, reflects a difference in inflammatory load compared with OAE, which essentially represents only outer hair cell function. In future work, other methods of measuring hearing should be considered, including speech in noise testing, many individuals with hearing loss not detectable via PTA will have a poor speech in noise capability due to dysfunction of auditory processing. As a measure that encompasses the entire auditory pathway, including auditory processing, this may be a more sensitive measure to changes in hearing.

Frailty describes individuals who are in a state of increased risk of vulnerability to disease, disability and death, compared to others of the same age²⁵⁰. Connecting the clinical state of age-related frailty with underlying biological age, as measured by biomarkers, is a goal. Frailty can be evaluated, and health status quantified, by the number of health deficits that individuals accumulate. Specifically, the frailty index (FI) is the ratio of the deficits present in a person, to the total number of potential deficits evaluated²⁵¹. The FI has been used in many epidemiological and clinical studies to grade the degree of risk of several adverse outcomes, including mortality, health service use, hospital-acquired complications, worsening health, and loss of independence²⁵²⁻²⁵⁴, as well as conditions such as cognitive impairment²⁵⁵, heart disease²⁵⁶ and osteoporosis²⁵⁷. Another functional indicator of frailty is hand-grip strength (HGS) which is associated with inflammatory biomarkers²⁵⁸. A recent study in a cohort of middle-aged and older adults has shown that HGS is strongly associated with cardiovascular disease and therefore has the potential to be a valuable screening tool for cardiovascular risk in clinical settings. Where blood sampling is not possible, this will be highly advantageous because HGS is easily measured and highly reproducible³³².

A recent systematic review of biomarkers related to ageing recommends a range of serum measures as well as physical and cognitive assays in order to cover the full spectrum of ageing across body systems³⁵. In contrast to physiological indices, there is a growing interest in the utility of molecular markers, specifically regarding DNA methylation³³³. The epigenetic clock is based on the measurement of DNA methylation at multiple sites and appears to correlate with biological

Chapter 2

age and age-related risk more than chronological age³³³⁻³³⁵. Advanced glycation end products represent another potential biomarker that accumulates with age and in several age-related diseases³³⁶. Furthermore, increased levels of some advanced glycation end products are also associated with increased mortality in humans³³⁷.

Glycoprotein A (GlycA), a composite nuclear magnetic resonance (NMR) biomarker reflecting diverse inflammatory pathway activation has been shown to have much greater stability and lower intra-individual variability than single acute-phase proteins³³⁸. In population studies, GlycA is a robust predictor of disease-specific mortality, cardiovascular disease and cancer, even after adjusting for other inflammatory biomarkers^{339,340}.

The attrition rate in this study was high (26%); however, on investigation, nothing about the individuals who dropped out of the study appears significant. Some individuals were removed from the study at their own request due to health or time restrictions and others became uncontactable when we tried to arrange follow-up. We looked to see if those with the poorest health or poorest inflammatory profiles were the ones to drop-out on the speculation that they may have greater time pressure from health appointments, or even such poor health they physically could not attend, or possibly had even passed away. However, nothing significant about the individuals who did not continue in the study was discovered. In future work, study attrition may be improved by offering individuals an incentive to complete the study, i.e. an inflammation-modifying intervention process.

There is developing enthusiasm in the idea that treating the underlying biological process of ageing may influence the onset of many age-related conditions and diseases with a single intervention. In 2018, a multi-organisation partnership in the United Kingdom announced the formation of the “Innovative Therapeutics for Ageing Consortium” (iTAc), which aspires to accelerate the discovery and development of therapeutics for ageing. The consortium aims to address the lack of therapeutic interventions for multimorbidity and diseases related to ageing processes. Early phase drug discovery in iTAc will scout for, explore and exploit targets that are considered to constitute four major cellular mechanisms underpinning ageing: inflammation, cellular senescence, DNA damage and repair, and metabolic dysfunction¹³⁷.

There is an emerging body of evidence in both animal models and humans that supports causative links between increased physical activity and disease prevention and management, mediated by improved immunity. Interventions involving physical activity have improved symptoms of disease in a range of inflammatory and autoimmune disorders, with the benefits seen including improvements in microvascular and macrovascular function³⁴¹ and decreased disease severity and pain in patients with rheumatoid arthritis³⁴². However, evidence would also suggest that high

levels of increased physical activity throughout adulthood and not just in late-adulthood is necessary. A study was performed on non-elite cyclists who had maintained a high level of physical activity for most of their adult lives. The findings showed these individuals lacked many of the physiological changes expected with advancing age, such as loss of muscle mass and function (sarcopenia), reduced insulin sensitivity, elevated cholesterol and high blood pressure³⁴³. They also exhibited fewer signs of immunosenescence, including reduced evidence of a decline in thymic output, with a frequency of recent thymic emigrants similar to that seen in younger adults²⁷⁸. An increase in systemic inflammation was also not observed with changes to regulatory T cell and B cell frequencies^{344,345} not being seen in the cyclists. However, the accumulation of senescent T cells was still observed comparably to age-matched non-exercising adults, suggesting that lifelong physical activity ameliorates rather than totally prevents immunosenescence²⁷⁸. Another study has also demonstrated maintained thymic output and naïve T cell frequency in males who had partaken in moderate-high intensity physical activity for an average of 25 years³⁴⁶.

2.6 Conclusions and Future Work

- Serial measurements of urine neopterin and neopterin volatility can determine an individuals' inflammatory baseline and identify those with chronic systemic inflammation (inflammaging)
- High neopterin volatility is associated with increased risk and co-occurrence of chronic age-related conditions
- Being a current smoker is associated with increased neopterin volatility
- Individuals with a recognised hearing loss increased from study baseline to end
- High inflammatory baseline was associated with greater progression of hearing loss (high-frequency hearing)
- Transient otoacoustic emissions (TEOAE) are not a sensitive measure to change in hearing in older adults due to the loss of recordable OAEs with age and reduced hearing

Future work will involve a longer study of at least five years with a larger cohort, this longer timespan will allow for greater change in hearing level to be observed which is greater than the test-retest reliability of pure tone audiometry. An investigation of other more sensitive measures of change in hearing as well as other measures of ageing, that could be incorporated would be beneficial. There is evidence that inflammatory changes even at a young age, can have an effect on inflammaging, so looking at a younger mid-life cohort may be interesting. Mid-life individuals may be more motivated to make lifestyle changes if they are found to be at risk of inflammaging.

Chapter 2

Finally, using such a study for the assessment of interventions that could reduce progression of age-related disease by reducing inflammation could highlight beneficial therapies. Identifying those that may benefit from interventions will be possible through easier testing that individuals are able to do in their own home. For example, tests that correspond to frailty (hand grip strength), progression of disease (hearing testing, such as speech in noise), and regular inflammatory monitoring using a technique that has the ability to measure markers in urine within the home, will aid identification of such individuals.

Chapter 3 Development of a spectroscopy-based method for detecting and quantifying an inflammatory biomarker in urine

3.1 Overview

Chapter 2 demonstrates that monitoring the level of an inflammatory marker in an individual's urine can give insight into their potential risk of age-related conditions. This chapter demonstrates the potential of Surface-Enhanced Raman spectroscopy (SERS) as an analytical tool for measuring a biomarker, neopterin, in urine.

3.2 Introduction

3.2.1 Barriers to routine monitoring using standard analytical approaches

Urinary neopterin concentration can be measured using enzyme-linked immunosorbent assay (ELISA), radioimmunoassay (RIA) and high-performance liquid chromatography (HPLC); their use for determination of neopterin in urine is widely reported^{9,11,13,58,347-351}. Whilst these techniques are established, they have drawbacks: tests are only performed in specialised laboratories, involve time-consuming assay-based tests (resulting in slow results turnaround), expensive enzymes, sophisticated instrumentation and equipment, and can in some cases lack sensitivity. For example, to run a single sample through HPLC for measurement of both neopterin and creatinine (including disinfection/cleaning of the column between samples) would take more than an hour¹², whereas in the same time you could measure hundreds of samples with ELISA/RIA. The cost to perform HPLC (in 2020) is around £7 per sample, although it varies considerably depending on what the sample is⁶³. ELISA is cheaper; however, it has poorer accuracy and precision of measurement. An additional drawback of RIA is the handling of radioactive materials which requires specialised laboratories and costly waste-streams.

For long-term monitoring of an individual's baseline systemic inflammation, an alternate method that is rapid and inexpensive would be preferable. Such a method, or tool, could be employed in the clinical setting or an individual's home due to its ease of use and low cost. Therefore, making it possible to regularly monitor an individual to identify those with consistently elevated neopterin levels (opposed to short periods of raised inflammation due to an acute illness) and therefore as demonstrated in chapter 2 'at risk' of worsening age-related disease.

3.2.2 Surface-Enhanced Raman spectroscopy as a portable and sensitive analytical approach

Surface-enhanced Raman spectroscopy (SERS) is a sensitive analytical technique with limits of detection down to fM and single-molecule^{14,352,353}. SERS utilizes the localized surface plasmon resonance (LSPR) of metallic nanomaterials to enhance Raman signals³⁵⁴⁻³⁵⁷. Raman enhancement is optimal when an analyte is located in close proximity to, or adsorbed onto, the metallic nanoscale surface. There is growth in the use of SERS for quantification of biologically relevant molecules^{133,358-364} as it provides molecularly-specific information, is label-free, and can be performed directly in biofluids^{64,365-368}. Raman spectroscopy has advantages over other well-known analytical methods, including the use of portable spectrometers, allowing for point-of-care analysis of clinical samples.

3.2.2.1 Improving reproducibility of SERS substrates

For quantitation and to allow comparison between different analytical measurements SERS substrates need to be reproducible. Reproducible SERS enhancements require strict control over the material's nanostructure and the location of the analyte. Colloidal SERS is commonly performed by aggregating nanoparticles with analytes resulting in plasmon "hot spots" of high enhancement. However, this approach offers poor control over the spatial proximity of the analyte to the "hot spot" resulting in low measurement reproducibility³⁶⁹. Other SERS substrates with good reproducibility exist, both commercially and in research, however, these usually involve high cost due to complex high-level manufacturing, making them unsuitable for high-throughput monitoring of samples.

One way to improve quantification with colloidal nanoparticles is to use the Standard addition method (SAM), which is a well-established technique in analytical chemistry. SAM is useful when dealing with complex matrices, where many analytes compete for the "hot spot", preventing accurate quantification of the desired analyte. SAM works by spiking known amounts of the analyte of interest into the sample, a plot of peak area against the concentration of spiked analyte will enable the unknown amount of analyte to be calculated. Several groups have demonstrated the use of SAM with SERS to quantify analytes in urine^{113,133,370}; however, the extra steps of spiking samples with multiple known amounts of target analyte, adds additional time and expense in terms of the number of samples, the number of measurements required and having a stock of target analyte. Therefore, such a method is less suitable for point-of-care SERS measurement.

Another way to improve reproducibility is to employ an internal standard in SERS measurements, as first reported by Bell et al., who used an internal standard to compensate for temporal signal

variation when quantifying dipicolinic acid from *Bacillus* spores^{371,372}. However, competitive adsorption between the target analyte and the standard is likely, and the method will not work above saturation of the nanoparticle surface³⁷³. Therefore, the ratio of analyte to standard is not a linear relationship. However, placing the internal standard molecules within the inside of core-shell nanoparticles has been shown to improve the quantitative analysis of target molecules over a large concentration range³⁷⁴. Use of spacer molecules to control the nanogap between colloidal nanoparticles has also been used to control and improve reproducibility³⁷⁵; however, this still requires the use of aggregation agents which may interfere with the analytes in solution.

An alternative approach is to use layer-by-layer (LbL) self-assembly to “freeze” plasmonic nanogaps between nanoparticles on a planar or colloidal substrate. Fabrication of plasmon-tuneable, sensitive, quantitative, and self-calibrating colloidal SERS sensors has been reported³⁷⁶. Alternating coatings of gold nanoparticles (AuNPs) and polyelectrolyte “spacer” layers, controls the nanoparticle spacing in the radial direction. AuNPs are adsorbed directly from their colloidal suspension without the addition of any salt. Consequently, AuNP assembly creates a uniform deposition without polydisperse aggregates, enabling the controlled fabrication of sensors which are sensitive and reproducible for quantitative SERS measurements. These sensors are easily fabricated and the cost to produce and use is equivalent to using colloidal AuNPs.

3.2.3 Measuring urinary neopterin to creatinine ratio

Neopterin is a small biomolecule present in urine which can be used as a marker of systemic inflammation. Chronic systemic inflammation has been shown to play a role in health prognosis in a multitude of age-related conditions such as frailty¹⁵⁹, cardiovascular disease³⁷⁷, hearing loss^{5,6} and dementia³⁷⁸. Neopterin is produced from guanosine triphosphate by human monocytes and macrophages, after stimulation by interferon-gamma (IFN- γ) derived from antigen-activated T lymphocytes⁴⁷. Compared to blood, urine sampling is non-invasive. Urine is less protein-rich, so is less likely to suffer from matrix effects. Urine carries abundant metabolic information which can reflect health conditions within the body.

Neopterin is expressed as the urinary neopterin-to-creatinine ratio (UNCR), measured in $\mu\text{mol/mol}$ to normalize for glomerular filtration rate. A healthy non-inflamed individual will have a UNCR $< 251\mu\text{mol/mol}$ ^{13,46,47,379}. The main techniques used for the analysis of neopterin in urine include enzyme-linked immunosorbent assay (ELISA)⁵⁸, radioimmunoassay (RIA)¹³ and high-performance liquid chromatography (HPLC)^{13,379}. HPLC is considered the gold-standard technique, however, as discussed in 3.2.1, Raman spectroscopy offers portable instrumentation capable of

point and shoot analysis, enabling the technique to be used in a point-of-care situation by clinical staff, or at home by the individual themselves.

3.2.4 Raman analysis of neopterin in biofluids: limited evidence of clinical application

There are few examples of Raman analysis of neopterin in biofluids. Raman spectroscopy has been performed on the urine of oral cancer patients¹²¹, using principal component analysis to characterise urine samples as 'normal' or 'cancer'. Numerous metabolites were detected in urine, the spectrum for neopterin and the normalised Raman spectra of commercially available metabolites were found to differ in patients with oral cancer. A vibration for neopterin at 1283 cm^{-1} was observed in both the normal and cancer subjects, however appearing as a shoulder in the normal subjects. Other peaks attributed to neopterin were seen at 1482 and 1512 cm^{-1} which were observed at higher intensity for cancer patients, than that of normal subjects, indicating there may be an increased contribution of neopterin in the urine of cancer patients. No other distinguishable neopterin peaks from the other components of urine were seen in the wavenumber region 500-1800 cm^{-1} .

Other work that has measured neopterin in body fluids is the work of Kamińska et al. utilising SERS with both zinc oxide films on silicon and gold-capped silicon substrates^{363,380,381}. In their most recent work, they have developed SERS substrates with high reproducibility of measured signals, both within-substrate (RSD= 6.7%) and between-substrate (RSD= 8%), due to the uniform distribution of SERS-active "hotspots" across the substrate. The uniformity of distribution on their silicon/gold substrate is due to using an electrochemical etching process to generate porous silicon, the porosity and thickness of which is controlled by the etching process. They then use physical vapour deposition (PVD) to sputter a gold layer on top. They have used these substrates to measure the SERS intensity of the 695 cm^{-1} peak of neopterin in cerebral spinal fluid (CSF). In this study, they have compared the concentration of neopterin in normal CSF samples (4.3 nmol/L) and samples infected by *Neisseria meningitidis* (54nmol/L). The demonstrated reproducibility of these substrates for measuring neopterin is excellent, however, the substrates require a fairly complex manufacturing process. A substrate with a simpler and cheaper manufacturing process would be preferable, although likely have a trade-off in reproducibility.

3.2.5 Urinalysis with SERS is largely confined to classification of samples using multivariate analysis

Label-free SERS analysis of urine has been largely confined to studies of cancers^{120,124,125,382}, diseases^{383,384} and pharmacology^{362,385}. Rather than absolute quantification of a biomarker, most

of these studies rely on multivariate analysis to classify a sample as healthy or diseased. For example, Huang et al.¹²⁴ applied silver nanoparticles to the urine of oesophageal cancer patients and healthy volunteers, then used principal component analysis (PCA) combined with linear discriminant analysis (LDA) to differentiate the SERS spectra between normal and cancerous urine samples. Their results demonstrate diagnostic sensitivity of 87.5% and specificity of 83.3%.

Label-free SERS analysis of urine without multivariate analysis has been demonstrated^{133,385-388}. For example, absolute quantification of uric acid in urine by employing the SAM¹³³. This method shows good agreement against HPLC with an average of <9% difference between the analytical approaches. However, despite improving quantitative accuracy, the SAM requires extra sample preparation and increased sample analysis, rendering it unsuitable for rapid point-of-care testing.

3.2.6 Considerations for developing a novel analytical sensor

The novel SERS sensors used in this work have been previously characterised³⁷⁶. They demonstrated highly reproducible measurements (RSD 8-12%) for a Raman reporter molecule (4-MBA) and an enhancement factor of approximately 9×10^5 . This characterisation was for sensors with two layers of AuNPs around a polystyrene core, using 633nm excitation. The enhancement factor is a useful measurement for eliminating the effects of both instrumental and Raman scattering cross-section differences. Such differences occur with different instrumentation and substrates utilised between laboratories. Caution is necessary when considering a substrate enhancement factor, as some of the numbers used in the calculation are not measured, but instead based on estimations and assumptions. Also, enhancement factor is based on a reporter molecule with strong surface affinity, and therefore complete surface coverage is assumed. Obviously, the affinity of “real-world” analytes will vary, and total surface coverage is not guaranteed.

When developing a novel analytical device, there are validation and performance characteristics that need to be considered. These characteristics will determine the effectiveness of the device as an analytical tool. The Eurachem guide is an accredited guide to method validation for all analytical methods³⁸⁹. For method validation, the guide recommends tools such as blanks, routine test samples, spiked samples and measurement standards. For method performance, the guide recommends characteristics such as selectivity, limit of detection/limit of quantification (LOD/LOQ), working range, analytical sensitivity, trueness and precision. Both the validation and performance of a novel analytical sensor need to be considered.

Most SERS studies that involve quantifying an analyte focus on LOD/LOQ as the main measurement of performance. These measurements are useful for establishing the lowest

concentration that a sensor can detect or quantify, but actually have little “real-world” relevance. For example, what is actually more useful to know is how the sensor performs in the concentration range that is likely to be encountered with the target analyte. It is therefore recommended that with biofluids, sensor development should aim to have good accuracy for the physiological concentration of the target biomolecule³⁹⁰.

Reproducibility of measurement with a SERS substrate is crucial for quantitative measurement. Reproducibility is notably very poor for colloidal SERS substrates and significantly better for solid, structured SERS substrates. Therefore, when developing a novel substrate, it is paramount that the reproducibility is assessed, ideally both within- and between- batches. In the SERS community, it is recommended that 100 individual measurements are made per batch when comparing colloidal batches, and tens of measurements of a surface for assemblies and solid substrates. To obtain a statistically significant result, SERS data should be averaged from 3-5 samples with a few 100s of individual measurements per sample recorded under the same conditions and distributed over the reported area³⁹¹.

3.2.7 Research Gap

In this work, we have developed a method that uses SERS sensors for quantitative analysis of an inflammatory marker (neopterin) in urine. Raman measurement of neopterin in biofluids has been demonstrated^{121,363,380,381}, but to our knowledge, this is the first example of neopterin quantification in urine. We show for the first time that unlike other SERS substrates, our sensors can be used as a colloidal suspension, simply mixing with a urine sample for analysis. The method demonstrates comparable quantitative ability to other colloidal SERS methods and has the benefit of requiring no sample pre-treatment or multivariate analysis, thus making it a suitable technique for point-of-care testing with a portable spectrometer. This technique offers high sensitivity, specificity, simplicity and cost-effectiveness. Such an analytical system available at point-of-care will allow long-term monitoring of a patient’s immune system activation, which would be revolutionary in the monitoring of disease and health prognosis.

3.2.8 Hypotheses

- SERS sensors produced by layer-by-layer synthesis give more reproducible results than colloidal AuNPs and with increased SERS intensity/enhancement.
- SERS sensors show both within- and between- batch reproducibility as well as being stable against deterioration in storage.

- Physiologically relevant concentrations of neopterin and creatinine can be quantified in urine with comparable values to the gold standard HPLC.

3.2.9 Aims

This chapter aims to demonstrate that SERS is a suitably sensitive technique for detecting neopterin in urine samples. In addition, the novel SERS sensors produce more reliable results for quantitative analysis than colloidal gold nanoparticles and that the ease of use and low-cost manufacturing of these sensors is far more suited to point-of-care testing than highly manufactured or commercially available SERS substrates.

3.3 Methods

3.3.1 Layer-by-layer SERS Sensor Fabrication

SERS sensors were fabricated using a layer-by-layer (LbL) method described by Anderson et al.³⁷⁶. Silica microparticles (7.5 μ M, Microparticles GmbH Berlin) were used as a core on which iterative layers of Poly(ethyleneimine) (PEI) (Mw \sim 750 000 gM⁻¹ 50% (wt) in water, Sigma-Aldrich), poly(sodium 4-styrenesulfonate) (PSS) (Mw \sim 70 000 gM⁻¹, Sigma-Aldrich) and citrate-capped AuNPs (40nm, 8% CV, 9 x 10¹⁰ particles per ml, BBI Solutions) were applied to form two AuNP layers. Sensors were diluted and stored in water at 4°C until use.

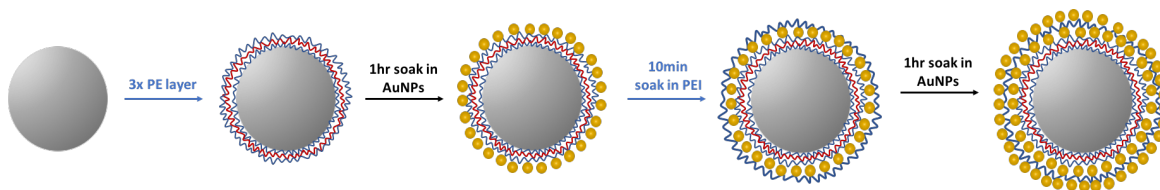


Figure 3.1 Procedure for preparation of layer-by-layer (LbL) SERS sensors involving iterative steps of applying polyelectrolyte layers and 40nm gold nanoparticles (AuNPs) to a silica microparticle.

3.3.2 Synthetic Urine Preparation

Synthetic urine was prepared according to the method of Villa and Poppi³⁹². Sodium chloride (NaCl, Acros organics), potassium chloride (KCl, Sigma-Aldrich), sodium dihydrogen phosphate (NaH₂PO₄, Sigma-Aldrich), urea (Sigma-Aldrich), citric acid (Fisher) and bovine albumin (Fisher)

were added to 18.2Ω Millipore water and pH adjusted with sodium hydroxide (NaOH, Sigma-Aldrich). Synthetic urine was stored at 4°C until use.

3.3.3 Human Urine Handling

Human urine samples were collected from healthy adults aged 65-75 years (NRES REC: 13/SC/0507 and University of Southampton ERGO 7923). When received, the urine samples were centrifuged at 2000rpm at a temperature of 4°C for 10 minutes and stored at -20°C. Prior to use, samples were thawed at 4°C and kept in the dark with a foil covering, as neopterin is light-sensitive. Prior to HPLC analysis, both synthetic and human urine samples were treated to remove protein by using spin-columns (Vivaspin 500μL 5kD, Sigma-Aldrich) and the filtrate taken for HPLC analysis.

3.3.4 Neopterin and Creatinine Standards

Neopterin (Tocris Bio-Techne cat no. 4656) and creatinine (Sigma-Aldrich C4255) standards were prepared by making a concentrated stock solution, 200 μM Neopterin and 50mM Creatinine by dissolving neopterin and creatinine respectively into 18.2Ω Millipore water. To enable dissolution of neopterin in water, the container was vortexed and placed into a sonicated water bath (37°C) for 2 hours. Both stock solutions were then stored at 4°C (neopterin covered in foil) until ready for use. Calibration standards of each analyte were then prepared by serial dilution when required.

3.3.5 UV-Vis analysis of layer-by-layer SERS sensors

For confirmation of successful LbL assembly and to characterise the sensors, light microscope images and UV-Vis scattering data were obtained. UV-Vis scattering measurements were performed using an Ocean Optics DH-2000 UV-Vis-NIR source and an Ocean Optics USB2000 spectrometer. The incident white light was collimated, and scattering spectra were collected orthogonal to incident radiation. Scattering measurements were taken of the prepared sensors, as well as colloidal 40nm AuNPs to characterise the red-shift in the scattering of the sensors demonstrating the surface plasmon resonance. The scattering measurements were normalised to correct for system spectral variation.

3.3.6 HPLC analysis

HPLC separation was conducted using a Gilson HPLC system (with a Shimadzu RF-10A Fluorescence detector and a Gilson UV/Vis- 155 detector) set up for reverse-phase using a 150 x

4.6 mm column with a 5 μ m particle size (Gemini C18 110A). For each injection, the run time was 40 minutes. The mobile phase consisted of 25mM Acetic Acid, 10mM Sodium 1-octane sulfonate at pH 3. The organic buffer with 50% acetonitrile was increased in gradient from 0% to 100% over 30 minutes at a flow rate of 1.0 ml min⁻¹. The sodium-1-octane sulfonate (Sigma-Aldrich) acts as an ion-pairing reagent to increase retention time. Urine samples were analysed undiluted and at a 1:4 dilution. Each sample (20 μ l) was introduced using an autoinjector. The retention time for creatinine was 21 minutes and neopterin 10 minutes, although the retention times were earlier when the urine samples were analysed. Neopterin was detected by fluorescence (excitation 353nm, emission 438nm) and creatinine detected by UV absorbance (235nm). Repeated measurements were made for each sample and averaged. For creatinine, the spectra were background subtracted for water. Spectral analysis was performed in UniPoint software.

3.3.7 SERS analysis

SERS analysis was performed on a Renishaw InVia spectrometer (633nm HeNe laser, 6mW max output). The instrument was calibrated using a silicon wafer with a static spectrum peak at 521cm⁻¹. Lbl SERS sensors (0.1%, 5 μ L) were mixed with analyte/sample (20 μ L) by pipetting and measurements taken after a 10-minute incubation. A drop (5 μ L) of mixture was then pipetted onto an aluminium disc, and the microscope used to focus onto a single sensor. Experimental parameters were a one accumulation extended scan (500-1000cm⁻¹ for neopterin measurement and 1500-2000cm⁻¹ for creatinine measurement (although for some initial experiments a creatinine peak was used in the 500-1000cm⁻¹ range)) with an exposure time of 10 seconds using a long working distance objective (Olympus, 50x, 0.55 N.A.). For each sample between 6 and 10 spectra were collected for averaging. Processing was performed with iRootlab³⁹³ and Renishaw's WiRE software (example of spectra before and after processing can be seen in Appendix D). Spectra were denoised using wavelet smoothing and baseline corrected with an 8th order polynomial in iRootlab. WiRE was used to curve fit and determine peak areas (example in Appendix E). For the batch reproducibility measurements, the measured creatinine peak (685 cm⁻¹) was not normalised to another. For the other results, the peak area of the peaks at 1760 cm⁻¹ and 1850 cm⁻¹ were taken with the 1760 cm⁻¹ peak being from creatinine and the 1850 cm⁻¹ peak being from the polyelectrolyte within the sensors and therefore acting as an internal standard to normalize the creatinine peak to. Similarly, for neopterin, the peak area of the peak at 695 cm⁻¹ was normalized to another internal standard peak at 887 cm⁻¹. The wavenumber regions of the extended scans were chosen to focus on known peaks for neopterin and creatinine.

3.3.8 Data Analysis

All data analysis was performed in GraphPad Prism 8 including correlations, regression analysis, Bland-Altman plots, paired t-tests, ANOVA and descriptive statistics. Mean peak areas were interpolated from standard curves produced for both neopterin and creatinine with both HPLC and SERS.

3.4 Results and Discussion

3.4.1 Development and Optimisation of Layer-by-layer SERS Sensors

The SERS sensors have been fabricated to achieve controlled spacing between the two layers of gold nanoparticles (AuNPs). Two polyelectrolytes are used to form these spacing layers. Figure 3.2 shows a schematic of a fully assembled SERS sensor, showing the layers and the formation of a “hot spot” (red circle) between the two layers of AuNPs. This fabrication process enables tight control over the separation of nanoparticles in the radial direction, therefore controlling with a degree of precision, the formation of “hot spots”. Compared to using colloidal AuNPs for SERS enhancement, these sensors should provide improved reproducibility.

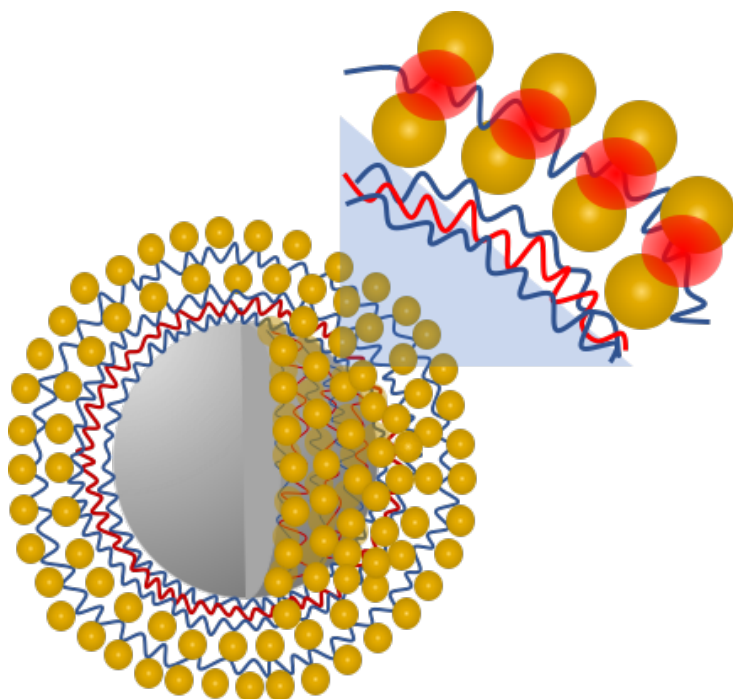


Figure 3.2 Schematic of a SERS sensor.

Fabricated using a layer-by-layer process of coating a silica microparticle with polyelectrolyte and two layers of gold nanoparticles. Nanoparticle separation in the

radial direction is controlled and thus “hot spot” formation is controlled between the two layers, producing reproducible SERS sensors.

UV-Vis scattering has been used to demonstrate the evolution of LSPR in the colloidal SERS sensors (Figure 3.3a). The λ_{\max} at 590nm represents singular AuNPs, whereas the red-shifted λ_{\max} at 850nm represents coupled AuNPs within the two layers on the SERS sensors. This information confirms that the two layers of AuNPs are in close enough proximity for LSPR to couple and form “hotspots”. This is similar to the λ_{\max} shift seen when colloidal AuNPs are aggregated; however, in the case of SERS sensors, the coupling is controlled as the AuNPs are fixed in space. Previous work has shown that colloidal SERS sensors prepared with 2 layers of AuNPs optimizes the SERS signal achieved using a 633nm excitation source³⁷⁶. In order to establish the optimum conditions for using the SERS sensors, several experiments were performed. Figure 3.3b shows that after a 10-minute soak of the analyte/sample with the colloidal SERS sensors, the SERS intensity obtained is at a peak, which then starts to decrease. For this reason, we chose to incubate every sample with colloidal SERS sensors for exactly 10 minutes before analysis. It could be sensible to leave the incubation period longer, until the signal is stable (around 30 minutes), and depending on the sample and the application of testing, this may be a preferred option. However, for a point-of-care type test, a smaller incubation time would be preferable. It is interesting that the intensity increases with incubation time to a peak, and then decreases again and before becoming stable. Reasoning for this could be due to movement of free analyte, it could be possible that over the initial 10 minutes, analyte is soaking into the sensors and signal intensity increases with analyte within the “hot spots” and close by, after 10 minutes, it is possible that analyte diffuses out of the sensors again, apart from that which has got “caught” within the layers. When multiple spectra are acquired from a single SERS sensor, the signal and therefore sensor are seen to deteriorate (figure 3.3c and 3.3d). Reducing laser power helps alleviate this, however this also leads to a reduction in SERS enhancement, which is counter-productive to what we are trying to achieve. For quantitative analysis, we have used maximum laser power, but each SERS acquisition is made from a separate SERS sensor within the sample rather than taking multiple acquisitions from a single sensor.

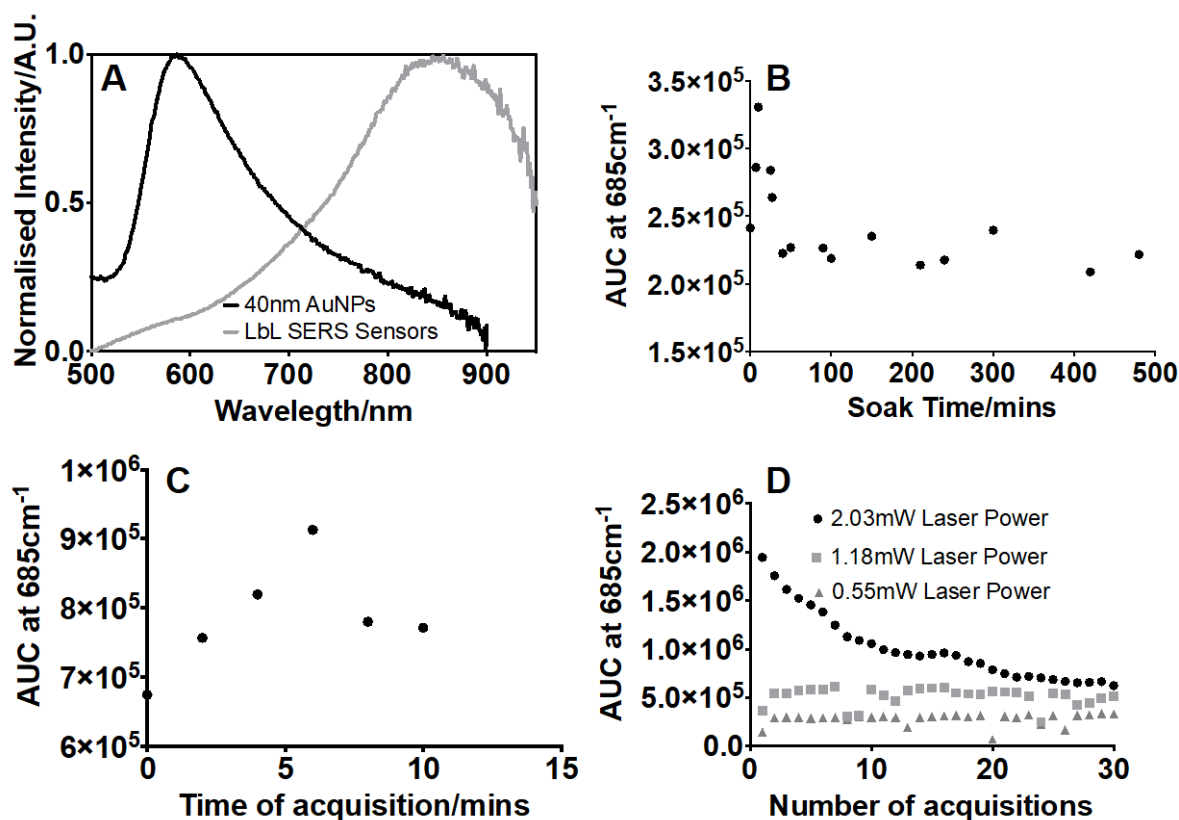


Figure 3.3 Results for optimisation testing of the SERS sensors.

(a) UV-Vis scattering measurement of prepared SERS sensors and colloidal 40nm AuNPs demonstrating the evolution of LSPR. (b) The area under curve of creatinine peak with an increasing soak time of analyte with the sensor. An increase and subsequent decrease in intensity is observed, with optimum soak time being 10-20 minutes. (c) The area under curve of creatinine peak with the time of acquisition. After 6 minutes (4 acquisitions) intensity obtained decreases as sensor degrades. (d) The area under curve of creatinine peak when multiple spectra are taken using a single sensor. With 100% laser power, maximum intensity is obtained; however, intensity decreases with each acquisition as the sensor degrades.

3.4.2 Batch reproducibility and stability of SERS Sensors

Assembly of the colloidal SERS sensors using the Lbl process was standardized to be as consistent as possible to ensure uniform SERS enhancement properties of the sensors. The reliability and stability of the fabrication process was assessed by taking multiple (100) SERS spectra of a standard sample (5mM creatinine) with two different batches of freshly prepared SERS sensors, a batch that had been stored at 4°C for one month, and with salt-aggregated 40nm colloidal AuNPs. All the spectra were analysed, and area under the curve of the peak at 675 cm⁻¹ plotted. Figure 3.4 shows the distribution of values within each batch as well as the consistently improved

enhancement achieved with SERS sensors over 40nm colloidal AuNPs. The mean areas under the peak for batch A and B were 7.0×10^5 and 7.1×10^5 respectively, compared to a mean of 4.1×10^4 when using the colloidal AuNPs. The variance within batch A was 26.0% (RSD), and batch B 27.8% (RSD) compared to a variance of 120.3% (RSD) between the 100 spectra taken with the colloidal AuNPs. Similarly, the batch-to-batch reproducibility was evaluated by performing a one-way ANOVA. No significant difference ($p=0.9655$) was shown between the measurements from batch A and B, however a significant difference ($p < 0.0001$) was observed when batch A and B were compared to 40nm colloidal AuNPs. The stability of the SERS sensors is demonstrated, analysis of the data by a one-way ANOVA, shows no significant difference ($p < 0.0001$) between the measurements taken with freshly prepared SERS sensors and those that had been stored for one month at 4°C prior to analysis.

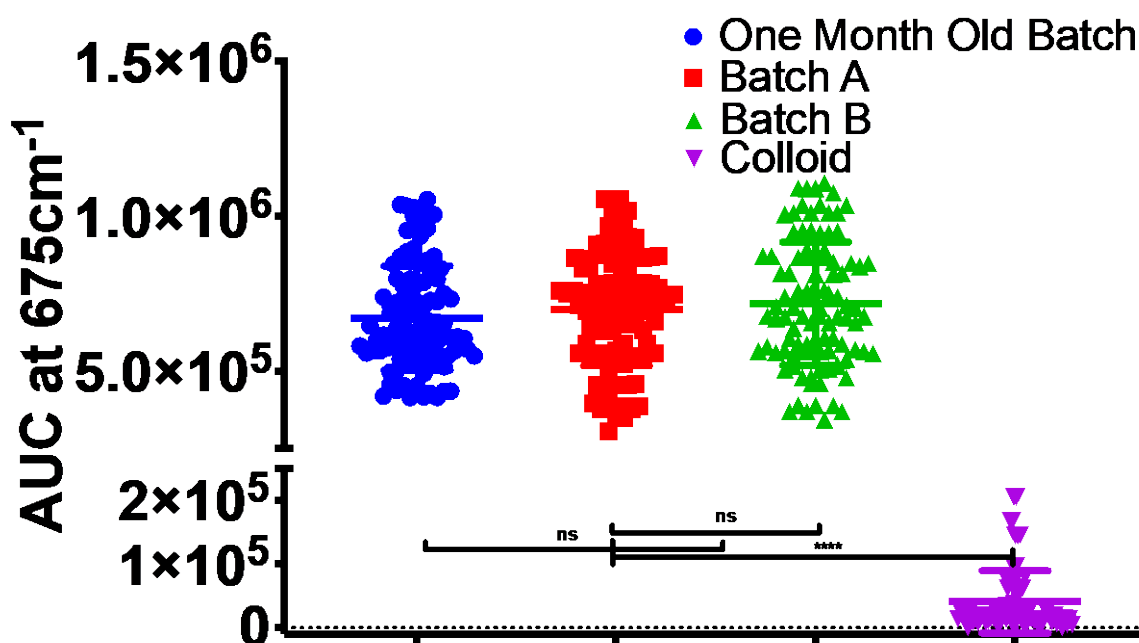


Figure 3.4 Verification of batch-to-batch reproducibility of the SERS sensors and improved enhancement over colloidal AuNPs.

Mean (RSD) values: One-month-old batch 6.7×10^5 (25.1), Batch A 7.0×10^5 (26.0), Batch B 7.1×10^5 (27.8), Colloid 4.1×10^4 (120.3). Appendix F shows processed spectra for these results. The raw and processed SERS spectra for this data can be seen in Appendix F.

These results demonstrate the increased enhancement of the SERS spectrum observed with the SERS sensors compared to SERS spectra obtained using salt-aggregated colloidal AuNPs. The within-batch reproducibility of the spectra obtained with SERS sensors shows variation (RSD 26.0 and 27.8%) but with significant improvement over the reproducibility obtained with colloidal

AuNPs (RSD 120.3%). Similar sample preparation and measurement is required whether using the SERS sensors or the colloidal AuNPs; therefore, the improved reproducibility with no additional sample preparation is a method enhancement. Analysis of the batch-to-batch reproducibility of the SERS sensors shows no difference in results obtained, suggesting there is no variation in formation or uniformity of the sensor in the manufacturing process. The SERS sensors are also shown to not deteriorate in storage, an additional promising feature.

3.4.3 Neopterin SERS verification

As with any analyte present in low concentration in a complex mixture, verification of SERS detection of neopterin in the presence of competing analytes was necessary. Known amounts of neopterin were spiked into samples of urine (standard addition method) with the peak height of the 685 cm^{-1} peak measured. 0, 5, 10, 20 and $40\mu\text{L}$ of $100\mu\text{M}$ neopterin were added to samples of urine specimen to give a $100\mu\text{L}$ total volume, including $12.5\mu\text{L}$ of urine sample, $5\mu\text{L}$ of sensors and water. For each prepared sample, 5 extended scans ($100\text{-}2000\text{ cm}^{-1}$) were collected, averaged and processed (baseline subtraction and smoothing). The results are shown in figure 3.5, where the peak corresponding to neopterin at 685 cm^{-1} can clearly be seen to increase in size with increasing neopterin concentration (figure 3.5B). The whole urine spectrum remains largely unchanged by the addition of the neopterin standard, as the changes are quite subtle and neopterin remains a weak Raman scatterer, however, knowing where to look in the spectrum it becomes more obvious (figure 3.5A and 3.5B). There is some change in the mid-spectrum region for the two higher volumes of neopterin, an overall increase in intensity in this region, and more defined peaks, this could be due to an interaction of the neopterin with other analytes in the urine, which only occurs when neopterin concentration reaches a critical amount within the sample. The measured peak heights of the 685 cm^{-1} peak are plotted against volume of neopterin added (figure 3.5C) which shows a sigmoidal concentration response similar to that of the calibration curve for pure neopterin. This figure could be used to calculate the concentration of neopterin in the urine sample as per the standard addition method, but this data is included here as a verification tool that neopterin concentration increases and is measurable despite being in the presence of competing analytes.

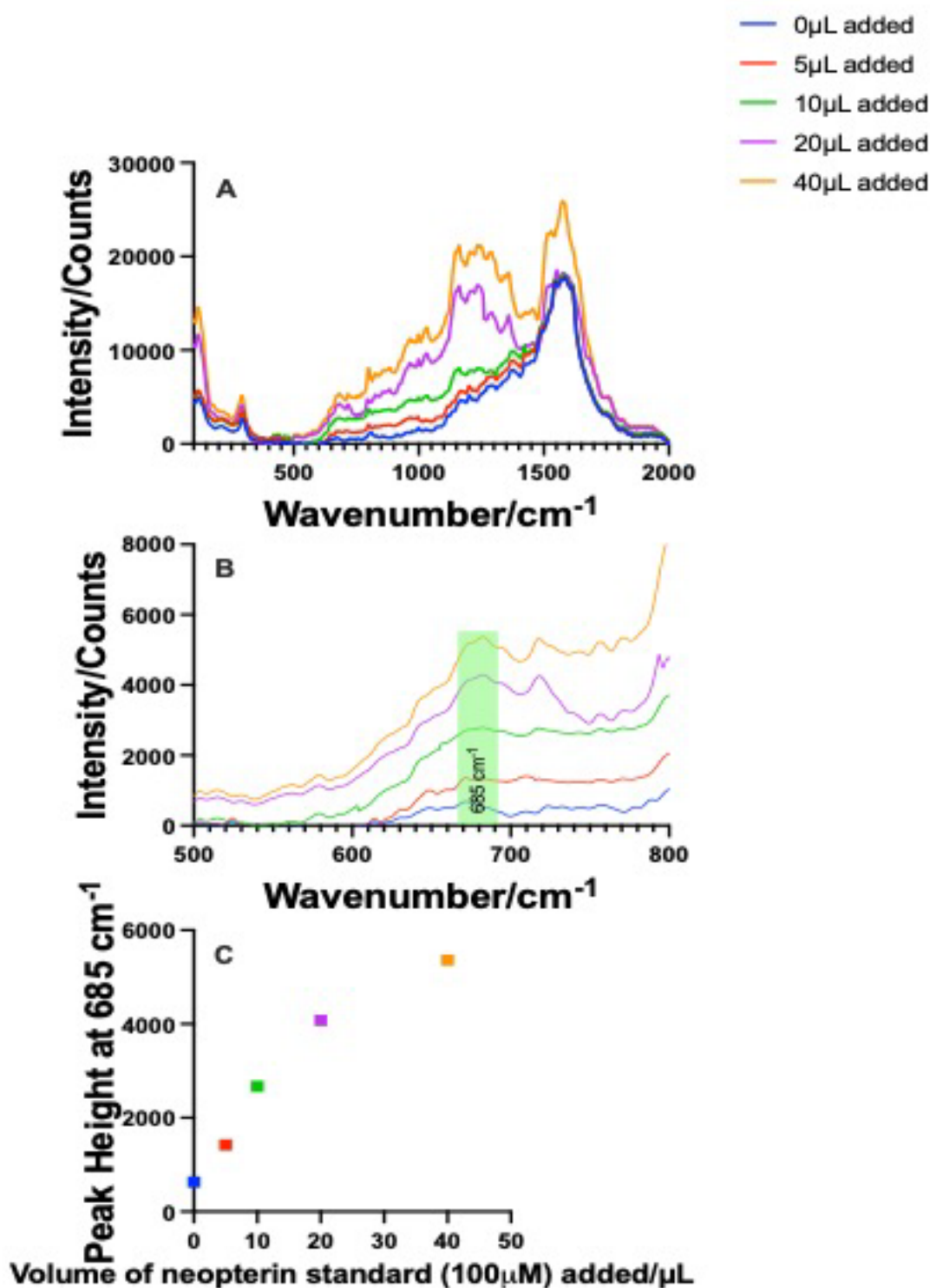


Figure 3.5 Verification of neopterin SERS measurement in a complex matrix of urine.

Increasing volumes of neopterin standard (100 μM) were added to samples of urine and SERS measurements made from SERS sensors within the sample. For each sample, 5 measurements were made before being averaged, baseline subtracted and smoothed. The volumes of neopterin added were 0, 5, 10, 20, and 40 μL of neopterin respectively.

3.4.4 Validation with synthetic urine samples

The use of colloidal SERS sensors has been demonstrated previously, and optimized conditions established³⁷⁶. However, this is the first use of such sensors in a complex matrix such as urine. A concern in the analysis of urine is being able to detect the analytes of interest accurately in a matrix of competing molecules and signals. We aimed to establish whether physiologically relevant concentrations of creatinine and neopterin could be detected and quantified and how the measurements obtained compared to both an expected value and a value obtained via HPLC. Synthetic urine samples were prepared with known concentrations of creatinine and neopterin and blinded prior to analyses. The concentrations calculated from the SERS measurement were found to be in very good agreement with the expected concentration of each sample (R^2 of 0.961 and 0.991 for creatinine and neopterin) as shown in figure 3.6 E and F. Additionally, the agreement between the two analytical methods was good (R^2 of 0.936 and 0.990 for creatinine and neopterin), demonstrating that at physiologically relevant concentrations, both methods perform equally well. The Bland-Altman analysis (figure 3.6 C and D) also shows the agreement between the two analytical methods, although there is bias for both creatinine (-0.0013) and neopterin (-0.24) these are both relatively small and insignificant for their concentration ranges. Measurements of neopterin have a larger associated error (error bars are 95% confidence intervals) which is most likely due to the much lower concentrations of the samples and possible deterioration of neopterin due to its light sensitivity¹³.

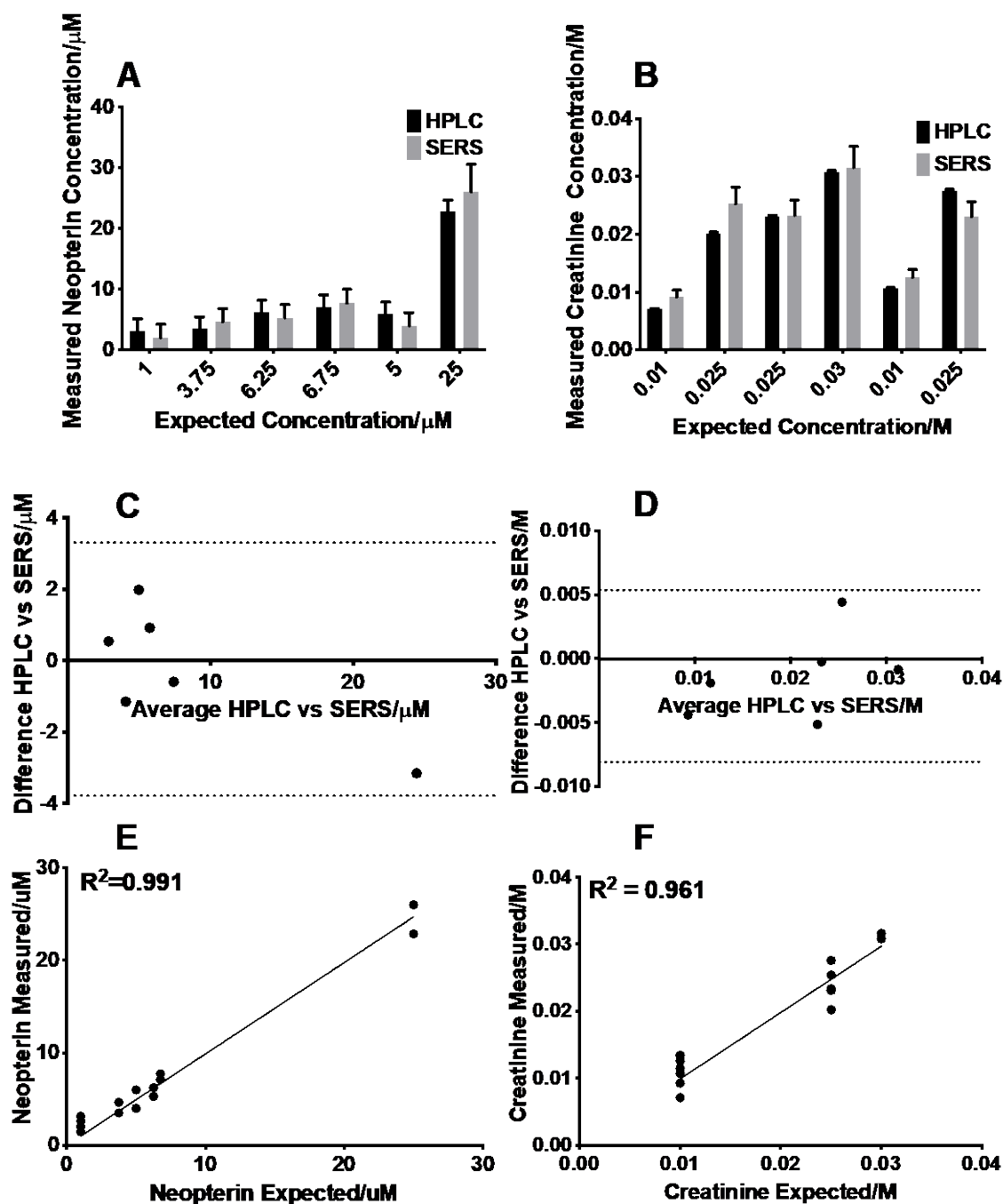


Figure 3.6 Results of expected vs measured synthetic urine samples

A and B) Expected vs measured concentrations of prepared synthetic urine samples analysed by SERS with SERS sensors and HPLC. Good agreement between SERS measurement and HPLC is observed. Each synthetic urine sample was measured 3 times for HPLC and 8 times for SERS before averaging. Mean plotted and error bars demonstrate 95% confidence intervals. C and D) Bland-Altman analysis of Neopterin and Creatinine concentrations measured by HPLC and SERS. -0.24 bias for neopterin and -0.0013 bias for creatinine. E and F) Correlation between expected and measured concentration (for SERS only) is $R^2 = 0.961$ and $R^2 = 0.991$ for creatinine and neopterin respectively. Appendix H shows processed SERS and HPLC data for

these results. Appendix G shows the standard curves for SERS and HPLC used for these results.

3.4.5 Measurement of urinary neopterin to creatinine ratio (UNCR)

To further evaluate the validity of the SERS sensors, experiments were repeated with human urine samples from a cohort of volunteers with unknown amounts of creatinine and neopterin. As unaware of the concentrations present within the samples, and the likely high concentrations of creatinine that risked saturating the system, it was deemed appropriate to measure each sample undiluted and at a 1:4 dilution. The undiluted samples were used to make measurement of neopterin and the 1:4 diluted samples were used to make measurement of creatinine due to creatinine being too concentrated in the undiluted samples to get an accurate measurement. This allowed both analytes to be measured in an optimum concentration range based on the concentration profiles already established for both HPLC and SERS.

The characteristic peaks for neopterin and creatinine were at 695 cm^{-1} , and 1760 cm^{-1} and these were both normalized to peaks present in the colloidal SERS sensors from the polyelectrolyte layers acting as an internal standard. Having an inbuilt internal standard within the SERS sensor allows normalization of the analyte peaks to that of the standard, allowing for fluctuations in intensity.

Table 3.1 shows a summary of the results from the two analytical approaches for each analyte, along with their associated percentage difference and the corresponding UNCR. As an example, for sample 03510, there was no difference in the creatinine predicted concentration between HPLC and SERS, HPLC predicted a neopterin concentration of $1.45\mu\text{M}$, compared to $1.24\mu\text{M}$ predicted from SERS, a difference of 15.61%. Overall, for all samples analysed, the percentage difference between the two analytical approaches ranged from 0% to 40%, with the average being 12.77% for creatinine and 17.85% for neopterin. Although somewhat larger than ideal, this is still encouraging considering the low concentrations being measured (for neopterin) and the simplicity, ease and speed of the method compared to others published, demonstrating the real potential for point-of-care testing.

Table 3.1 Summary of results for human urine samples: HPLC, SERS and the associated percentage difference (RSD) between the two analytical approaches for neopterin(μM), creatinine(M) and UNCR($\mu\text{mol/mol}$).

The neopterin measurements were performed on undiluted samples and the creatinine measurements were performed on 1:4 dilution samples. Appendix I shows processed SERS and HPLC data for these results.

Sample	Creatinine HPLC/M	Creatinine SERS/M	Difference/%	Neopterin HPLC μM	Neopterin SERS/ μM	Difference/%	UNCR HPLC/ μMM^{-1}	UNCR SERS/ μMM^{-1}	Difference/%
SAMPLE 1 (0577)	0.006	0.006	0.000	0.70	0.71	1.42	121.13	126.93	4.68
SAMPLE 2 (03510)	0.004	0.004	0.000	1.45	1.24	15.61	340.30	296.05	13.91
SAMPLE 3 (0549)	0.004	0.003	28.571	0.81	0.99	20.00	225.98	295.53	26.67
SAMPLE 4 (05712)	0.002	0.002	0.000	0.77	0.52	38.76	368.46	284.19	25.82
SAMPLE 5 (05711)	0.010	0.009	10.526	2.50	3.40	30.51	257.89	391.16	41.07
SAMPLE 6 (0207)	0.010	0.009	10.526	3.79	3.44	9.68	381.31	363.72	4.72
SAMPLE 7 (05412)	0.015	0.012	22.222	3.58	3.47	3.12	238.47	288.80	19.09
SAMPLE 8 (0518)	0.008	0.006	28.571	2.13	2.63	21.01	264.83	410.76	43.20
SAMPLE 9 (0309)	0.006	0.004	40.000	1.22	0.82	39.22	196.93	215.90	9.19
SAMPLE 10 (04810)	0.016	0.016	0.000	4.22	3.56	16.97	263.78	229.39	13.95
SAMPLE 11 (0458)	0.013	0.017	26.67	6.49	6.34	2.34	512.47	374.55	31.10

To further establish the reproducibility of this SERS approach, we have analysed 6 samples (one synthetic and 5 human urine) in triplicate (table 3.2). Batch-to-batch variation and reproducibility of SERS enhancement are significant factors for determining a SERS substrate's suitability for quantitative measurement³⁹⁴. Inconsistent enhancements are often seen with colloidal substrates due to variations in colloidal concentrations and nanoparticle aggregation. Colloidal SERS sensors overcome these issues, and we have already shown that there is no statistical significance between measurements taken with separate batches (figure 3.4).

Table 3.2 Measured concentrations of Creatinine (M) and Neopterin (μM) in urine samples, measured in triplicate with SERS using Lbl sensors.

Each triplicate sample was prepared and analysed separately. Appendix H and I show processed spectra for these results.

Sample	Creatinine/M			Creatinine/M		Neopterin/ μM			Neopterin/ μM	
				<i>Mean</i>	<i>%CV</i>				<i>Mean</i>	<i>%CV</i>
A	0.0115	0.0134	0.0092	<i>0.011</i>	<i>18.35</i>	2.595	1.447	2.028	<i>2.023</i>	<i>28.36</i>
Sample 2 (03510)	0.0044	0.0042	0.0038	<i>0.004</i>	<i>7.34</i>	1.255	1.243	0.926	<i>1.141</i>	<i>16.33</i>
Sample 12 (0355)	0.0016	0.0020	0.0018	<i>0.002</i>	<i>12.28</i>	0.686	0.632	0.719	<i>0.679</i>	<i>6.48</i>
Sample 1 (0577)	0.0056	0.0060	0.0057	<i>0.006</i>	<i>3.98</i>	0.709	0.811	0.597	<i>0.706</i>	<i>15.11</i>
Sample 5 (05711)	0.0087	0.0078	0.0072	<i>0.008</i>	<i>9.61</i>	3.398	2.839	2.307	<i>2.848</i>	<i>19.15</i>
Sample 4 (05712)	0.0018	0.0027	0.0032	<i>0.003</i>	<i>26.15</i>	0.525	0.583	0.928	<i>0.678</i>	<i>32.11</i>

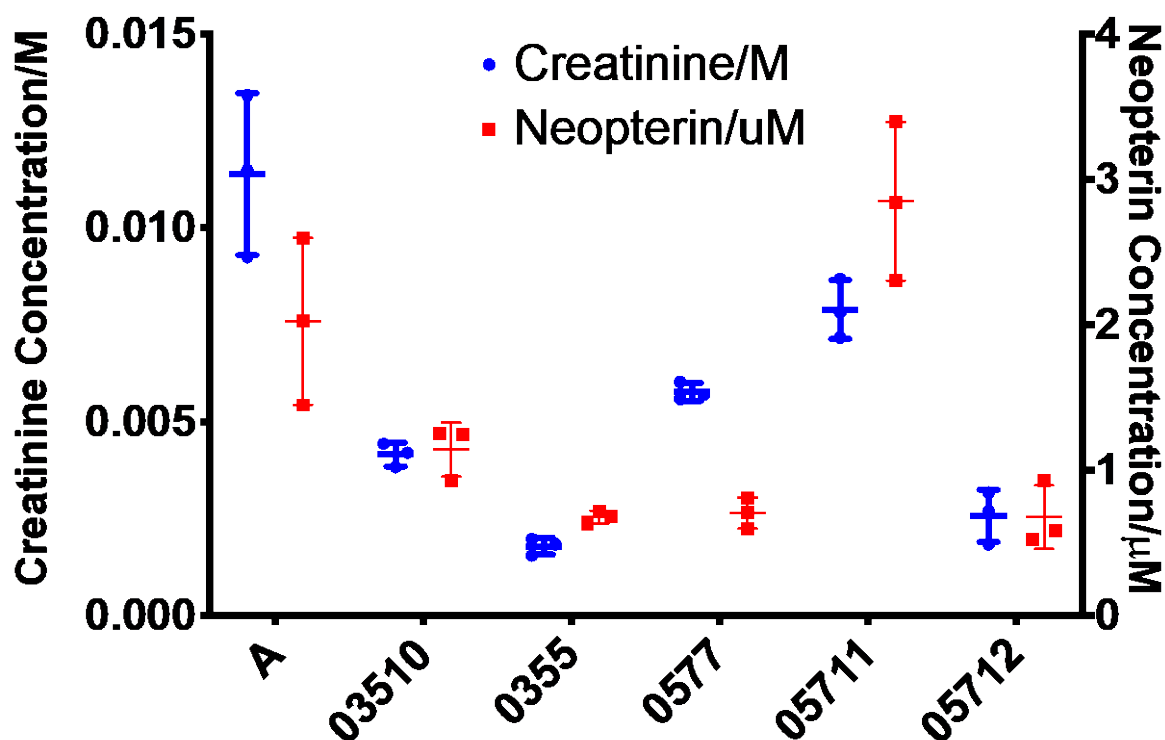


Figure 3.7 Summary of results for the triplicate analysis of urine samples.

Average concentration from triplicate measurement for neopterin(μM), creatinine(M) and the relative standard deviation (RSD, % difference) between measurements. Appendix H and I shows processed SERS spectra for these results.

As an example, for sample 0577, the percentage difference in the three measurements obtained for creatinine was 3.98% and for neopterin 15.11%. The average percentage difference for triplicate analysis is 12.45% for creatinine and 17.75% for neopterin, thus demonstrating reasonable precision and overall reproducibility.

As a quick and simple analytical alternative to HPLC that does not require any sample preparation steps (other than dilution and mixing), the addition of standards such as that required for SAM, use of expensive immunochemistry or multivariate analysis; quantification with colloidal SERS sensors can be achieved with good enough accuracy and precision to be considered a valid method.

3.4.6 Stratification of results into 'risk' categories/screening tool

We have demonstrated that SERS using the colloidal SERS sensors can quantify two analytes of interest, creatinine and neopterin, in the complex matrix of urine. The benefit of measuring these two compounds is to determine the UNCR as a marker of immune system activation. Individuals with a consistently raised UNCR ($>251\mu\text{mol/mol}$ (cut off value from literature⁴⁷)) are more

susceptible to age-related diseases and poorer prognosis of disease. Therefore, can this analytical method be used as a screening method to determine a clinically relevant factor? i.e. which individuals are 'at risk' of poorer disease prognosis. After calculating the UNCR for each urine sample, we have then stratified it as high or low risk depending on the 251 $\mu\text{mol/mol}$ threshold and compared the stratification results to those obtained via the HPLC measurements and looked at the agreement (taking the HPLC measurements as gold standard).

Screening sensitivity was found to be 83%, and screening accuracy 72%

$$\text{Sensitivity} = \frac{\text{True Positive}}{\text{True Positive} + \text{False Negative}}$$

$$\text{Accuracy} = \frac{\text{True Positive} + \text{True Negative}}{\text{True Positive} + \text{False Positive} + \text{True Negative} + \text{False Negative}}$$

Table 3.3 UNCR($\mu\text{mol/mol}$) values obtained for urine samples via HPLC and SERS and agreement of risk stratification between two methods (presuming HPLC correct as gold standard).

Results demonstrate agreement in risk stratification as high/low UNCR (above or below 251 $\mu\text{mol/mol}$) for 8 of the 11 samples, demonstrating for screening 72% accuracy and 83% sensitivity.

Sample	UNCR HPLC/ μMM^{-1}	UNCR SERS/ μMM^{-1}	Correct stratification as high/low risk
0577	121.13	126.93	Yes
03510	340.30	296.05	Yes
0549	225.98	295.53	No (false +ve)
05712	368.46	284.19	Yes
05711	257.89	391.16	Yes
0207	381.31	363.72	Yes
05412	238.47	288.80	No (false +ve)
0518	264.83	410.76	Yes
0309	196.93	215.90	Yes
04810	263.78	229.39	No (false -ve)
0458	512.47	374.55	Yes

Assuming the stratification based on HPLC results to be accurate (as gold standard), we found 8 of our 11 samples made the correct assignment of high/low risk based on UNCR < or > 251 $\mu\text{mol/mol}$. Allowing for a small sample size (n=11) this demonstrates the SERS method to have 72% accuracy and 83% sensitivity as an analytical tool to stratify individuals into risk category based on their

level of inflammatory marker -neopterin in their urine. Two of the three samples that weren't correctly assigned are close in concentration to the 251 $\mu\text{mol/mol}$ cut-off, therefore, it may be advisable to have a testing protocol whereby if a sample concentration comes out as within 15% of the cut-off value (213-289 $\mu\text{mol/mol}$), then it should be re-analysed at a different dilution.

3.5 Limitations

This work has demonstrated within batch reproducibility of novel SERS sensors of 26% (RSD) when measuring a single analyte peak. Improved reproducibility is shown when using an internal standard peak against which to normalise the analyte peak. Urine samples measured in triplicate have shown reproducibility in the range of 12-18% (RSD). These measurements compare well to even commercially available SERS substrates. Reproducibility has been assessed with two commercially available substrates, Klarite and QSERS, using Rhodamine-6G as an analyte, the reported reproducibility range from 13- 21.41% (RSD) depending on whether peak area or peak intensity was measured³⁹¹. Equally, reproducibility of neopterin measurement in urine with ELISA has been shown to be around 14%. Therefore, our obtained reproducibility with analytes in a complex matrix such as urine, without the cost of commercially available substrates or expensive reagents, is promising. Additionally, when considering the method proposed in this chapter, utilising the SERS sensors to measure UNCR in urine samples, the sensitivity of screening an individual's urine to categorise them as 'at risk' is 83% which is a reasonable sensitivity for a screening test. Other screening tests that are based on lateral flow devices or ELISA for example, show sensitivities with similar values. For example, a ELISA and lateral flow immunoassays for SARS-CoV-2, are on average around 80%³⁹⁵.

Although promising, it is likely that the SERS sensors performance in measuring analytes in urine samples could be improved, as chapter 4 will demonstrate. Additional validation measurements are also recommended for good analytical practice, such as recovery rate and root mean square error (RMSE)³⁹⁰. Recovery rate is the ratio of the detected concentration to the actual known concentration in the sample. RMSE gives an estimation of the precision of the SERS sensor and is best calculated on a validation data set to determine the predictive power of the sensors.

3.6 Conclusions

We have demonstrated for the first time the use of colloidal SERS sensors as a substrate for SERS of urine. Optimized conditions for using the sensors have been established and used to measure two analytes- neopterin and creatinine, with improved enhancement and reproducibility over using colloidal AuNPs.

Chapter 3

To validate the use of colloidal SERS sensors, we analysed synthetic urine that was prepared with known concentrations of neopterin and creatinine and established that the SERS method could quantify the concentration of each analyte with good accuracy. There was good agreement between the SERS and HPLC results that were used for benchmarking.

We have further demonstrated the analytical capability of this technique when using human urine samples and found promising results with good reproducibility when performed in triplicate.

We can conclude that the technique provides promise as an analytical method for absolute quantification of two biologically relevant biomarkers in urine. As a tool for stratifying individuals into 'risk' categories based on their level of immune system activation, the technique works well.

The benefits of SERS as an analytical technique are clear; the acquisition is fast allowing multiple spectra to be taken (averaging would improve results), portable equipment would allow it to be used at point-of-care in a clinical or home setting, it is highly sensitive and molecularly specific, and requires no need for markers or labels. Additionally, our technique requires no sample preparation or complex spectral analysis; therefore, could easily be carried out by an 'untrained' individual such as clinical staff or patient.

Chapter 4 Towards Point-of-Care testing: a paper-based lateral flow assay for SERS detection of inflammatory marker in urine

4.1 Overview

Chapter 2 evidenced the clinical reasoning behind measuring neopterin and creatinine in urine, and the benefit that monitoring at point-of-care would provide. Chapter 3 demonstrated that SERS, as a technique in combination with our fabricated sensors, can with reasonable accuracy and reproducibility, measure these molecules in samples of urine. This chapter aims to develop the SERS sensor technique into something that would be useable at the point-of-care; the feasibility of paper-based devices for a SERS lateral flow assay is demonstrated, and the proof-of-concept that the paper device can separate the analytes of interest via paper chromatography is shown.

4.2 Introduction

4.2.1 The challenge of developing point-of-care testing

Point-of-care testing (POCT) is defined as biochemical testing at or near the site of patient care, whenever the medical care is needed³⁹⁶ and that yields immediate acquisition of information on an individual's condition to facilitate treatment decisions or more extensive testing³⁹⁷. There is a clinical drive towards POCT for more efficient clinical diagnosis and improved patient care³⁹⁸.

The global POCT market is expected to reach USD 39.96 billion by 2021 with a compound annual growth rate of 9.8%³⁹⁹. Emerging technological innovations in smartphones, biosensors, lab-on-a-chip and wearable devices are transforming the point-of-care diagnostic market. The driving force behind these innovations in healthcare is to provide expedited, clinically informative results, whether the patient is seen in a clinical setting or their own home. The point-of-care (POC) diagnostics industry will be part of a paradigm shift from curative medicine to predictive, personalised and pre-emptive medicine.

The required features of point-of-care devices are³⁹⁸:

1. Simple to use
2. Reagents and consumables are robust in storage and usage

Chapter 4

3. Results should be concordant with an established laboratory method
4. Device together with associated reagents and consumables are safe to use

Currently, most chemical and biochemical analysis is performed using mass spectrometry (MS), liquid chromatography (LC) or the combination of the two LC/MS, which is unrivalled for both sensitivity and specificity. However, these methods are confined to laboratories and analysis turnaround times are prolonged. Compact and lightweight instrumentation that can be used at the POC is desirable.

The biggest challenge for emerging POCT technologies to be translated into clinically and commercially viable products, is the demonstration of high analytical precision and reproducibility, for analyte quantification in large numbers of patient samples, without significant interference from other substances. Additionally, the technology needs to be validated by accredited technologies. Batch-to-batch variability and quality control can also be problematic, particularly for paper-based assays^{400,401}.

For early diagnosis of a disease, a POCT relies on detection of biomarkers in low concentration in complex body fluids such as blood and urine. Many devices currently being used for POCT are colorimetry-based lateral flow assays (LFA) because they are low in cost, provide rapid analysis in a user-friendly (non-expert) format. However, detection sensitivity is limited, and they cannot provide a quantitative measurement. The obvious example of this is the pregnancy test, a lateral flow immunoassay. These assays typically use gold nanoparticle (AuNP) labelled antibodies to give selective detection of the target analyte, with the colour change being detected by eye. If the analyte is present in too low a concentration, it may be insufficient to elicit a colour change and therefore would give a false negative result. Equally, at high analyte concentrations, the intensity of the coloured line reaches a ceiling effect because it is limited by the number of labelled antibodies becoming saturated. Using a reader to determine the colour density can give a semiquantitative measurement, but this is limited by low sensitivity and precision^{402,403}. It is also not possible to detect multiple analytes at the same time because although different antibodies conjugated to AuNPs can be used for different target analytes, a reader cannot distinguish between the two. Raman spectroscopy (Surface-enhanced Raman spectroscopy (SERS)) combined with a lateral flow assay can overcome these issues as it combines high sensitivity, quantification and multiplexing which has been extensively demonstrated⁴⁰⁴⁻⁴¹⁵. Several reports have demonstrated combination of SERS with LFA for health diagnostic applications^{405,409,416-418}.

4.2.2 The need for point of care testing- a global pandemic driving force

With the current global pandemic (SARS-CoV-2) highlighting the need for super-rapid diagnostic tests, never has there been a greater demand for on-the-spot, user-friendly testing methods. This year (2020) has seen a huge drive in diagnostic research led by a need to find cheaper, better, faster, diagnostics with exceptional sensitivity.

In the first 6 months of 2020, more than 20,000 articles have been published on SARS-CoV-2. Research into testing has focused on both direct molecular diagnostic testing for current viral infection, as well as antibody testing to assess possible immunity to subsequent infection. A global pandemic certainly motivates research efforts worldwide.

There are a lot of questions and considerations including how to collect a specimen, which specimen to collect, when to collect it during the course of the disease, as well as which are the best methods of testing. At present, the recommended diagnostic test involves detection of viral RNA using nucleic acid amplification tests (NAAT) such as polymerase chain reaction (PCR)-based tests, with the recommended sample being a nasopharyngeal swab. The virus can be detected in other specimens, such as blood, saliva and stools, but these have generally been shown to be less reliable at present⁴¹⁹. However, it is strikingly apparent that the upscaling of these tests to process the volumes of samples that require testing is inadequate.

Other testing has focused on antigen detection; several rapid antigen tests have been proposed⁴²⁰ mostly focusing on lateral flow immunoassays. The advantages of the antigen tests are their rapidity, 10-30 min instead of hours, for NAAT testing, ease of interpretation, and limited technical skill and infrastructure required. However, the sensitivity is low, and the specificity is poor⁴²¹ as there is potential for the non-specific cross-reaction with other human coronaviruses⁴²². Monoclonal antibodies specifically against SARS-CoV-2 are in development. In published studies on the diagnostic performance of rapid assays, the sensitivity and specificity ranged from 9% to 88.6% and from 88.9% to 91.7%, respectively⁴²³⁻⁴³⁵. Of note, the sensitivity of these tests performed in countries other than China were substantially lower than those reported for studies conducted in China. Antibody-based approaches are hampered by their relatively slow development compared to nucleic acid tests and are time-consuming and expensive to produce. Reviews of current commercialised technologies focused on COVID-19 diagnosis have been published^{436,437}.

The severity of disease with SARS-CoV-2 is greater in those with pre-existing comorbidities such as cardiovascular conditions⁴³⁸⁻⁴⁴⁰. As well as comorbidities, several risk factors such as high D-dimer⁴⁴¹, neutrophils⁴⁴², liver damage⁴⁴³, and deranged clotting⁴⁴⁴ have been associated with

disease severity. Zhou et al. have developed a predictive risk model to accurately predict those who will have severe disease without taking into account disease symptoms or requiring chest imaging. Their risk score includes gender, age, hypertension, stroke, diabetes mellitus, ischaemic heart disease/heart failure, respiratory disease, renal disease, increases in neutrophil count, monocyte count, sodium, potassium, urea, alanine transaminase, alkaline phosphatase, high sensitive troponin-I, prothrombin time, activated partial thromboplastin time, D-dimer and C-reactive protein, as well as decreases in lymphocyte count, base excess and bicarbonate levels⁴⁴⁵. Their model is based on test results taken on the day of admission into hospital and looked at an outcome of need for intensive care admission, intubation or all-cause mortality. This model showed an excellent predictive outcome value in the 4445 patients included who tested positive for SARS-CoV-2. Those patients with the outcome of intensive care admission, intubation, or all-cause mortality, had a significantly higher risk score (median: 19, 95% CI: 14-24, max: 37) than those who did not (median:8, 95% CI:5-11, max: 34)⁴⁴⁵.

Currently, the availability of simple clinical risk scores for risk stratification is limited. The COVID-GRAM predicts the development of critical illness, based on symptoms, radiograph results, clinical and laboratory details⁴⁴⁶. Similarly, the 4C Mortality Score includes eight variables readily available at initial hospital assessment: age, sex, number of comorbidities, respiratory rate, peripheral oxygen saturation, level of consciousness, urea level, and C-reactive protein⁴⁴⁷.

The First Affiliated Hospital, Zhejiang University School of Medicine also recommends the surveillance of inflammatory response biomarkers for the SARS-CoV-2 infection: C-reactive protein, procalcitonin, ferritin, D-dimer, IL-4, IL-6, IL-10, TNF- α and INF- γ . Low total number of lymphocytes at the onset of disease is also an indicator of poor prognosis.

FebriDx is a commercially available POC device that measures C-reactive protein and myxovirus resistance protein A (stimulated by interferon-alpha/beta cells), to distinguish between acute bacterial and viral infections. FebriDx has been shown to have reasonable diagnostic accuracy in a hospital setting with high COVID-19 prevalence, outside of influenza season. More research is needed to establish the accuracy of the test when used in a lower COVID-19 prevalence area, or when other respiratory infections are in circulation⁴⁴⁸.

Clearly, the use of additional biomarkers such as inflammatory markers could help diagnose and predict risk of severity of SARS-CoV-2. The biosensing community has been urged to create affordable, rapid, sensitive and multiplexed systems amenable to mass production in order to detect these biomarkers simultaneously.

4.2.3 Utilising intrinsic molecular characteristics of the target analyte-Raman spectroscopy for point-of-care testing

Raman spectroscopy is a form of vibrational spectroscopy. Molecularly-specific information is gleaned from the spectrum of scattered light that occurs due to the vibrations that occur within each molecule. The spectrum of scattered light is characteristic of, and can therefore be used to identify, molecules. Raman spectroscopy is an ideal analytical technique for POCT; it is suitable for measuring aqueous samples without any destruction to the sample or need for labels. One disadvantage is that the Raman signal can be weak and difficult to detect, particularly with molecules in low concentration, thus limiting its use in biomedical applications. However, the inherently weak Raman signal can be enhanced by utilising plasmonic metal nanostructures, a technique known as surface-enhanced Raman spectroscopy (SERS). In recent years, studies have begun to be published which use SERS to detect human diseases such as neurological diseases^{449,450}, diabetes⁴⁵¹, kidney disease⁴⁵² and cardiovascular diseases⁴⁵³. Additionally, multiple cancers, such as breast, lung, colorectal, and viral diseases including influenza, hepatitis, HIV and those responsible for tropical diseases, have also been detected by SERS⁴⁴⁹.

Research in the Raman field largely uses benchtop spectrometers because they provide good accuracy, high sensitivity, excellent resolution and multiple excitation wavelengths. However, due to their size and complex operation, they are not suitable to be used at POC. Portable hand-held Raman devices are also available and have been used for on-site, real-time Raman spectroscopy⁴⁵⁴⁻⁴⁵⁶. The miniaturisation of the Raman components that is necessary to make a hand-held device results in some loss to the sensitivity of the Raman signal, but with a suitable low-cost but well-performing SERS substrate, the amplification of the Raman signal can make SERS-based POCT possible. Another alternative is smartphone-based Raman systems; a smartphone Raman spectrometer in combination with SERS devices made from low-cost filter paper and silver nanoparticles has been demonstrated⁴⁵⁷.

In a recent review, Restaino and White identify critical criteria that should be met for POC SERS⁴⁵⁸:

- Individual sensors (devices) must be inexpensive, enabling a low per-test cost
- Instrumentation must be portable, preferably handheld
- The usage procedure must be rapid and easy-to-perform, preferably single-step with minimal instrument precision required
- Detection limits must be sufficiently low in order to measure trace levels of the target

There is growing interest in the use of microfluidic devices with SERS^{459,460}. Microfluidics are attractive for POCT with SERS analysis due to the possibility of integrated sample preparation

within the device. However, fabrication becomes complex when trying to engineer the interactions between the analyte and plasmonic nanostructures within the device. This fabrication complexity is costly and would not result in devices suitable for POCT as they would be expensive to produce in bulk. Additionally, sample-loading into a microfluidic device is non-trivial, a desirable device would have a world-to-device interface that enables easy sample collection, e.g. a dipstick that is pipette and tubing free.

4.2.4 Using paper as an alternative cost-effective but reproducible substrate

Nanoparticles in colloidal aqueous solutions have routinely been used as SERS substrates; however, their use is limited due to poor stability and low reproducibility. Micro- and nanofabricated sensors deliver large enhancement with high-level reproducibility because they are very controlled, each location on a sensor is very much like all other locations on that sensor, and all sensors from a batch are alike. Current methods of fabricating efficient SERS substrates include the immobilisation of metallic nanoparticles on rigid substrates (glass, quartz and silicon)^{461,462}, or the fabrication of metallic nanostructures using lithography¹⁰⁷. However, these methods are high cost, have long preparation times and sophisticated manufacturing techniques.

An alternative approach is to use paper-based substrates with their low-cost, ease of manufacture and lower environmental impact⁴⁶³. Paper is porous, and therefore metal nanostructures can easily be deposited into it. Paper is also inexpensive and flexible, making it suitable for low-cost, high-throughput production. Other useful features of paper-based devices are its flexibility and large surface area, making it suitable for collecting samples by way of swabbing as reported by Lee et al.⁴⁶⁴. Another advantage for sample collection is that liquids can wick through paper, enabling the passive transfer of samples without the need for manual pipetting or pumps. This means devices can be used as a dipstick rather than manually collecting the sample and transferring it to the device, it can simply be dipped into the sample and analysed.

To achieve SERS enhancement, the nanoparticles (similar to colloidal systems) need to be closely spaced or aggregated within the paper substrate to achieve high signal enhancement. The distribution of the plasmonic nanostructures in paper substrates is likely to be completely random because of the surface topology of the paper and the deposition/formation of the nanoparticles. This may result in clustering, leading to the SERS signals from one spot on the device being unequivalent to another spot. The best reproducibility across paper SERS devices that have been reported range between 10 and 15%⁴⁶⁵⁻⁴⁷¹. Reproducibility can be improved by sample averaging across the device, averaging across multiple devices, and some handheld spectrometers feature rastering and line scanning⁴⁷².

Conventional SERS devices manufactured on silicon or silica have virtually no background signal, whereas paper results in larger background signals due to the composition of organic polymers and the chemicals that are often used to enhance strength and colour. The background signal that originates from such chemicals may dominate the spectrum when measuring analytes in low concentration, affecting both reproducibility and the detection limit. Filter paper and chromatography paper have been found to have the smallest background for SERS⁴⁷³.

4.2.5 Producing SERS active paper devices

To form hot spots and achieve better Raman enhancement, metal nanostructures have been integrated into paper via soaking/dip coating^{474,475}, inkjet printing^{114,473}, screen printing⁴⁷⁶ and filtration⁴⁷⁷. Figure 4.1 depicts some of these methods.

In-situ synthesis involves forming metallic nanostructures on either the surface of or within the pores of the paper substrate. An example of this is cellulose paper being oxidised to expose aldehyde groups and Tollens' reagent added to form silver nanoparticles via the silver mirror reaction⁴⁶⁵. Another example is to alternately soak unmodified cellulose paper in AgNO_3 and NaBH_4 to form silver nanoparticles in-situ⁴⁷⁸. As these methods require immersion of the paper, the resulting nanoparticles form across the whole surface. Another method has been demonstrated whereby the nanoparticles are patterned onto one area by inkjet printing lecithin and potassium iodide onto printing paper before immersing the paper into HAuCl_4 solution, thus forming gold nanostructures in the printed area only⁴⁶⁶. Similarly, silver and halide solutions have been inkjet-printed onto paper, whereupon adding photographic developer solution and exposing the paper to light the plasmonic nanostructures are formed⁴⁷⁹. Although the materials are inexpensive for these in-situ methods, the soaking/rinsing/printing steps that they require leaves them unsuitable for high-throughput manufacturing.

Nanoparticles can be deposited onto paper by simply dipping the paper into a prepared solution of nanoparticles. Lee et al. first demonstrated this by soaking cellulose paper in a colloid of gold nanorods⁴⁶⁴. Dip-coated substrates are a lot quicker to produce than those by in-situ synthesis; however, there are still drawbacks because patterning of sensors is not possible, and there is no control over the distribution of them. Also, a significant volume of nanoparticle colloid is wasted in production.

White's group prepared nanosized silver colloids by Lee and Meisel's method and then printed them onto chromatography paper with an inkjet-printer to obtain a sensitive SERS substrate^{114,473}. Other groups have since reported similar techniques^{480,481}, and others have reported spraying colloid ink to form patterned arrays of nanoparticles^{468,482,483}. Spray-coating plasmonic AuNPs onto

paper has been shown to notably improve loading efficiency and distribution in a much shorter time compared to dip- or drop-coating methods⁴⁸³. Sensing capability was also 2 times higher than with a dip-coated sensor, and adding a second layer of AuNPs greatly enhanced SERS signals.

Others have simply spotted nanoparticles onto the paper^{484,485}, or used pens or brushes to apply nanoparticles^{469,486,487}. A slightly more high-throughput option has been achieved by screen-printing a colloid ink onto paper^{476,488,489}.

By far the simplest and most common approach to introducing nanoparticles onto a paper substrate is through either spin or dip/drop coating⁴⁹⁰⁻⁴⁹². However, the inkjet-printing technology allows the loading of the plasmonic nanoparticles to be precisely controlled^{480,493,494}, which is, of course, advantageous for reproducibility of the substrate.

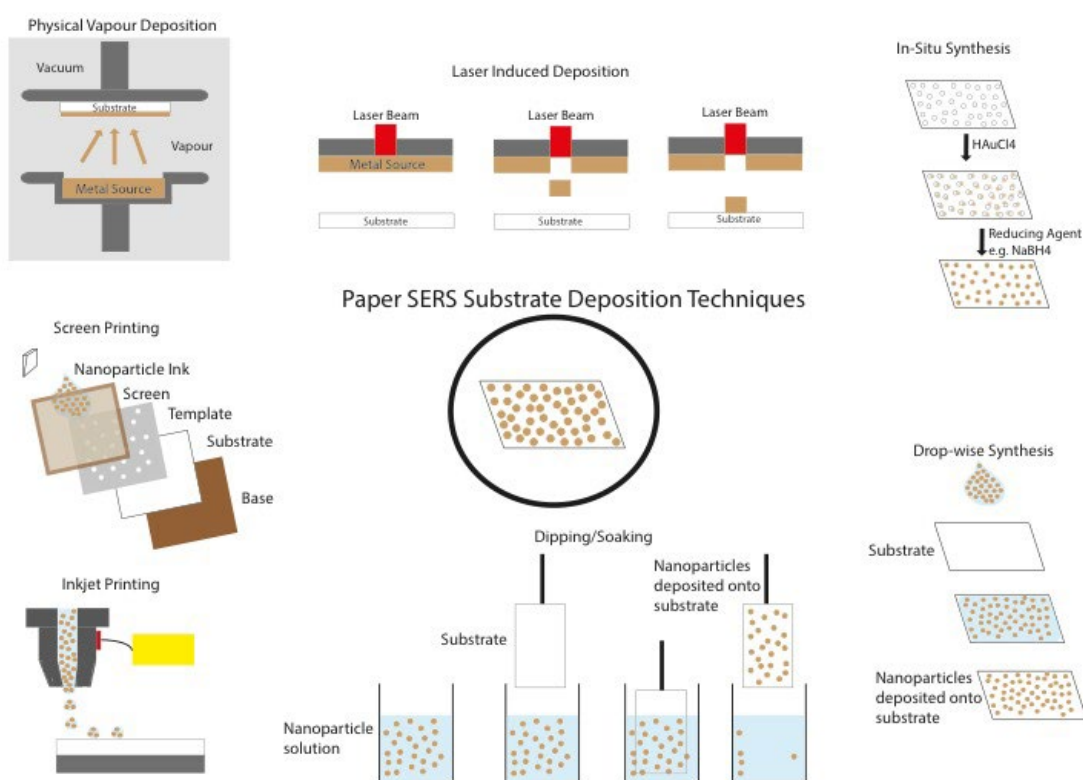


Figure 4.1 Methods of depositing gold nanoparticles onto paper substrates to make SERS active paper devices.

4.2.6 Utilising paper substrates can allow sample separation

When the sample is a mixture of analytes, e.g. a biofluid, there is usually a need to separate the components of the mixture, to improve detection. One of the benefits of paper is the overlapped cellulose fibres provide numerous micro-cavities and gaps, enabling the quick adsorption of solution samples by capillary force. Using paper substrates or paper-based chromatography is a

straightforward way to separate a target analyte from other compounds without the need for complex or expensive equipment (see Figure 4.2).

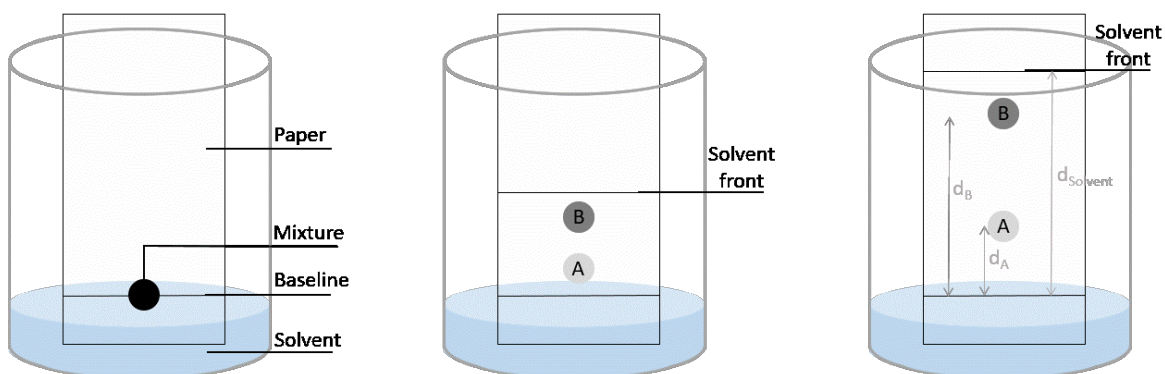


Figure 4.2 Paper chromatography, before, during and after development and visualisation.

Distance travelled by analyte A and B (d_A and d_B) and distance travelled by solvent (d_{solvent}) are used to calculate each analyte's retention factor (R_f).

Cellulose fibres in paper attract water molecules from the atmosphere and the manufacturing process; therefore, the paper fibres in cellulose have a thin layer of water molecules attached to the surface, it is the interaction of molecules with this water that is important in paper chromatography. The stronger the adsorption of a molecule (through hydrogen bonding, van der Waals forces and dipole-dipole attractions), the less distance it will travel up the paper, and the smaller the R_f value. Different molecules have different R_f values and can therefore be separated.

Such sample separation with a paper SERS device can be done with lateral or vertical flow chromatography and both have been reported in the literature^{136,495-498}. This type of separation can also be useful for mixtures containing proteins, as the proteins being large will block the target analytes from reaching the metal nanostructures, therefore separating them from the analytes of interest, will improve detection ability. Lateral-flow separation has been used to separate melamine from infant formula with both polyvinylidene fluoride membranes and paper^{136,499} a vertical flow design has also been demonstrated to separate an antimicrobial drug from serum⁴⁹⁷. Their vertical flow device uses stacks of nitrocellulose membranes, and when the sample is applied to the top, it wicks through the layers to the SERS active zone at the bottom of the stack, but the proteins are removed by the intervening layers.

4.2.7 Employing paper-based SERS for healthcare

Paper-based SERS substrates have been demonstrated^{109,386,392,418,480,490,500-503}. The most-reported technique combining SERS with paper substrates has been to utilise analyte-specific antibodies for immunoassays or DNA aptamer probes for analyte capture^{386,418,501,503-506}. However, the expense

of using antibodies is considerable, and DNA aptamers have an expensive and rigorous design and validation procedure; therefore, not desirable for a product designed for multiple measures from individuals.

A microfluidic paper-based device for quantitative measurement of a cardiac biomarker without the need for a calibration curve has been developed. It uses predictive models to accurately quantify three unknown cardiac biomarkers in serum based on previously obtained Raman data about these biomarkers⁵⁰⁷. However, this method is still using antibody detection, which is expensive.

In another recent paper, a novel paper-based SERS assay for simultaneous detection of two cytokines (MCP-1 and IL-10) in human serum is demonstrated⁴⁵³. The system utilises a polymer membrane fabricated from polypropylene with a polytetrafluoroethylene coating, forming a three-dimensional fibrous network. The increased surface area offers high loading of capture antibodies, thus improving sensing sensitivity. Due to its unique feature of two-layers of AuNPs in a sandwich design, a small gap is generated between the AuNPs producing a “hot-spot” effect that enhances the SERS signal, allowing a more sensitive detection. However, this technique still requires expensive capture antibodies.

A recent example of a paper-based SERS system not utilising antibodies is that described by Shende et al.⁴⁹⁸. They have developed a 5-minute LFA to measure codeine and fentanyl in saliva, blood plasma and whole blood. Their flow separation strips rapidly separate drugs from these biofluids. The strips consist of a sample introduction/separation pad, nitrocellulose flow membrane, the SERS active pad (glass-fibre impregnated with AuNPs), and an absorbent/wicking pad, all positioned on a thin plastic support. The test strips are placed in a plastic tube containing the sample, which then flows up the strip driven by capillary action. The strips are removed from the tube for measurement. This straightforward assay demonstrates the use of paper to separate components of a biofluid before SERS acquisition, without the need for antibodies or use of Raman reporter tags. They achieved spectra with a very good signal-to-noise ratio with just a 3s acquisition time, demonstrating the real potential of such devices for POCT.

4.2.8 Research Gap

We demonstrated for the first time in Chapter 3, SERS sensors fabricated by layer-by-layer synthesis whereby nanoparticle layers are formed around a silica microsphere, which controls the spacing between the nanoparticles and therefore “hotspot” formation. We demonstrated the use of these sensors as an alternative to colloidal nanoparticles for measurement of a clinically interesting biomolecule in urine. The method demonstrated reasonable accuracy and precision

compared to the gold-standard method of HPLC. However, to further improve the reliability of these SERS sensors, we hypothesise that fabricating them into paper devices will improve the technique by removing some of the uncontrollable factors that arise with performing SERS in liquids. The sensors deposited into paper also opens up the system to the separation of sample components via paper chromatography, which will further improve sensitivity to the analyte of interest without the need for capture antibodies. Finally, a paper-based SERS device is more suitable to POCT in combination with a portable Raman spectrometer, than traditional colloidal/aqueous-based SERS measurement. We demonstrate paper SERS devices that incorporate high-throughput deposition of SERS microsensors onto paper as well as devices where the sensors are drop-coated onto the paper.

4.2.9 Hypotheses

- Layer-by-layer fabricated SERS sensors can be deposited onto paper-based (cellulose and nitrocellulose) strips and reliable SERS measurements obtained
- Neopterin can be mobile via capillary action on paper-based SERS devices and detected by SERS
- The paper device can be used to separate a mixture of creatinine and neopterin prior to SERS detection

4.2.10 Aims

In this chapter, we aim to demonstrate the proof-of-concept that a paper-based device with embedded SERS sensors can be used to separate and reliably measure two molecules of interest present in urine samples.

4.3 Methods

4.3.1 Preparation of neopterin and creatinine samples

A 200 μ M stock solution of neopterin was prepared in water and synthetic urine (see method of synthetic urine preparation in Chapter 3). Neopterin (2.53mg (M_w 253.21), Tocris Bio-technie) was added to sterile water (50mL, Millipore, 18 m Ω) or synthetic urine (50mL). The tube was covered in foil and vortexed for 30 seconds, before being placed in a sonicator bath for 2 hours. Aliquots were then stored in the freezer until required. When required, neopterin standards were produced via serial dilution of the 200 μ M stock.

Chapter 4

A 50mM stock solution of creatinine was prepared in water and synthetic urine. Creatinine (56.6mg (M_w 113.12), Sigma-Aldrich) was added to sterile water (10mL, Millipore, 18 m Ω) or synthetic urine (10mL) and mixed well by inversions and vortex. Dilutions of this stock were then prepared as required.

4.3.2 Preparation of layer-by-layer SERS sensors

Poly(ethyleneimine) (PEI) (M_n ~60000, M_w ~750000, 50 wt. % in water) and poly(sodium4-styrenesulfonate) (PSS) (M_w ~70000, powder) were purchased from Sigma-Aldrich and diluted in 0.5M NaCl to the required concentrations. Polyelectrolyte solutions were sterile filtered (0.22 μ M) after preparation. Citrate capped gold nanoparticles (AuNPs) (40nm 8% CV, 9×10^{10} particles/mL) were purchased from BBI Solutions and used as received. Silica microparticles (~8 μ M aqueous suspension) were purchased from Microparticles GmbH.

The initial polyelectrolyte cushion was applied by injecting 20 μ L of 8 μ m silica microparticles into 100 μ L PEI solution (10mg/mL) immediately vortexed for 10s and then vigorously mixed for 20 minutes on a shaker. The microparticles were then washed three times by centrifugation, with supernatant removal and resuspension in water (100 μ L and 25 μ L on final wash). This was repeated with PSS (10mg/mL) and again with PEI (10mg/mL) with four washes after this final coating. AuNPs were then applied by injecting the cushioned microparticles into a volume of AuNPs that allowed 2x coverage of the entire surface of the microparticles and ensured an excess (5 μ L of particles into 1mL of 40nm AuNPs) then vortexed for 10s and vigorously mixed for 1 hour on a shaker. The microparticles were then washed as before until the supernatant was clear and finally resuspended in 25 μ L of water. The microparticles were then injected into 100 μ L PEI (5mg/mL) vortexed for 10s and left to soak for 10 minutes on a shaker, followed by four washes and resuspension in 25 μ L of water. A second addition into AuNPs (5 μ L of particles into 1mL of 40nm AuNPs) of the microparticles was carried out which were then vortexed for 10s and vigorously mixed for 1 hour on a shaker. The microparticles were then washed as before until the supernatant was clear and finally resuspended into 100 μ L of water and stored at 4°C.

4.3.3 Preparation of Whatman No.1 Paper devices with SERS sensors

Strips 10cm long and 0.5cm wide were cut from Whatman No.1 filter papers. A pencil line was drawn 0.5cm from the base to identify the baseline. A pencil marking was also made 5cm from the base, to mark the location of the SERS sensors. SERS sensors were mixed for 20s with a vortex mixer, and then a drop (10 μ L) pipetted onto the top surface of the paper at the marked site. The paper strip was covered with foil and allowed to dry at room temperature overnight.

4.3.4 Preparation of G1 devices with SERS sensors

The preparation of these devices was performed by Panagiotis Galanis, postgraduate researcher in Optoelectronics Research Centre, University of Southampton.

The substrate materials used to make the paper-based devices are Whatman™ grade 1 qualitative filter paper (cellulose) with nominal thickness 180 μm and pore size 11 μm from GE Healthcare and a UniSart CN 95 nitrocellulose membrane with a thickness of 140-170 μm, pore size of roughly 15 μm and a capillary flow speed of 90-135 s/40 mm from Sartorius Stedim Biotech GmbH, Germany. For the device fabrication work, we used an acrylate-based negative photo-polymer DeSolite® 3471-3-14 from DSM Desotech, Inc., USA. The photo-polymer is deposited on the substrate using a PICO® Pμlse™ dispenser platform from Nordson EFD, UK, which deposits micro-droplets through a tip with diameter 100 μm with volumes as small as 0.5 nL at a frequency at 100 Hz. The laser used for the polymerization of the photo-polymer was a fibre-coupled continuous wave (c.w.) diode laser (Cobolt MLD, Cobolt AB Sweden) operating at 405 nm with a maximum output power of 60 mW.

The fluidic devices were created within the cellulose paper and the nitrocellulose membrane via the local deposition of the photo-polymer following by the subsequent exposure to the laser source (spot size ~5 mm and fluence 40 mJ/cm²). The polymer penetrates throughout the entire thickness of the substrate before the laser curing in order to create solid polymeric structures that extend through the thickness of the substrate and can guide the flow of liquids without any side leakage observed. SERS sensors were mixed and deposited onto the devices using the dispenser platform, 5 cm from the base.

4.3.5 Brightfield microscopy of SERS sensors within devices

A Zeiss Axioplan 2 microscope was used to take brightfield images of the prepared paper-based devices, a 40x (N.A. 0.75), 20x (N.A. 0.50) and 10x (N.A. 0.30) air objectives were used.

4.3.6 Optimisation of run-time with paper-based devices

Whatman no.1 devices were prepared according to 4.3.3. Neopterin (200 μM in water) was spotted onto the baseline using a 0.5 μL pipette. Two drops were spotted, allowed to dry and this repeated three times. In between spotting, the device was covered with foil. The spots were checked under UV light (365 nm) to ensure enough sample had been loaded. Each device was placed into a well of a 96-well plate containing water (80 μL) as the solvent. The solvent front was left to run to 5.5 cm, 6.0 cm, 6.5 cm and 7.0 cm from the base of the device before being removed

from the solvent and the solvent front marked with a pencil. The devices were covered with foil and left to dry, before being visualised under UV again and the position of the neopterin spot marked. SERS spectra were then obtained from the SERS sensors positioned at the 5cm from the base position.

4.3.7 Single samples run on devices

For analysis of a single neopterin sample run on a paper device, the method in 4.3.6 was followed. The solvent front was left to run to 6cm. Images depicting the steps in this process can be seen in Figure 4.3.

4.3.8 Creatinine/neopterin mixture run on devices

For analysis of two analytes (neopterin and creatinine) on a paper device, the method was altered. Whatman no.1 devices were prepared according to 4.3.3. Neopterin (200 μ M in water) was spotted onto the baseline using a 0.5 μ L pipette. Two drops were spotted, allowed to dry, and this repeated three times. Creatinine (1mM) was spotted onto the baseline next to the neopterin spot, using the same method. Finally, a mixture of both neopterin and creatinine was spotted onto the baseline. Once all the spots had dried, the device was run in a small beaker(25ml) with 70% Ethanol (500 μ L) as the solvent. The solvent front was left to run to 7.5cm from the base of the device before being removed from the solvent, the solvent front marked, and covered with foil and left to dry. UV was used to visualise the position of neopterin on the device and I₂ for the position of creatinine. SERS spectra were then collected from the SERS sensors positioned at 5cm and 6.5cm from the base.

For prepared mixed samples of creatinine and neopterin, this process was followed but with just the sample being spotted on the device.

4.3.9 SERS measurement of SERS sensors within paper device/spectra acquisition

SERS measurements were performed on a Renishaw InVia spectrometer (633nm, HeNe laser, 6mW max output). The instrument was calibrated using a silicon wafer with a static spectrum peak at 521 cm^{-1} . The intensity of this calibration peak was used to monitor the power of the instrument and adjust results accordingly. A single SERS sensor within the device was identified using brightfield microscopy mode prior to the irradiation with the laser, for observing scattering before SERS spectral acquisition (see figure 4.3). For each measurement, 10 acquisitions were taken with an exposure time of 1s over the wavenumber range of interest (500-1000 cm^{-1} for neopterin and 1500-2000 cm^{-1} for creatinine) using an Olympus objective (20x, 0.40 N.A). Spectral

pre-processing was performed with iRootlab³⁹³ and Renishaw's WiRE software. Spectra were denoised using wavelet smoothing and baseline corrected with an 8th order polynomial in iRootlab. The 10 acquisitions were averaged before WiRE was used to curve fit and determine peak height.

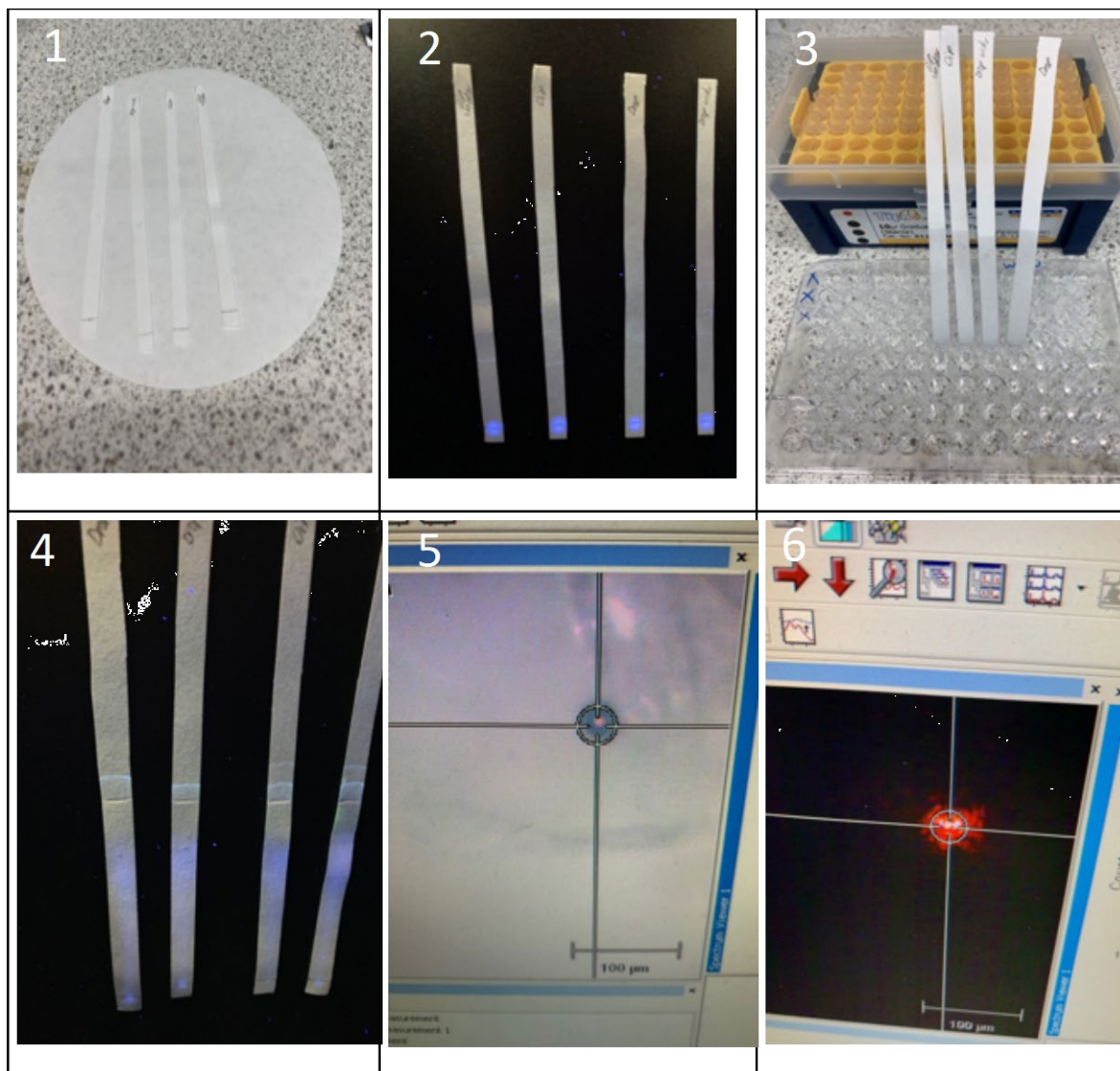


Figure 4.3 Images depicting the process of running a sample on a device and obtaining SERS measurement.

1) The paper substrates are embedded with SERS sensors in the predetermined location, and drops of sample are added to the baseline, and allowed to dry (4.3.3 and 4.3.6) 2) Once dried, the paper substrate is viewed under UV to check the positioning and loading of the sample (4.3.6) 3) The paper substrates are placed into individual wells of a 96-well plate containing the solvent and the device is left to run

for the required length (4.3.6) 4) After being dried, the paper substrates are viewed under UV light and the spot of highest intensity observed in the correct location of the SERS sensors (4.2.6) 5) The brightfield microscope of the Raman spectrometer is used to locate and focus on a single SERS sensor on the paper device (4.3.9) 6) Laser is switched on, and scattering is observed from the SERS sensor.

4.3.10 Visualisation of analyte spots

Neopterin spots on the paper devices were visualised in a UV Viewing cabinet using 254nm light. Creatinine spots were visualised by eye on being highlighted by iodine adsorption after placing the devices into a sealed container with iodine crystals (Sigma Aldrich, UK) and left for 2 hours.

4.3.11 Data analysis and statistics

SERS spectra were averaged and pre-processed in Renishaw's WiRE software and irootlab as detailed in 4.3.9. Once spectra were averaged and processed, curve fitting was used to measure peak height of the peaks of interest and their subsequent ratios.

Data processing and analysis was then performed in GraphPad Prism 8. For the data in this chapter, this included plotting standard curves (regression models) and interpolating results, descriptive statistics including means, standard deviations and coefficients of variation.

Paired t-tests were used to compare means for significance. For example, comparing results obtained on Whatman No.1 devices vs. G1 devices (section 4.4.1).

For section 4.4.6 reproducibility of measurements was assessed by relative standard deviation (coefficient of variation) calculated in GraphPad Prism 8. For comparison of predicted concentration vs expected concentration, correlation coefficients and root mean square error (RMSE) of prediction were calculated in GraphPad Prism 8.

Other information on how results were obtained are detailed in their relevant sections.

4.4 Results and Discussion

4.4.1 Choosing a membrane for the device

Sartorius CN95 nitrocellulose (CN95) and Whatman grade 1 cellulose (G1) with plastic backing and Whatman no.1 (WN1) filter paper without backing were selected. These membranes were selected for their pore size and membrane thickness. The Sartorius CN95 nitrocellulose

membrane has a pore size of 15 μm and the Whatman No.1/G1 a pore size of 11 μm , both of which are just slightly larger than the size of the SERS sensors (8 μm silica core) which allows the sensors to sit within the membrane pores rather than on the surface. With the SERS sensors within the membrane, they should be immobile and therefore not likely to move with the solvent front moving up the device. Brightfield images of the sensors on each of the different devices can be seen in figure 4.4.

The speed at which a liquid (synthetic urine) travelled up the membranes was assessed. A 2cm in length CN95 and G1 devices were placed in synthetic urine (40 μL) in a 96 well plate, it took 20s and 120s for the liquid to travel to the end of the membrane for the two devices. Through our testing with the three membranes, we established that the length of the membrane would need to be a lot longer for CN95 due to the liquid travelling up the membrane more rapidly. Therefore, a longer membrane would be needed for separation to be achieved. With 10cm long membranes, the run time was 4-5 minutes for the CN95 and 10-15 minutes for the G1 devices.

To further investigate the suitability of the membranes, neopterin samples were run, and R_f values calculated. The retention factor (R_f) is the distance the analyte travels up the membrane, relative to the distance the solvent travels. For each 10cm membrane, neopterin (200 μM) was spotted 0.5cm from the base and allowed to dry under foil. The device was placed in water or synthetic urine (80 μL) and allowed to run for a length of time dependent on the type of membrane.

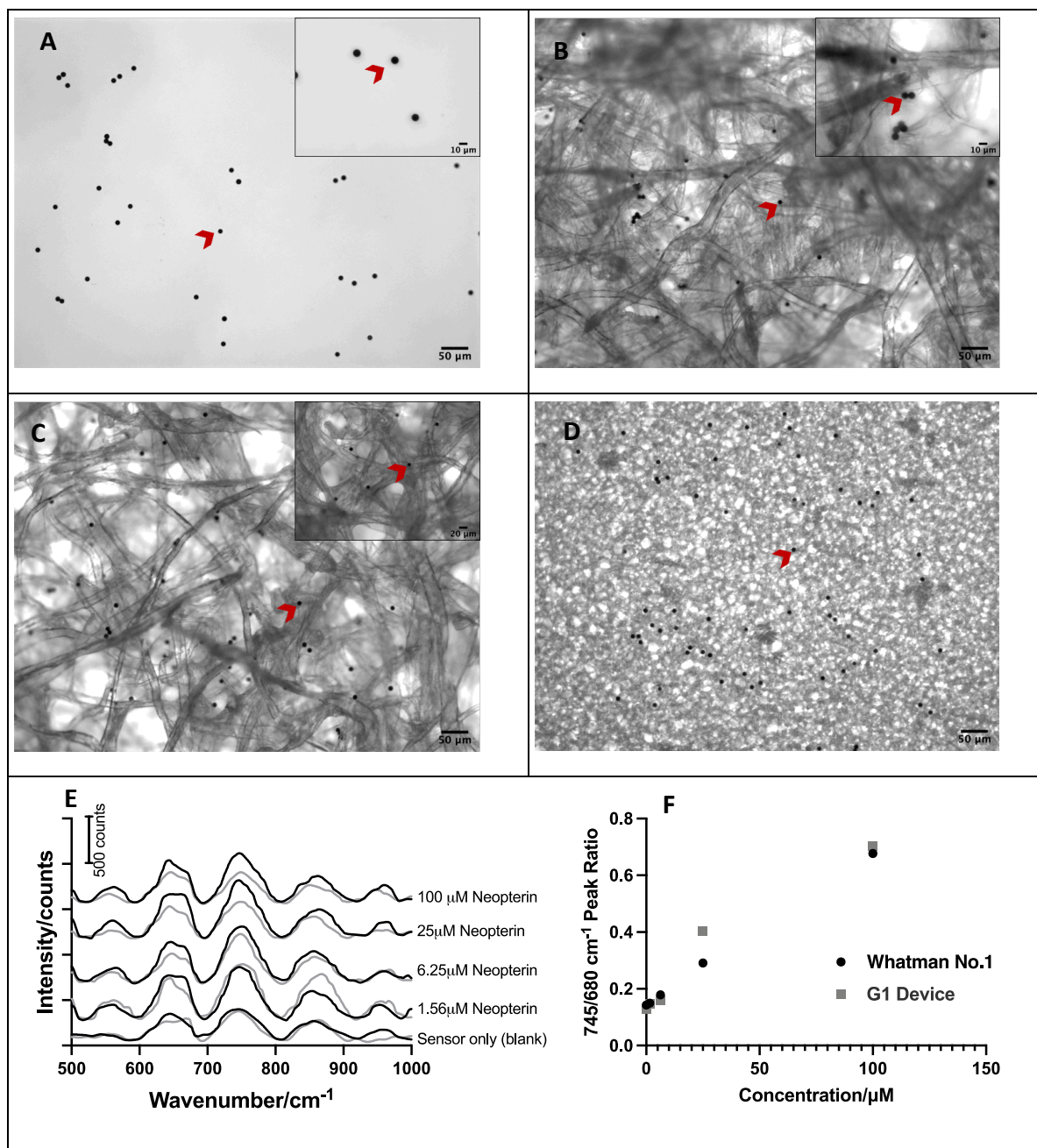


Figure 4.4 Brightfield microscope images of SERS sensors (example identified by a red arrow) on paper device membranes and SERS spectra of neopterin on devices.

A) Sensors in water, scale bar 50 μm , inset scale bar 10 μm B) Sensors on Whatman No.1 filter paper, scale bar 50 μm , inset scale bar 10 μm C) Sensors on G1 paper devices, scale bar 50 μm , inset scale bar 20 μm D) Sensors on CN95 nitrocellulose devices, scale bar 50 μm . E) SERS spectra of neopterin standards run on Whatman No.1 filter paper (black) and G1 devices (grey), as well as the blank spectrum with just the sensor (no neopterin) for each device. F) The calculated peak ratio of neopterin peak (680 cm^{-1}) for each concentration on both the Whatman No.1 (black) and G1 devices (grey).

Table 4.1 Run times and R_f values for the three different paper devices used. R_f values for both neopterin in water and synthetic urine.

No significant difference in R_f values between Whatman G1 devices and Whatman no.1 devices, and no significant difference between neopterin in water and neopterin in synthetic urine.

	Whatman G1	Sartorius CN95	Whatman no.1
Run time	15 minutes	5 minutes	10 minutes
Rf (water) 1	0.868	No spot under UV	0.843
Rf (water) 2	0.863	No spot under UV	0.830
Rf (water) 3	0.821	No spot under UV	0.784
Rf (synthetic urine) 1	0.831	No spot under UV	0.820
Rf (synthetic urine) 2	0.820	No spot under UV	0.824

The results demonstrate that the retention factor (R_f) for neopterin is consistent between repeats and consistent between the Whatman G1 membranes with polymer backing and the Whatman No.1 filter paper membranes with no backing. When synthetic urine is used as the solvent, the R_f value is slightly smaller than when water is used, this is most likely due to interactions from the components within the urine, with the neopterin; therefore, it does not move so far up the membrane. A search in the literature for paper chromatography R_f values of neopterin in urine did not reveal any values for water as the solvent; therefore, no comparison can be made. R_f values for neopterin in urine with other solvents have been published^{508,509}. For example, both papers report paper chromatography with 3% ammonium chloride, with an R_f value of 0.58 and 0.68, respectively. The difference in reported R_f value for the same solvent, highlight that the other conditions of the paper chromatography process will cause variation in this value and this is why it is imperative to keep all conditions the same. According to Kealey and Haines⁵¹⁰, mobile phase eluting power should be adjusted so that solute R_f values fall between 0.2 and 0.8 to maximise resolution. The experimental R_f values in this chapter are at the upper end of what is acceptable. In future work, adjusting the solvent system to reduce the R_f value may be advised. However, the

reasoning for using water as the solvent was to demonstrate the potential of this system for POCT, whereby the user may be performing the chromatography in their home, and solvent use would need to be controlled.

When the CN95 membranes were run, no visible spot was seen under UV corresponding to neopterin, and this was because under UV the whole membrane was active (seen in figure 4.7c, second device from left). Therefore, further use of these membranes was not deemed appropriate to requirement.

The G1 devices were prepared for use on a polymer backing and the sensors deposited via instrumental deposition to demonstrate what a potential point-of-care device would be like. The WN1 membranes were equivalent in fibre, but without the backing or superior deposition of sensors, but were more than adequate for testing purposes. Figure 4.4e show the spectra for the same range of samples run on both the G1 and WN1 substrates. The spectra are different concentrations of neopterin, but the same samples and the same number of samples, tested on each device. The spectra are largely equivalent, although the overall intensity of the G1 devices appears to be slightly lower, however Figure 4.4f demonstrates that the calculated peak ratios from each are comparable.

4.4.2 Membrane and sensor background

The SERS sensors consist of a silica core, polyelectrolyte layers (PSS and PEI) and gold nanoparticles (AuNPs), the preparation of which is detailed in chapter 3. These sensors have a background signal, as does the cellulose of the devices. Figure 4.5 shows the background SERS signal for the SERS sensor, along with Raman spectra of each component.

The background signal of the SERS sensors was measured in the two wavenumber regions of interest ($500\text{-}1000\text{ cm}^{-1}$ for neopterin peak, and $1500\text{-}2000\text{ cm}^{-1}$ for creatinine peak). The peaks in the background signal of the SERS sensors, largely correspond to the Raman peaks of the two polyelectrolytes. PEI has Raman peaks at 560 cm^{-1} , 740 cm^{-1} , 845 cm^{-1} , 960 cm^{-1} , 1530 cm^{-1} , 1600 cm^{-1} which correspond to prominent peaks in the sensor SERS spectrum (with increased intensity and slight wavenumber shift discernible from SERS enhancement). Similarly, PSS has Raman peaks at 665 cm^{-1} , 825 cm^{-1} , 1600 cm^{-1} and 1625 cm^{-1} , at much higher intensity than the peaks of PEI, as it is more Raman active as a compound; however, the SERS spectrum of the sensors appears to have a definite contribution from both polyelectrolytes.

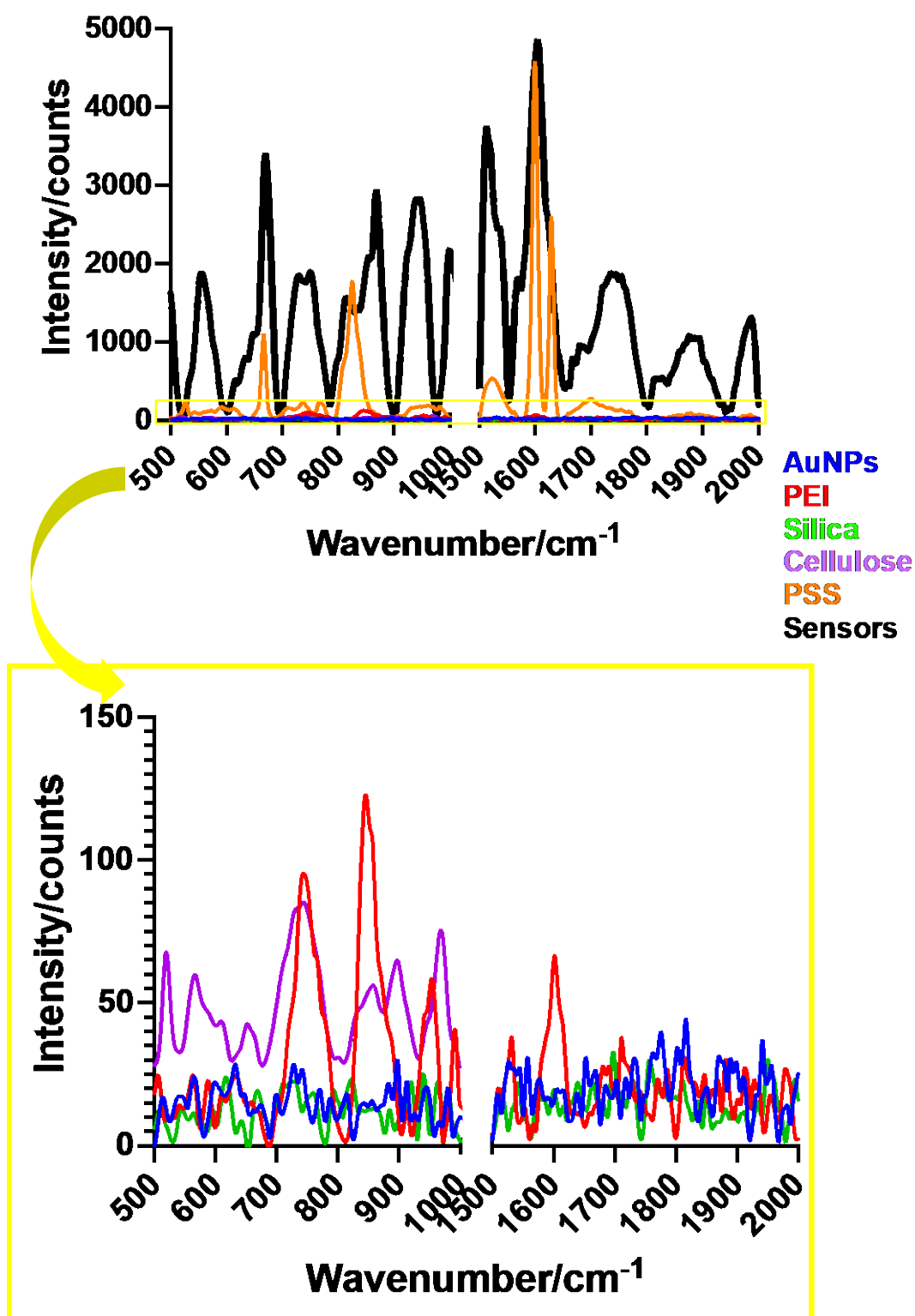


Figure 4.5 SERS background signal from SERS sensors at 500-1000 cm^{-1} and 1500-2000 cm^{-1} , as well as the spectra for the contributing components and cellulose.

The main peaks visible in the sensor spectrum are contributed to by the PEI and PSS layers within the sensor make-up.

4.4.2.1 Peak ratio

The benefit of the SERS sensors having a robust background signal is that the peaks attributed to PEI and PSS can be used as reference peaks. The polyelectrolytes act as an internal standard within the sensor. The peak height of any given analyte is likely to vary depending on the exact environment of the SERS acquisition (changes in the position of the sensor, variation in laser power and positioning of laser over the sensor, temperature fluctuations), by taking a peak height ratio relative to one of the internal standard (from the polyelectrolytes) peaks, some of this variation can be controlled for as presented in figure 4.6.

To demonstrate the benefit of using the above stated internal standard normalisation approach SERS spectra were obtained for neopterin at different concentrations (1.56 μ M- 200 μ M) using SERS sensors embedded in Whatman No.1 filter paper. Peak height was measured at 680 cm^{-1} , a peak corresponding to neopterin, and peak height was measured at 745 cm^{-1} , a peak corresponding to PEI in the sensor, acting as an internal standard. The 745 cm^{-1} peak is broad, most likely because it can be devolved into more than one peak for multiple vibrations, however, the broadness is consistent each time, and peak height rather than peak area is used for measurement. For each concentration measured, the variation in peak height is considerable. Using peak height alone to determine neopterin concentration from unknown samples, would not be accurate enough. However, when the neopterin peak height is considered relative to the internal standard peak height, the resulting ratio eliminates variation that occurs in SERS measurements due to variability in the actual measurement acquisition. The values for peak ratio demonstrate improved precision and therefore, more useful for quantitative analysis. Although, using internal standards to improve measurement reproducibility has been shown³⁷¹, there can be competitive adsorption between the analyte of interest and the internal standard for the metal surface, therefore the signal may vary with concentration in a non-linear way, and will not work above saturation of the metal surface³⁷³. An alternative method of placing an internal standard within the inside of core-shell nanoparticles has been demonstrated³⁷⁴, but to our knowledge, this is the first time the composition of the sensor itself has been used as an internal standard.

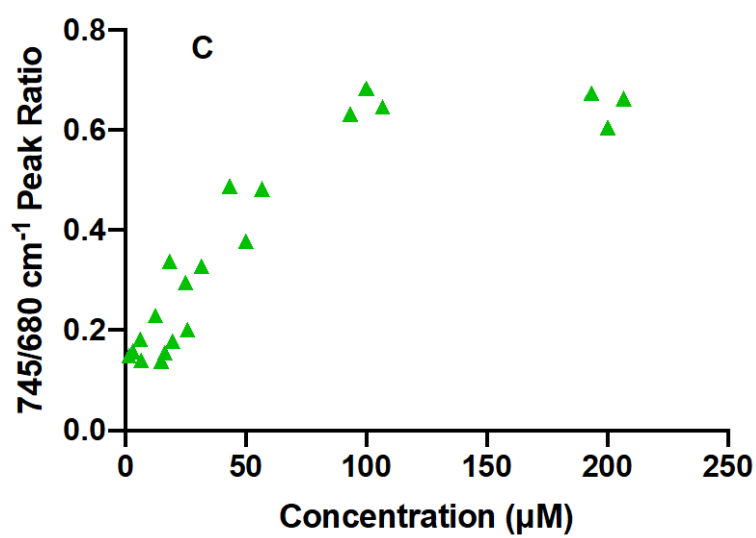
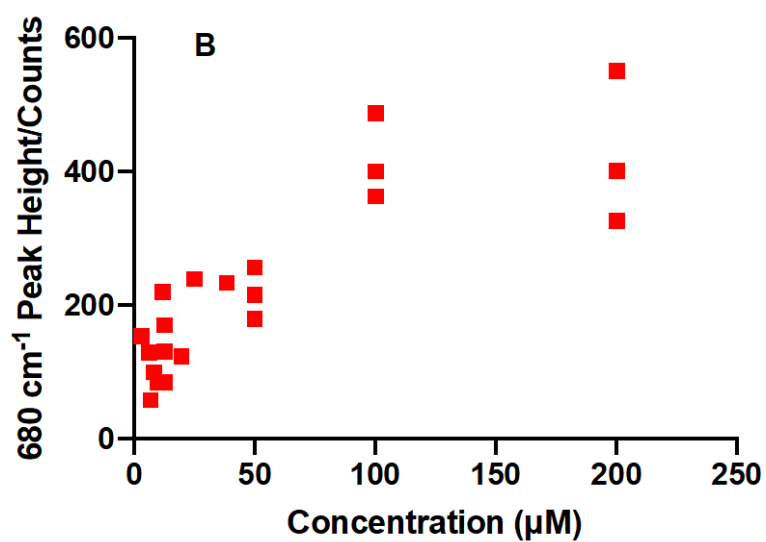
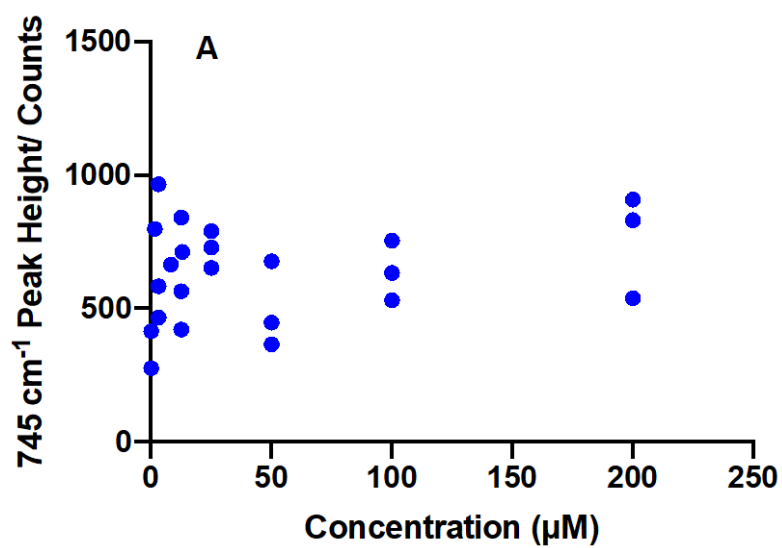


Figure 4.6 Using peak height ratio gives useable data.

A&B) These graphs demonstrate the fluctuation in absolute peak height for a peak at 745 cm^{-1} (internal standard) and peak at 680 cm^{-1} (neopterin), C) Shows when the ratio of corresponding peaks is taken, the variability in results for each concentration is reduced as experimental variations are eliminated, the data becomes more robust and useable.

4.4.3 Optimising the run-length of the assay

To determine that the analyte of interest (neopterin) travelled up the paper device to the sensor region, the length of 'run' time of the device was varied, to extend the length of time the device was left in solvent before being removed, the solvent front marked, and allowed to dry.

Sensors were deposited on the devices 5cm from the base (4.5cm from the baseline), analyte ($200\mu\text{M}$ neopterin) was spotted on each device 0.5cm from the base. The devices used were a Whatman G1 membrane on polymer backing, a Sartorius CN95 membrane on polymer backing and Whatman no.1 filter paper with no backing. The two devices with backing were allowed to run until the solvent front reached 6cm from the base. With the WN1 devices, they were allowed to run to 5.5, 6.0, 6.5 and 7.0 cm from the base.

In figure 4.7, images are seen that show the membranes under UV when the neopterin has been spotted on them, the membranes being run using water as the solvent and the membranes again under UV post-run, showing the movement of the neopterin up each membrane (excluding the CN95 nitrocellulose membrane which is largely UV active across the whole run length). Figure 4.7c depicts the increased height that the UV active neopterin moves with increased run length.

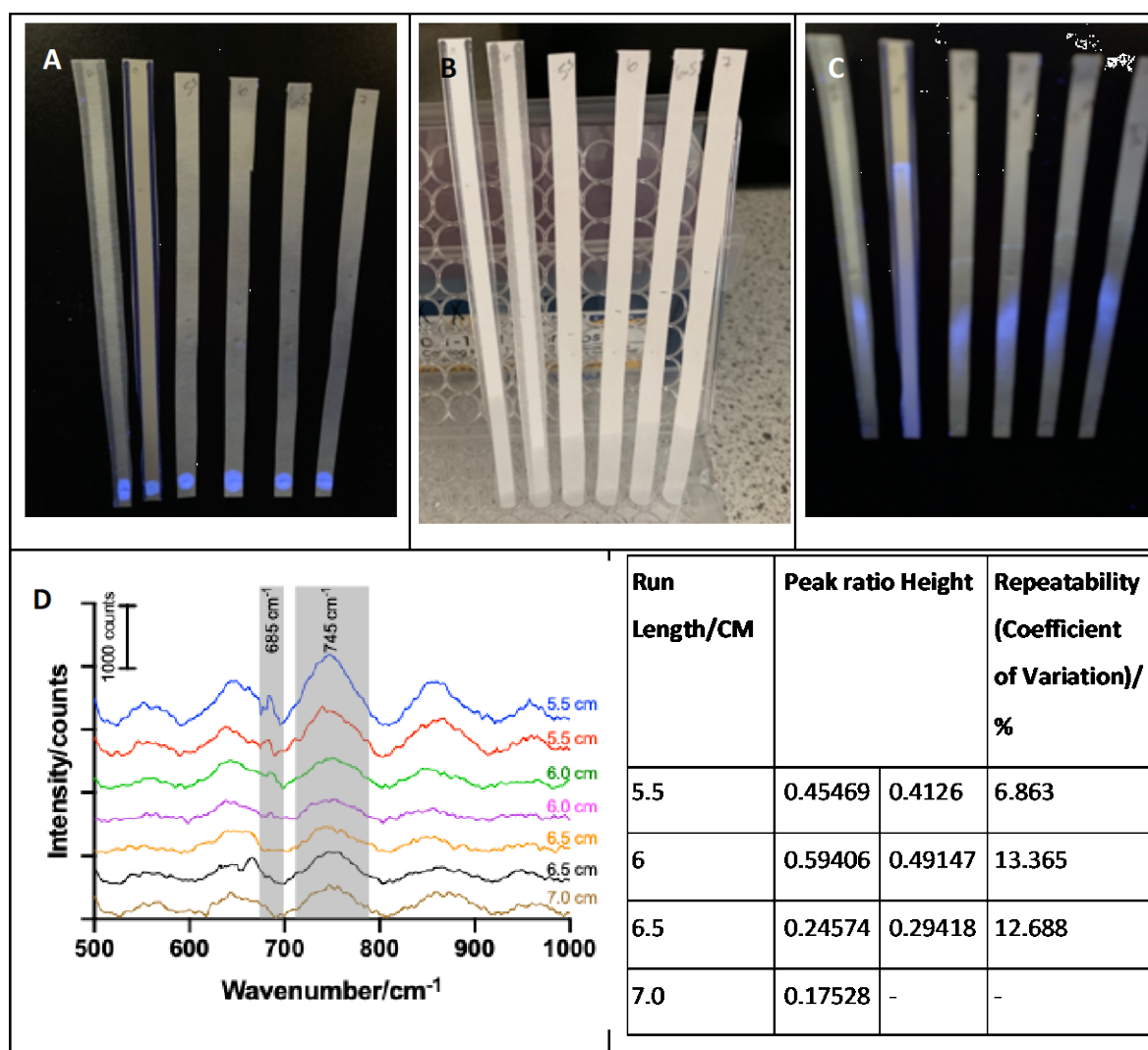


Figure 4.7 Optimising assay run time for neopterin.

A) Devices under UV after neopterin has been spotted on the baseline. B) Devices being run in water as the solvent. C) Devices under UV post-run showing different UV spot height with different run time. D) SERS spectra of devices for each length of run, peak height was measured at 685 cm^{-1} and 745 cm^{-1} and the ratio taken. E) Table of measured peak ratio for the different length runs (in duplicate) and the repeatability of these measurements.

In order to decide which run length put the neopterin in the most optimum position for the SERS sensors, spectra of the sensors were obtained and analysed. Figure 4.7d, shows the acquired SERS spectra for each run length and a repeat after pre-processing, peak height was measured at 685 cm^{-1} and 745 cm^{-1} , and a ratio of peaks taken.

When the solvent front was left to run 6cm up the device, the largest value for peak ratio height was obtained from SERS spectra being taken from SERS sensors placed at 5cm up the device. This implies the greatest number of neopterin molecules were bound to SERS sensors after this run length. This also corresponds with our experimental R_f value of neopterin being 0.820-0.868, if the solvent front were run for 6cm, the neopterin spot would be expected to be around 5cm and this was also evident by the location of the neopterin spot under UV. However, the SERS results for run length and visualising the devices under UV both demonstrate that the location of neopterin up the device is not confined to a small distinct spot, but instead is present over an area of a few cm, therefore not a 'clean' chromatogram. However, irrespective of this, there is a point of brightest intensity under UV and increased peak height ratio with the SERS which is the area we want to be located at the position of the SERS sensors. The tailing of the spot is caused by slow desorption as the solute migrates, or saturation of adsorption sites by high concentrations of the solute (overloading)⁵¹⁰. This does mean that if trying to separate a compound such as neopterin from others (e.g. in urine), a solvent other than water is needed to achieve a clean separation.

4.4.4 Neopterin SERS measurement on paper-based devices

As shown in the preceding sections, paper devices embedded with SERS sensors were used to measure samples of neopterin and the optimum length of a run has been established that allows neopterin to move to the location of the SERS sensors. SERS spectra are then gathered from individual sensors within the paper device. Multiple spectra (10 acquisitions) are taken with fast (1s) acquisition and then averaged. Neopterin samples prepared in both water and synthetic urine were measured. Whether the neopterin was in water or synthetic urine did not alter its mobility along the device, and with the same run-length of 6cm, the neopterin spot moved to approximately the same position with similar R_f value (table 4.1). When visualising the devices under UV, it was observed that the spots from neopterin were in a similar place after being run in both water and synthetic urine.

To measure neopterin using the paper-based devices, the same averaging, and pre-processing is applied to the spectra as those in Chapter 3. A neopterin peak is present at 685 cm^{-1} and is taken as a ratio to an internal standard peak at 745 cm^{-1} . Figure 4.8a shows the SERS spectra generated by the sensor itself, a neopterin standard, and neopterin in synthetic urine. The neopterin peak at 685 cm^{-1} is small but still distinguishable even in the synthetic urine samples.

A standard curve of peak height ratio for different neopterin concentrations was generated. Neopterin concentrations in the range $1.56\mu\text{M}$ - $200\mu\text{M}$ were prepared via serial dilution of the $200\mu\text{M}$ neopterin stock. Figure 4.8, shows the G1 and WN1 paper devices after being run, using

water as the solvent, to the 6cm mark. Concentration increases left to right, which can be seen in the increase in UV intensity; a UV spot was not visible by eye for concentrations $<25\mu\text{M}$. The standard curve is non-linear and fitted with a 4PL sigmoidal curve with an R^2 of 0.972 for WN1 membranes and R^2 of 0.9860 for G1 devices. The concentration measurements were repeated in triplicate, with good repeatability (error bars represent the standard deviation of triplicate measurement).

The peak in the spectra at 685 cm^{-1} was used for neopterin measurement. This was, in fact, the average wavenumber observed for this peak, with the actual range being $680\text{-}695\text{ cm}^{-1}$, this variation in peak position is not uncommon in SERS, as the interaction of the molecules with the SERS substrate affects the peak position. The ionic environment, such as that due to synthetic urine, can also have an effect on how the molecules interact with the substrate. A SERS peak for neopterin is reported at 695 cm^{-1} corresponding to a C-C vibration and ring modes³⁸¹, and the standard Raman spectrum of neopterin has a reported intense peak at 696 cm^{-1} which corresponds with the findings from this device. Raman and SERS spectra can often be different, due to the selection rules being modified by the adsorption of the molecules onto the surface used for SERS. However, with neopterin, the most obvious peaks in the range we are measuring are reported as $668, 698$ and 963 cm^{-1} for standard Raman of neopterin powder by Kaminska et al.³⁸¹ and $667, 696$ and 958 cm^{-1} reported by Elumalai et al.¹²¹, all of which are observed in our SERS spectra of neopterin.

Using this method for measuring neopterin concentration, the limit of detection (LoD) was estimated using $3x$ the standard deviation of blank samples³⁸⁹. The results gave a LOD of 3 nM which is higher than the reported LOD of neopterin with other SERS substrates where 1 nM is reported³⁸¹, but this is with a more complex substrate and in-depth spectral processing, compared to our fast and simple technique. The physiological 'normal' concentration of neopterin in urine is expected to be a few μM ¹²; therefore, this should be readily detectable with this paper-based technique.

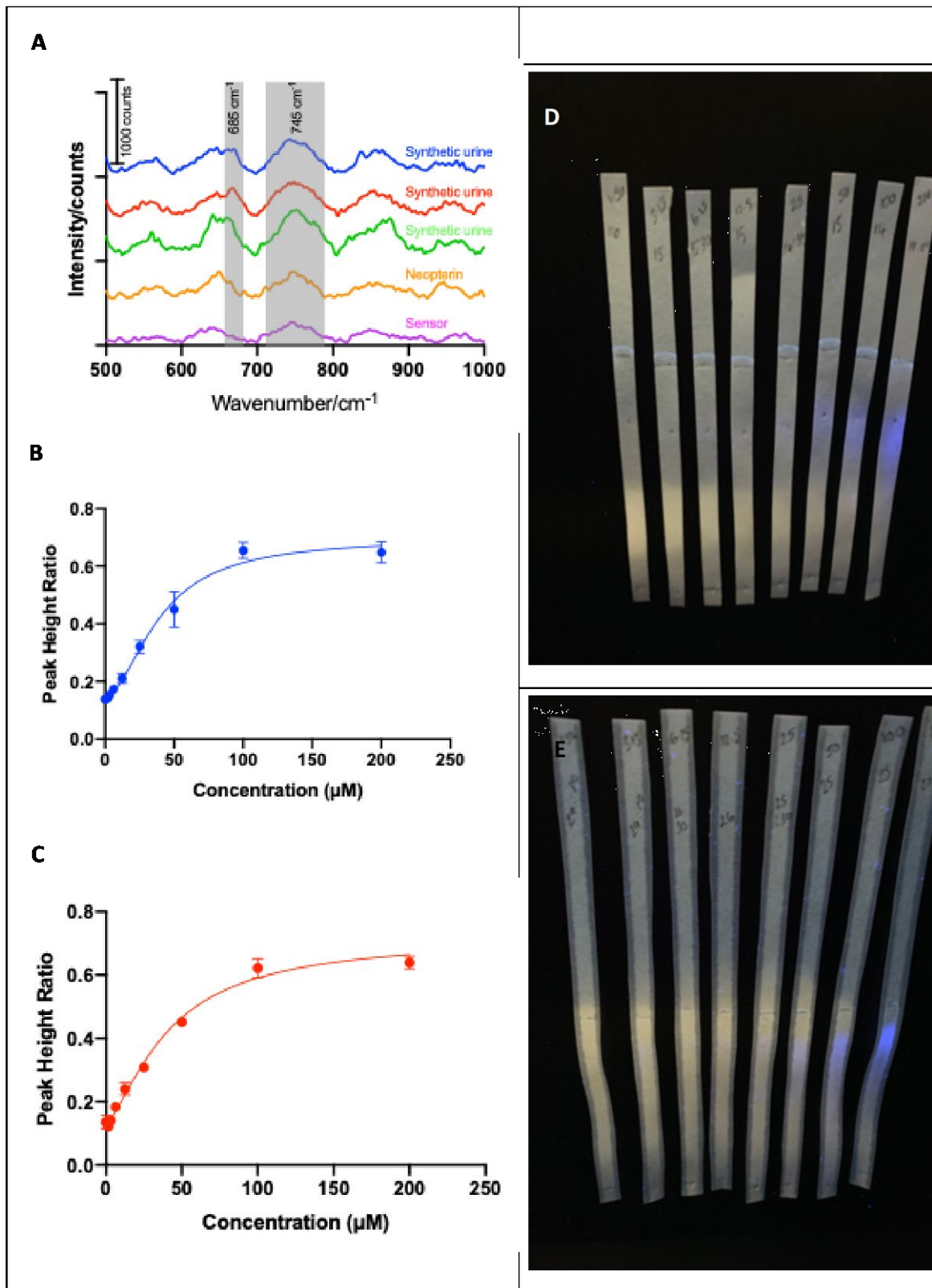


Figure 4.8 SERS measurement of neopterin on paper devices.

A) SERS spectra for sensor background, neopterin standard, and neopterin in synthetic urine (triplicate), demonstrating the two peaks used to measure peak height ratio, for neopterin measurement. B) Calibration curve for neopterin standards (in water) on Whatman No.1 devices, each concentration measured in triplicate, error bars represent the standard deviation of triplicate measurement. $R^2 = 0.972$. C) Calibration curve for neopterin standards (in water) on Whatman G1 membranes, each concentration measured in triplicate, error bars represent the standard deviation of triplicate measurement. $R^2 = 0.9860$, D) Whatman No.1 devices under UV after being run for 6cm in water. Concentration increases from left (1.56 μ M) to right (200 μ M), and increase in UV intensity seen with increasing concentration, below 25 μ M, UV spot not visible by eye. E) Whatman G1 devices under UV after being run for 6cm in water. Concentration increases from left (1.56 μ M) to right (200 μ M), and increase in UV intensity seen with increasing concentration, below 25 μ M, UV spot not visible by eye.

4.4.5 Using paper-based devices for separation of components

A key benefit of using paper-based devices as SERS substrates is the ability to use simple paper chromatography to separate components of a mixture, such as urine, to eliminate the matrix effect and improve robustness of the technique, and to quantify low concentration analytes. To further demonstrate suitability of these devices for clinical use, a mixture of neopterin and creatinine was separated and analysed. To give clinical meaning, neopterin in urine is measured as urinary neopterin to creatinine ratio (UNCR) to account for variation in urine state.

As demonstrated in Chapter 3, neopterin and creatinine have similar SERS spectra but with some distinctive peaks. Figure 4.9 shows where the peaks used for analysis are in relation to each other, and also in relation to the background signal from the SERS sensors themselves, peaks of which are used for internal standard. Neopterin has distinctive peaks present at 685 cm^{-1} and 960 cm^{-1} , for the analysis in this chapter, the 685 peak is used. Spectra for creatinine are collected in a different wavenumber range (1500-2000 cm^{-1}) and a peak corresponding to creatinine at 1760 cm^{-1} is used for analysis.

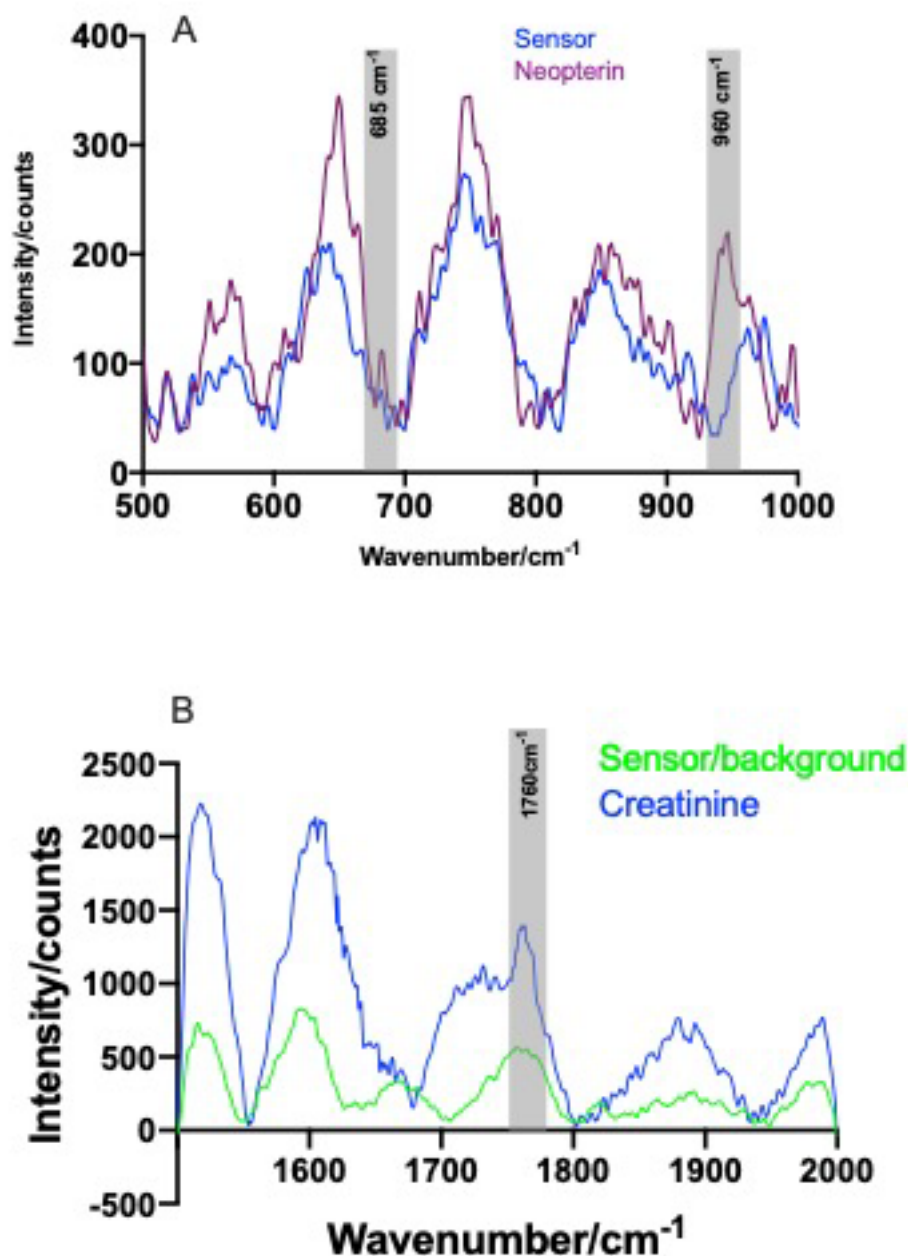


Figure 4.9 SERS spectra for neopterin (500-1000 cm^{-1})

(A) and creatinine (1500-2000 cm^{-1}) (B) showing the distinguishable peaks from the background SERS sensor spectrum.

Neopterin measurements are made using the peak at 685 cm^{-1} and creatinine using the peak at 1760 cm^{-1} .

In order to separate neopterin and creatinine on a single paper device, so that both could be measured independently, some optimisation of the method was required. Unlike neopterin, creatinine is not UV active, and therefore, Iodine adsorption was used to generate contrast to allow observation of the position of creatinine on the paper devices. The separation was carried out using water as a solvent. As already demonstrated in this chapter, neopterin moves up the

paper device when water is used as a solvent with an R_f value of around 0.83. However, creatinine continues to move with the solvent front, after the device is removed from the solvent.

Alternative solvents isopropanol (IPA) and 70% ethanol (EtOH) were tested. With IPA, neither the neopterin or creatinine moved with the solvent and remained on the baseline. With 70% EtOH, neopterin moved up the paper with an R_f value of 0.6 and creatinine moved further with an R_f value of 0.85, distinctly separating the two analytes from each other in their position on the paper. In Figure 4.10, the neopterin under UV and the creatinine after iodine treatment can be seen, with three channels, one creatinine or neopterin only, and another lane with a mixture of the two. The middle plate of the figure has marked where the two analytes end up after a 6cm run, and these positions can be taken as the points to place SERS sensors in devices to enable SERS spectra of both analytes to be obtained.

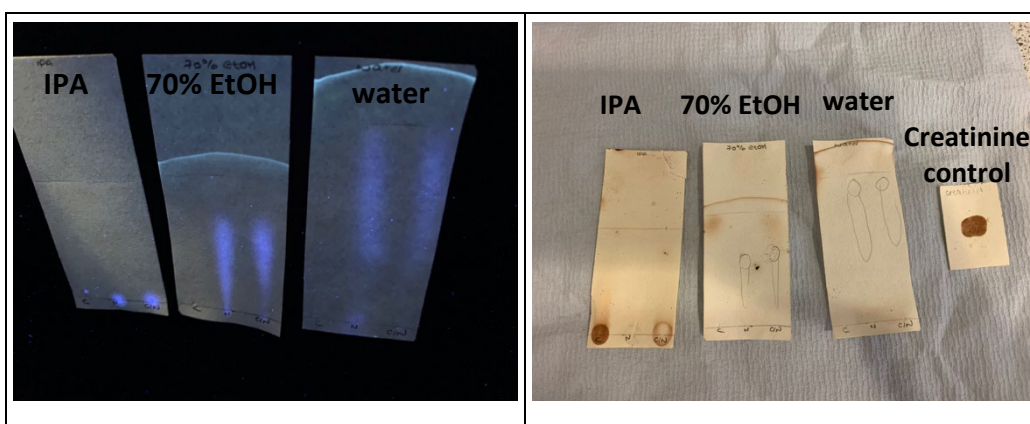


Figure 4.10 Paper chromatography separation of creatinine and neopterin.

All three paper substrates are spotted with creatinine (left channel), neopterin (middle channel) and a mixture of creatinine and neopterin (right channel). The three substrates were run in different solvents, IPA (left), 70% EtOH (middle) and water (right). The image on the left identifies the position of the neopterin, under UV illumination, on the paper substrate. With IPA as the solvent, the neopterin spot remains on the baseline, with 70% EtOH the neopterin moves up the plate with an R_f value of 0.60, with water the neopterin moves up the plate with an R_f value of 0.83. The image on the right shows the same paper substrates after being placed in iodine vapour, which makes the creatinine visible (the neopterin spots identified under UV illumination are marked in pencil). With IPA as solvent, the creatinine spot remains on the baseline, with 70% EtOH the creatinine spot moves up the plate with an R_f value of 0.85, with water the creatinine continues to move up the substrate with the solvent front.

Paper devices of WN1 filter paper were prepared with SERS sensors deposited in two distinct areas, 5cm from the base and 6.5cm from the base, with the solvent run length being 7.5cm. In both regions, SERS measurements were obtained from a single sensor. Spectra were collected at both positions in the 500-1000 cm^{-1} wavenumber region where we look for the neopterin peak, and also the 1500-2000 cm^{-1} wavenumber region where we look for the creatinine peak. In Figure 4.11a, the spectra show the distinct neopterin peak at 685 cm^{-1} which is not present in the creatinine spectrum or the background sensor spectrum. In figure 4.11b we see that the average spectrum collected from the sensors located at the 5cm position shows a peak at 685 cm^{-1} in both replicates of this type of run, but no distinct peak at this wavenumber in the average spectrum collected from the 6.5cm position. The 5cm position spectra are similar to the neopterin spectrum of 4.11a and the 6.5cm position spectra show similarity to the creatinine spectrum of the 4.11a.

A similar result is seen when the two positions have SERS spectra obtained at the 1500-2000 cm^{-1} region. Creatinine has a distinct peak at 1760 cm^{-1} (figure 4.11c) which is present in the spectra obtained from the 6.5cm position but is not present in the spectra obtained at the 5cm position shown in figure 4.11d. Equally, there are peaks at 1645 and 1670 cm^{-1} in the spectra obtained from the 5cm position which are likely neopterin peaks and are not present in the spectra obtained from the 6.5cm position.

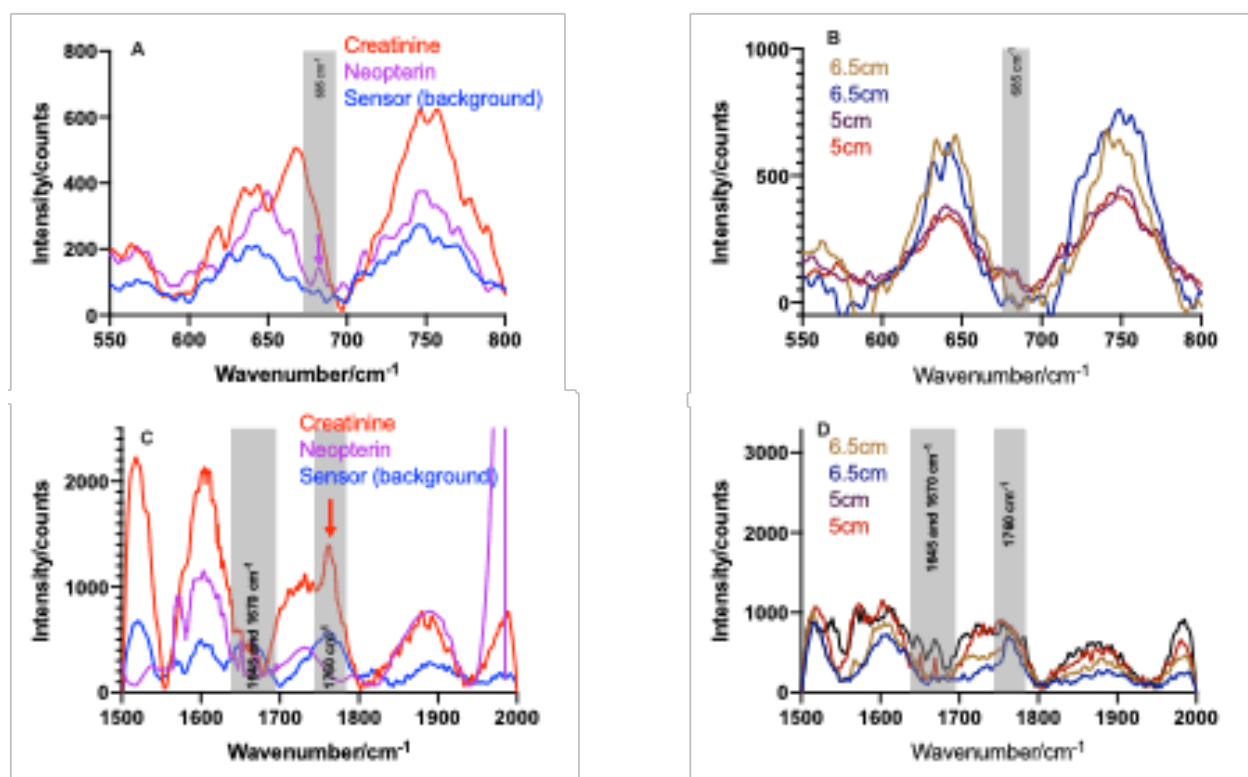


Figure 4.11 SERS spectra of creatinine and neopterin measured after paper chromatography separation.

A) SERS spectra for the 550-800 cm^{-1} region for neopterin, creatinine and the sensors background signal. B) SERS spectra obtained in the region 550-800 cm^{-1} from sensors located 5cm and 6.5cm up the substrate. The 5cm are positioned where neopterin is expected to travel to, and we see a peak at 685 cm^{-1} where neopterin is measured. The sensors at 6.5cm are positioned where creatinine is expected to travel to, and we do not see a peak at 685 cm^{-1} . C) SERS spectra for the 1500-2000 cm^{-1} region for creatinine, neopterin and the sensors background signal. D) SERS spectra obtained in the region 1500-2000 cm^{-1} from sensors located at 5cm and 6.5cm up the substrate. The SERS spectra collected at the 6.5cm position show a peak at 1760 cm^{-1} which is also present in the creatinine reference spectrum.

4.4.6 Paper-based devices for quantitative SERS measurement

To demonstrate the ability of these paper devices to report quantitative differences between samples, test samples were prepared with known concentrations and blinded to the researcher. These samples were a neopterin sample, four synthetic urine samples spiked with neopterin, and three creatinine/neopterin mixtures.

SERS measurements were taken from the SERS sensors within the paper devices. After spectral processing, the measurement of the peak ratio 685/745 cm^{-1} was taken for each sample. The calibration curve shown in figure 4.8, was used to interpolate the value of the measured concentration of neopterin in μM . Results are displayed in Table 4.2. The table also displays a % value for accuracy and recovery, which indicates how close to the known concentration the measured concentration is. It also shows the direction of bias, i.e. over- or under-estimation. The results are mostly under-estimates, which is more commonly expected, but the randomness of both positive and negative difference would suggest there is no systematic bias in the model. Notably, there are fewer samples measured at higher concentrations of neopterin. To fully confirm the reliability of the technique, an even spread of samples across the concentration range would be beneficial. However, the physiological range of neopterin expected in an individual is of the order of a few μM ; therefore, we are more interested in the bias at these lower concentrations.

The quantitation of neopterin in the mixed creatinine/neopterin samples consistently gave the poorest accuracy of the samples measured, and were all under-estimated. This may well be due to interactions between the two molecules altering the binding of neopterin with the sensors. The calibration curve used for quantitation of these samples was from standards of just neopterin, therefore for improved accuracy, a calibration curve of neopterin standards prepared in a mix

Chapter 4

with creatinine may be useful. Plot of predicted vs expected concentration of neopterin is shown in figure 4.12, the high correlation but with an offset may indicate a systemic error which could be due to the calibration curve being a source of error.

Table 4.2 Quantitative measurements of neopterin in prepared samples using paper devices with SERS sensors.

Table details the expected concentration, the measured concentration, the accuracy and recovery. The measured neopterin concentration where measured in triplicate or duplicate also shows the average with percentage variation (coefficient of variation)/reproducibility.

Sample	Expected Neopterin Concentration/ μ M	Measured Neopterin Concentration/ μ M				Accuracy/ % Bias	Recovery/ %
Neopterin	40.0						
WN1		41.9	34.2	37.3	37.8 (10.21%)	-5.5	94.5
G1		40.1	36.8	-	38.5 (5.94%)	-3.75	96.25
Neopterin spiked synthetic urine A	100.0						
WN1		89.0	122.2		105.6 (22.26%))	5.6	105.6
G1		101.7				1.7	101.7
Neopterin spiked synthetic urine B	50.0						
WN1		35.5				-29	71
G1		33.6				-32.8	67.2
Neopterin spiked synthetic urine C	25.0						

WN1		-		
G1		27.4	9.6	109.6
Neopterin spiked synthetic urine D	12.5			
WN1		11.8	-5.6	94.4
G1		-		
Creatinine/neopterin mix A	20.0			
WN1		17.1	-14.5	85.5
G1		18.0	-10	90
Creatinine Neopterin mix B	5.0			
WN1		3.7	-26	74
G1		2.8	-44	56
Creatinine/neopterin mix C	10.0			
WN1		8.2	-18	82
G1		8.5	-15	85

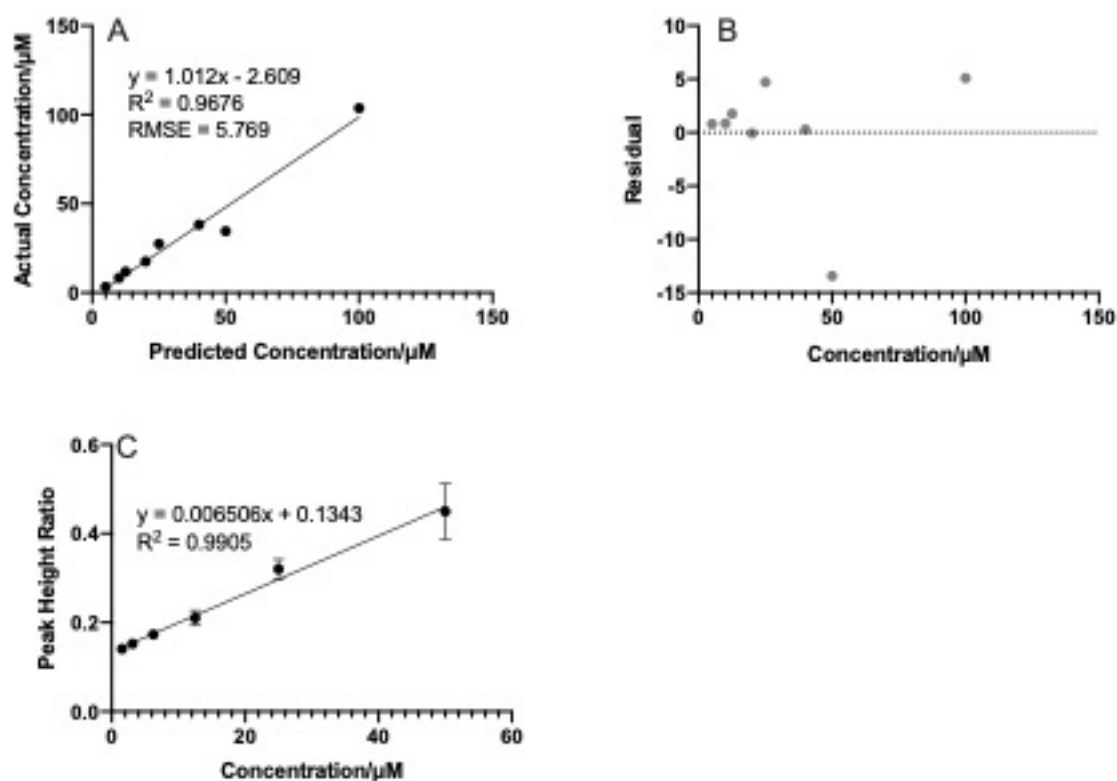


Figure 4.12 Validation plots for paper SERS of neopterin

A) Plot of predicted concentration vs expected concentration of neopterin, the response is linear with a correlation coefficient of 0.9676 and root mean square error (RMSE) of prediction of 5.769. B) Plot of residual error between the experimentally observed concentration of neopterin and expected concentration of neopterin. C) Plot of the linear range of neopterin calibration (1.56-50 μM) with a correlation coefficient of 0.9905.

When any sensor or substrate is being developed for quantitative measurement, there are important analytical parameters that need to be considered to assess its viability as an analytical tool. In chapter 3, we have demonstrated the accuracy, reproducibility and batch-to-batch repeatability of colloidal SERS sensors. To further assess the analytical capability of these sensors within paper devices, we sought to obtain further measurements. The limit of detection (LOD) and limit of quantification (LOQ) are often used to demonstrate the capability of analytical techniques. There are various methods used for calculating LOD and LOQ, but one of the most well accepted is to multiply the standard deviation of replicate measurements of samples, by 3 for LOD and 10 for LOQ³⁸⁹. The standard deviation is obtained from sufficient replicate measurements of blank or low concentration samples. For our results, we used the SD of the blanks ($n=2$) and 1.56 μM ($n=3$) samples, giving a value of 0.006. Equation 1 was used to calculate the standard deviation per replicate. Where S_0' is the SD used for calculating LOD and LOQ, S_0 is the estimated

SD of n single repeats of samples at or close to zero concentration, and n is the number of replicate measurements³⁸⁹.

Equation 1:

$$S_0' = S_0 / \sqrt{n}$$

Therefore, S_0' would be $0.003\mu\text{M}$ the LOD would be calculated as $0.009\mu\text{M}$ and the LOQ as $0.03\mu\text{M}$. In practice, however, anything below $1\mu\text{M}$ would be difficult to distinguish above the background of the sample. Kaminska et al. have developed a solid SERS substrate with a zinc oxide film surface, which they have used to measure neopterin in blood plasma³⁸¹. They have used the same neopterin peak for measurement, as in this study, and have calibrated with neopterin in buffer in the range of 0-250 nM (linear range 0-40nM). They report a LOD of 1.4 nM for neopterin in blood plasma, which they have estimated using the signal-to-noise method, whilst a valid method for determining LOD with an analytical method in which there is significant baseline noise, the technique involves trial and error and is inherently unreliable. The upper limit of normal for neopterin in blood is 8.7nM, whereas for urine this is $251\mu\text{mol/mol creatinine}$ ¹², with the average creatinine concentration being 12.475mM ⁵¹¹, the expected neopterin concentration would be in the region of $3\mu\text{M}$. The lowest mean neopterin concentration for a young healthy adult is reported as $101 \pm 33 \mu\text{mol/mol creatinine}$ ⁴⁷, so assumed lowest concentration of $68 \mu\text{mol/mol creatinine}$, would give a neopterin concentration of around $1\mu\text{M}$. The actual value of LOD/LOQ is only relevant to the lowest analyte concentration you are experimentally trying to measure, for example as long as the LOD/LOQ are sufficiently lower than the expected lower limit of physiological concentration, the actual value isn't as important. It is more important to be able to predict concentrations of samples with accuracy at concentrations relevant to the known physiological range. The purpose of the devices demonstrated in this chapter is to identify those with higher-than-normal neopterin concentration, rather than to accurately quantify those with lower-than-average neopterin concentration, as a low concentration doesn't indicate a health issue.

Figure 4.12a shows the root mean square error (RMSE) of predicting neopterin concentration from the calibration data set is 5.769, and this value is largely because of a particularly poor agreement between predicted and expected concentration for the $50\mu\text{M}$ sample. This sample is perhaps erroneous and should be re-measured. For most of the samples measured, the predictive power of the paper devices was small, if the $50\mu\text{M}$ sample is excluded from the analysis, the RMSE is only 1.641, suggesting a variance of around $1.6\mu\text{M}$ in the model's prediction ability. The interpretation of this varies on what concentration range you are considering. When considering

samples of concentration greater than a few μM , then variance of 1.6 in the measurement is unlikely to make a significant difference. If measuring the concentration of a sample that is less than a few μM , a variation of 1.6 could be rather significant, depending on what the clinical significance of the concentration is.

The reproducibility of the SERS sensors in liquid measured as relative standard deviation was found to be 27% (RSD, chapter 3), Kaminska et al. have used a solid SERS substrate to measure neopterin and report a RSD of 11% which is comparable to commercially available substrates such as Klarite (RSD = 14%). Although reproducibility has not been determined for the method described in this chapter, it is likely that the combination of the SERS sensors embedded in a paper substrate, with the paper chromatography separation, will result in a significantly improved reproducibility. We have observed a reproducibility of 5.94-10.21 % when measuring a $40\mu\text{M}$ sample of neopterin in triplicate (see Table 4.2). However, for further validation purposes, reproducibility of the substrates would need to be assessed by measuring the same sample at least 50-100 times. The benefit of this technique is the simplistic substrate preparation (with potential for low-cost high-throughput production) and potential for testing in a patient's home or at point-of-care with cheap, disposable devices and a portable Raman instrument. Therefore, some trade-off in reproducibility comparable to other substrates that require costly manufacture and bench-top spectrometers would be outweighed by the benefits of the device.

4.5 Conclusions and Future Work

- SERS sensors have successfully been deposited onto filter paper, with both a simple drop coating method and a superior instrumental 'printing' technique suitable for large-scale production.
- Neopterin and creatinine peaks are distinguishable from the sensor/paper background, and peaks corresponding to the sensor make-up can be used as an internal standard.
- Neopterin and creatinine can be separated on the paper devices using 70% ethanol as a solvent, with R_f values of 0.6 and 0.85 for neopterin and creatinine respectively.
- The concentration of neopterin within samples run on the paper devices can be quantified with acceptable accuracy and performance. Further validation of the paper substrates is required though, along with re-analysis of calibration standards.
- The concept of using the paper SERS substrates for simultaneous separation of analytes and SERS measurement has been demonstrated. Further development is required utilising a hand-held spectrometer and testing multiple samples at point-of-care.

Chapter 5 General Discussion

This study set out to demonstrate the clinical utility of longitudinal monitoring of systemic inflammation in older individuals, and to demonstrate a potential technique that would allow point-of-care monitoring in the individuals' home.

This study demonstrates serial measurements of neopterin in urine, which allows neopterin volatility to be assessed. This better identified those with chronic systemic inflammation than any single time-point measures. When participants were grouped according to their neopterin volatility, similar trends were seen with the other measured inflammatory markers.

This work has demonstrated Raman spectroscopy with novel sensors that provide surface-enhancement, is a suitable technique for quantifying neopterin concentration in urine samples, and this can be further implemented into a paper device suitable for a point-of-care test.

5.1 Ageing and inflammation

Ageing is an inevitable process, and although life expectancy continues to rise due to advancements in medical care, nutrition, and better environments, the process of ageing has not slowed¹⁴². However, individuals age differently. Some individuals, such as centenarians, achieve both longevity and maximal healthspan, whilst others are living longer but with multiple age-related morbidities¹⁴³. Quality of life, is therefore, not equal in older adults. Additionally, increased numbers of older adults living with multiple age-related disorders has both social and economic consequences. Blue Zone project communities have benefited from better health, significant medical cost savings, productivity improvements, increased economic vitality, and lower obesity and smoking rates^{512,513}.

The human immune system protects from pathogens and from damaged or altered tissues and cells, whilst limiting damage to the body's own healthy tissues. The immune system also develops a memory of exposure to pathogens, so that with successive encounters, the response is more rapid and specific. With age, these aspects of immune response deteriorate. Older individuals are more susceptible to both bacterial and viral pathogens, the incidence of cancer is age-related, as is tolerance of one's own tissues, as evidenced by increased autoimmunity⁵¹⁴. Additionally, the ability of the body to mount an adequate, protective vaccination response declines with age. The decline of these functions with age is referred to as immunosenescence⁴.

Ageing is also associated with a state of low-grade chronic systemic inflammation, termed inflammaging⁴. Older adults experience inflammaging to differing degrees, dependent on their individual immunobiography²³⁰. Inflammaging is an upregulation in inflammatory markers, or impaired induction of anti-inflammatory signalling and is a component of the progression of many age-related conditions, such as cardiovascular disease¹⁶⁰, frailty³¹⁸, and dementia⁵¹⁵.

Inflammaging is the best studied aspect of immunosenescence, particularly the measurement of inflammatory cytokines (IL-6, IL-1 β , TNF- α and CRP)⁴. Higher plasma concentrations of IL-6 and TNF- α have been associated with physiological measures of frailty, lower grip strength and gait speed in older adults^{29,45}. Measurement of inflammatory cytokines has also been incorporated into longitudinal aging studies and also studies including in centenarians⁵¹⁶. However, the purpose of this work has been to focus on an excreted marker that can be easily and readily measured, more suited to longitudinal testing.

5.1.1 Age-related hearing loss

Sensory functions are critical for maintaining activities of daily living and social interactions in older life. Studies have investigated and shown associations between inflammaging/inflammation and age-related hearing loss^{5-7,162,190,245}, with some of these being large cohort studies, therefore showing a robust association which has also been repeatable in our small cohort of 45. There are also longitudinal studies which show the relationship between inflammation and ARHL whilst eliminating the confounding effect of acute inflammatory episodes. Nash et al. (2014) show that long-term raised CRP levels in younger adults are associated with 10-year increased incidence of hearing loss⁵. Showing not only does raised inflammation correlate with hearing level, but also increases the likelihood of developing hearing loss.

Our longitudinal study has investigated the effect of inflammatory state on the progression of hearing loss in older adults. We have found high inflammatory baseline (high neopterin volatility) to be associated with greater progression in high-frequency hearing loss from the start to the end of the study, as measured by change in Puretone audiometry (PTA) hearing threshold. The higher frequencies of hearing are most affected by deterioration due to age²⁰². This study also measured transient otoacoustic emissions (TEOAE). PTA is the standard method for assessing hearing loss change over time. However, as measures of progression of age-related hearing loss, both PTA and TEOAE have significant limitations. PTA has a test-retest reliability of 5dB³²⁴, so only changes of greater than 5dB can be deemed a deterioration in hearing level. Over the course of this study, the mean change in hearing level was 2dB for the lowest neopterin volatility group, and 9dB for the highest neopterin volatility group. The use of TEOAEs was included in this study as an

objective assessment of hearing level which is sensitive to small changes. TEOAEs are used to assess outer hair cell function in the cochlea; it is the method of assessment used in the newborn hearing screening program (NHSP). However, if there is damage to the outer hair cells (as occurs with age-related hearing loss) resulting in a mild hearing loss or greater, TEOAEs are not evoked. Therefore, many older people do not have recordable TEOAEs, a finding confirmed in this cohort, where measures varied from strong to no evoked response.

Standard PTA measures hearing level at frequencies in the range of 250-8000 Hz; however, the human range of hearing is 20-20,000 Hz. Therefore, in any future work, extended high-frequency audiometry (up to 16,000 Hz) would be recommended as a greater change in hearing level is likely to be seen at even higher frequencies, particularly in a cohort of this age where higher frequencies would be expected to be intact but sensitive to change. Additionally, if standard PTA is being used, it would be advisable to extend study duration to between 5 and 10 years. ARHL is thought to progress at a rate of about 1dB per year, so over a longer time period, the progression of ARHL would be higher than the test-retest reliability of PTA.

Age-related changes to the auditory system are believed to typically occur in the inner ear. There is evidence from murine studies that inflammatory processes in the inner ear are responsible for the degeneration in function, however this is not yet well defined in relation to age-related damage. Age-related degenerative changes can occur in the organ of Corti, stria vascularis, auditory nerve and basilar membrane. There is also potential for age-related changes in the central auditory system. Assessing central auditory deficits is not possible with routine audiometric testing such as PTA and TEOAE.

Other measures of hearing function that should be considered for future work are speech testing, and electrophysiological measures such as Auditory Brainstem Response (ABR) and Cortical evoked response audiometry (ERA). Speech testing is a test of functional hearing and gives a speech-recognition threshold, which is a level or signal-to-noise ratio at which the listener can identify and repeat 50% of words. Speech discrimination is affected by both cochlear loss and by certain auditory processing disorders⁵¹⁷, so speech recognition threshold is sensitive to deficits other than threshold elevation. It has been shown that noise exposure, ageing and ototoxic drugs can destroy synapses between cochlear nerve fibres and their hair cell targets, even when hair cells and thresholds recover^{210,211,518-520}.

Until this type of synaptopathy becomes extreme, behavioural thresholds would not be seen to be elevated⁵²¹, because the most vulnerable cochlear neurons to ageing and noise, do not contribute to threshold detection in quiet^{522,523}. With high thresholds and low spontaneous rates, these neurons are important in deciphering transient stimuli in the presence of background

noise^{522,523}. The loss of these neurons could be a major contributor for those who experience difficulty hearing speech in noise^{519,524-526}. In the human ageing ear, the rate of cochlear neural loss is more significant than the rate of sensory cell loss^{527,528}. Measurements of auditory evoked potentials include a contribution from the cochlear regions tuned to the extended high frequencies which are not assessed by standard PTA. Therefore, auditory evoked potentials can detect changes in neural amplitudes in subjects with normal standard-frequency thresholds which could be due to neural damage throughout the cochlea or to hair cell damage at the basal end of the cochlea.

In our study, we have seen those that are inflammaged have high neopterin volatility. It is believed that people with ongoing inflammaging are prone to have repeated episodes of inflammation. Initially, inflammatory episodes may fully resolve, however with the progression of inflammaging, full resolution of inflammation becomes less likely and inflammatory markers may remain elevated for longer. Initially, the body reacts to inflammation to bring the body back to homeostasis; however, prolonged periods of inflammation cause maladaptive processes such as changes in homeostatic set points and tissue injury²³¹. Therefore, it is important to know how often inflammatory state is raised in individuals, by using neopterin volatility rather than mean neopterin level. Regular monitoring highlights the frequency of raised inflammation, as well as how long it takes to resolve, therefore, recognising good resolvers and poor resolvers. Neopterin volatility, however, does not distinguish between those who have frequent inflammatory episodes and those who had prolonged resolution of inflammation.

Our study demonstrates serial measurements of neopterin in urine, which allows neopterin volatility to be assessed. This better identified those with chronic systemic inflammation than any single time-point measures. When participants were grouped according to their neopterin volatility, similar trends were seen with the other measured inflammatory markers.

This work also demonstrates that high neopterin volatility is associated with increased risk and co-occurrence of chronic age-related conditions as well as hearing loss, such as cardiovascular disease and type 2 diabetes. This is strong evidence for these individuals being inflammaged, as their consistently elevated inflammatory baseline would seemingly be affecting multiple systems in the body. Inflammaging is a predictor of frailty^{32,159}, those who are at increased risk of vulnerability to disease, disability and death. The frailty index is another biomarker that could be used to assess inflammaging; it is the ratio of the deficits present in a person, to the number of deficits evaluated²⁵¹. The frailty index has been used in many epidemiological and clinical studies. Another functional indicator of frailty is hand-grip strength (HGS) which has been shown to be associated with inflammatory biomarkers²⁵⁸.

Factors driving inflammaging are not inevitable, and there is evidence to suggest that lifestyle changes such as diet and exercise, can reduce inflammation and halt or reduce inflammaging⁵²⁹. Biomarkers of healthy ageing would be useful as outcome measures in trials of interventions designed to extend healthspan.

Healthy eating patterns are associated with lower circulating concentrations of inflammatory markers, including CRP and several cytokines^{530,531}. Subjects with greater adherence to a Mediterranean diet had 17% lower IL-6 and 20% lower CRP concentrations than those with the poorest adherence to the diet⁵³². Among the components of a healthy diet, higher intake of whole grains, vegetables and fruits, nuts and fish, are all associated with lower inflammation⁵³⁰.

Regular physical activity in older adults has been associated with lower levels of pro-inflammatory cytokines such as IL-6, TNF- α ⁵³³, improved neutrophil chemotaxis⁵³⁴, increased T-cell proliferation⁵³⁵ and improved vaccination responses⁵³⁶. There is also evidence that physically active older adults have fewer infections⁵³⁷. A study has looked at older non-elite cyclists compared to their sedentary counterparts. There was evidence that the cyclists showed reduced decline in thymic output, inflammaging, and increased Th17 cell responses, although the accumulation of senescent T cells still occurred²⁷⁸. The non-elite cyclists also had evidence of a thymoprotective environment due to high serum levels of IL-7 and IL-15 and low IL-6⁵³⁸, which also help to maintain naïve T cells in the periphery⁵³⁹.

However, prolonged exhaustive exercise is actually associated with increased stress hormones and impaired immune responses, but moderate exercise has been shown to have immunomodulatory effects^{540,541}. A comparative study of individuals undertaking an aerobic exercise regime, with those undertaking a flexibility/strength regime, has shown immunological benefits in the aerobic exercise group only⁵⁴². In a murine study on male C57Bl/6J mice, the effect of life-time exercise on longevity and health parameters was investigated. Life-long exercise (spontaneous wheel running), did not prolong longevity but did prevent several signs of frailty, and therefore concluded that exercise is an intervention that increases healthspan by delaying age-associated frailty⁵²⁹.

Inconsistencies in the literature regarding the immunological response to exercise may be due to lack of consistency in methods of physical activity evaluation and the exercise regime used. Other inconsistencies may be due to the lack of considering potential confounders, such as nutritional state, depressive symptoms, gender, or consumption habits, all of which could influence the results. The mechanisms by which physical activity may reduce inflammation need to be better understood⁵⁴³. However, there is definite evidence that maintained physical activity from middle into older age, can protect against many aspects of immune ageing.

Pharmacological interventions are also worth consideration. Many elderly individuals use lipid-lowering drugs, such as statins, because atherosclerosis and the risk of cardiovascular diseases increase with age. The cohort in this study had 37.8% diagnosed with hypertension and 13.3% diagnosed with other cardiovascular disease and 35.6 % using statins. As well as lipid-lowering effects, statins have been shown to reduce cardiovascular risk by improving endothelial function, maintain plaque stability and reducing the inflammatory response. Statins have been shown to reduce CRP levels by almost 17%³²⁰. In a large-scale population study, those who had never used statins were three times as likely to develop age-related hearing loss, compared to those who used statins⁵. The results of this study, do not show this same relationship, although on entering the study, half of those in the lowest neopterin volatility group were prescribed statins, but no overall conclusion can be drawn.

Other studies have evaluated the use of statins as otoprotectants. Simvastatin has been shown to reduce gentamicin-induced outer hair cell loss in rat cochlear cultures⁵⁴⁴. In a mouse model of presbycusis, atorvastatin has been shown to preserve outer hair cell function⁵⁴⁵. Pravastatin and Fluvastatin have been shown to reduce noise-induced hearing loss and hair cell death^{546,547}. A further recent study has demonstrated that lovastatin reduces cisplatin-induced hearing loss in adult mice⁵⁴⁸.

Another drug of interest is Aspirin, a non-steroidal anti-inflammatory drug (NSAID). Aspirin has been tested for pro-longevity in genetically heterogenous mice⁵⁴⁹, but a positive result was only seen in male mice⁵⁵⁰. It was suggested that the lack of effect in female mice was due to differences in drug disposition and metabolism. The ASPREE-HEARING study is investigating the potential therapeutic benefits of low-dose aspirin on ARHL. This large Australian-based clinical trial is targeting 1262 individuals age 70 years old or older, but is still currently in progress³⁰⁵. This trial provides huge potential for an incredibly inexpensive yet feasible treatment option for preventing or reducing ARHL.

Other limitations of note in this study are the small cohort size and the ratio of males to females. A sample size of 45 is rather small; however, findings are similar to those seen in studies on much larger populations. As a pilot study, this work provides evidence for long-term neopterin volatility as a measurement of inflammaging. Future work will involve a study of increased duration, on a large multi-centre population. This study had a disproportionate number of females to males, and this will be better controlled in future work as males are known to have poorer hearing than females³²³, particularly at high-frequencies. Additionally, progression of hearing loss has been shown to be greater in males⁵⁵¹. This is often attributed to males being exposed to greater noise through occupational and lifestyle differences⁵⁵², but studies have shown that when the effect of

noise exposure is eliminated, the incidence and progression of hearing loss in males remained higher^{323,551}. A theory for this is that female hormones play a protective role as there is evidence of oestrogen receptors in the cochlea^{553,554}.

There are also several differences in the immunological response of males and females, most likely because women are known to produce more robust humoral and cellular immune responses. However, the reason for the gender disparity in immunosenescence is still a matter of discussion⁵⁵⁵.

5.2 SERS-based neopterin measurement at point-of-care

If the current global pandemic can teach us anything, it is that lab-based diagnostic testing such as PCR, is not suitable for mass testing, and point-of-care diagnostics are not yet sufficiently developed. A major focus of SERS research is the development of novel and highly active SERS substrates. Whilst many are aiming to achieve the highest possible enhancement factors and lowest limits of detection, it is also vitally important to develop substrates which are simple to use, cheap, and suitable for point-of-care testing.

As most have the aim of high enhancement, reproducibility and low detection limits, many have developed approaches integrating SERS with microfluidic devices^{370,460,556-558}. These devices have shown promising results; however, they still utilise polymer and plastic devices that are complex to produce and add cost. Utilising paper-based devices for chromatographic separation with inkjet-printed nanoparticles has been extensively demonstrated^{114,136,464,471,473,480,481,493,494,559-563} and brilliant results observed. A limitation of using printed silver and gold nanoparticles is the shelf-life. Silver and gold nanoparticles are prone to oxidation and become unstable if exposed for too long. Therefore, most of these devices have a limited shelf-life of a few days to weeks. Commercially available substrates have superior shelf lives, although still limited. Currently, commercially available substrates cost in the range of £6 to £40 per test, due to the cost of the manufacturing process and even these do not report the best reproducibility for quantitative measurements.

Enhancement factor (EF) and the limit of detection (LOD) are widely used to promote the usefulness of SERS substrates. However, in the arena of point-of-care devices for quantitation of clinical markers, these parameters are fairly irrelevant. Devices suitable for POC are required to be simple and cheap, SERS substrates that offer the largest enhancements and lowest LOD, are largely those with complex manufacturing, and although devices such as microfluidics are

promoted as POC suitable, in reality, they are not. More recent recommendations for devices that are suitable for this type of use is to focus on whether they can actually accurately quantify the samples they have been designed for. Can the substrate measure the concentration of a clinically relevant biomarker in the region of its physiological concentration, whilst keeping the device as cheap and easy to use as possible³⁹⁰? There are also multiple ways of measuring LOD and LOQ, some of which are slightly subjective; therefore, some of the extremely low reported values, could be questioned. If these types of measurements are to be used in the SERS community, then there needs to be a consensus on the approach, and it needs to be as objective as possible.

Paper chromatography is a well-established quick, easy and inexpensive way to separate and analyse components in a mixture. Just like other chromatography techniques, the principle of the separation is based on the different affinity of analytes for the stationary phase and the solubility of the analytes in the mobile phase. This research demonstrates that paper SERS substrates can be used to chromatographically separate a target from a complex matrix without the need for additional sample clean-up steps. Compared to traditional analytical techniques such as high-performance liquid chromatography (HPLC) and mass spectrometry (MS), paper SERS chromatography detects the presence of target analytes without any sample processing whilst eliminating complicated and laborious sample clean up and analyte extraction steps. In addition, unlike other SERS techniques for multi-analyte detection, the analytes can be well separated in the chromatogram, eliminating the need for multivariate analysis of the SERS spectra.

We have demonstrated that the SERS sensors have a shelf-life of at least one month, and most likely longer. We did not assess the long-term stability of the sensors on the paper devices, as they were always made fresh for use. Silver and gold nanoparticles are liable to oxidation and others have shown that the SERS active life-time for paper SERS substrates can vary from days (for silver) to weeks (for gold), depending on storage conditions such as humidity, temperature and oxygen concentration⁴⁷⁹. The use of foil packs with humectants and oxygen scavengers could be used to control and improve the storage conditions.

Control of hotspot formation between the nanoparticles (rather than between the layers) could be further controlled by using molecules that link, space, or cap the nanoparticles. Formation of nanoparticle dimers and clusters have been demonstrated using different linker molecules⁵⁶⁴⁻⁵⁶⁶. The spacing between nanoparticles can be controlled, with differing sized linker molecules, depending on the size of the analyte of interest, therefore acting as a sieve to other molecules.

SERS detection relies on the adsorption of the analyte onto the nanoparticles. This relies on the analyte having an affinity for the nanoparticle surface as well as there being little competitive adsorption with competing molecules. Also, because of the large number of different chemical

bonds within biological molecules, and the random orientation of molecules, it can make identification exceptionally difficult. One way of overcoming this obstacle is to employ the use of labelled biorecognition elements such as antibodies, enzymes and aptamers. This allows for the generation of a specific signal upon binding, which enables the detection of target biomolecules.

Nucleic acid aptamers can specifically capture biological analytes^{502,567-570}. The binding affinity of aptamers for their targets is comparable and can even be better than antibodies, and are not just limited to protein targets⁵⁷¹⁻⁵⁷³. Once identified by the Systematic Evolution of Ligands by Exponential Enrichment (SELEX) process⁵⁷⁴, nucleic acid sequences can be synthesised very simply in a short time period, and on a large scale in a test tube, using basic nucleic acid components. Aptamers are also much more resistant to degradation compared to antibodies and enzymes and can be made to bind to targets under diverse conditions. By using multiple aptamers with affinity for different antigen targets, it is possible to detect multiple analytes within a single assay.

Another concern with using a SERS technique to quantify neopterin, is the stability of neopterin itself. The urine samples that were used in this study had been stored at -20°C for several years and would have been subjected to some freeze-thaw cycles by nature of being used by different researchers over the study duration. Such handling of the samples may have affected the neopterin concentration within the samples. Stability experiments on urine samples from primates have considered the changes in urinary neopterin levels to multiple freeze-thaw cycles, extended exposure to room temperature, extended storage, and exposure to light²⁴⁷. Urine samples were stored at -20°C for 2 years, and overall urinary neopterin levels remained the same after 2 years. Neopterin levels in urine increased with the number of freeze-thaw cycles they were subjected to. Neopterin levels in human serum, have also been found to be affected by frequent thawing cycles, and in macaques, urinary neopterin significantly increased after three freeze-thaw cycles⁵⁷⁵. For future work, freeze-thaw of samples should be avoided. If it is necessary to freeze and thaw samples, then all samples must be subjected to the same number of cycles, if the values within the samples are to be compared. Keeping urine samples at room temperature for 24-48 hours, showed a decrease initially, but then an increase in urinary neopterin levels²⁴⁷. Therefore, it is recommended that samples should be frozen promptly after collection. It has also been shown that sunlight significantly degrades neopterin levels^{576,577}; however, artificial light does not²⁴⁷. In another study, urinary neopterin was found to be remarkably stable over time. However, rises in creatinine indexed urinary neopterin were detected due to degradation of the creatinine⁵⁷⁵, and it has been suggested that urinary neopterin concentrations should be indexed for specific gravity instead of creatinine⁵⁷⁸.

5.3 Clinical Implications and Future Work

Healthcare is moving towards predictive, preventative and personalised medicine. This will provide treatment of health conditions that are tailored to an individual's specific need.

Techniques and technologies which allow the profiling of individuals at the molecular level are what is needed. Based on the results of this work, it is entirely feasible that those identified to be at greater risk of age-related hearing loss, or at greater risk of progression of age-related hearing loss, could be treated more holistically than just being provided with amplification. For middle-aged individuals, knowing their risk category would allow them to make significant lifestyle changes, which could alter, or reduce, their risk of developing an age-related condition in the future. For older adults already diagnosed with one (or more) conditions linked to inflammaging, they would have the chance to reduce the risk of progression of disease. As there is no current disease altering management for age-related hearing loss, research into interventions that reduce inflammaging, with potential to reduce the progression of hearing loss, would be revolutionary.

The inflammaging and hearing loss study presented here is useful pilot evidence for a much larger study. Future work should involve a large scale, multi-centre, population study, of minimum 5-year duration. The study would further investigate the effect of systemic inflammation on the progression of age-related hearing loss, incorporating additional measures of both hearing and inflammaging. Such a study would also allow investigation of intervention measures, such as diet, exercise and pharmacology.

Further work into developing a point-of-care test for urinary neopterin will involve additional development of the SERS paper chromatography, to optimise further for neopterin and creatinine quantification. Work on developing an actual device with an encasement, that functions with a handheld Raman spectrometer would be necessary in the immediate future. The device would then need to undergo stringent validation and quality assurance measurements before potentially being taken to market.

5.4 Conclusions

The body of work of this thesis has provided evidence for the necessity for point-of-care testing of neopterin volatility and has outlined how best this might be achieved using the method of Surface-enhanced Raman spectroscopy. The novel contributions to the scientific community are:

- Neopterin volatility, measured from serial monthly urine samples, is a good measure of inflammaging and allows individual's risk category to be predicted.

- High neopterin volatility is associated with increased risk and co-occurrence of chronic age-related conditions, as well as specifically being associated with greater progression of high-frequency hearing loss.
- Surface-enhanced Raman spectroscopy using our colloidal SERS sensors has demonstrated the quantitative measurement of neopterin and creatinine in urine samples, with improved enhancement and reproducibility over colloidal gold nanoparticles. This provides evidence for the feasibility of using SERS for point-of-care testing, due to its fast and sensitive data acquisition, using samples that do not require sample preparation and without the need for multivariate analysis.
- Although the use of paper chromatography with SERS has previously been demonstrated, this is the first demonstration of our colloidal SERS sensors being incorporated into a paper chromatography device.
- The use of paper chromatography SERS to separate and quantify neopterin and creatinine has been demonstrated, which validates the use of this technique for potential point-of-care monitoring of urinary neopterin.

Appendix A InflammHear Subject Questionnaire



Version 1

Date: 4/07/2013

PARTICIPANT INFORMATION SHEET

Project Title: THE EFFECT OF INFLAMMATION ON THE PROGRESSION OF AGE-RELATED HEARING LOSS

InflammHear

Questionnaire

Please tick the answer that best describes your situation

DEMOGRAPHICS

Identification number:

Age:

Gender:

Have you lived most of your adult life in the city or rural setting?

City Rural

What is/was your principal occupation?

HEARING (without wearing hearing aids)

a. Do you find it difficult to follow a conversation if there is background noise? For example children playing, TV or radio on?

Yes No

b. How well can you follow a conversation with one other person when there is no background noise?

1. Not at all

Appendix A

2. With great difficulty
3. With moderate difficulty
4. With slight difficulty
5. With no difficulty

c. How well can you follow a conversation in a noisy location such as a shop, restaurant or busy street?

1. Not at all
2. With great difficulty
3. With moderate difficulty
4. With slight difficulty
5. With no difficulty

d. How long altogether have you worked in noisy places where you had to shout to be heard?

1. Never
2. For less than 6 months
3. For 6 to 11 months
4. For 1 to 5 years
5. For more than 5 years

e. During your lifetime have you fired more than a total of 10 rounds from a shotgun or military rifle (not counting a .22 rifle)?

Yes No

f. Do you get noises in your head or ears such as ringing, buzzing or whistling, that usually lasts for more than 5 minutes and occurs **not** only after loud sounds?

Yes No

g. Did any of your close relatives (parents, siblings, grandparents, children) have difficulty with their hearing before age 65 years?

Yes No Unsure

h. Did you suffer from ear infections as a child?

Yes No Unsure

i. Do you use or have you been prescribed a hearing aid?

Yes No

LIFESTYLE

j. Have you ever smoked regularly (i.e. at least once a day for a year or more)?

Yes No

k. If you no longer smoke, did you give it up before the age of 40?

Yes No

MEDICAL

l. Have you been ever prescribed medication for high blood pressure?

Yes No

m. Have you ever been prescribed Statins?

Yes No

n. Have you ever been told by a doctor that you have heart failure?

Yes No

o. Have you ever been told by a doctor that you have problems with your heart valves?

Yes No

p. Have you ever had a heart attack or angina?

Yes No

q. Have you been ever had a stroke?

Yes No

r. Do you have diabetes?

Yes No

Appendix B InflammHear Subject Questionnaire Results

Tables

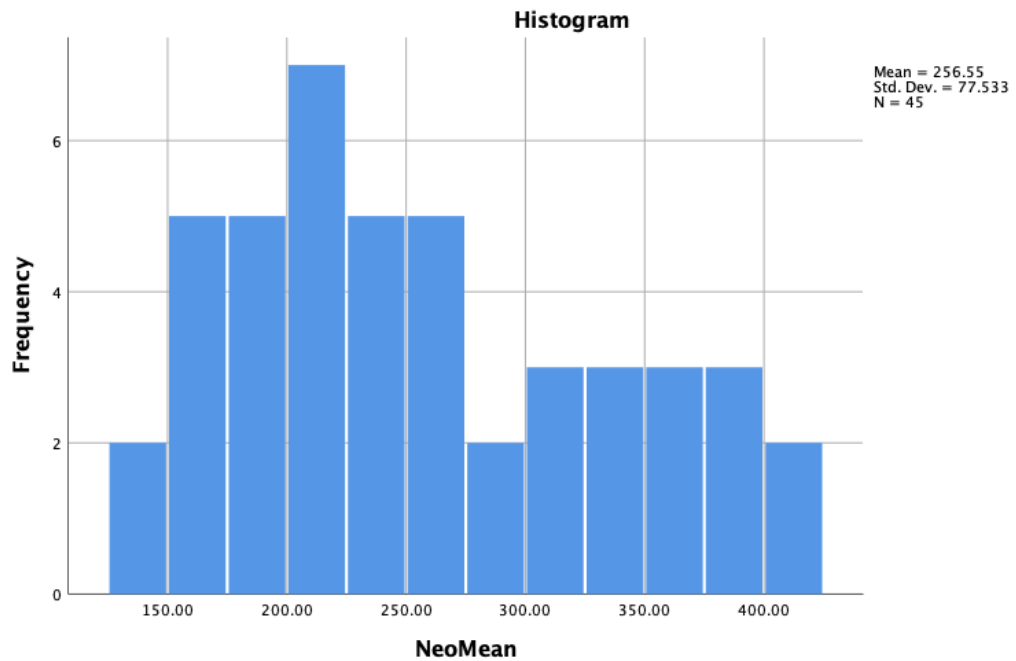
Characteristic	Baseline		Study End	
	Number	Percentage (%)	Number	Percentage (%)
Smoking				
No	28	62.2	25	55.6
Yes	17	37.8	20	44.4
Gave up before age 40				
Yes	8	47.1	7	65
No	9	52.9	13	35
One or more chronic disease	18	40	22	48.9
Hypertension				
No	28	62.2	24	53.3
Yes	17	37.8	21	46.7
Heart disease				
No	39	86.7	38	84.4
Yes	6	13.3	7	15.6
Stroke				
No	45	100	44	97.8
Yes	0	0	1	2.2
Diabetes				
No	44	97.8	43	95.6
Yes	1	2.2	2	4.4
Statin use				
No	29	64.4	29	64.4
Yes	16	35.6	16	35.6

Appendix B

Characteristic	Baseline		Study End	
	Number	Percentage (%)	Number	Percentage (%)
Difficulty hearing in quiet				
No difficulty	34	75.6	29	64.4
Slight difficulty	7	15.6	10	22.2
Moderate difficulty	4	8.9	5	11.1
Great difficulty	0	0	1	2.2
Difficulty hearing in noise				
No difficulty	8	17.8	8	17.8
Slight difficulty	18	40.0	18	40.0
Moderate difficulty	14	31.1	14	31.1
Great difficulty	5	11.1	5	11.1
History of noise exposure				
No	35	77.8	34	75.6
Yes	10	22.2	11	24.4
Hearing aids prescribed				
No	36	80.0	32	71.1
Yes	9	20.0	13	28.9
Tinnitus				
No	30	66.7	30	66.7
Yes	15	33.3	15	33.3
Recurrent ear infections				
No	28	62.2	29	64.4
Yes	11	24.4	13	28.9
Unsure	6	13.3	3	6.7
Family history of hearing loss				
No	23	51.1	20	44.4
Yes	15	33.3	15	33.3
Unsure	7	15.6	10	22.2

Appendix C Assessing normality of InflammHear Data

C.1 Example Variable- Neopterin Mean



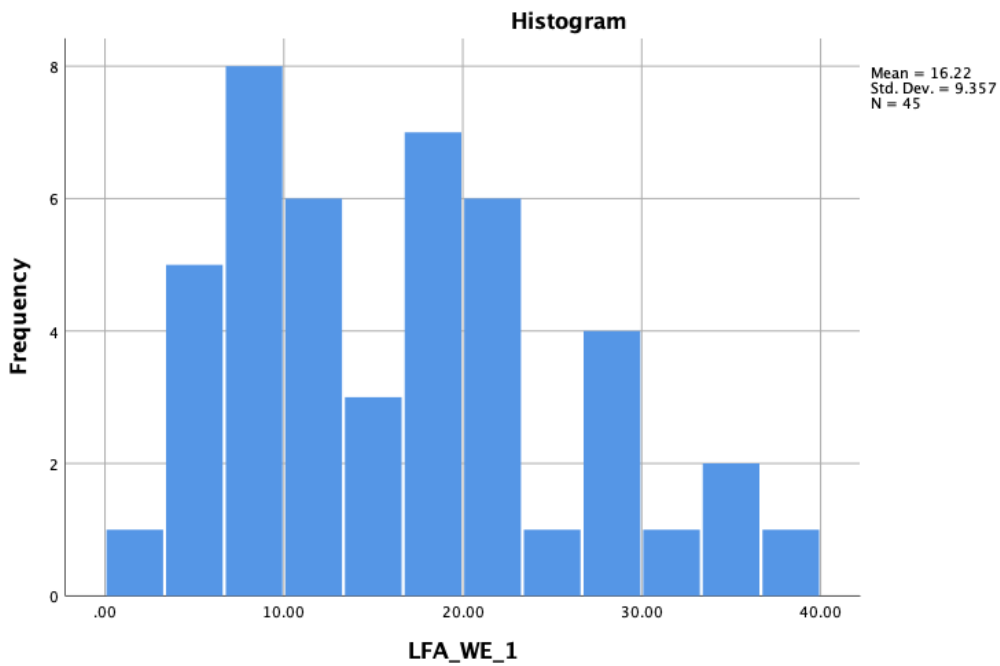
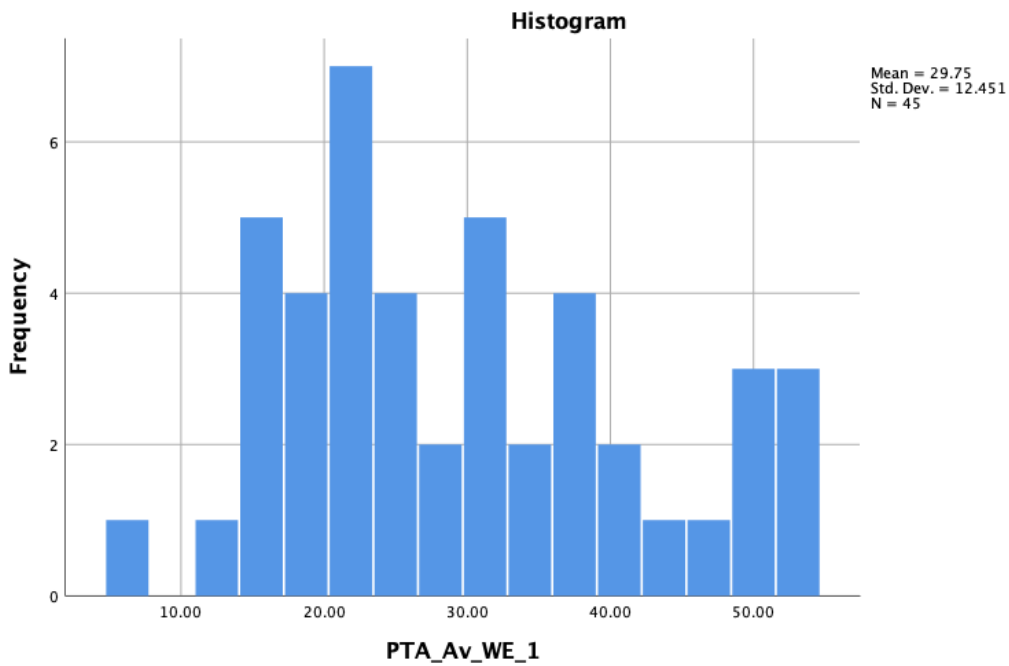
Tests of Normality

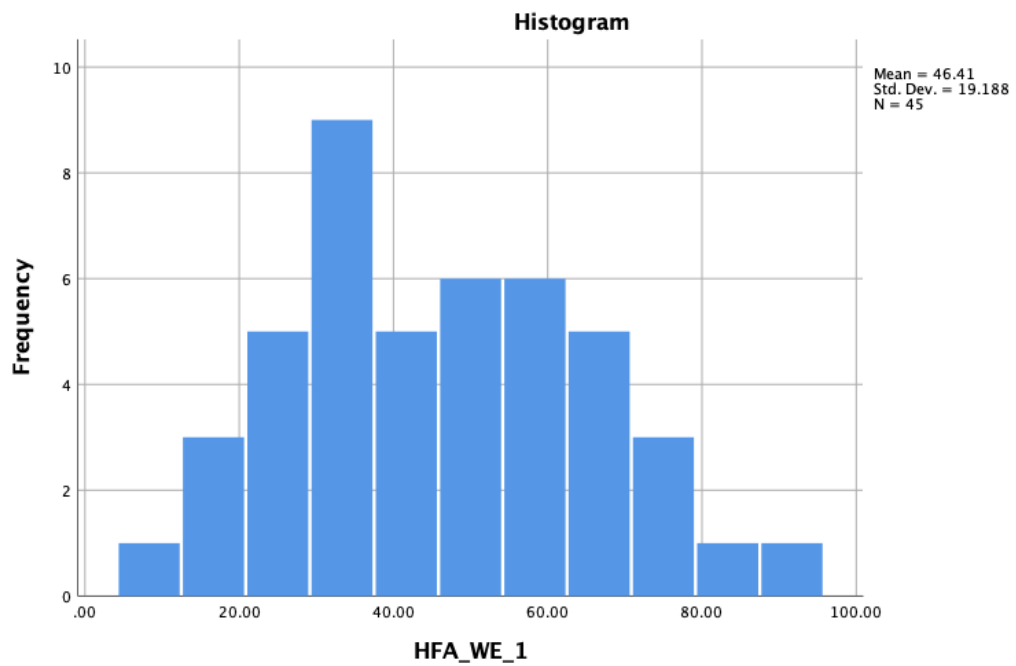
	Kolmogorov-Smirnov ^a			Shapiro-Wilk		
	Statistic	df	Sig.	Statistic	df	Sig.
NeoMea n	.098	45	.200*	.950	45	.050

*. This is a lower bound of the true significance.

a. Lilliefors Significance Correction

C.2 Example Variables- PTA Average, High Frequency Average and Low Frequency Average





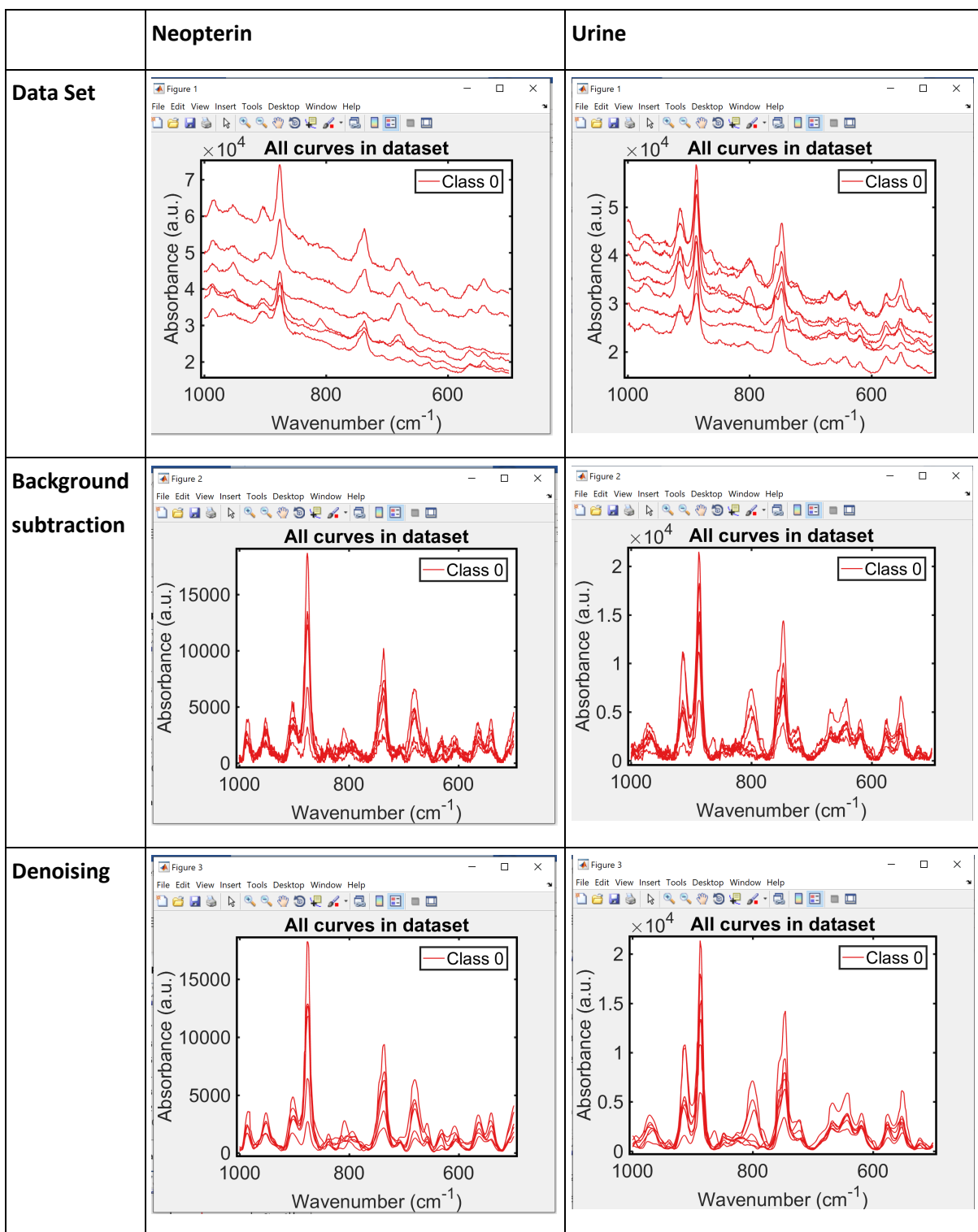
Tests of Normality

	Kolmogorov-Smirnov ^a			Shapiro-Wilk		
	Statistic	df	Sig.	Statistic	df	Sig.
PTA_Av_WE_1	.103	45	.200	.951	45	.055
LFA_WE_1	.113	45	.184	.959	45	.108
HFA_WE_1	.120	45	.109	.975	45	.449

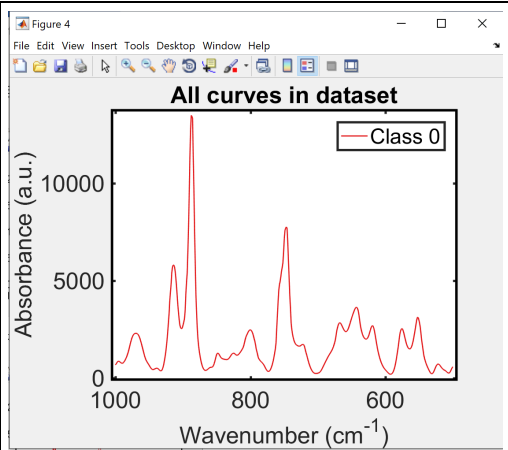
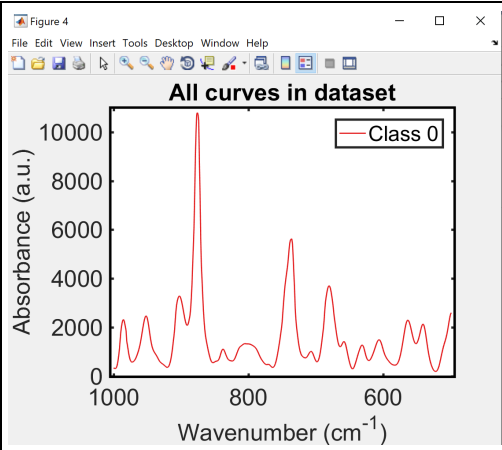
*. This is a lower bound of the true significance.

a. Lilliefors Significance Correction

Appendix D Example of SERS spectra pre-processing

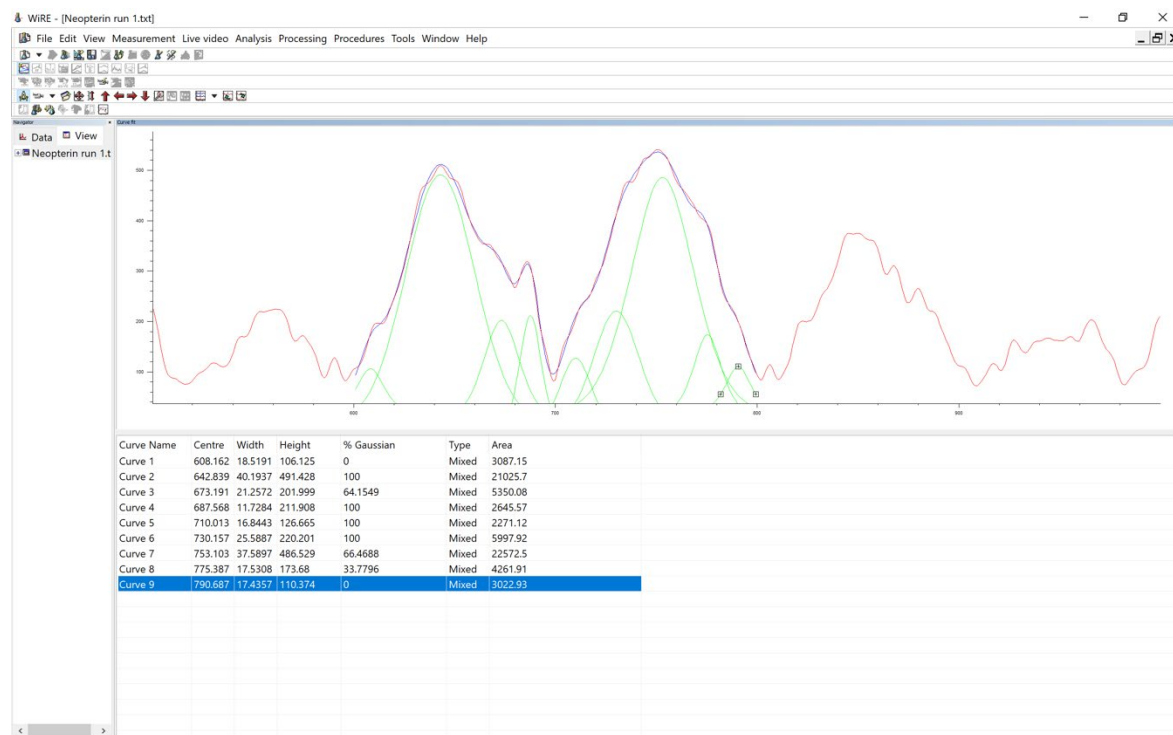


Averaging



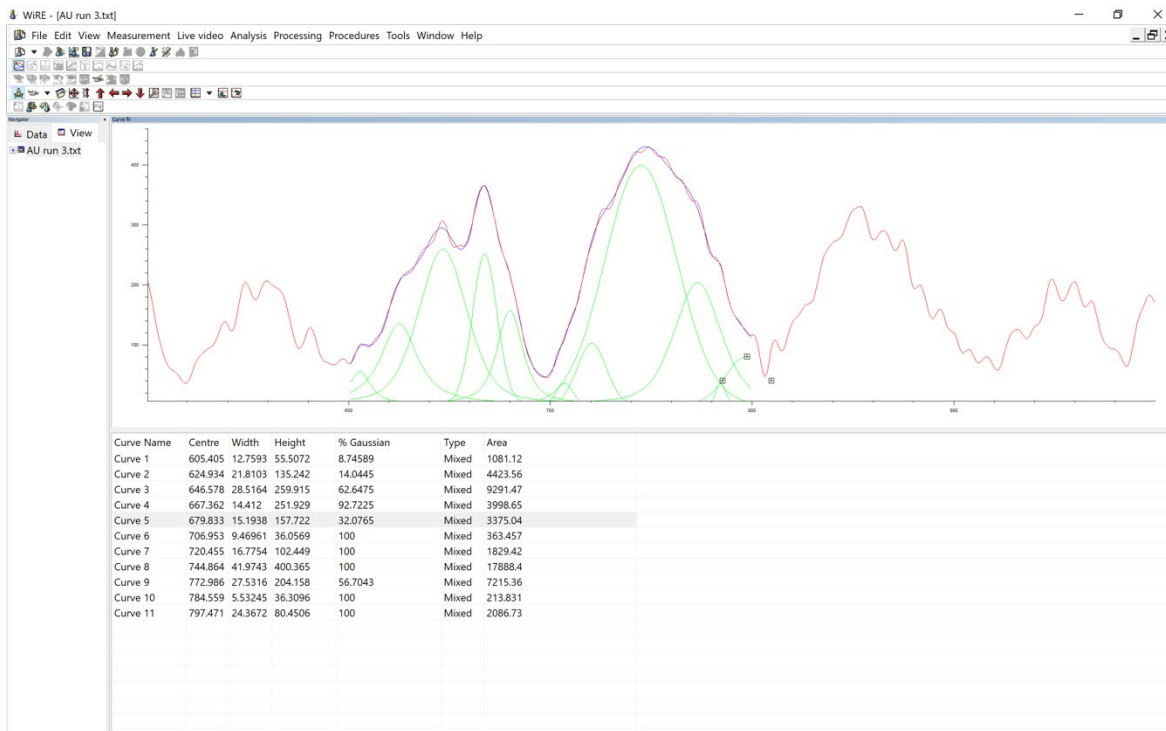
Appendix E Example of curve fitting SERS spectra

Neopterin Sample A



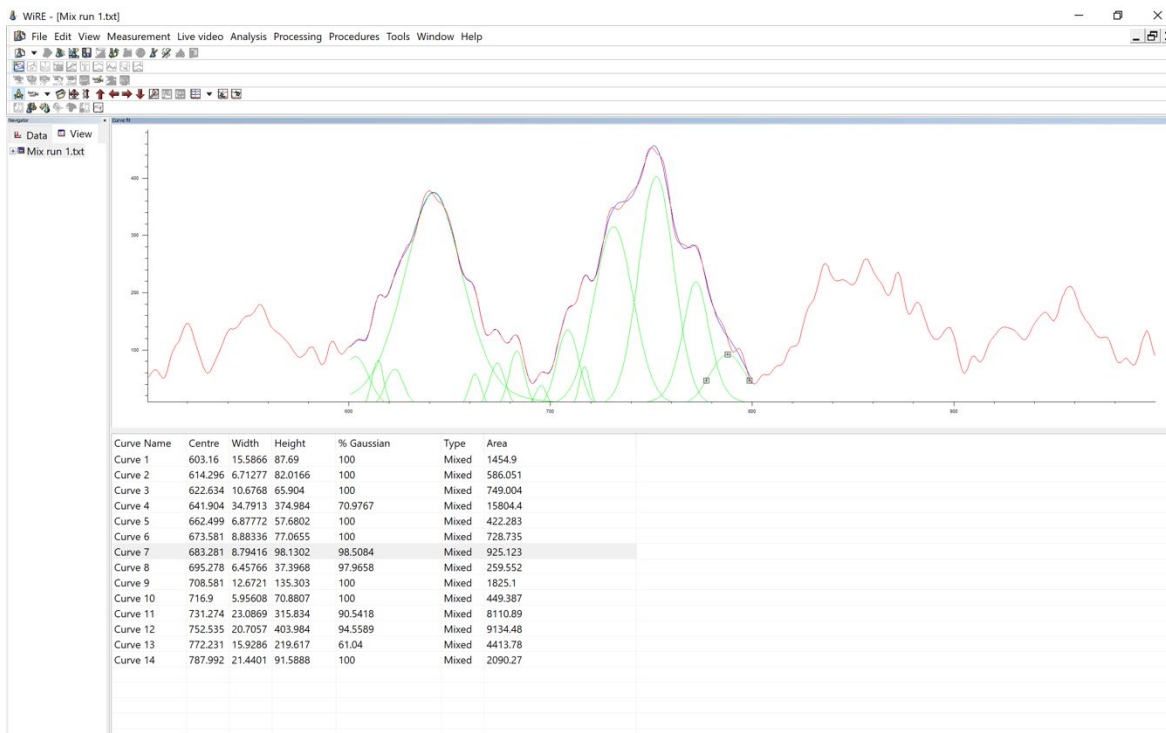
After curve fitting: Peak height at 687.568 cm^{-1} is 211.908 and 753.103 cm^{-1} is 486.529. Peak ratio height is 0.4355506. Interpolation from the standard curve gives a concentration of $41.907\mu\text{M}$.

Neopterin spiked artificial urine C



After curve fitting: Peak height at 679.833 cm^{-1} is 157.722 and 744.864 cm^{-1} is 400.365. Peak ratio height is 0.39394552. Interpolation from the standard curve gives a concentration of $35.526\mu\text{M}$.

Neopterin/Creatinine Mix A

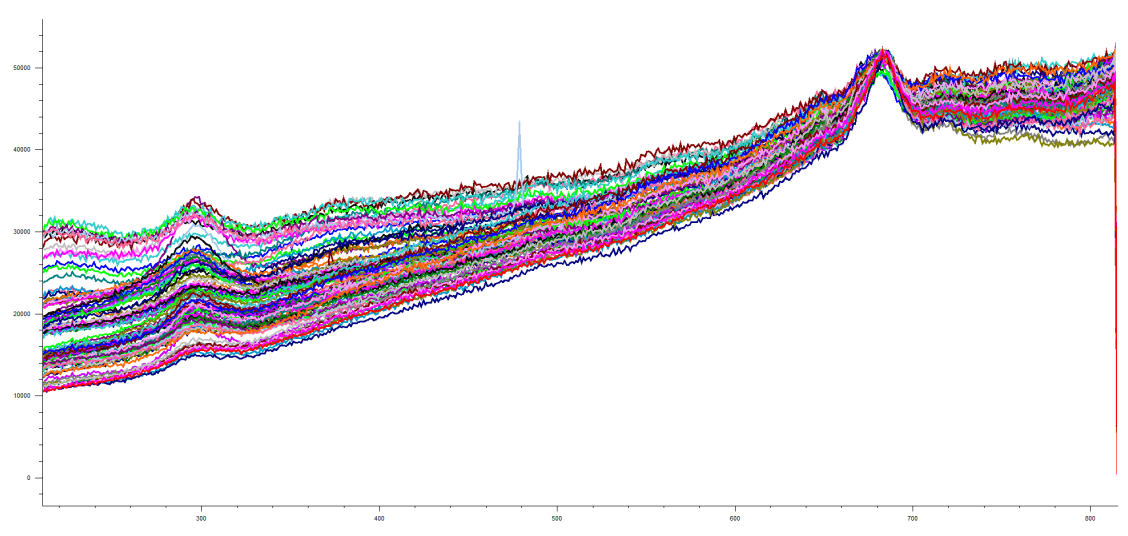


After curve fitting: Peak height at 683.281 cm^{-1} is 98.1302 and 752.535 cm^{-1} is 403.984. Peak ratio is 0.24290615. Interpolation from the standard curve gives a concentration of $17.050\text{ }\mu\text{M}$.

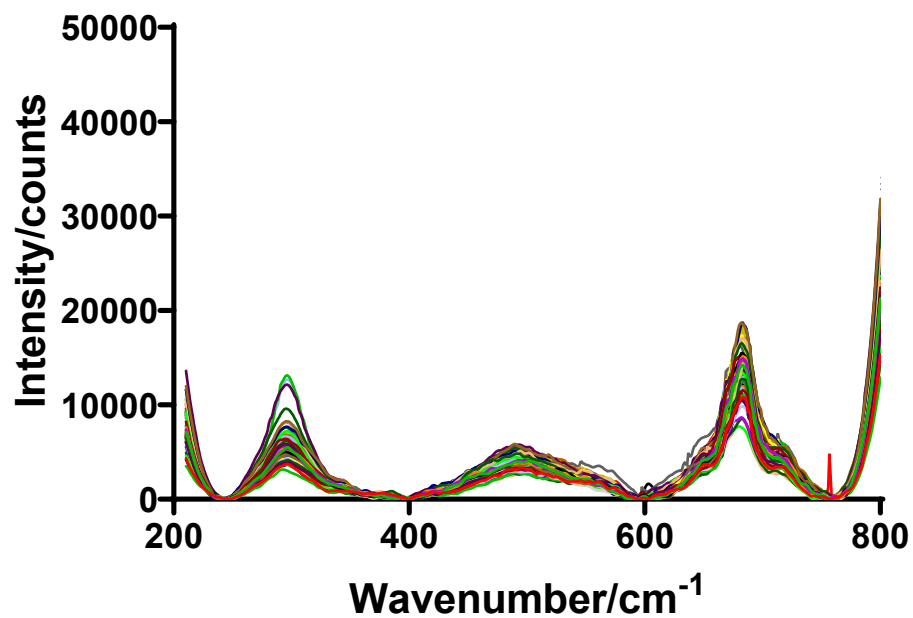
Appendix F Batch to batch reproducibility SERS spectra

One-month old batch

Unprocessed SERS spectra

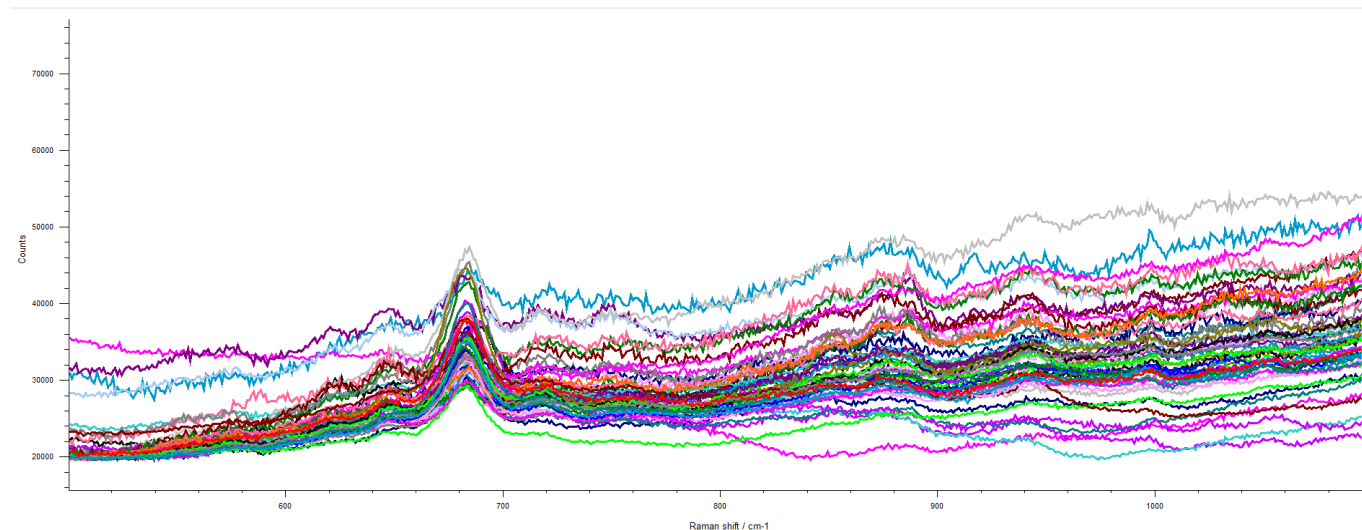


Baseline corrected and denoised

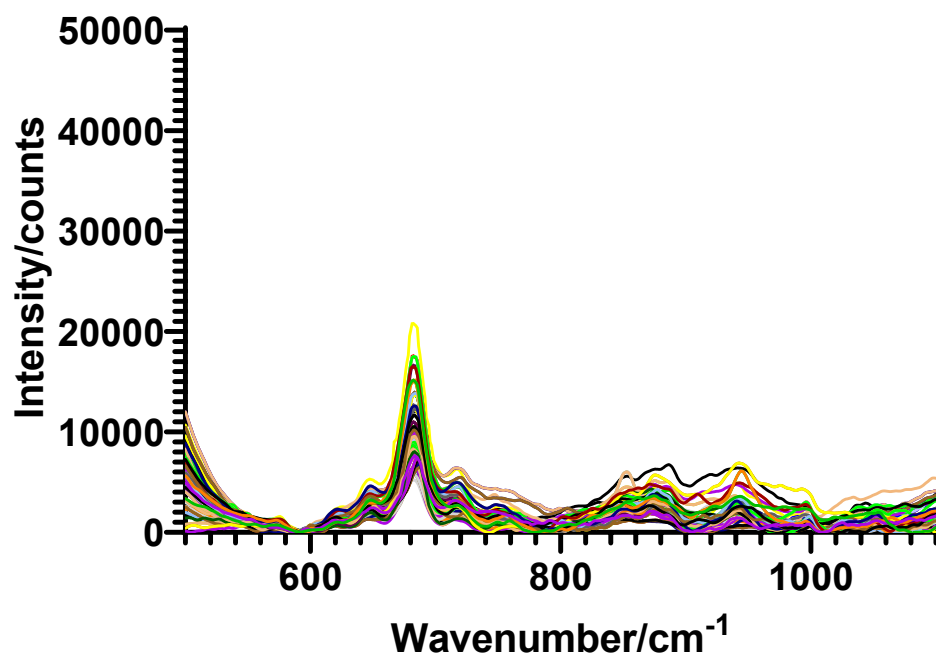


Batch A

Unprocessed SERS spectra

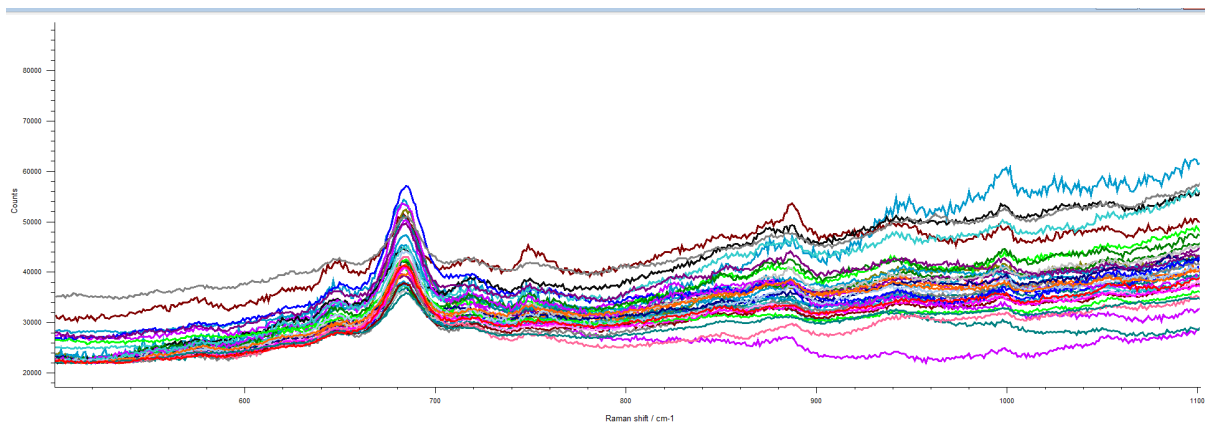


Baseline corrected and denoised

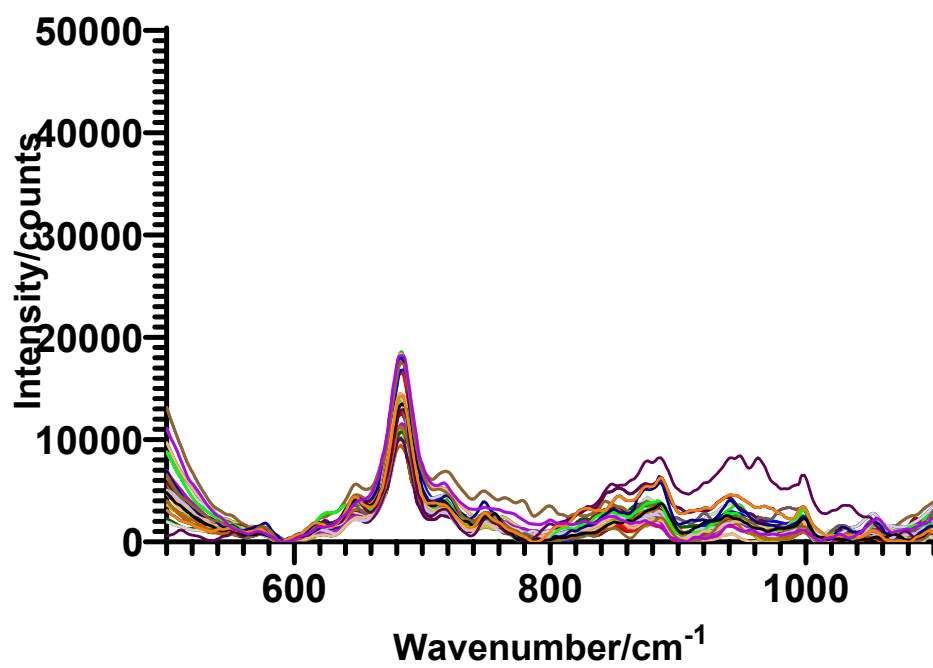


Batch B

Unprocessed SERS spectra

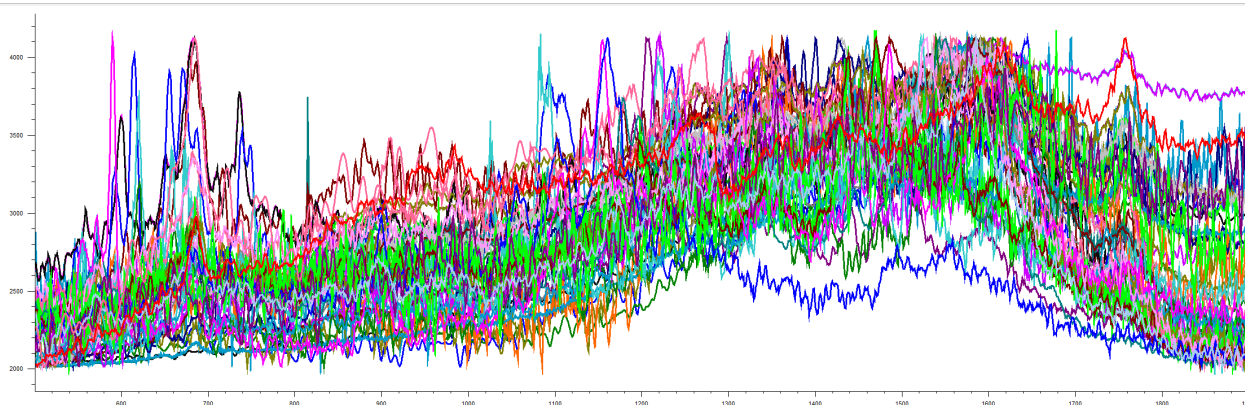


Baseline corrected and denoised

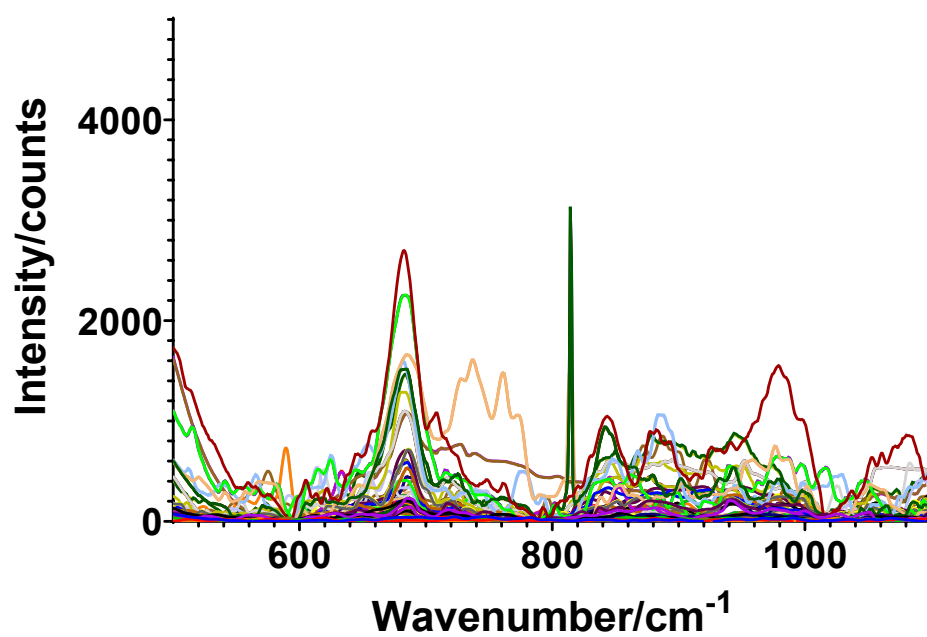


Colloid

Unprocessed SERS spectra



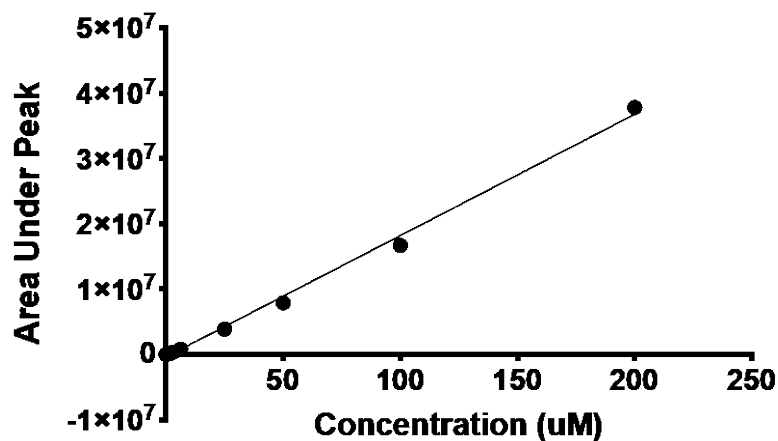
Baseline corrected and denoised



Appendix G Neopterin and Creatinine standard curves

HPLC

Neopterin in synthetic urine



Straight line

Best-fit values

Yintercept -380037

Slope 185853

95% CI (profile likelihood)

Yintercept -759108 to -965.7

Slope 180402 to 191305

Goodness of Fit

Degrees of Freedom 20

R squared 0.9961

Sum of Squares 10809602653379

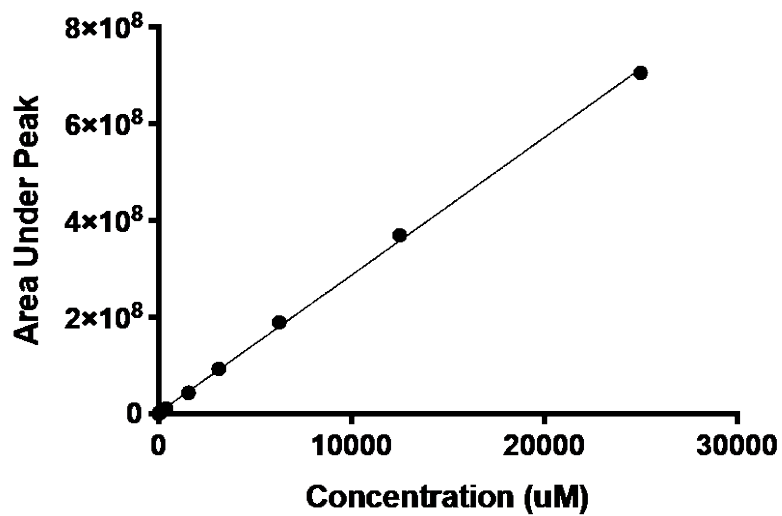
Sy.x 735174

Number of points

of X values 36

Y values analyzed 22

Creatinine in synthetic urine



Straight line

Best-fit values

YIntercept 2613049

Slope 28466

95% CI (profile likelihood)

YIntercept -39704 to 5265802

Slope 28175 to 28756

Goodness of Fit

Degrees of Freedom 28

R squared 0.9993

Sum of Squares 1.002e+015

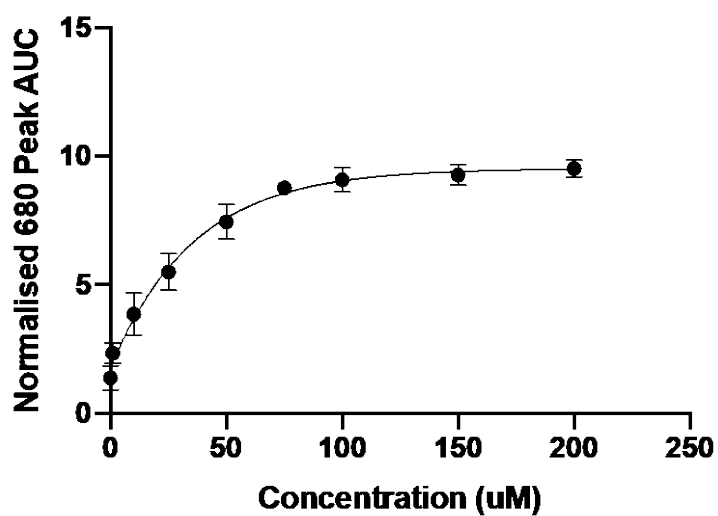
Sy.x 5983378

Number of points

of X values 36

Y values analyzed 30

SERS

Neopterin

One-phase association

Best-fit values

Y0	1.770
Plateau	9.519
K	0.02780
Tau	35.97
Half-time	24.93
Span	7.750

95% CI (profile likelihood)

Y0	1.317 to 2.217
Plateau	9.079 to 10.01
K	0.02219 to 0.03473
Tau	28.79 to 45.07
Half-time	19.96 to 31.24

Goodness of Fit

Degrees of Freedom	6
R squared	0.9946
Sum of Squares	0.4364

Sy.x 0.2697

Constraints

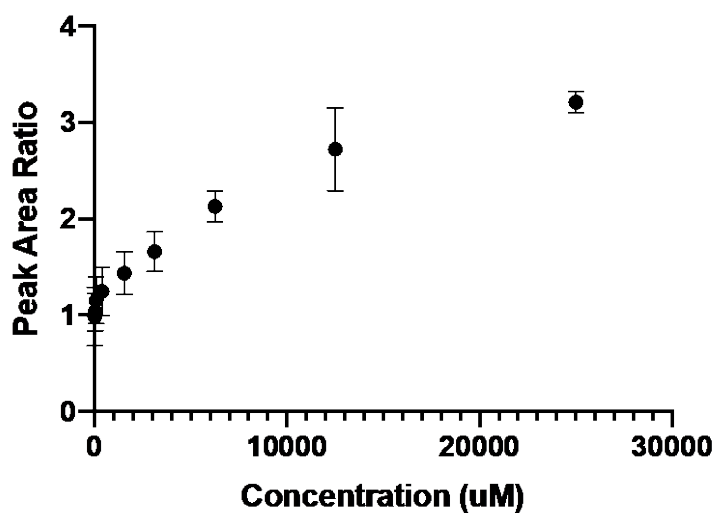
K $K > 0$

Number of points

of X values 9

Y values analyzed 9

Creatinine



Line

Best-fit values

YIntercept 1.233

Slope $8.938e-005$

95% CI (profile likelihood)

YIntercept 1.132 to 1.335

Slope $7.895e-005$ to $9.981e-005$

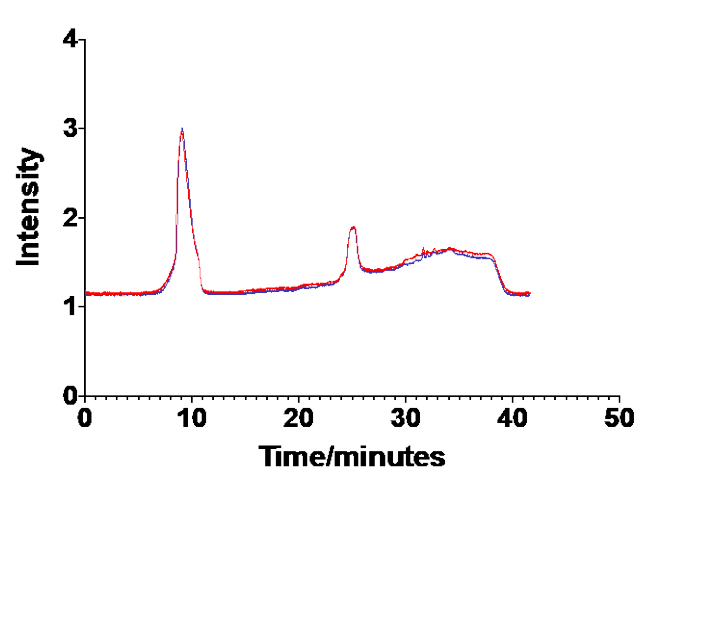
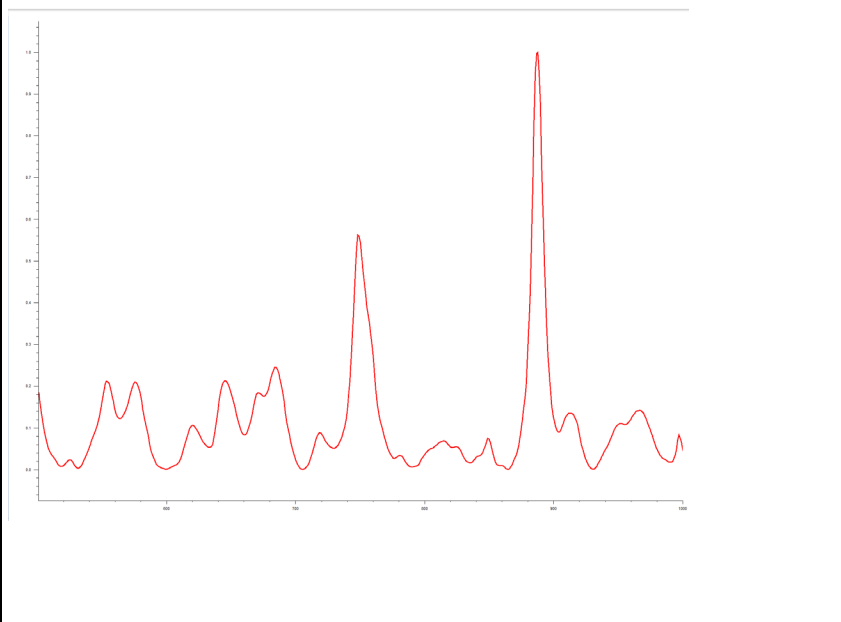
Goodness of Fit

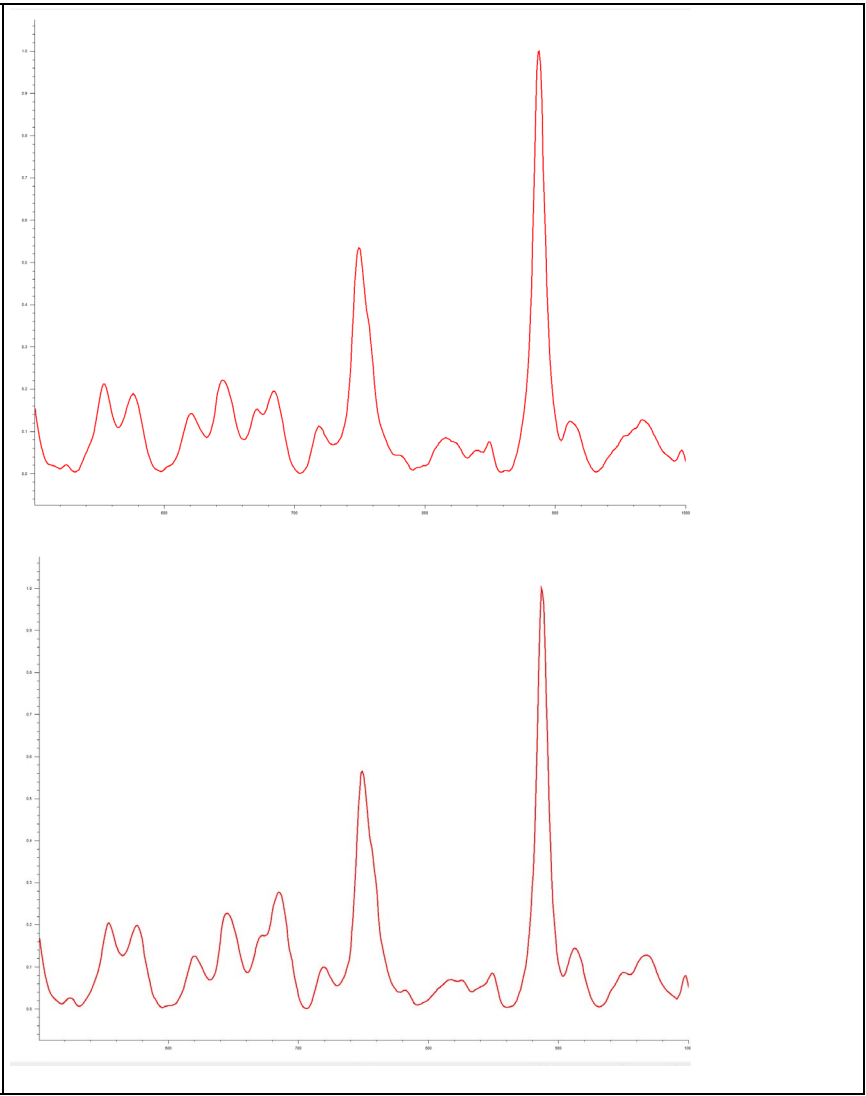
Degrees of Freedom 57

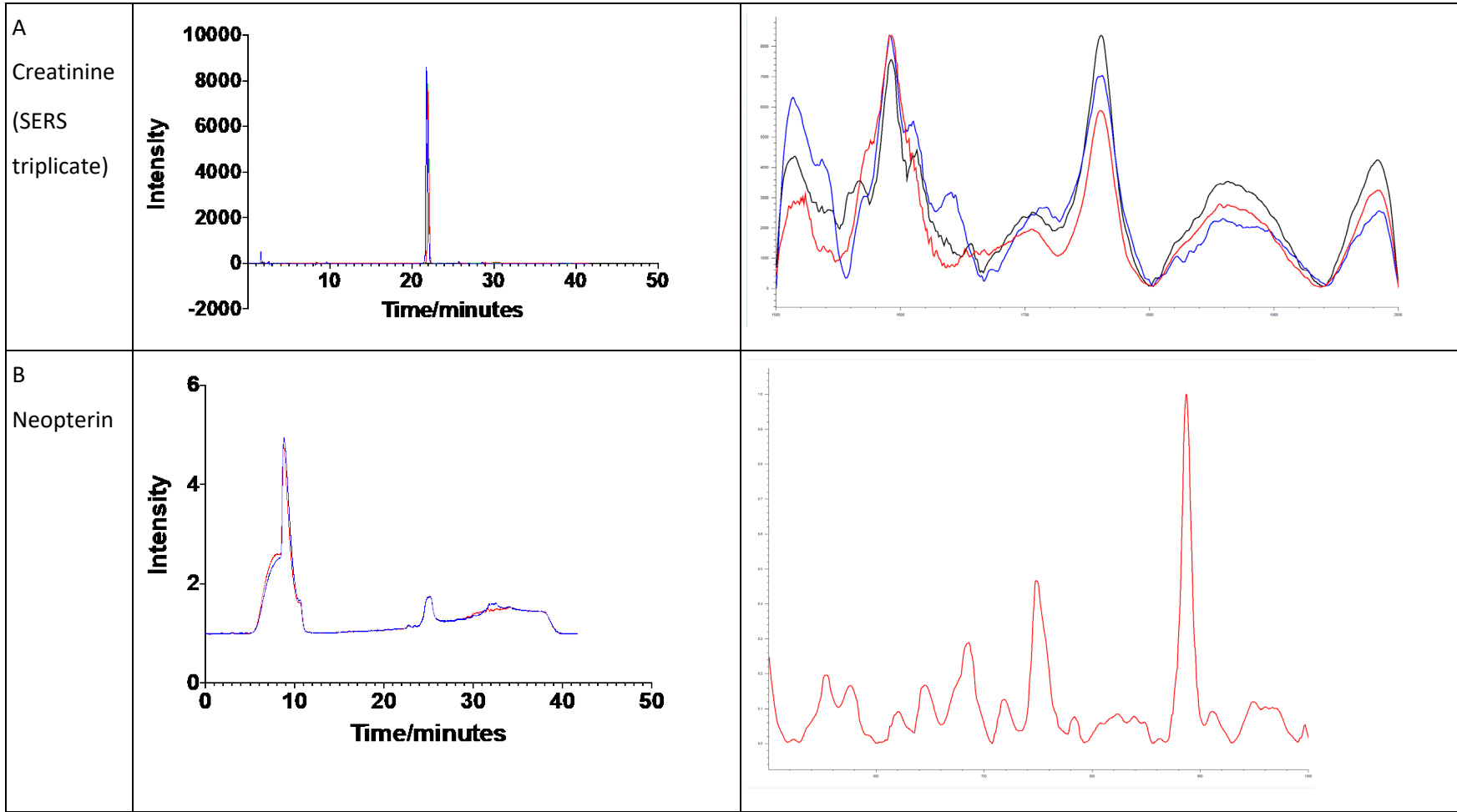
R squared 0.8378

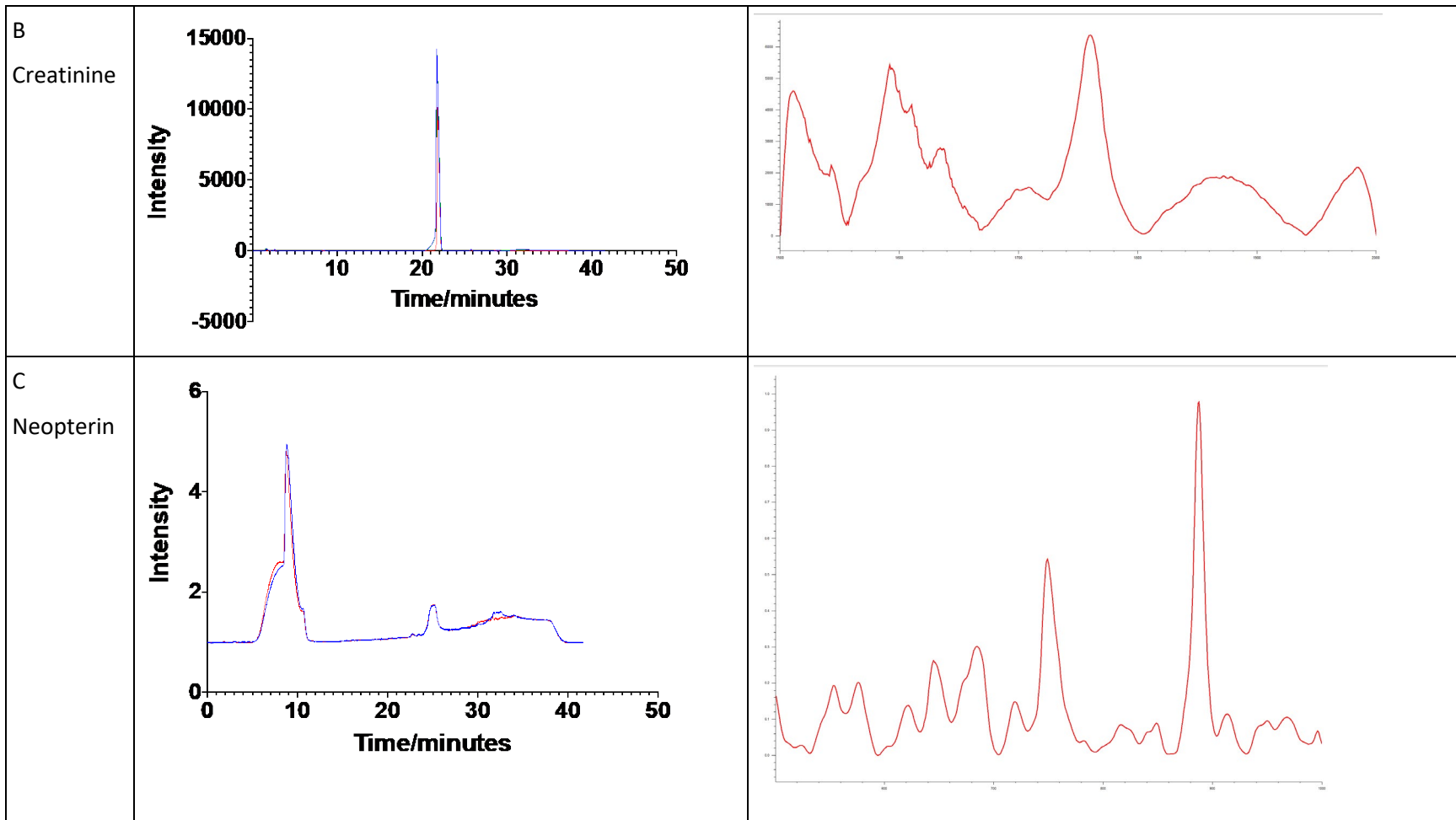
Sum of Squares	6.001
Sy.x	0.3245
Number of points	
# of X values	59
# Y values analyzed	59

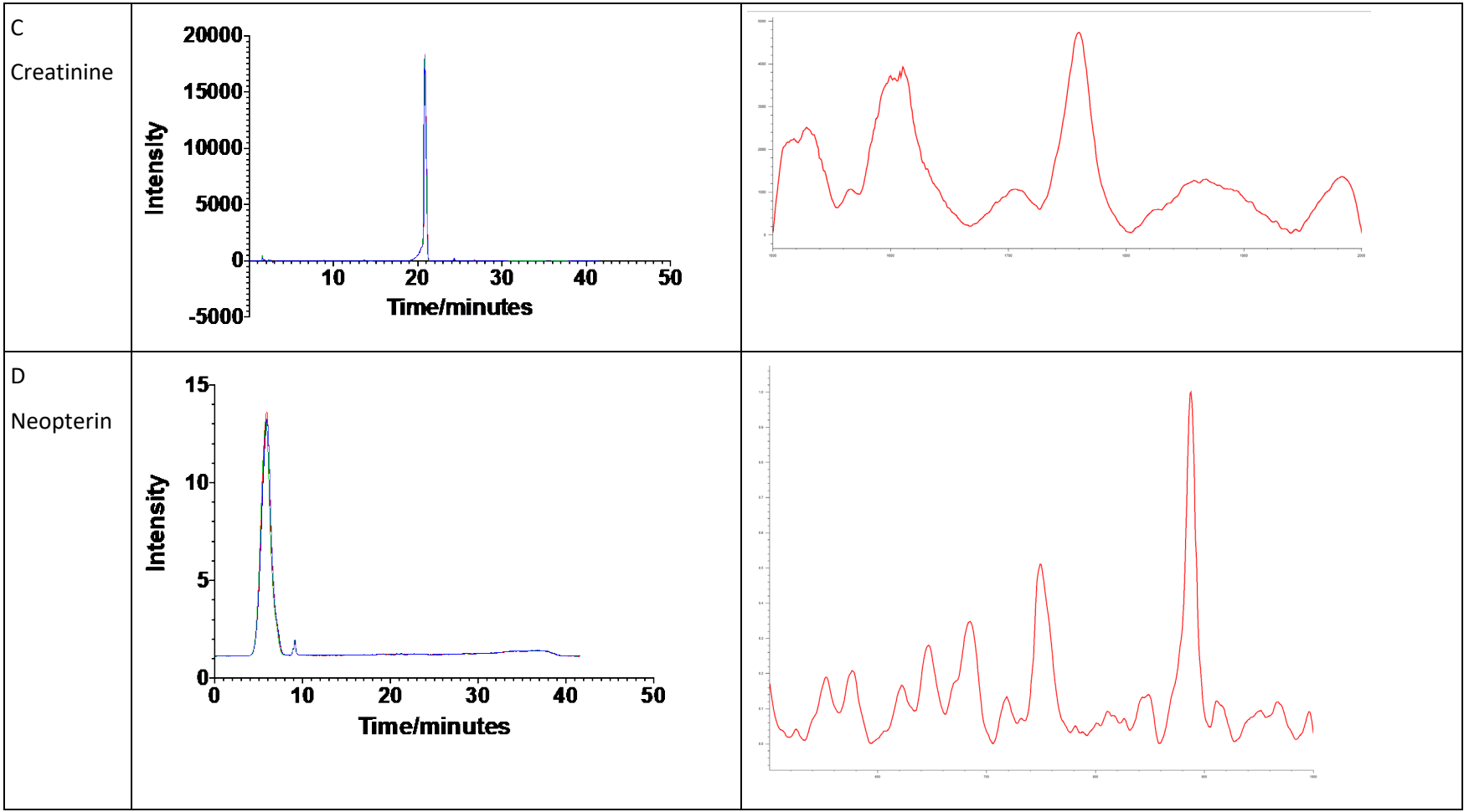
Appendix H Synthetic Urine spectra and chromatograms

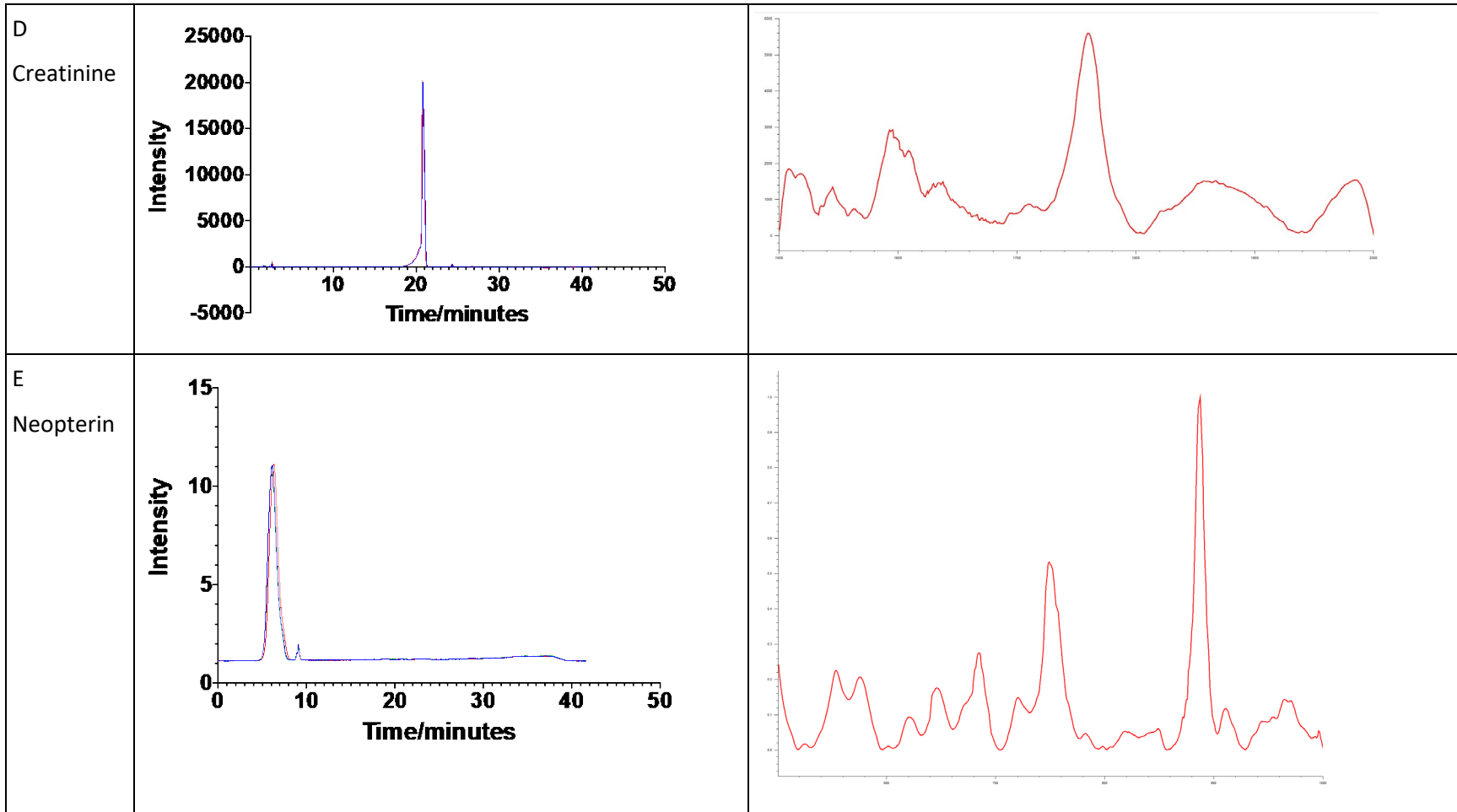
	HPLC	SERS
A Neopterin (SERS triplicate)		

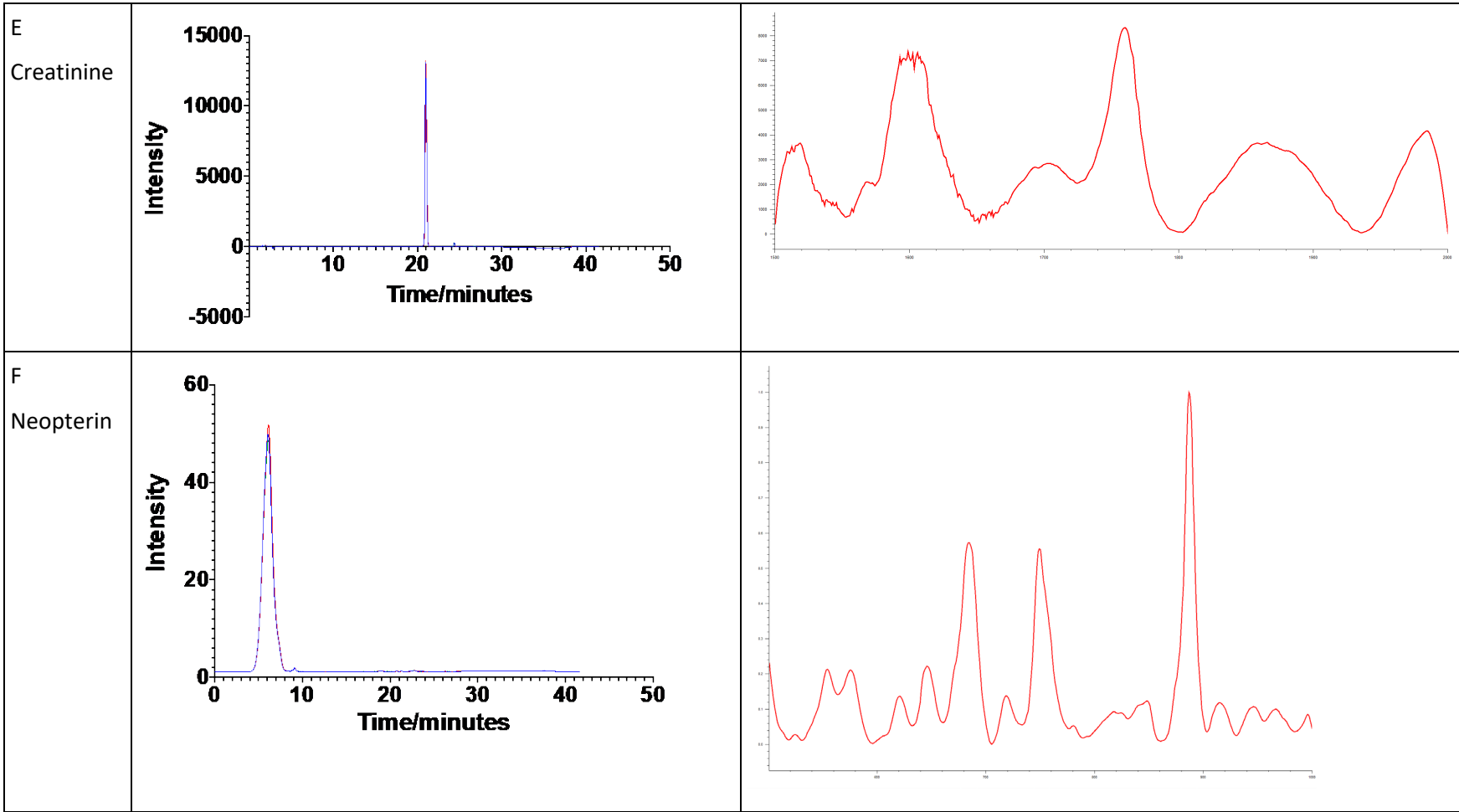




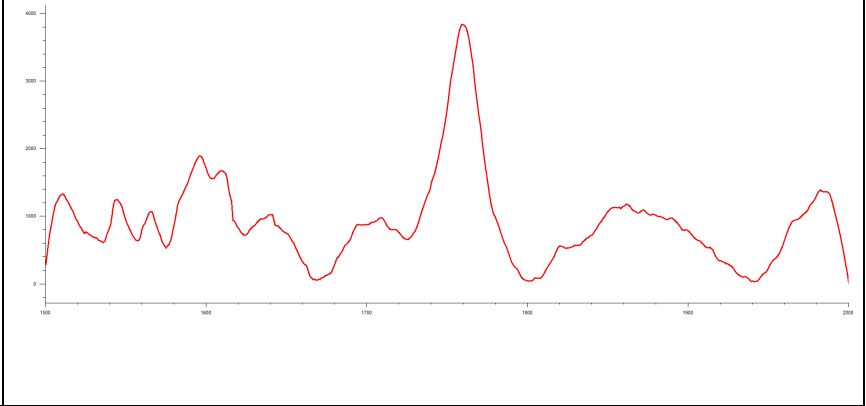
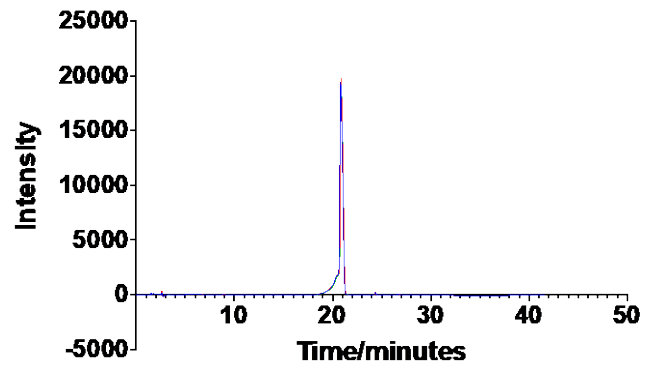




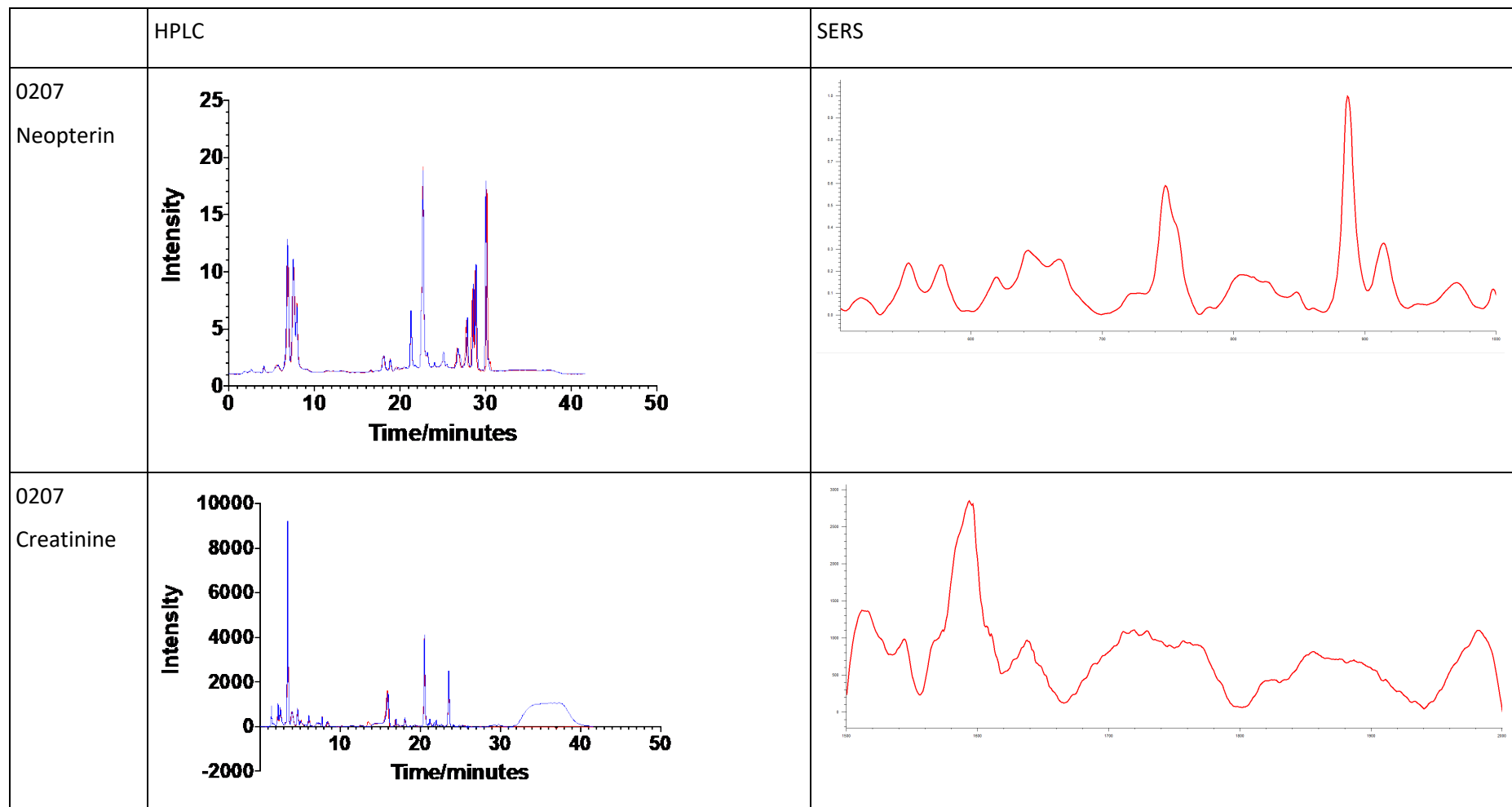




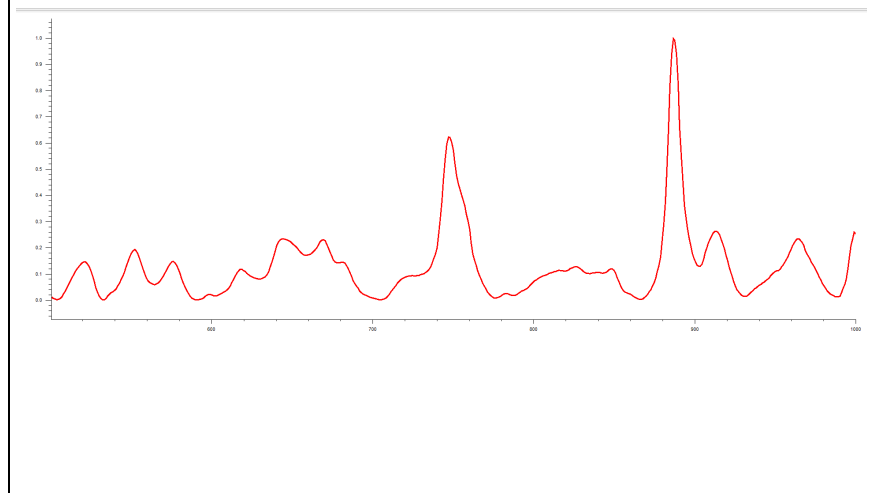
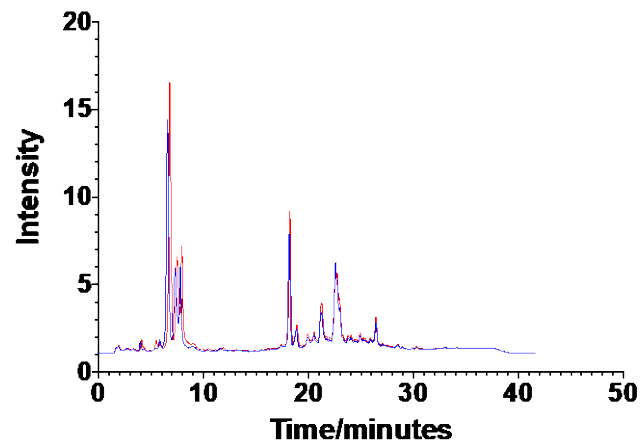
F
Creatinine



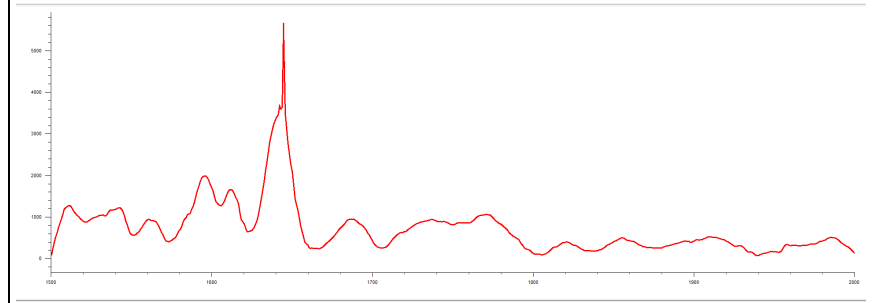
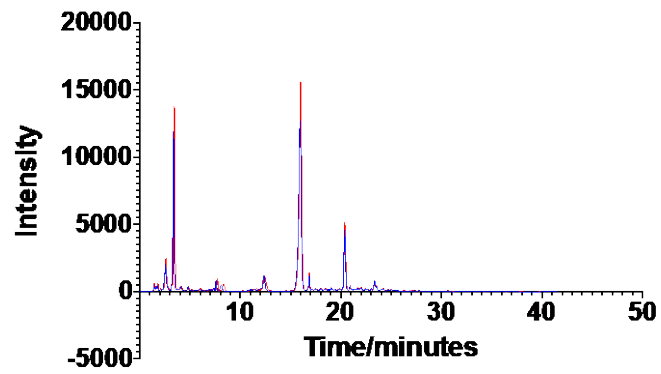
Appendix I Real Urine spectra and chromatograms



0309
Neopterin

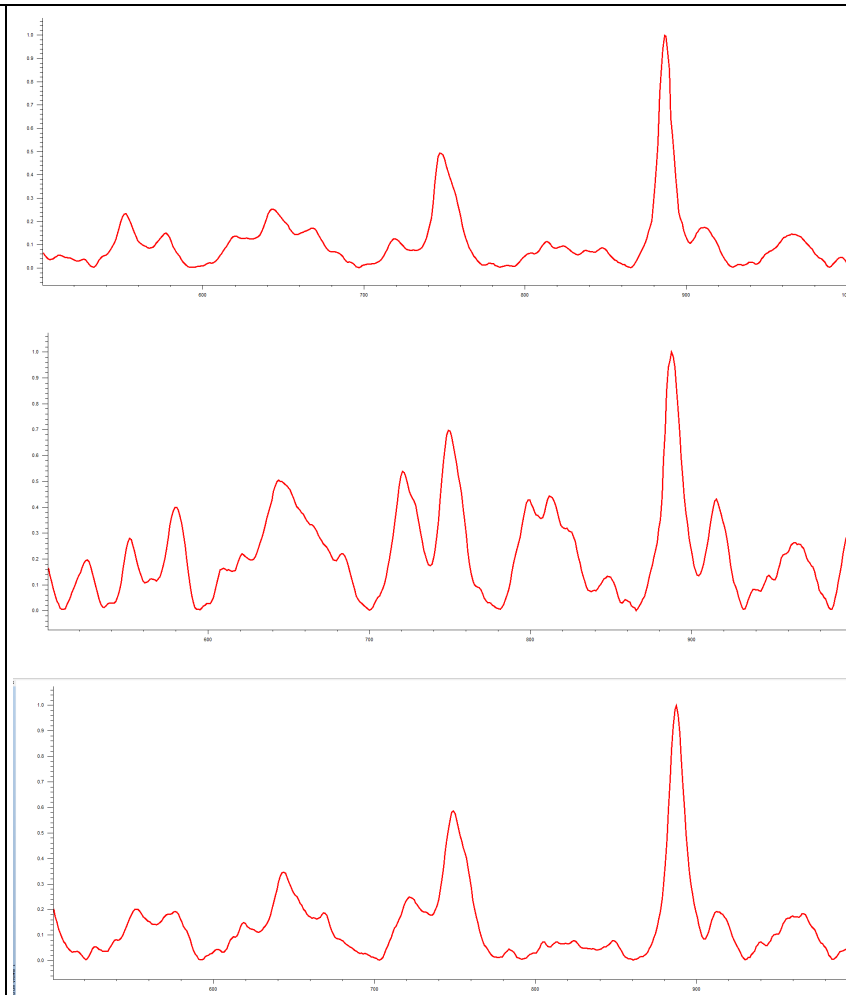
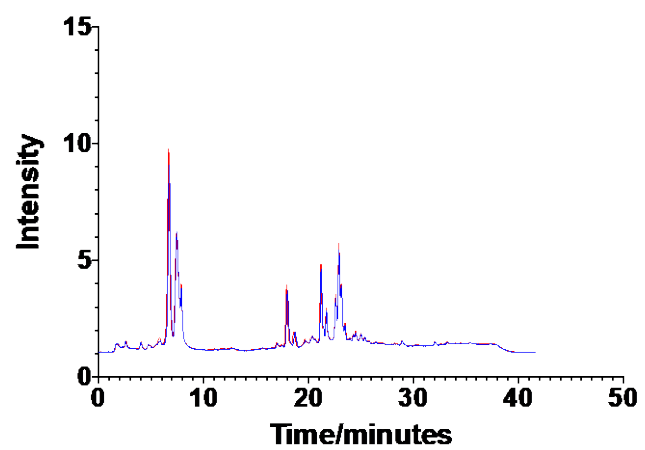


0309
Creatinine

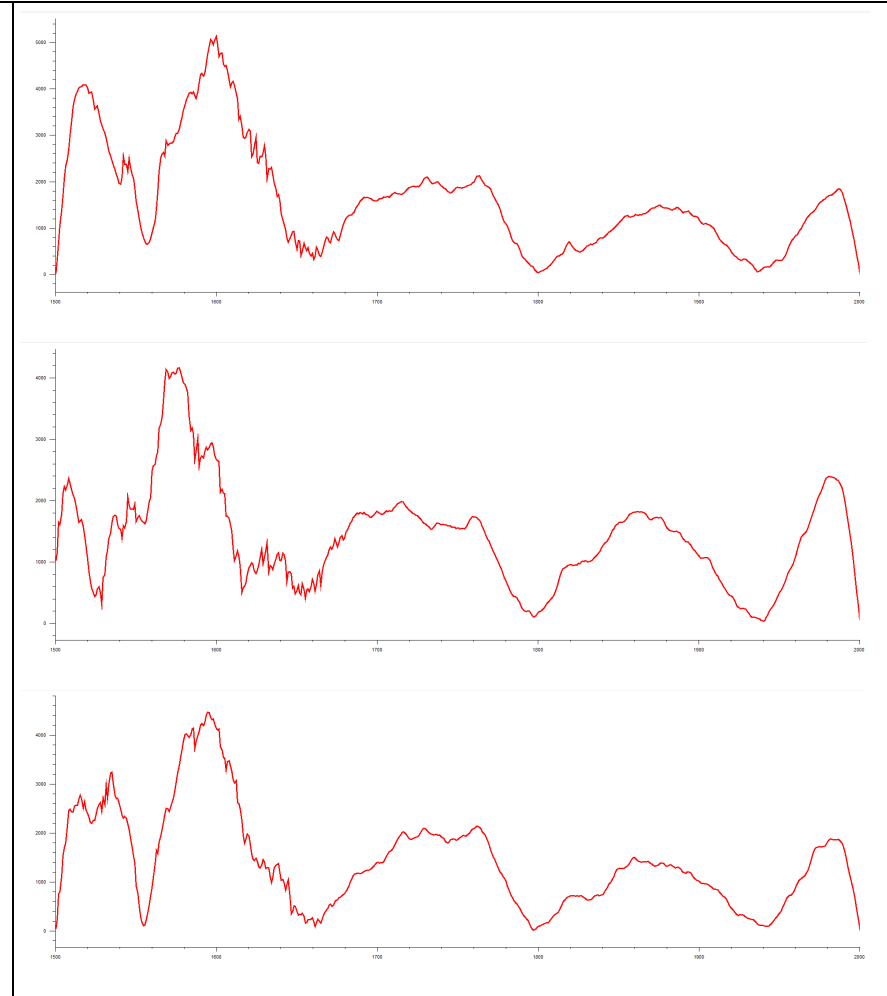
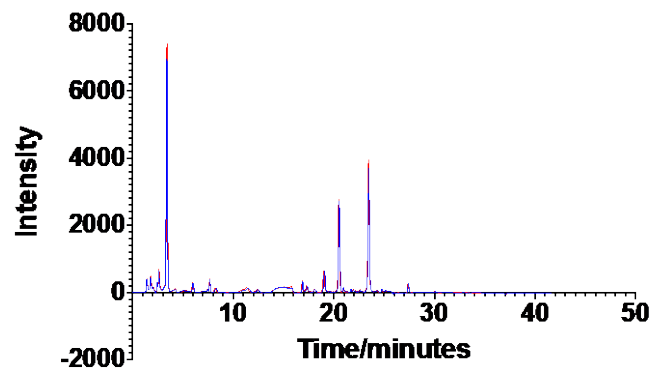


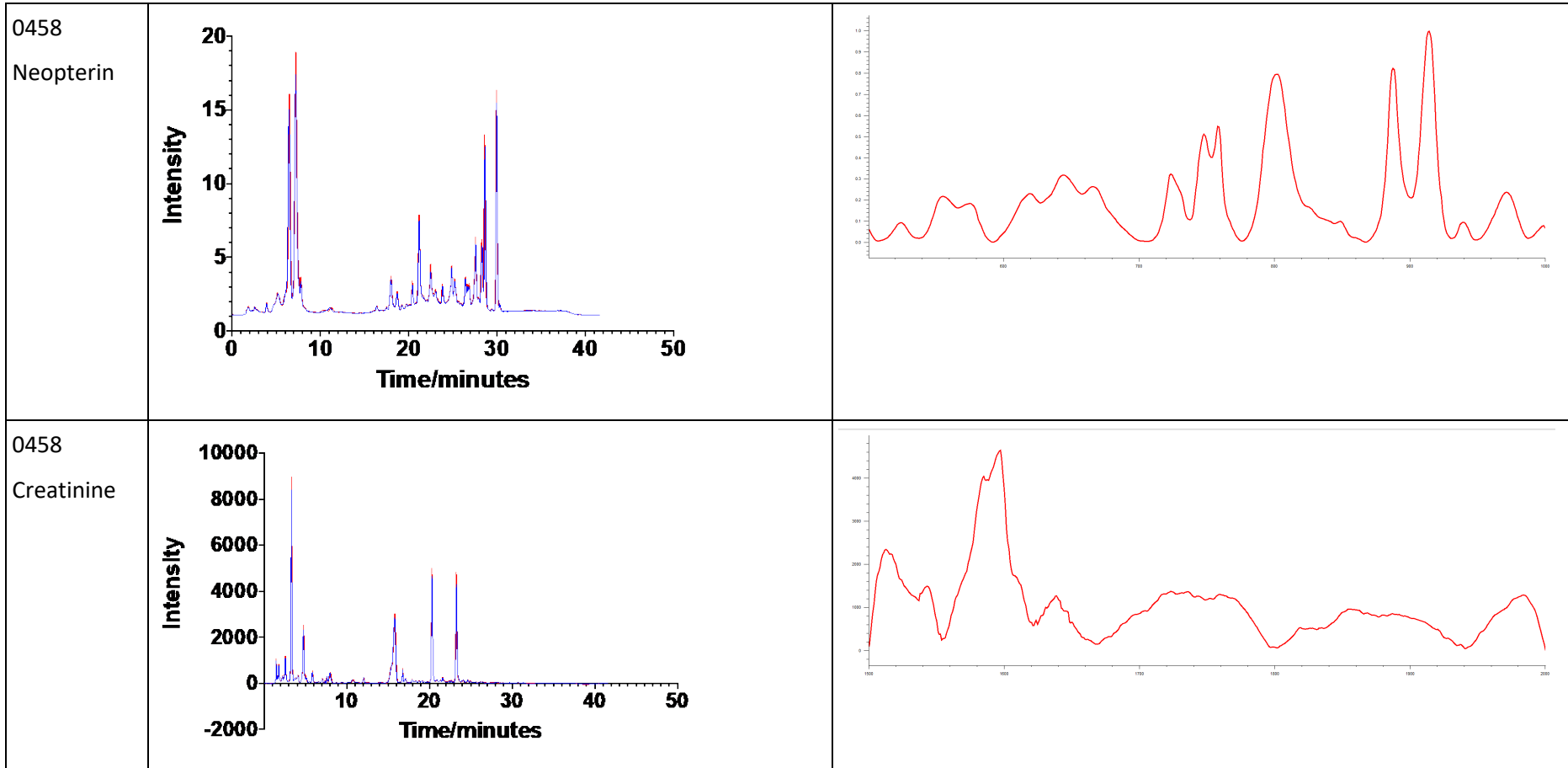
0355

Neopterin

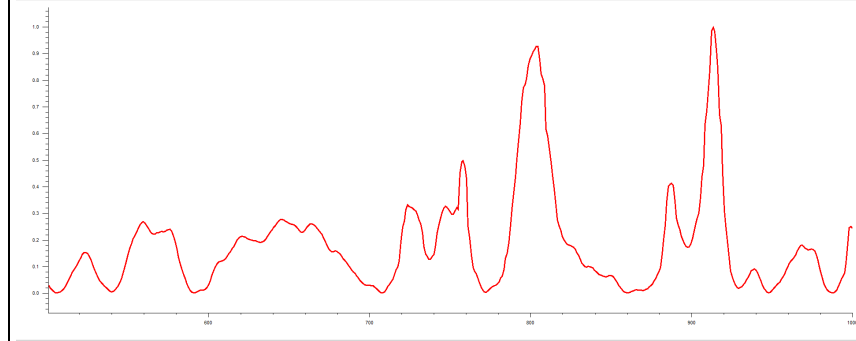
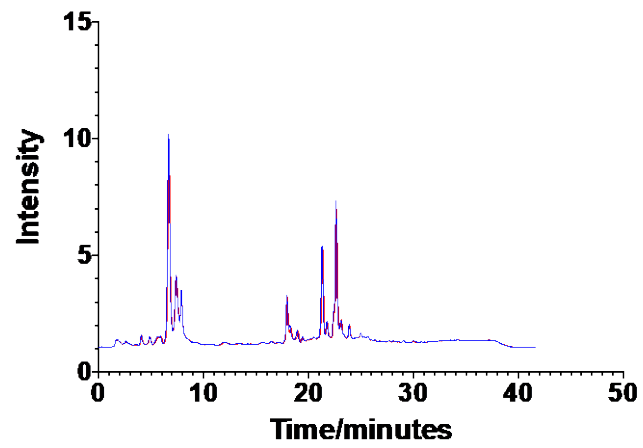
(SERS in
triplicate)

0355
Creatinine
(SERS in
triplicate)

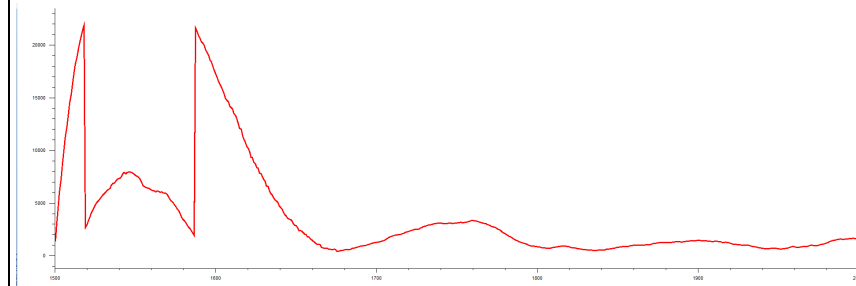
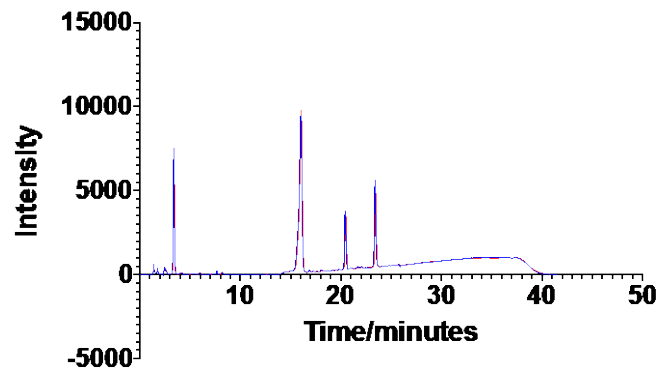


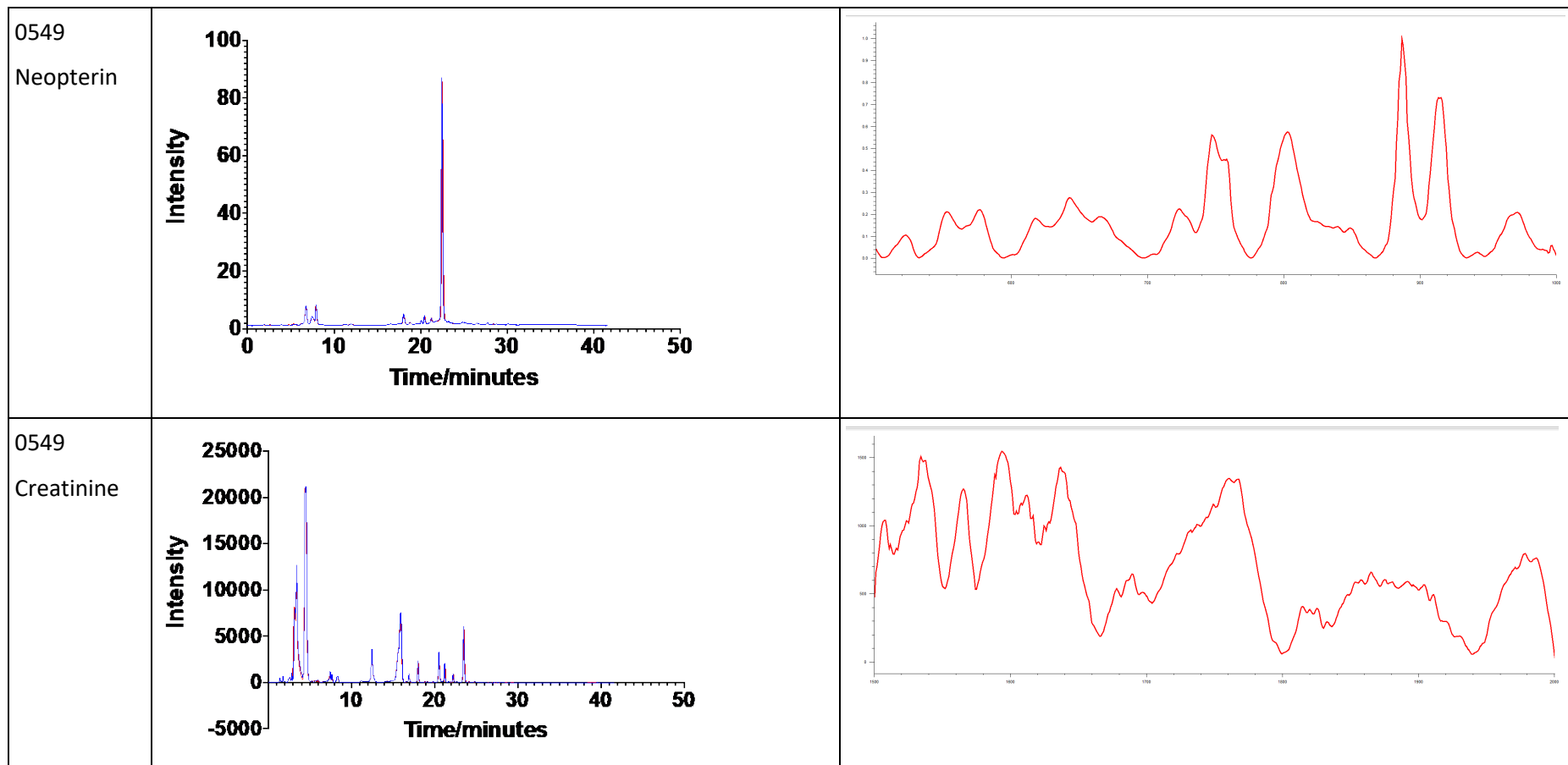


0518
Neopterin

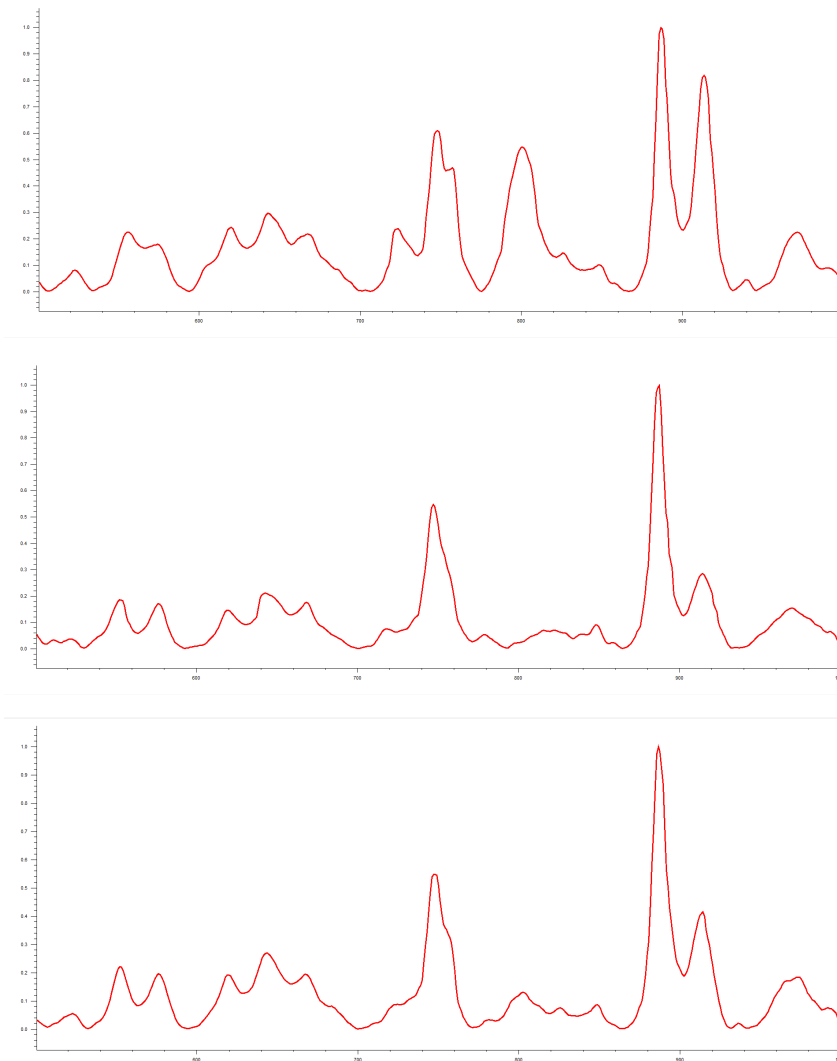
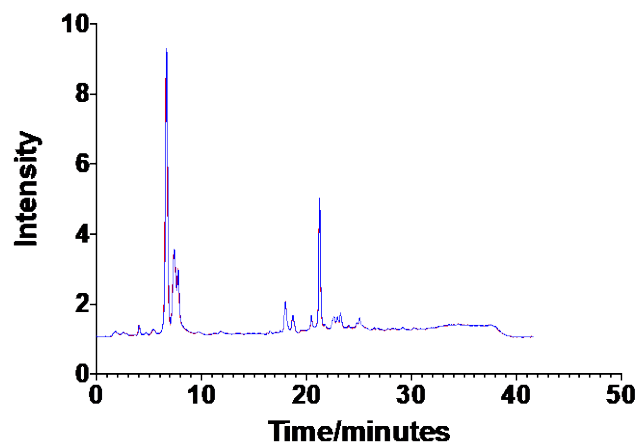


0518
Creatinine

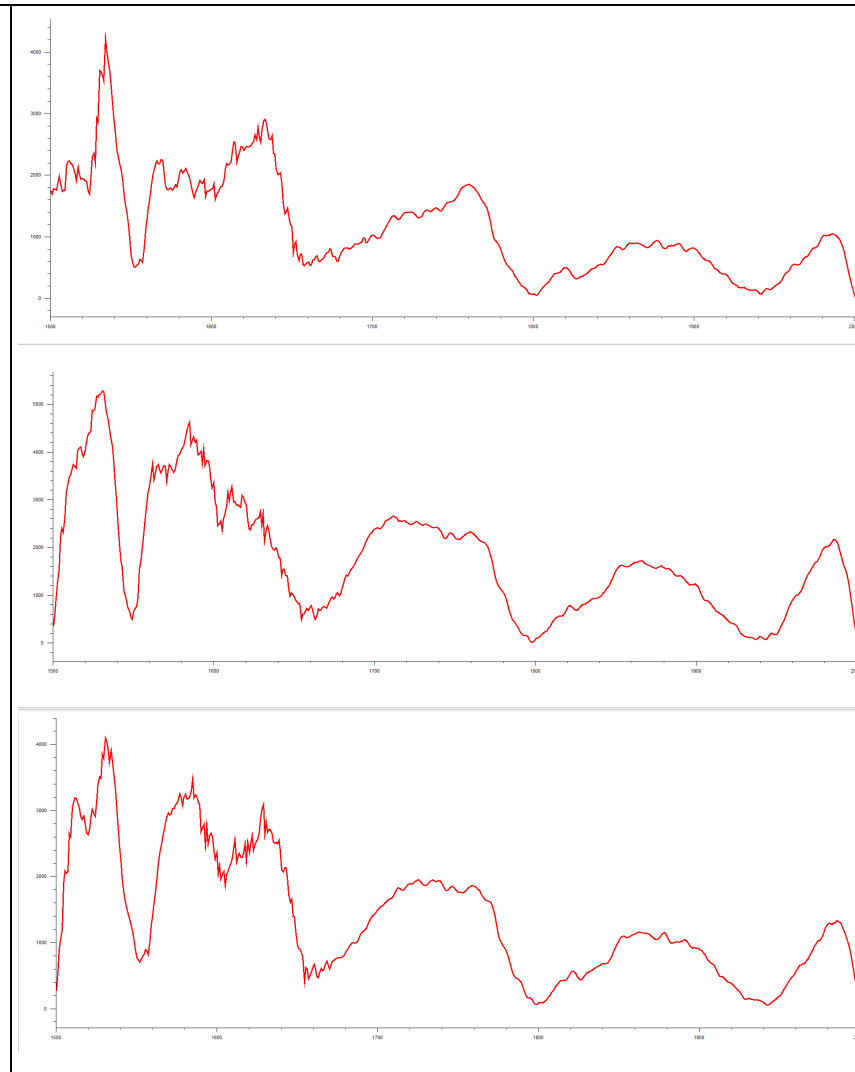
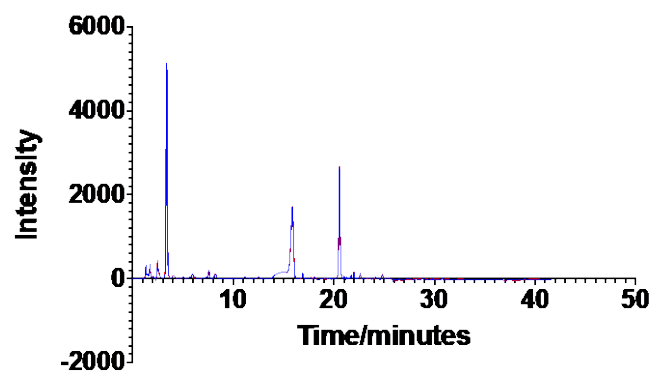




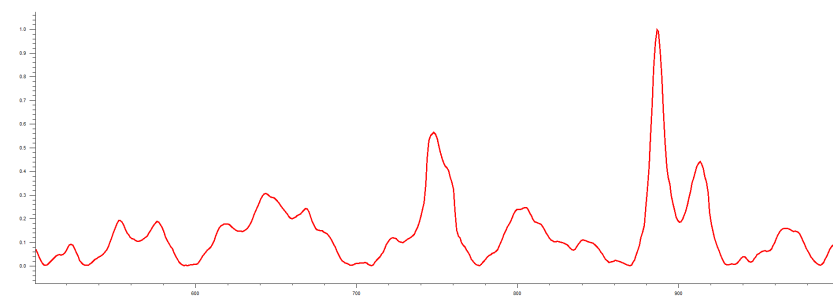
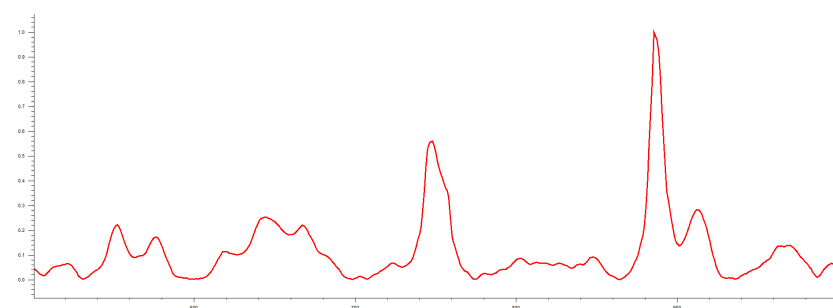
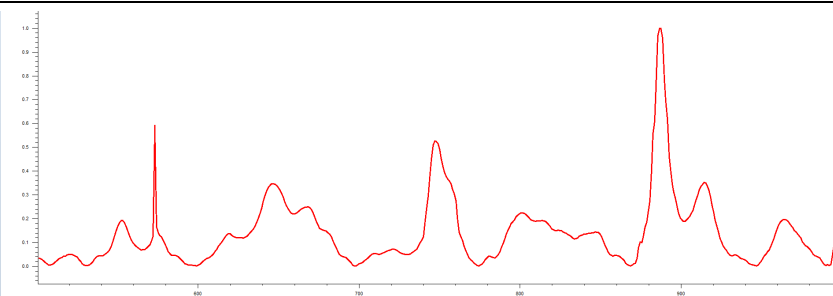
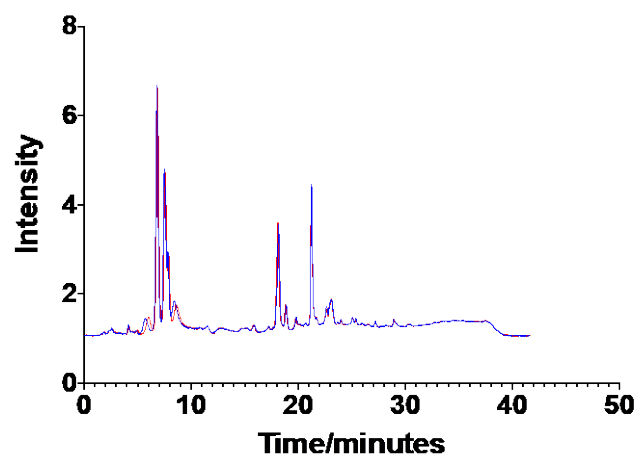
0577
Neopterin
(SERS in
triplicate)



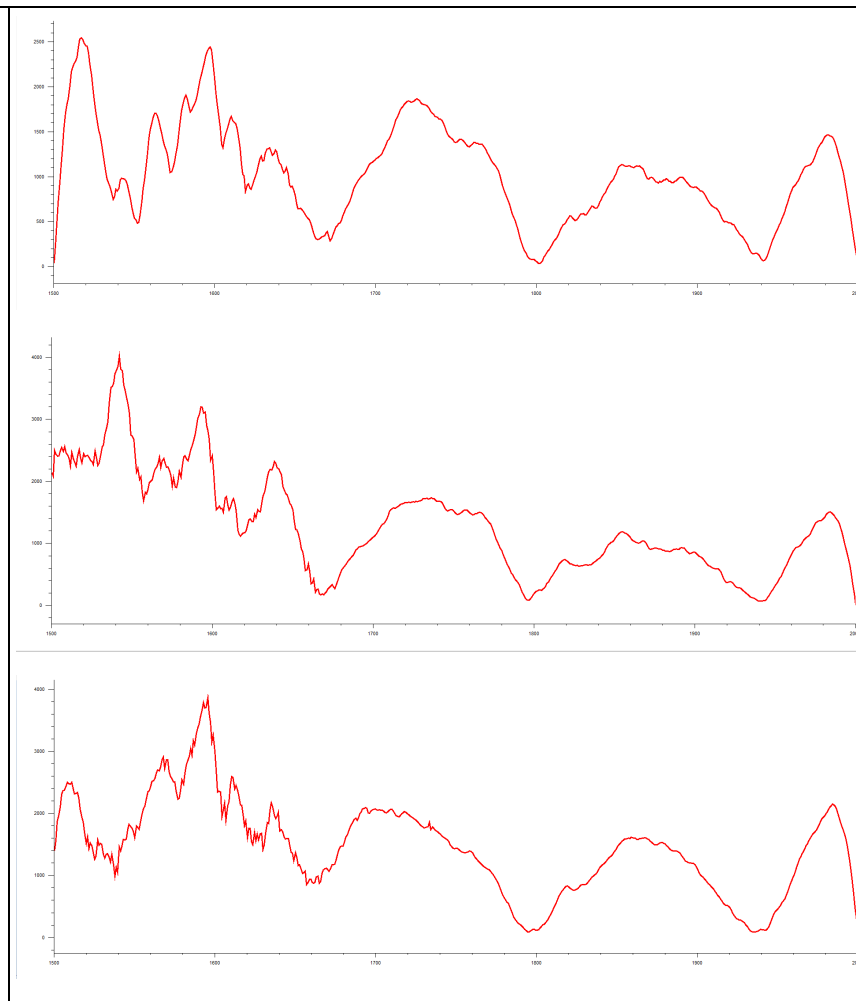
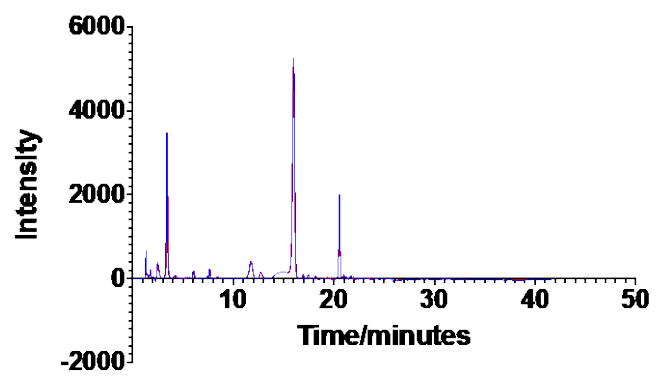
0577

Creatinine
(SERS in
triplicate)

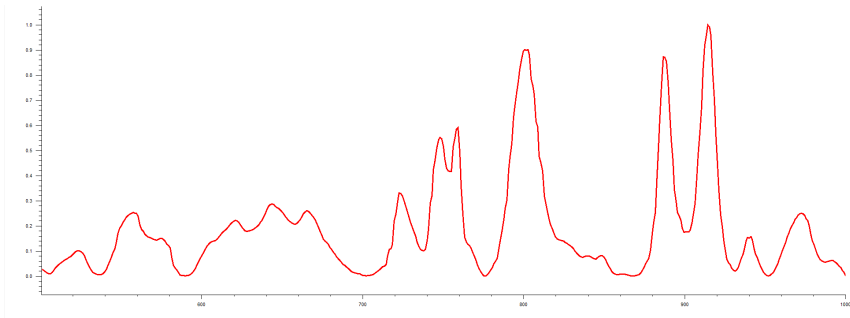
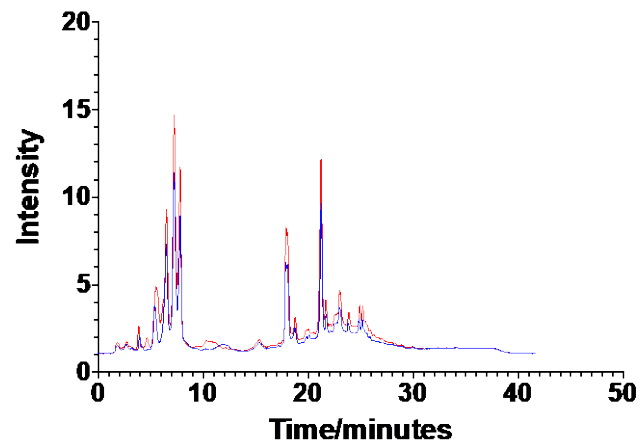
03510
Neopterin
(SERS in
triplicate)



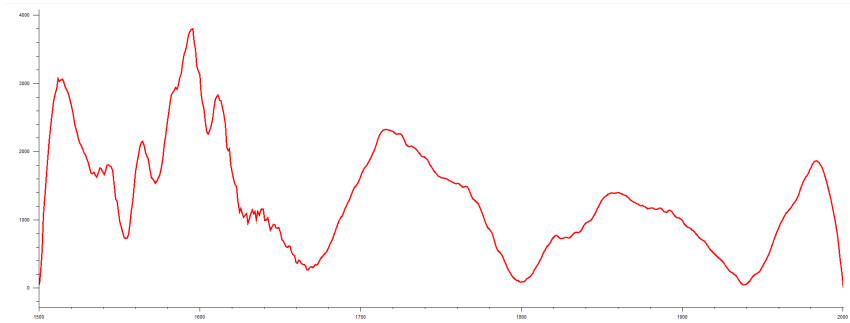
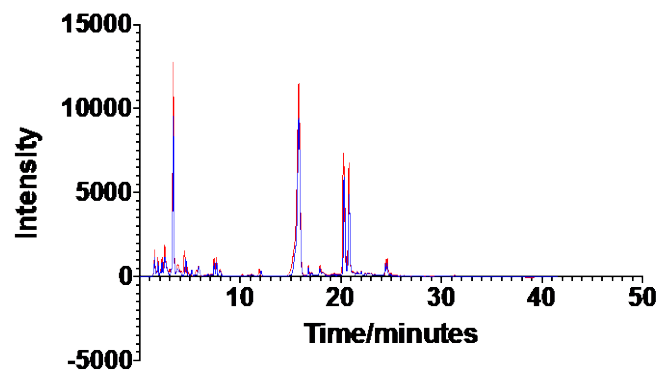
03510
Creatinine
(SERS in
triplicate)

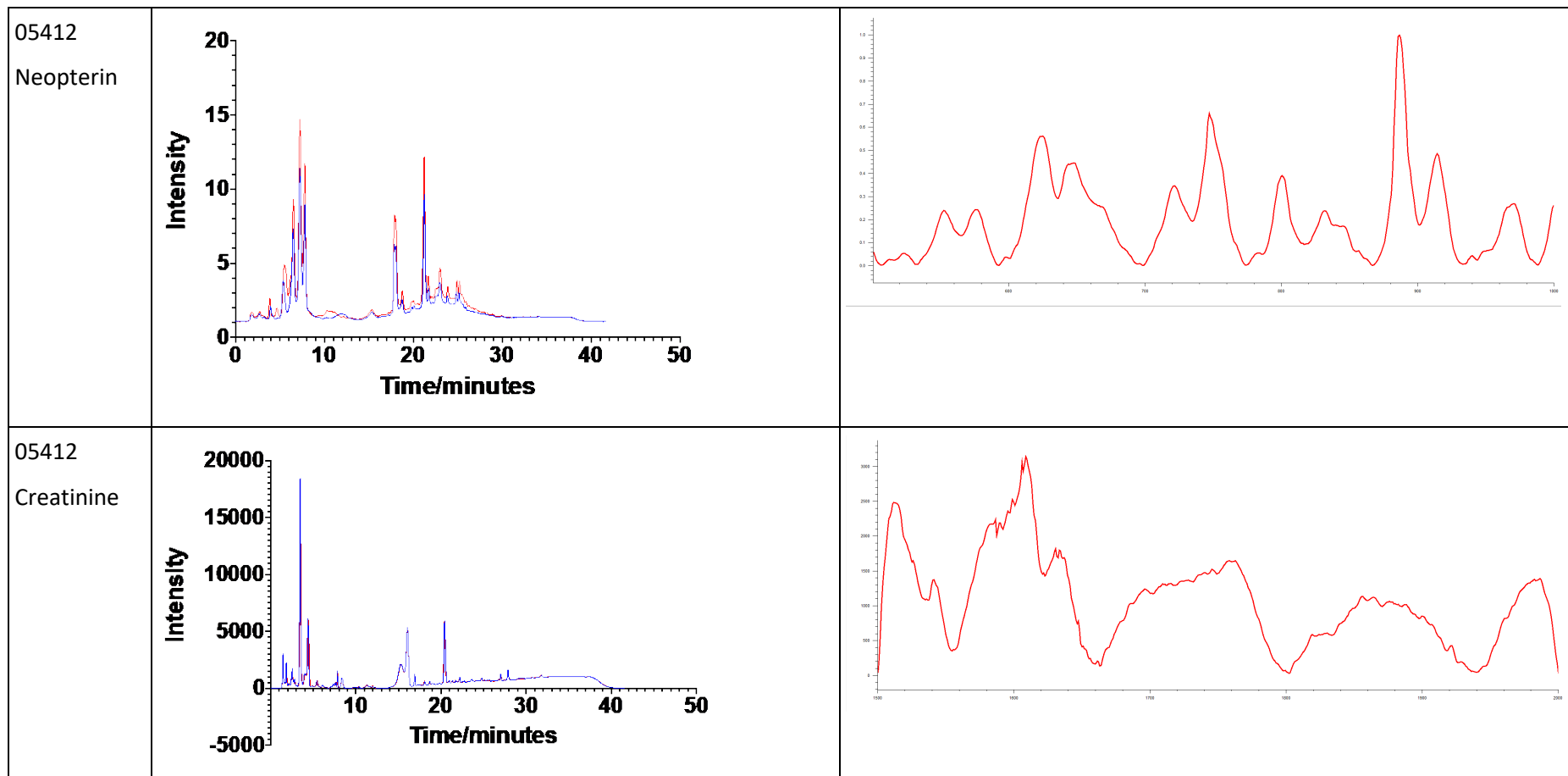


04810
Neopterin

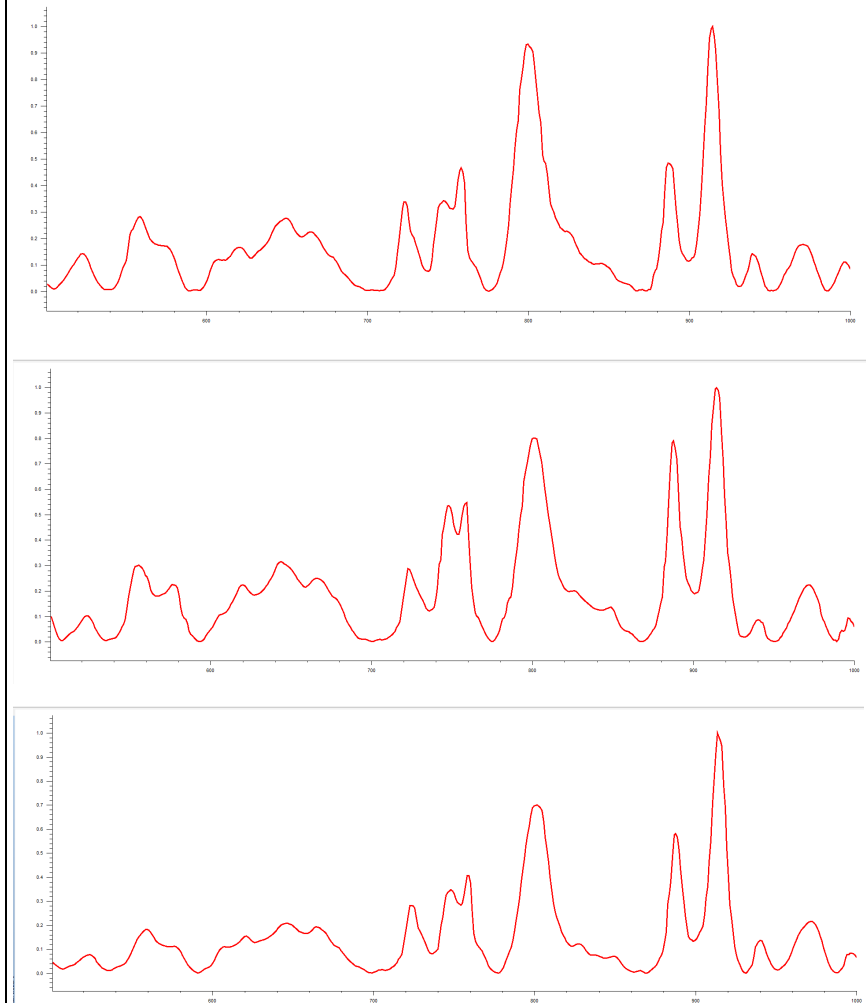
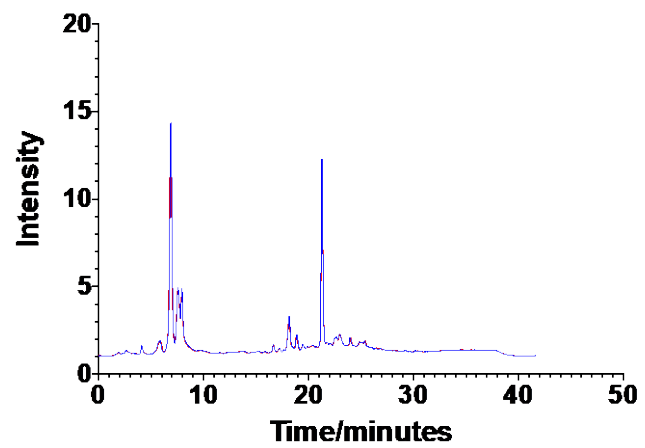


04810
Creatinine

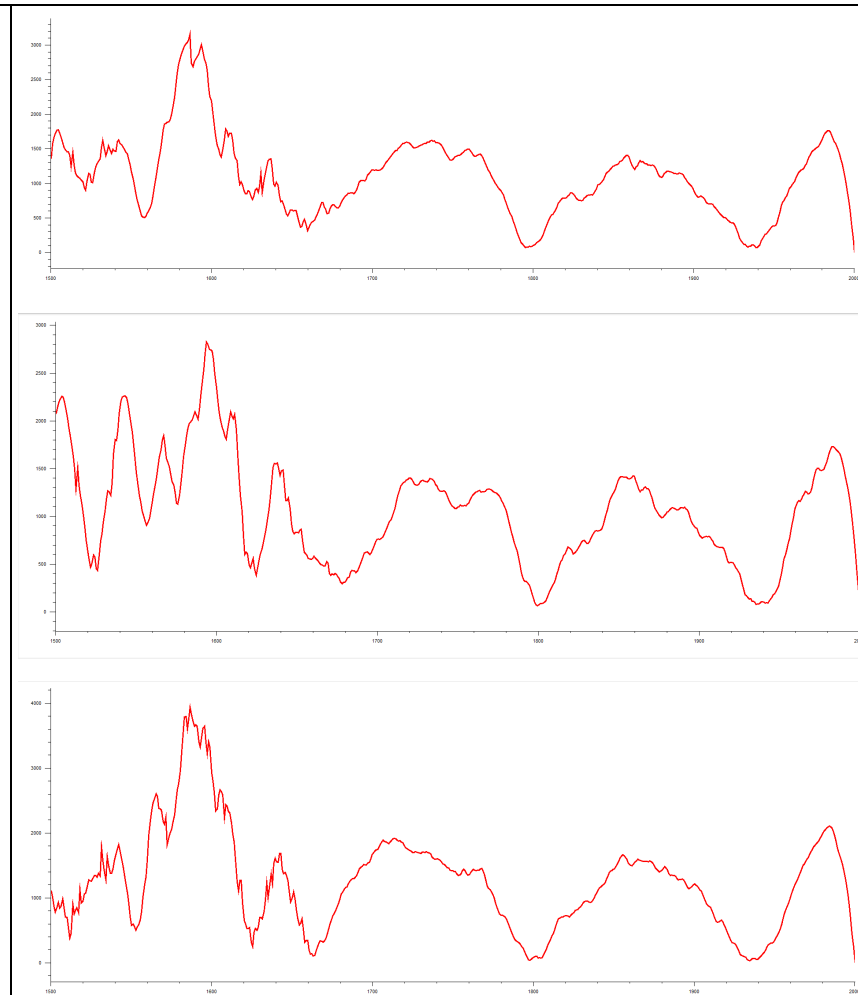
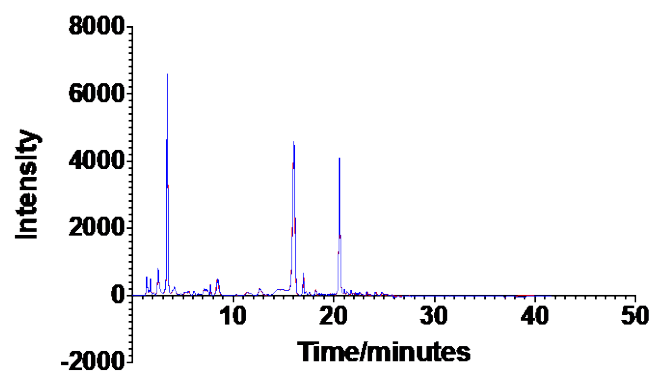




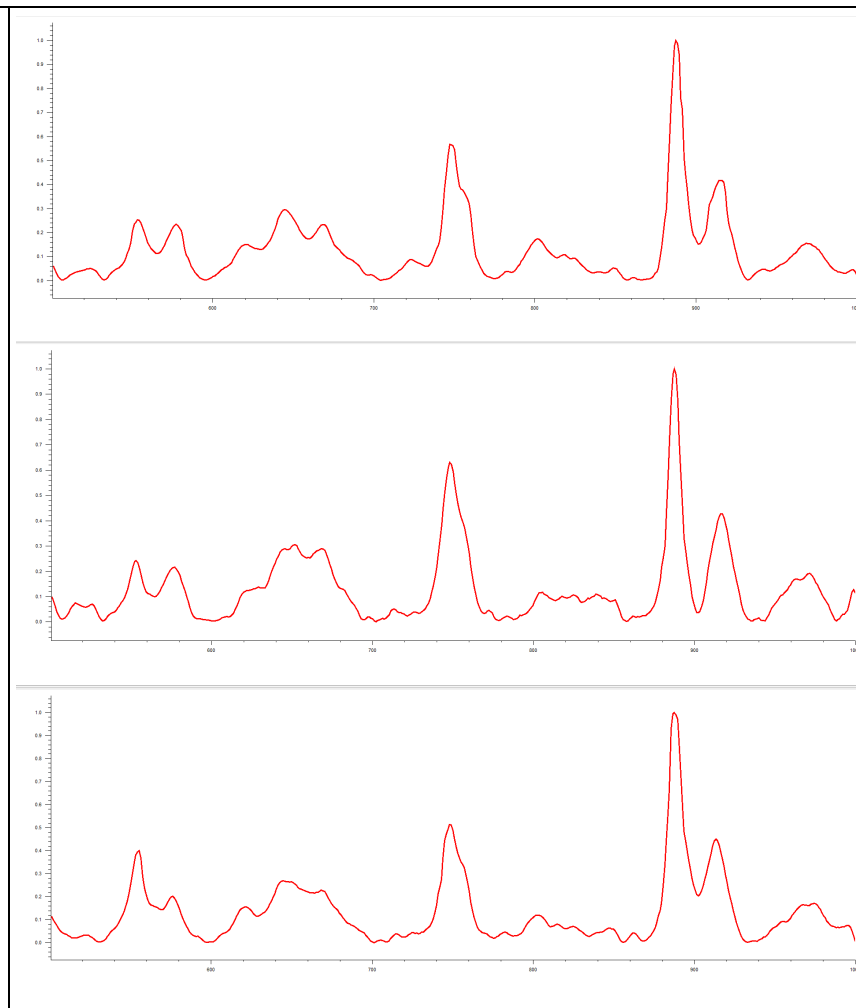
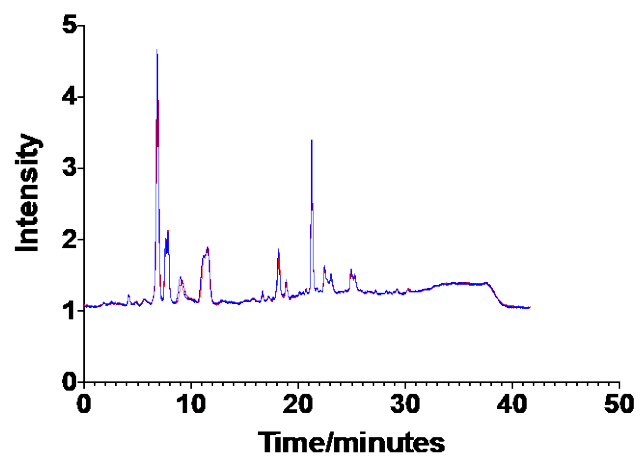
05711
Neopterin
(SERS in
triplicate)



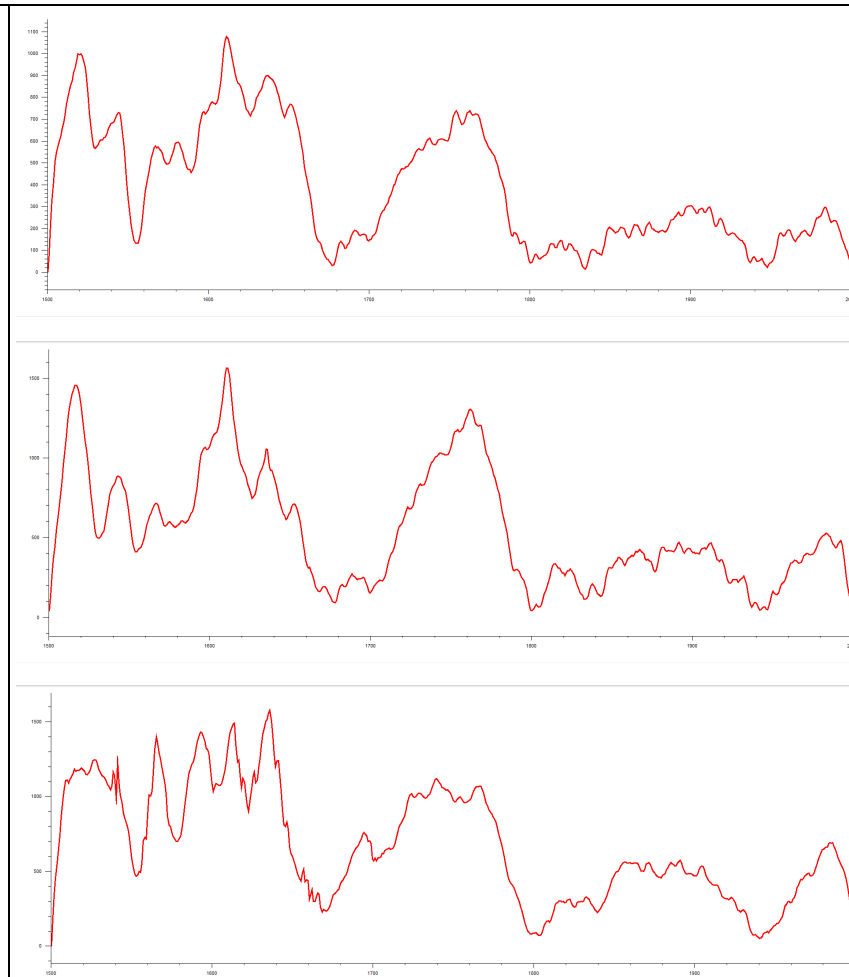
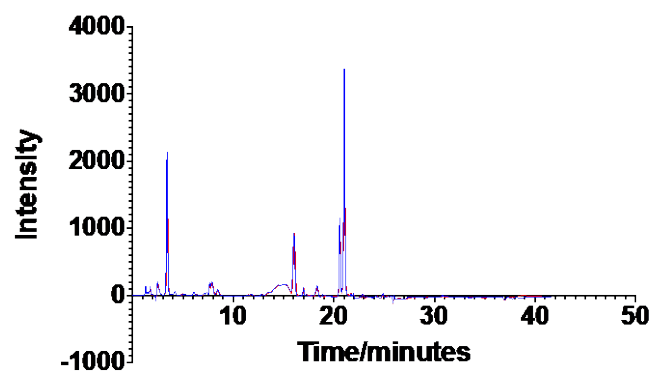
05711

Creatinine
(SERS in
triplicate)

05712
Neopterin
(SERS in
triplicate)



05712
Creatinine
(SERS in
triplicate)



List of References

1. ONS. Population Estimates for UK, England and Wales, Scotland and Northern Ireland: mid-2015. 2016.
2. Science GOf. *Future of an Ageing Population*; 2016.
3. Franceschi C, Campisi J. Chronic Inflammation (Inflammaging) and Its Potential Contribution to Age-Associated Diseases. *The Journals of Gerontology Series A: Biological Sciences and Medical Sciences* 2014;69(Suppl 1):S4-S9.
4. Franceschi C, Bonafè M, Valensin S, et al. Inflamm - aging: an evolutionary perspective on immunosenescence. *Annals of the New York Academy of Sciences* 2000;908(1):244-54.
5. Nash SD, Cruickshanks KJ, Zhan W, et al. Long-term Assessment of Systemic Inflammation and the Cumulative Incidence of Age-related Hearing Impairment in the Epidemiology of Hearing Loss Study. *Journals of Gerontology Series a-Biological Sciences and Medical Sciences* 2014;69(2):207-14.
6. Verschuur C, Agyemang-Prempeh A, Newman TA. Inflammation is associated with a worsening of presbycusis: Evidence from the MRC national study of hearing. *International Journal of Audiology* 2014;53(7):469-75.
7. Verschuur CA, Dowell A, Syddall HE, et al. Markers of inflammatory status are associated with hearing threshold in older people: findings from the Hertfordshire ageing study. *Age and Ageing* 2012;41(1):92-97.
8. Eisenhut M. Neopterin in Diagnosis and Monitoring of Infectious Diseases. *J Biomark* 2013;2013:196432.
9. Plata-Nazar K, Jankowska A. Clinical Usefulness of Determining the Concentration of Neopterin. *Pteridines* 2011;22(3):77-89.
10. Berdowska A, Zwirska-Korczala K. Neopterin measurement in clinical diagnosis. *Journal of Clinical Pharmacy and Therapeutics* 2001;26(5):319-29.
11. Nancey S, Perret - Liaudet A, Moussata D, et al. Urinary neopterin is a valuable tool in monitoring Crohn's disease activity. *Inflammatory bowel diseases* 2008;14(11):1548-54.
12. Prasanna J, Sumadhura C, Karunakar P. Neopterin as a diagnostic biomarker for diagnosis of inflammatory diseases like periodontitis. *Journal of Oral Research and Review* 2017;9(1):45-49.
13. Werner ER, Bichler A, Daxenbichler G, et al. DETERMINATION OF NEOPTERIN IN SERUM AND URINE. *Clinical Chemistry* 1987;33(1):62-66.
14. Yang S, Dai X, Stogin BB, et al. Ultrasensitive surface-enhanced Raman scattering detection in common fluids. *Proceedings of the National Academy of Sciences* 2016;113(2):268-73.
15. Nations U. World Population Prospects 2019: Highlights, 2019.
16. Evans J, Fletcher A, Wormald R, et al. Prevalence of visual impairment in people aged 75 years and older in Britain: results from the MRC trial of assessment and management of older people in the community. *British Journal of Ophthalmology* 2002;86(7):795-800.
17. Dodds RM, Granic A, Davies K, et al. Prevalence and incidence of sarcopenia in the very old: findings from the Newcastle 85+ Study. *Journal of cachexia, sarcopenia and muscle* 2017;8(2):229-37.

List of References

18. Collerton J, Davies K, Jagger C, et al. Health and disease in 85 year olds: baseline findings from the Newcastle 85+ cohort study. *BMJ* 2009;339:b4904.
19. Ward BW, Schiller JS. Peer reviewed: prevalence of multiple chronic conditions among US adults: estimates from the National Health Interview Survey, 2010. *Preventing chronic disease* 2013;10.
20. Emori TG, Banerjee SN, Culver DH, et al. Nosocomial infections in elderly patients in the United States, 1986–1990. *The American journal of medicine* 1991;91(3):S289-S93.
21. Fleming DM, Elliot AJ. The impact of influenza on the health and health care utilisation of elderly people. *Vaccine* 2005;23:S1-S9.
22. Marston BJ, Plouffe JF, File TM, et al. Incidence of community-acquired pneumonia requiring hospitalization: results of a population-based active surveillance study in Ohio. *Archives of internal medicine* 1997;157(15):1709-18.
23. Thompson WW, Shay DK, Weintraub E, et al. Mortality associated with influenza and respiratory syncytial virus in the United States. *Jama* 2003;289(2):179-86.
24. Fein AM. Pneumonia in the elderly: overview of diagnostic and therapeutic approaches. *Clinical infectious diseases* 1999;28(4):726-29.
25. Aw D, Silva AB, Palmer DB. Immunosenescence: emerging challenges for an ageing population. *Immunology* 2007;120(4):435-46.
26. Leonardi GC, Accardi G, Monastero R, et al. Ageing: from inflammation to cancer. *Immunity & Ageing* 2018;15(1):1.
27. Bruunsgaard H, Skinhøj P, Pedersen AN, et al. Ageing, tumour necrosis factor - alpha (TNF - α) and atherosclerosis. *Clinical & Experimental Immunology* 2000;121(2):255-60.
28. Bruunsgaard H, Andersen-Ranberg K, Jeune B, et al. A high plasma concentration of TNF- α is associated with dementia in centenarians. *Journals of Gerontology Series A: Biomedical Sciences and Medical Sciences* 1999;54(7):M357-M64.
29. Visser M, Pahor M, Taaffe DR, et al. Relationship of interleukin-6 and tumor necrosis factor- α with muscle mass and muscle strength in elderly men and women: the Health ABC Study. *The Journals of Gerontology Series A: Biological Sciences and Medical Sciences* 2002;57(5):M326-M32.
30. Fried LP, Tangen CM, Walston J, et al. Frailty in older adults: evidence for a phenotype. *The Journals of Gerontology Series A: Biological Sciences and Medical Sciences* 2001;56(3):M146-M57.
31. Wilson D, Jackson T, Sapey E, et al. Frailty and sarcopenia: The potential role of an aged immune system. *Ageing research reviews* 2017;36:1-10.
32. Baylis D, Bartlett DB, Syddall HE, et al. Immune-endocrine biomarkers as predictors of frailty and mortality: a 10-year longitudinal study in community-dwelling older people. *Age* 2013;35(3):963-71.
33. Butcher S, Chahal H, Nayak L, et al. Senescence in innate immune responses: reduced neutrophil phagocytic capacity and CD16 expression in elderly humans. *Journal of Leukocyte Biology* 2001;70(6):881-86.

34. Ogata K, An E, Shioi Y, et al. Association between natural killer cell activity and infection in immunologically normal elderly people. *Clinical & Experimental Immunology* 2001;124(3):392-97.
35. Lara J, Cooper R, Nissan J, et al. A proposed panel of biomarkers of healthy ageing. *BMC Medicine* 2015;13(1):222.
36. Cooper R, Kuh D, Hardy R. Objectively measured physical capability levels and mortality: systematic review and meta-analysis. *BMJ* 2010;341:c4467.
37. Cooper R, Strand BH, Hardy R, et al. Physical capability in mid-life and survival over 13 years of follow-up: British birth cohort study. *BMJ* 2014;348:g2219.
38. Cooper R, Kuh D, Cooper C, et al. Objective measures of physical capability and subsequent health: a systematic review. *Age and Ageing* 2011;40(1):14-23.
39. Steptoe A, Kivimäki M. Stress and cardiovascular disease. *Nature Reviews Cardiology* 2012;9(6):360-70.
40. Rosmond R, Wallerius S, Wanger P, et al. A 5 - year follow - up study of disease incidence in men with an abnormal hormone pattern. *Journal of internal medicine* 2003;254(4):386-90.
41. De Martinis M, Franceschi C, Monti D, et al. Inflammation markers predicting frailty and mortality in the elderly. *Experimental and molecular pathology* 2006;80(3):219-27.
42. Krabbe KS, Pedersen M, Bruunsgaard H. Inflammatory mediators in the elderly. *Experimental gerontology* 2004;39(5):687-99.
43. Franceschi C, Capri M, Monti D, et al. Inflammaging and anti-inflammaging: a systemic perspective on aging and longevity emerged from studies in humans. *Mechanisms of ageing and development* 2007;128(1):92-105.
44. Bruunsgaard H, Pedersen M, Pedersen BK. Aging and proinflammatory cytokines. *Current opinion in hematology* 2001;8(3):131-36.
45. Verghese J, Holtzer R, Oh-Park M, et al. Inflammatory markers and gait speed decline in older adults. *Journals of Gerontology Series A: Biomedical Sciences and Medical Sciences* 2011;66(10):1083-89.
46. Fuchs D, Weiss G, Reibnegger G, et al. The role of neopterin as a monitor of cellular immune activation in transplantation, inflammatory, infectious, and malignant diseases. *Critical reviews in clinical laboratory sciences* 1992;29(3-4):307-44.
47. Murr C, Widner B, Wirleitner B, et al. Neopterin as a marker for immune system activation. *Current Drug Metabolism* 2002;3(2):175-87.
48. Giunta B, Fernandez F, Nikolic WV, et al. Inflammaging as a prodrome to Alzheimer's disease. *Journal of Neuroinflammation* 2008;5(1):51.
49. Hunt KJ, Walsh BM, Voegeli D, et al. Inflammation in aging part 1: physiology and immunological mechanisms. *Biological research for nursing* 2010;11(3):245-52.
50. Fuchs D, Stahl-Hennig C, Gruber A, et al. Neopterin--Its clinical use in urinalysis. *Kidney International Supplement* 1994(47).
51. Lim KL, Muir K, Powell RJ. Urine neopterin: a new parameter for serial monitoring of disease activity in patients with systemic lupus erythematosus. *Annals of the Rheumatic Diseases* 1994;53(11):743-48.

List of References

52. Zouridakis E, Avanzas P, Arroyo-Espliguero R, et al. Markers of inflammation and rapid coronary artery disease progression in patients with stable angina pectoris. *Circulation* 2004;110(13):1747-53.
53. Weimer R, Suesal C, Yildiz S, et al. Post - Transplant sCD30 and Neopterin as Predictors of Chronic Allograft Nephropathy: Impact of Different Immunosuppressive Regimens. *American journal of transplantation* 2006;6(8):1865-74.
54. Zvarik M, Martinicky D, Hunakova L, et al. Differences in pteridine urinary levels in patients with malignant and benign ovarian tumors in comparison with healthy individuals. *Journal of Photochemistry and Photobiology B: Biology* 2015;153:191-97.
55. Koc E, Tunca M, Akgul EO, et al. Effects of etanercept on urine neopterin levels in patients with psoriasis in a controlled, open-label study. *Journal of Dermatology* 2009;36(4):191-96.
56. Wirleitner B, Schroecksnadel K, Winkler C, et al. Neopterin in HIV-1 infection. *Molecular Immunology* 2005;42(2):183-94.
57. Yuksekol I, Ozkan M, Akgul O, et al. Urinary neopterin measurement as a non-invasive diagnostic method in pulmonary tuberculosis. *International Journal of Tuberculosis and Lung Disease* 2003;7(8):771-76.
58. Ozmeric N, Baydar T, Bodur A, et al. Level of neopterin, a marker of immune cell activation in gingival crevicular fluid, saliva, and urine in patients with aggressive periodontitis. *Journal of Periodontology* 2002;73(7):720-25.
59. Hausen A, Fuchs D, Konig K, et al. DETERMINATION OF NEOPTERINE IN HUMAN-URINE BY REVERSED-PHASE HIGH-PERFORMANCE LIQUID-CHROMATOGRAPHY. *Journal of Chromatography* 1982;227(1):61-70.
60. Parker DC, Mielke MM, Yu Q, et al. Plasma neopterin level as a marker of peripheral immune activation in amnesic mild cognitive impairment and Alzheimer's disease. *International journal of geriatric psychiatry* 2013;28(2):149-54.
61. Spencer ME, Jain A, Matteini A, et al. Serum levels of the immune activation marker neopterin change with age and gender and are modified by race, BMI, and percentage of body fat. *The Journals of Gerontology Series A: Biological Sciences and Medical Sciences* 2010;65(8):858-65.
62. Lhee HY, Kim H, Joo KJ, et al. The clinical significance of serum and urinary neopterin levels in several renal diseases. *Journal of Korean medical science* 2006;21(4):678-82.
63. Kazakevich YV, Lobrutto R. *HPLC for pharmaceutical scientists*: John Wiley & Sons; 2007.
64. Bonifacio A, Cervo S, Sergo V. Label-free surface-enhanced Raman spectroscopy of biofluids: fundamental aspects and diagnostic applications. *Analytical and Bioanalytical Chemistry* 2015;407(27):8265-77.
65. Mathers CD, Loncar D. Projections of global mortality and burden of disease from 2002 to 2030. *PLoS Medicine* 2006;3(11):e442.
66. Saito H, Nishiwaki Y, Michikawa T, et al. Hearing Handicap Predicts the Development of Depressive Symptoms After 3 Years in Older Community - Dwelling Japanese. *Journal of the American Geriatrics Society* 2010;58(1):93-97.
67. Lin FR, Metter EJ, O'Brien RJ, et al. Hearing loss and incident dementia. *Archives of neurology* 2011;68(2):214-20.

68. Lin FR, Yaffe K, Xia J, et al. Hearing loss and cognitive decline in older adults. *JAMA internal medicine* 2013;173(4):293-99.
69. Gurgel RK, Ward PD, Schwartz S, et al. Relationship of hearing loss and dementia: a prospective, population-based study. *Otology & neurotology: official publication of the American Otological Society, American Neurotology Society [and] European Academy of Otology and Neurotology* 2014;35(5):775.
70. Albers MW, Gilmore GC, Kaye J, et al. At the interface of sensory and motor dysfunctions and Alzheimer's disease. *Alzheimer's & Dementia* 2015;11(1):70-98.
71. Horikawa C, Kodama S, Tanaka S, et al. Diabetes and risk of hearing impairment in adults: a meta-analysis. *The Journal of Clinical Endocrinology & Metabolism* 2012;98(1):51-58.
72. Rosenhall U, Sundh V. Age-related hearing loss and blood pressure. *Noise and Health* 2006;8(31):88.
73. Formby C, Phillips D, Thomas R. Hearing loss among stroke patients. *Ear and hearing* 1987;8(6):326-32.
74. Gopinath B, Schneider J, Rochtchina E, et al. Association between age-related hearing loss and stroke in an older population. *Stroke* 2009;40(4):1496-98.
75. Helzner EP, Patel AS, Pratt S, et al. Hearing sensitivity in older adults: associations with cardiovascular risk factors in the health, aging and body composition study. *Journal of the American Geriatrics Society* 2011;59(6):972-79.
76. Cruickshanks KJ, Nondahl DM, Dalton DS, et al. Smoking, central adiposity, and poor glycemic control increase risk of hearing impairment. *Journal of the American Geriatrics Society* 2015;63(5):918-24.
77. Mizutari K, Michikawa T, Saito H, et al. Age-related hearing loss and the factors determining continued usage of hearing aids among elderly community-dwelling residents. *PLoS One* 2013;8(9):e73622.
78. AOHL. Hearing Matters. London: Action on Hearing Loss, 2016.
79. Davis AC. The prevalence of hearing impairment and reported hearing disability among adults in Great Britain. *International Journal of Epidemiology* 1989;18(4):911-17.
80. Huang Q, Tang J. Age-related hearing loss or presbycusis. *European Archives of Oto-Rhino-Laryngology* 2010;267(8):1179-91.
81. Tan WJT, Thorne PR, Vlajkovic SM. Characterisation of cochlear inflammation in mice following acute and chronic noise exposure. *Histochemistry and Cell Biology* 2016;146(2):219-30.
82. Fujioka M, Kanzaki S, Okano HJ, et al. Proinflammatory cytokines expression in noise - induced damaged cochlea. *Journal of neuroscience research* 2006;83(4):575-83.
83. Wakabayashi K, Fujioka M, Kanzaki S, et al. Blockade of interleukin-6 signaling suppressed cochlear inflammatory response and improved hearing impairment in noise-damaged mice cochlea. *Neuroscience research* 2010;66(4):345-52.
84. Prochazka M. *Surface-Enhance Raman Spectroscopy: Bioanalytical, Biomolecular and Medical Applications*. Switzerland: Springer; 2016.
85. Carey PR. *Biochemical applications of Raman and resonance Raman spectroscopies*. San Diego: Academic Press; 1982.

List of References

86. Fleischmann M, Hendra PJ, McQuillan A. Raman spectra of pyridine adsorbed at a silver electrode. *Chemical Physics Letters* 1974;26(2):163-66.
87. Ru ECL, Etchegoin PG. Single-Molecule Surface-Enhanced Raman Spectroscopy. *Annual Review of Physical Chemistry* 2012;63(1):65-87.
88. Stiles PL, Dieringer JA, Shah NC, et al. Surface-enhanced Raman spectroscopy. *Annu Rev Anal Chem (Palo Alto Calif)* 2008;1:601-26.
89. Lee PC, Meisel D. Adsorption and surface-enhanced Raman of dyes on silver and gold sols. *The Journal of Physical Chemistry* 1982;86(17):3391-95.
90. Le Ru EC, Etchegoin PG. *Principles of Surface-Enhanced Raman Spectroscopy*. Amsterdam: Elsevier; 2009.
91. Oldenburg SJ, Averitt RD, Westcott SL, et al. Nanoengineering of optical resonances. *Chemical Physics Letters* 1998;288:243-47.
92. Oldenburg SJ, Jackson JB, Westcott SL, et al. Infrared extinction properties of gold nanoshells. *Applied Physics Letters* 1999;75(19):2897-99.
93. Prodan E, Nordlander P. Structural Tunability of the Plasmon Resonances in Metallic Nanoshells. *Nano Letters* 2003;3(4):543-47.
94. Li JF, Tian XD, Li SB, et al. Surface analysis using shell-isolated nanoparticle-enhanced Raman spectroscopy. *Nat Protoc* 2013;8(1):52-65.
95. Li JF, Huang YF, Ding Y, et al. Shell-isolated nanoparticle-enhanced Raman spectroscopy. *Nature* 2010;464(7287):392-5.
96. Wentrup-Byrne E, Sarinas S, Fredericks PM. Analytical Potential of Surface-Enhanced Fourier Transform Raman Spectroscopy on Silver Colloids. *Applied Spectroscopy* 1993;47(8):1192-97.
97. Zhang X, Chen H, Zhang H. Layer-by-layer assembly: from conventional to unconventional methods. *Chemical Communications* 2007(14):1395-405.
98. Anderson WJ, Nowinska K, Mahajan S, et al. Quantitative Colloidal SERS Sensors- Tuning Plasmon Properties Layer-by-Layer. *Nanoscale* (in press).
99. Fan M, Andrade GF, Brolo AG. A review on the fabrication of substrates for surface enhanced Raman spectroscopy and their applications in analytical chemistry. *Analytica Chimica Acta* 2011;693(1-2):7-25.
100. Romo-Herrera JM, Alvarez-Puebla RA, Liz-Marzan LM. Controlled assembly of plasmonic colloidal nanoparticle clusters. *Nanoscale* 2011;3(4):1304-15.
101. Baia M, Astilean S, Iliescu T. New developments in SERS-active substrates *Raman and SERS Investigations of Pharmaceuticals*. Berlin: Springer; 2008 p187-205.
102. Jang YH, Chung K, Quan LN, et al. Configuration-controlled Au nanocluster arrays on inverse micelle nano-patterns: versatile platforms for SERS and SPR sensors. *Nanoscale* 2013;5(24):12261-71.
103. Wang H, Kundu J, Halas NJ. Plasmonic Nanoshell Arrays Combine Surface-Enhanced Vibrational Spectroscopies on a Single Substrate. *Angew. Chem. Int. Ed.* 2007;46:9040-44.

104. Han Y, Sukhishvili S, Du H, et al. Layer-by-Layer Self-Assembly of Oppositely Charged Ag Nanoparticles on Silica Microspheres for Trace Analysis of Aqueous Solutions Using Surface-Enhanced Raman Scattering. *Journal of Nanoscience and Nanotechnology* 2008;8(11):5791-800.
105. Olson LG, Lo Y-S, Beebe, et al. Characterization of Silane-Modified Immobilized Gold Colloids as a Substrate for Surface-Enhanced Raman Spectroscopy. *Analytical Chemistry* 2001;73(17):4268-76.
106. Toderas F, Baia M, Baia L, et al. Controlling gold nanoparticle assemblies for efficient surface-enhanced Raman scattering and localized surface plasmon resonance sensors. *Nanotechnology* 2007;18(25):255702.
107. Kahl M, Voges E, Kostrewa S, et al. Periodically structured metallic substrates for SERS. *Sensors and Actuators B: Chemical* 1998;51(1):285-91.
108. Zhang J, Li Y, Zhang X, et al. Colloidal self-assembly meets nanofabrication: from two-dimensional colloidal crystals to nanostructure arrays. *Advanced Materials* 2010;22(38):4249-69.
109. Lin CC, Lin CY, Kao CJ, et al. High efficiency SERS detection of clinical microorganism by AgNPs-decorated filter membrane and pattern recognition techniques. *Sensors and Actuators B-Chemical* 2017;241:513-21.
110. Bell SEJ, Sirimuthu NMS. Quantitative surface-enhanced Raman spectroscopy. *Chemical Society Reviews* 2008;37(5):1012-24.
111. Bell SEJ, Stewart A. Quantitative SERS methods. In: Schlucker S (ed.) *Surface Enhanced Raman Spectroscopy: Analytical, Biophysical and Life Science Applications*: Wiley; 2011 p71-86.
112. Brown RJC, Milton MJT. Nanostructures and nanostructured substrates for surface—enhanced Raman scattering (SERS). *Journal of Raman Spectroscopy* 2008;39(10):1313-26.
113. Mamian-Lopez MB, Poppi RJ. Standard addition method applied to the urinary quantification of nicotine in the presence of cotinine and anabasine using surface enhanced Raman spectroscopy and multivariate curve resolution. *Analytica Chimica Acta* 2013;760:53-59.
114. Yu WW, White IM. Inkjet-printed paper-based SERS dipsticks and swabs for trace chemical detection. *Analyst* 2013;138(4):1020-25.
115. Chen X, Zheng X, Ding K, et al. A quantitative LC-MS/MS method for simultaneous determination of cocaine and its metabolites in whole blood. *Journal of pharmaceutical and biomedical analysis* 2017;134:243-51.
116. Han XX, Ozaki Y, Zhao B. Label-free detection in biological applications of surface-enhanced Raman scattering. *TrAC Trends in Analytical Chemistry* 2012;38:67-78.
117. Xie W, Schluecker S. Medical applications of surface-enhanced Raman scattering. *Physical Chemistry Chemical Physics* 2013;15(15):5329-44.
118. Rodriguez-Lorenzo L, Fabris L, Alvarez-Puebla RA. Multiplex optical sensing with surface-enhanced Raman scattering: A critical review. *Analytica Chimica Acta* 2012;745:10-23.
119. Pahlow S, März A, Seise B, et al. Bioanalytical application of surface- and tip-enhanced Raman spectroscopy. *Engineering in Life Sciences* 2012;12(2):131-43.

List of References

120. Del Mistro G, Cervo S, Mansutti E, et al. Surface-enhanced Raman spectroscopy of urine for prostate cancer detection: a preliminary study. *Analytical and Bioanalytical Chemistry* 2015;407(12):3271-75.
121. Elumalai B, Prakasarao A, Ganesan B, et al. Raman spectroscopic characterization of urine of normal and oral cancer subjects. *Journal of Raman Spectroscopy* 2015;46(1):84-93.
122. Bhattacharjee T, Khan A, Maru G, et al. A preliminary Raman spectroscopic study of urine: diagnosis of breast cancer in animal models. *Analyst* 2015;140(2):456-66.
123. Huang S, Wang L, Chen W, et al. Non-invasive optical detection of esophagus cancer based on urine surface-enhanced Raman spectroscopy. *Proceedings of the SPIE - Progress in Biomedical Optics and Imaging* 2014;9230:923020 (6 pp.)-20 (6 pp.).
124. Huang S, Wang L, Chen W, et al. Potential of non-invasive esophagus cancer detection based on urine surface-enhanced Raman spectroscopy. *Laser Physics Letters* 2014;11(11).
125. Yang T, Guo X, Wu Y, et al. Facile and Label-Free Detection of Lung Cancer Biomarker in Urine by Magnetically Assisted Surface-Enhanced Raman Scattering. *Acs Applied Materials & Interfaces* 2014;6(23):20985-93.
126. Shapiro A, Gofrit ON, Pizov G, et al. Raman molecular imaging: a novel spectroscopic technique for diagnosis of bladder cancer in urine specimens. *European urology* 2011;59(1):106-12.
127. Saatkamp CJ, de Almeida ML, Bispo JA, et al. Quantifying creatinine and urea in human urine through Raman spectroscopy aiming at diagnosis of kidney disease. *J Biomed Opt* 2016;21(3):37001.
128. Goodall BL, Robinson AM, Brosseau CL. Electrochemical-surface enhanced Raman spectroscopy (E-SERS) of uric acid: a potential rapid diagnostic method for early preeclampsia detection. *Physical Chemistry Chemical Physics* 2013;15(5):1382-88.
129. Wang H, Malvadkar N, Koytek S, et al. Quantitative analysis of creatinine in urine by metalized nanostructured parylene. *Journal of Biomedical Optics* 2010;15(2).
130. Chi J, Zaw T, Cardona I, et al. Use of surface-enhanced Raman scattering as a prognostic indicator of acute kidney transplant rejection. *Biomedical Optics Express* 2015;6(3):761-69.
131. Martins Bispo JA, Silveira L, Jr., de Sousa Vieira EE, et al. Determining the amounts of urea and glucose in urine of patients with renal complications from diabetes mellitus and hypertension by near-infrared Raman spectroscopy. In: Cote GL (ed.) *Optical Diagnostics and Sensing Xiii: Toward Point-of-Care Diagnostics*; 2013.
132. Martins Bispo JA, de Sousa Vieira EE, Silveira L, Jr., et al. Correlating the amount of urea, creatinine, and glucose in urine from patients with diabetes mellitus and hypertension with the risk of developing renal lesions by means of Raman spectroscopy and principal component analysis. *Journal of Biomedical Optics* 2013;18(8).
133. Westley C, Xu Y, Thilaganathan B, et al. Absolute Quantification of Uric Acid in Human Urine Using Surface Enhanced Raman Scattering with the Standard Addition Method. *Analytical Chemistry* 2017;89(4):2472-77.
134. Beleites C, Neugebauer U, Bocklitz T, et al. Sample size planning for classification models. *Anal Chim Acta* 2013;760:25-33.

135. Zhang K, Qing J, Gao H, et al. Coupling shell-isolated nanoparticle enhanced Raman spectroscopy with paper chromatography for multi-components on-site analysis. *Talanta* 2017;162:52-56.
136. Yu WW, White IM. Chromatographic separation and detection of target analytes from complex samples using inkjet printed SERS substrates. *Analyst* 2013;138(13):3679-86.
137. López-Otín C, Blasco MA, Partridge L, et al. The hallmarks of aging. *Cell* 2013;153(6):1194-217.
138. Assar ME, Angulo J, Rodríguez-Mañas L. Diabetes and ageing-induced vascular inflammation. *The Journal of Physiology* 2016;594(8):2125-46.
139. Loeser RF, Collins JA, Diekman BO. Ageing and the pathogenesis of osteoarthritis. *Nature Reviews Rheumatology* 2016;12:412.
140. Hou Y, Dan X, Babbar M, et al. Ageing as a risk factor for neurodegenerative disease. *Nature Reviews Neurology* 2019.
141. Calabrese V, Santoro A, Monti D, et al. Aging and Parkinson's Disease: Inflammaging, neuroinflammation and biological remodeling as key factors in pathogenesis. *Free Radical Biology and Medicine* 2018;115:80-91.
142. Vaupel JW. Biodemography of human ageing. *Nature* 2010;464(7288):536-42.
143. Perry DP. Introduction to Aging, Cancer, and Age-related Diseases. *Annals of the New York Academy of Sciences* 2010;1197(1):vii-x.
144. Olshansky SJ, Carnes BA, Cassel C. In search of Methuselah: estimating the upper limits to human longevity. *Science* 1990;250(4981):634-40.
145. Martin GM, LaMarco K, Strauss E, et al. Research on aging: the end of the beginning: American Association for the Advancement of Science, 2003.
146. Hubert HB, Bloch DA, Oehlert JW, et al. Lifestyle Habits and Compression of Morbidity. *The Journals of Gerontology: Series A* 2002;57(6):M347-M51.
147. Franceschi C, Monti D, Sansoni P, et al. The immunology of exceptional individuals: the lesson of centenarians. *Immunology today* 1995;16(1):12-16.
148. Franceschi C, Bonafè M. Centenarians as a model for healthy aging: Portland Press Limited, 2003.
149. Evert J, Lawler E, Bogan H, et al. Morbidity profiles of centenarians: survivors, delayers, and escapers. *The Journals of Gerontology Series A: Biological Sciences and Medical Sciences* 2003;58(3):M232-M37.
150. Arai Y, Martin-Ruiz CM, Takayama M, et al. Inflammation, but not telomere length, predicts successful ageing at extreme old age: a longitudinal study of semi-supercentenarians. *EBioMedicine* 2015;2(10):1549-58.
151. Rubino G, Bulati M, Aiello A, et al. Sicilian centenarian offspring are more resistant to immune ageing. *Aging Clinical and Experimental Research* 2019;31(1):125-33.
152. Aiello A, Ligotti ME, Cossarizza A. Centenarian Offspring as a Model of Successful Ageing. In: Caruso C (ed.) *Centenarians: An Example of Positive Biology*. Cham: Springer International Publishing; 2019 p35-51.
153. Organization WH. *World report on ageing and health*: World Health Organization; 2015.

List of References

154. Goronzy JJ, Fang F, Cavanagh MM, et al. Naive T cell maintenance and function in human aging. *The Journal of Immunology* 2015;194(9):4073-80.
155. Fulop T, Larbi A, Dupuis G, et al. Immunosenescence and Inflamm-Aging As Two Sides of the Same Coin: Friends or Foes? *Frontiers in Immunology* 2018;8(1960).
156. Franceschi C, Garagnani P, Parini P, et al. Inflammaging: a new immune–metabolic viewpoint for age-related diseases. *Nature Reviews Endocrinology* 2018;14(10):576-90.
157. Fulop T, Witkowski JM, Pawelec G, et al. On the immunological theory of aging *Aging: Karger Publishers; 2014 p163-76.*
158. Franceschi C, Zaikin A, Gordleeva S, et al. Inflammaging 2018: An update and a model. *Seminars in Immunology* 2018;40:1-5.
159. Gale CR, Baylis D, Cooper C, et al. Inflammatory markers and incident frailty in men and women: the English Longitudinal Study of Ageing. *Age* 2013;35(6):2493-501.
160. Libby P, Okamoto Y, Rocha VZ, et al. Inflammation in atherosclerosis: transition from theory to practice. *Circulation journal* 2010;74(2):213-20.
161. Paolisso G, Rizzo MR, Mazziotti G, et al. Advancing age and insulin resistance: role of plasma tumor necrosis factor- α . *American Journal of Physiology-Endocrinology And Metabolism* 1998;275(2):E294-E99.
162. Wang J, Sung V, Carew P, et al. Inflammation and hearing status in mid-childhood and mid-life: a population-based cross-sectional study. *International Journal of Epidemiology* 2019.
163. Watson N, Ding B, Zhu X, et al. Chronic inflammation–inflammaging–in the ageing cochlea: a novel target for future presbycusis therapy. *Ageing research reviews* 2017;40:142-48.
164. Lio D, Scola L, Crivello A, et al. Gender-specific association between– 1082 IL-10 promoter polymorphism and longevity. *Genes and immunity* 2002;3(1):30.
165. Pawelec G. Hallmarks of human “immunosenescence”: adaptation or dysregulation?: BioMed Central, 2012.
166. Cevenini E, Monti D, Franceschi C. Inflamm-aging. *Current Opinion in Clinical Nutrition & Metabolic Care* 2013;16(1):14-20.
167. Cevenini E, Caruso C, Candore G, et al. Age-related inflammation: the contribution of different organs, tissues and systems. How to face it for therapeutic approaches. *Current pharmaceutical design* 2010;16(6):609-18.
168. Shaygani E, Bahmani M, Asgary S, et al. Inflammaging and cardiovascular disease: Management by medicinal plants. *Phytomedicine* 2016;23(11):1119-26.
169. Kim Y-W, Byzova TV. Oxidative stress in angiogenesis and vascular disease. *Blood* 2014;123(5):625-31.
170. Lawes S, Demakakos P, Steptoe A, et al. Combined influence of depressive symptoms and systemic inflammation on all-cause and cardiovascular mortality: evidence for differential effects by gender in the English Longitudinal Study of Ageing. *Psychological Medicine* 2019;49(9):1521-31.
171. Ferrucci L, Fabbri E. Inflammageing: chronic inflammation in ageing, cardiovascular disease, and frailty. *Nature Reviews Cardiology* 2018;15(9):505-22.

172. Davis BK, Wen H, Ting JP-Y. The inflammasome NLRs in immunity, inflammation, and associated diseases. *Annual review of immunology* 2011;29:707-35.
173. Khansari N, Shakiba Y, Mahmoudi M. Chronic inflammation and oxidative stress as a major cause of age-related diseases and cancer. *Recent patents on inflammation & allergy drug discovery* 2009;3(1):73-80.
174. Reuter S, Gupta SC, Chaturvedi MM, et al. Oxidative stress, inflammation, and cancer: how are they linked? *Free Radical Biology and Medicine* 2010;49(11):1603-16.
175. Ostan R, Lanzarini C, Pini E, et al. Inflammaging and Cancer: A Challenge for the Mediterranean Diet. *Nutrients* 2015;7(4).
176. Stringhini S, Zaninotto P, Kumari M, et al. Lifecourse socioeconomic status and type 2 diabetes: the role of chronic inflammation in the English Longitudinal Study of Ageing. *Scientific Reports* 2016;6:24780.
177. Prattichizzo F, De Nigris V, La Sala L, et al. "Inflammaging" as a Druggable Target: A Senescence-Associated Secretory Phenotype-Centered View of Type 2 Diabetes. *Oxidative Medicine and Cellular Longevity* 2016;2016:10.
178. Ahima RS. Connecting obesity, aging and diabetes. *Nature medicine* 2009;15(9):996.
179. Deleidi M, Jäggle M, Rubino G. Immune aging, dysmetabolism, and inflammation in neurological diseases. *Frontiers in Neuroscience* 2015;9:172.
180. Holmes C, Butchart J. Systemic inflammation and Alzheimer's disease. *Biochem Soc Trans* 2011;39(4):898-901.
181. Dalle S, Rossmeislova L, Koppo K. The Role of Inflammation in Age-Related Sarcopenia. *Frontiers in Physiology* 2017;8(1045).
182. Kauppinen A, Paterno JJ, Blasiak J, et al. Inflammation and its role in age-related macular degeneration. *Cellular and Molecular Life Sciences* 2016;73(9):1765-86.
183. White J, Kivimäki M, Jokela M, et al. Association of inflammation with specific symptoms of depression in a general population of older people: The English Longitudinal Study of Ageing. *Brain Behav Immun* 2017;61:27-30.
184. Tanner A, Vassallo M, Kwan JSK, et al. The pulmonary rehabilitation regimen: a treatment for frailty and 'inflammaging'? *British Journal of Hospital Medicine* 2018;79(8):432-37.
185. Van Epps P, Oswald D, Higgins PA, et al. Frailty has a stronger association with inflammation than age in older veterans. *Immunity & Ageing* 2016;13(1):27.
186. Tay L, Lim WS, Chan M, et al. The independent role of inflammation in physical frailty among older adults with mild cognitive impairment and mild-to-moderate Alzheimer's disease. *The journal of nutrition, health & aging* 2016;20(3):288-99.
187. Soysal P, Stubbs B, Lucato P, et al. Inflammation and frailty in the elderly: A systematic review and meta-analysis. *Ageing research reviews* 2016;31:1-8.
188. Mekli K, Nazroo JY, Marshall AD, et al. Proinflammatory genotype is associated with the frailty phenotype in the English Longitudinal Study of Ageing. *Aging Clinical and Experimental Research* 2016;28(3):413-21.

List of References

189. Lassale C, Vullo P, Batty GD, et al. Inflammatory markers are associated with age-related hearing impairment: The English longitudinal study of ageing. *Revue d'Épidémiologie et de Santé Publique* 2018;66:S237-S38.
190. Simpson AN, Matthews LJ, Dubno JR. Lipid and C-reactive Protein Levels as Risk Factors for Hearing Loss in Older Adults. *Otolaryngology-Head and Neck Surgery* 2013;148(4):664-70.
191. Kuek A, Hazleman BL, Östör AJ. Immune-mediated inflammatory diseases (IMIDs) and biologic therapy: a medical revolution. *Postgraduate medical journal* 2007;83(978):251-60.
192. Ginaldi L, Di Benedetto MC, De Martinis M. Osteoporosis, inflammation and ageing. *Immunity & Ageing* 2005;2(1):14.
193. Correia C, Lopez KJ, Wroblewski KE, et al. Global Sensory Impairment in Older Adults in the United States. *Journal of the American Geriatrics Society* 2016;64(2):306-13.
194. Gershon RC, Wagster MV, Hendrie HC, et al. NIH Toolbox for Assessment of Neurological and Behavioral Function. *Neurology* 2013;80(11 Supplement 3):S2.
195. Doty RL. Olfactory dysfunction in Parkinson disease. *Nature Reviews Neurology* 2012;8(6):329-39.
196. Pinto JM, Wroblewski KE, Kern DW, et al. Olfactory Dysfunction Predicts 5-Year Mortality in Older Adults. *PLoS One* 2014;9(10):e107541.
197. Gallenga CE, Parmeggiani F, Costagliola C, et al. Inflammaging: should this term be suitable for age related macular degeneration too? *Inflammation Research* 2014;63(2):105-07.
198. Göde S, Turhal G, Kaya İ, et al. Evaluation of Procalcitonin and hs-CRP Levels in Sudden Sensorineural Hearing Loss. *The journal of international advanced otology* 2018;14(1):44-47.
199. Chen L, Zhang G, Zhang Z, et al. Neutrophil-to-lymphocyte ratio predicts diagnosis and prognosis of idiopathic sudden sensorineural hearing loss: A systematic review and meta-analysis. *Medicine* 2018;97(38):e12492-e92.
200. Mathers CD, Loncar D. Projections of global mortality and burden of disease from 2002 to 2030. *PLoS medicine* 2006;3(11):e442.
201. Dalton DS, Cruickshanks KJ, Klein BE, et al. The impact of hearing loss on quality of life in older adults. *The Gerontologist* 2003;43(5):661-68.
202. Gates GA, Mills JH. Presbycusis. *The Lancet* 2005;366(9491):1111-20.
203. Schuknecht HF, Gacek MR. Cochlear pathology in presbycusis. *Ann Otol Rhinol Laryngol* 1993;102(1 Pt 2):1-16.
204. Gacek RR, Schuknecht HF. Pathology of presbycusis. *International Audiology* 1969;8(2-3):199-209.
205. Sugawara M, Corfas G, Liberman MC. Influence of supporting cells on neuronal degeneration after hair cell loss. *J Assoc Res Otolaryngol* 2005;6(2):136-47.
206. Sha SH, Taylor R, Forge A, et al. Differential vulnerability of basal and apical hair cells is based on intrinsic susceptibility to free radicals. *Hearing Research* 2001;155(1-2):1-8.
207. Chen G-D, Zhao H-B. Effects of intense noise exposure on the outer hair cell plasma membrane fluidity. *Hearing Research* 2007;226(1):14-21.

208. Schmiedt RA. The Physiology of Cochlear Presbycusis. In: Gordon-Salant S, Frisina RD, Popper AN, et al. (eds.) *The Aging Auditory System*. New York, NY: Springer New York; 2010 p9-38.
209. Glueckert R, Bitsche M, Miller JM, et al. Deafferentation - associated changes in afferent and efferent processes in the guinea pig cochlea and afferent regeneration with chronic intrascalar brain - derived neurotrophic factor and acidic fibroblast growth factor. *Journal of Comparative Neurology* 2008;507(4):1602-21.
210. Kujawa SG, Liberman MC. Adding insult to injury: cochlear nerve degeneration after “temporary” noise-induced hearing loss. *Journal of Neuroscience* 2009;29(45):14077-85.
211. Sergeyenko Y, Lall K, Liberman MC, et al. Age-related cochlear synaptopathy: an early-onset contributor to auditory functional decline. *Journal of Neuroscience* 2013;33(34):13686-94.
212. Dubno JR, Eckert MA, Lee F-S, et al. Classifying human audiometric phenotypes of age-related hearing loss from animal models. *Journal of the Association for Research in Otolaryngology* 2013;14(5):687-701.
213. Humes LE, Dubno JR, Gordon-Salant S, et al. Central presbycusis: a review and evaluation of the evidence. *Journal of the American Academy of Audiology* 2012;23(8):635-66.
214. Gray DT, Engle JR, Recanzone GH. Age - related neurochemical changes in the rhesus macaque cochlear nucleus. *Journal of Comparative Neurology* 2014;522(7):1527-41.
215. Frisina RD, Walton JP. Age-related structural and functional changes in the cochlear nucleus. *Hearing Research* 2006;216:216-23.
216. Willott JF, Schacht J. Interventions and Future Therapies: Lessons from Animal Models. In: Gordon-Salant S, Frisina RD, Popper AN, et al. (eds.) *The Aging Auditory System*. New York, NY: Springer New York; 2010 p275-93.
217. Stamatakis S, Francis HW, Lehar M, et al. Synaptic alterations at inner hair cells precede spiral ganglion cell loss in aging C57BL/6J mice. *Hearing Research* 2006;221(1-2):104-18.
218. Tremblay M-È, Lowery RL, Majewska AK. Microglial interactions with synapses are modulated by visual experience. *PLoS Biol* 2010;8(11):e1000527.
219. Kettenmann H, Kirchhoff F, Verkhratsky A. Microglia: new roles for the synaptic stripper. *Neuron* 2013;77(1):10-18.
220. Harris JP. Immunology of the inner ear: response of the inner ear to antigen challenge. *Otolaryngology—Head and Neck Surgery* 1983;91(1):18-23.
221. Harris JP. Immunology of the inner ear: evidence of local antibody production. *Annals of Otolaryngology & Laryngology* 1984;93(2):157-62.
222. McCabe BF. Autoimmune inner ear disease: therapy. *Otology & Neurotology* 1989;10(3):196-97.
223. Frye MD, Yang W, Zhang C, et al. Dynamic activation of basilar membrane macrophages in response to chronic sensory cell degeneration in aging mouse cochleae. *Hearing Research* 2017;344:125-34.
224. Hirose K, Discolo CM, Keasler JR, et al. Mononuclear phagocytes migrate into the murine cochlea after acoustic trauma. *Journal of Comparative Neurology* 2005;489(2):180-94.

List of References

225. Zhang W, Dai M, Fridberger A, et al. Perivascular-resident macrophage-like melanocytes in the inner ear are essential for the integrity of the intrastrial fluid–blood barrier. *Proceedings of the National Academy of Sciences* 2012;109(26):10388-93.
226. Fujioka M, Okano H, Ogawa K. Inflammatory and immune responses in the cochlea: potential therapeutic targets for sensorineural hearing loss. *Frontiers in pharmacology* 2014;5:287.
227. Koo J-W, Quintanilla-Dieck L, Jiang M, et al. Endotoxemia-mediated inflammation potentiates aminoglycoside-induced ototoxicity. *Science translational medicine* 2015;7(298):298ra118-298ra118.
228. Wong ACY, Ryan AF. Mechanisms of sensorineural cell damage, death and survival in the cochlea. *Frontiers in Aging Neuroscience* 2015;7.
229. Morrisette-Thomas V, Cohen AA, Fülöp T, et al. Inflamm-aging does not simply reflect increases in pro-inflammatory markers. *Mechanisms of ageing and development* 2014;139:49-57.
230. Franceschi C, Salvioli S, Garagnani P, et al. Immunobiography and the Heterogeneity of Immune Responses in the Elderly: A Focus on Inflammaging and Trained Immunity. *Frontiers in Immunology* 2017;8(982).
231. Medzhitov R. Origin and physiological roles of inflammation. *Nature* 2008;454(7203):428-35.
232. Wood MB, Zuo J. The contribution of immune infiltrates to ototoxicity and cochlear hair cell loss. *Frontiers in Cellular Neuroscience* 2017;11:106.
233. Yang W, Vethanayagam RR, Dong Y, et al. Activation of the antigen presentation function of mononuclear phagocyte populations associated with the basilar membrane of the cochlea after acoustic overstimulation. *Neuroscience* 2015;303:1-15.
234. Mitchell P, Gopinath B, McMahon CM, et al. Relationship of Type 2 diabetes to the prevalence, incidence and progression of age - related hearing loss. *Diabetic Medicine* 2009;26(5):483-88.
235. Kim M-B, Zhang Y, Chang Y, et al. Diabetes mellitus and the incidence of hearing loss: a cohort study. *International Journal of Epidemiology* 2016;46(2):717-26.
236. Fortunato S, Forli F, Guglielmi V, et al. A review of new insights on the association between hearing loss and cognitive decline in ageing. *Acta Otorhinolaryngologica Italica* 2016;36(3):155.
237. Panza F, Solfrizzi V, Logroscino G. Age-related hearing impairment [mdash] a risk factor and frailty marker for dementia and AD. *Nature Reviews Neurology* 2015;11(3):166-75.
238. Su P, Hsu C-C, Lin H-C, et al. Age-related hearing loss and dementia: a 10-year national population-based study. *European Archives of Oto-Rhino-Laryngology* 2017;274(5):2327-34.
239. Dalton DS, Schubert CR, Pinto A, et al. Cadmium, obesity, and education, and the 10-year incidence of hearing impairment: The beaver dam offspring study. *The Laryngoscope* 2019;0(0).
240. Wang J, Sung V, Lycett K, et al. How body composition influences hearing status by mid-childhood and mid-life: The Longitudinal Study of Australian Children. *International Journal of Obesity* 2018;42(10):1771-81.

241. Dhanda N, Taheri S. A narrative review of obesity and hearing loss. *International Journal of Obesity* 2017;41(7):1066-73.
242. Lin Y-Y, Wu L-W, Kao T-W, et al. Secondhand Smoke is Associated with Hearing Threshold Shifts in Obese Adults. *Scientific Reports* 2016;6:33071.
243. Scherer EQ, Yang J, Canis M, et al. Tumor necrosis factor- α enhances microvascular tone and reduces blood flow in the cochlea via enhanced sphingosine-1-phosphate signaling. *Stroke* 2010;41(11):2618-24.
244. Huang C-M, Chen H-J, Huang P-H, et al. Retrospective cohort study on risk of hearing loss in patients with rheumatoid arthritis using claims data. *BMJ Open* 2018;8(1):e018134.
245. Gupta S, Curhan SG, Curhan GC. Biomarkers of Systemic Inflammation and Risk of Incident Hearing Loss. *Ear and hearing* 2019;40(4):981-89.
246. Löhrich T, Behringer V, Wittig RM, et al. The Use of Neopterin as a Noninvasive Marker in Monitoring Diseases in Wild Chimpanzees. *EcoHealth* 2018;15(4):792-803.
247. Behringer V, Stevens J, Leendertz F, et al. Validation of a method for the assessment of urinary neopterin levels to monitor health status in non-human-primate species. *Frontiers in Physiology* 2017;8(51).
248. Winkler C, Wirleitner B, Werner E, et al. Urinary Neopterin Concentrations in Healthy Individuals with Household Contact. *Pteridines* 2003;14.
249. Justice JN, Ferrucci L, Newman AB, et al. A framework for selection of blood-based biomarkers for geroscience-guided clinical trials: report from the TAME Biomarkers Workgroup. *Geroscience* 2018;40(5-6):419-36.
250. Clegg A, Young J, Iliffe S, et al. Frailty in elderly people. *The Lancet* 2013;381(9868):752-62.
251. Mitnitski AB, Mogilner AJ, Rockwood K. Accumulation of deficits as a proxy measure of aging. *The Scientific World Journal* 2001;1:323-36.
252. Yang Y, Lee LC. Dynamics and heterogeneity in the process of human frailty and aging: evidence from the US older adult population. *Journals of Gerontology Series B: Psychological Sciences and Social Sciences* 2009;65(2):246-55.
253. Rockwood K, Mitnitski A. Frailty defined by deficit accumulation and geriatric medicine defined by frailty. *Clinics in geriatric medicine* 2011;27(1):17-26.
254. Goggins WB, Woo J, Sham A, et al. Frailty index as a measure of biological age in a Chinese population. *The Journals of Gerontology Series A: Biological Sciences and Medical Sciences* 2005;60(8):1046-51.
255. Song X, Mitnitski A, Rockwood K. Nontraditional risk factors combine to predict Alzheimer disease and dementia. *Neurology* 2011;77(3):227-34.
256. Wallace LM, Theou O, Kirkland SA, et al. Accumulation of non-traditional risk factors for coronary heart disease is associated with incident coronary heart disease hospitalization and death. *PLoS One* 2014;9(3):e90475.
257. Kennedy C, Ioannidis G, Rockwood K, et al. A Frailty Index predicts 10-year fracture risk in adults age 25 years and older: results from the Canadian Multicentre Osteoporosis Study (CaMos). *Osteoporosis International* 2014;25(12):2825-32.

List of References

258. Semmarath W, Seesen M, Yodkeeree S, et al. The Association between Frailty Indicators and Blood-Based Biomarkers in Early-Old Community Dwellers of Thailand. *International Journal of Environmental Research and Public Health* 2019;16(18):3457.
259. Michaud M, Balardy L, Moulis G, et al. Proinflammatory cytokines, aging, and age-related diseases. *Journal of the American Medical Directors Association* 2013;14(12):877-82.
260. Wei J, Xu H, Davies JL, et al. Increase of plasma IL-6 concentration with age in healthy subjects. *Life sciences* 1992;51(25):1953-56.
261. Hager K, Machein U, Krieger S, et al. Interleukin-6 and selected plasma proteins in healthy persons of different ages. *Neurobiology of aging* 1994;15(6):771-72.
262. Fagiolo U, Cossarizza A, Scala E, et al. Increased cytokine production in mononuclear cells of healthy elderly people. *European journal of immunology* 1993;23(9):2375-78.
263. Ferrucci L, Corsi A, Lauretani F, et al. The origins of age-related proinflammatory state. *Blood* 2005;105(6):2294-99.
264. Leng SX, McElhaney JE, Walston JD, et al. ELISA and Multiplex Technologies for Cytokine Measurement in Inflammation and Aging Research. *The Journals of Gerontology: Series A* 2008;63(8):879-84.
265. ARMSTRONG R, CATTELL R, JONES S, et al. ELEVATED URINARY NEOPTERIN SUGGESTS IMMUNE ACTIVATION IN ALZHEIMERS-DISEASE AND DOWNS-SYNDROME. *Neuroscience research communications* 1994;14(2).
266. Savas S, Kabaroglu C, Alpman A, et al. No relationship between lipoprotein-associated phospholipase A2, proinflammatory cytokines, and neopterin in Alzheimer's disease. *Experimental gerontology* 2016;77:1-6.
267. Zis P, Strydom A, Buckley D, et al. Cognitive ability in Down syndrome and its relationship to urinary neopterin, a marker of activated cellular immunity. *Neuroscience Letters* 2017;636:254-57.
268. Sucher R, Schroecksnadel K, Weiss G, et al. Neopterin, a prognostic marker in human malignancies. *Cancer Letters* 2010;287(1):13-22.
269. Yildirim Y, Gunel N, Coskun U, et al. Serum neopterin levels in patients with breast cancer. *Medical Oncology* 2008;25(4):403-07.
270. Wietlicka-Kokoszane I, Jablecka A, Smolarek I, et al. Neopterin as a prognostic marker in patients with chronic heart failure. *Medical Science Monitor* 2010;16(5):CR232-CR37.
271. Valdiglesias V, Sánchez-Flores M, Maseda A, et al. Immune biomarkers in older adults: Role of physical activity. *Journal of Toxicology and Environmental Health, Part A* 2017;80(13-15):605-20.
272. Stuart CM, Zotova E, Koster G, et al. High-Throughput Urinary Neopterin-to-Creatinine Ratio Monitoring of Systemic Inflammation. *The Journal of Applied Laboratory Medicine* 2019;5(1):101-13.
273. Schafer MJ, White TA, Evans G, et al. Exercise prevents diet-induced cellular senescence in adipose tissue. *Diabetes* 2016;65(6):1606-15.
274. DeBoer MD. Obesity, systemic inflammation, and increased risk for cardiovascular disease and diabetes among adolescents: a need for screening tools to target interventions. *Nutrition* 2013;29(2):379-86.

275. Hallal PC, Andersen LB, Bull FC, et al. Global physical activity levels: surveillance progress, pitfalls, and prospects. *The Lancet* 2012;380(9838):247-57.
276. Lee I-M, Shiroma EJ, Lobelo F, et al. Effect of physical inactivity on major non-communicable diseases worldwide: an analysis of burden of disease and life expectancy. *The Lancet* 2012;380(9838):219-29.
277. Pollock RD, Carter S, Velloso CP, et al. An investigation into the relationship between age and physiological function in highly active older adults. *The Journal of Physiology* 2015;593(3):657-80.
278. Duggal NA, Pollock RD, Lazarus NR, et al. Major features of immunesenescence, including reduced thymic output, are ameliorated by high levels of physical activity in adulthood. *Aging cell* 2018;17(2):e12750.
279. Stessman J, Hammerman-Rozenberg R, Cohen A, et al. Physical activity, function, and longevity among the very old. *Archives of internal medicine* 2009;169(16):1476-83.
280. Moore SC, Lee I-M, Weiderpass E, et al. Association of leisure-time physical activity with risk of 26 types of cancer in 1.44 million adults. *JAMA internal medicine* 2016;176(6):816-25.
281. Pollock RD, O'Brien KA, Daniels LJ, et al. Properties of the vastus lateralis muscle in relation to age and physiological function in master cyclists aged 55–79 years. *Aging cell* 2018;17(2):e12735.
282. Franco OH, de Laet C, Peeters A, et al. Effects of physical activity on life expectancy with cardiovascular disease. *Archives of internal medicine* 2005;165(20):2355-60.
283. Moore SC, Patel AV, Matthews CE, et al. Leisure time physical activity of moderate to vigorous intensity and mortality: a large pooled cohort analysis. *PLoS medicine* 2012;9(11):e1001335.
284. Lee D-c, Brellenthin AG, Thompson PD, et al. Running as a key lifestyle medicine for longevity. *Progress in cardiovascular diseases* 2017;60(1):45-55.
285. WHO. *Global recommendations on physical activity for health* (accessed 6.6.2020).
286. Wen CP, Wai JPM, Tsai MK, et al. Minimum amount of physical activity for reduced mortality and extended life expectancy: a prospective cohort study. *The Lancet* 2011;378(9798):1244-53.
287. McPhee JS, French DP, Jackson D, et al. Physical activity in older age: perspectives for healthy ageing and frailty. *Biogerontology* 2016;17(3):567-80.
288. Katz D, Meller S. Can we say what diet is best for health? *Annual review of public health* 2014;35:83-103.
289. Colman RJ, Anderson RM, Johnson SC, et al. Caloric restriction delays disease onset and mortality in rhesus monkeys. *Science* 2009;325(5937):201-04.
290. Blagosklonny MV. Calorie restriction: decelerating mTOR-driven aging from cells to organisms (including humans). *Cell Cycle* 2010;9(4):683-88.
291. Cuervo AM, Bergamini E, Brunk UT, et al. Autophagy and aging: the importance of maintaining "clean" cells. *Autophagy* 2005;1(3):131-40.

List of References

292. Belsky DW, Huffman KM, Pieper CF, et al. Change in the rate of biological aging in response to caloric restriction: CALERIE Biobank analysis. *The Journals of Gerontology: Series A* 2017;73(1):4-10.
293. Harrison DE, Strong R, Sharp ZD, et al. Rapamycin fed late in life extends lifespan in genetically heterogeneous mice. *Nature* 2009;460(7253):392.
294. Nadon NL, Strong R, Miller RA, et al. NIA Interventions Testing Program: investigating putative aging intervention agents in a genetically heterogeneous mouse model. *EBioMedicine* 2017;21:3-4.
295. Martin-Montalvo A, Mercken EM, Mitchell SJ, et al. Metformin improves healthspan and lifespan in mice. *Nature communications* 2013;4:2192.
296. Zaseck LW, Miller RA, Brooks SV. Rapamycin attenuates age-associated changes in tibialis anterior tendon viscoelastic properties. *Journals of Gerontology Series A: Biomedical Sciences and Medical Sciences* 2016;71(7):858-65.
297. Flynn JM, O'Leary MN, Zambataro CA, et al. Late - life rapamycin treatment reverses age - related heart dysfunction. *Aging cell* 2013;12(5):851-62.
298. Lin A-L, Zheng W, Halloran JJ, et al. Chronic rapamycin restores brain vascular integrity and function through NO synthase activation and improves memory in symptomatic mice modeling Alzheimer's disease. *Journal of Cerebral Blood Flow & Metabolism* 2013;33(9):1412-21.
299. Barzilai N, Crandall JP, Kritchevsky SB, et al. Metformin as a tool to target aging. *Cell metabolism* 2016;23(6):1060-65.
300. Bannister C, Holden S, Jenkins - Jones S, et al. Can people with type 2 diabetes live longer than those without? A comparison of mortality in people initiated with metformin or sulphonylurea monotherapy and matched, non - diabetic controls. *Diabetes, Obesity and Metabolism* 2014;16(11):1165-73.
301. Group UPDS. Effect of intensive blood-glucose control with metformin on complications in overweight patients with type 2 diabetes (UKPDS 34). *The Lancet* 1998;352(9131):854-65.
302. Knowler WC, Barrett-Connor E, Fowler SE, et al. Reduction in the incidence of type 2 diabetes with lifestyle intervention or metformin. *The New England journal of medicine* 2002;346(6):393-403.
303. . *Seminars in immunopathology*: Springer.
304. Mora S, Glynn RJ, Hsia J, et al. Statins for the Primary Prevention of Cardiovascular Events in Women with Elevated High-Sensitivity C-Reactive Protein or Dyslipidemia: Results from JUPITER and meta-analysis of women from primary prevention trials. *Circulation* 2010;121(9):1069.
305. Lowthian JA, Britt C, Rance G, et al. Slowing the progression of age-related hearing loss: Rationale and study design of the ASPIRIN in HEARING, retinal vessels imaging and neurocognition in older generations (ASPREE-HEARING) trial. *Contemporary clinical trials* 2016;46:60-66.
306. Audiology B, Committee BPP. Recommended Procedure Pure-Tone Airconduction and Bone-Conduction Threshold Audiometry With and Without Masking.(2018). *The British Society of Audiology: Reading*.

307. Cohen J. *Statistical power analysis for the behavioral sciences*: Academic press; 2013.
308. Botelho CT, Carvalho SAdS, Silva IN. Increased prevalence of early cochlear damage in young patients with type 1 diabetes detected by distortion product otoacoustic emissions. *International Journal of Audiology* 2014;53(6):402-08.
309. Dorn PA, Konrad-Martin D, Neely ST, et al. Distortion product otoacoustic emission input/output functions in normal-hearing and hearing-impaired human ears. *The Journal of the Acoustical Society of America* 2001;110(6):3119-31.
310. Helleman HW, Dreschler WA. Overall versus individual changes for otoacoustic emissions and audiometry in a noise-exposed cohort. *International Journal of Audiology* 2012;51(5):362-72.
311. Abdala C, Visser-Dumont L. Distortion product otoacoustic emissions: A tool for hearing assessment and scientific study. *The Volta Review* 2001;103(4):281.
312. Keppler H, Dhooge I, Maes L, et al. Transient-evoked and distortion product otoacoustic emissions: A short-term test-retest reliability study. *International Journal of Audiology* 2010;49(2):99-109.
313. Perry VH, Cunningham C, Holmes C. Systemic infections and inflammation affect chronic neurodegeneration. *Nat Rev Immunol* 2007;7(2):161-7.
314. Barnett K, Mercer SW, Norbury M, et al. Epidemiology of multimorbidity and implications for health care, research, and medical education: a cross-sectional study. *The Lancet* 2012;380(9836):37-43.
315. Schroecksadel K, Murr C, Winkler C, et al. Neopterin to monitor clinical pathologies involving interferon- γ production. *Pteridines* 2004;15(3):75-90.
316. Avanzas P, Arroyo-Espliguero R, Cosin-Sales J, et al. Prognostic value of neopterin levels in treated patients with hypertension and chest pain but without obstructive coronary artery disease. *The American journal of cardiology* 2004;93(5):627-29.
317. Avanzas P, Arroyo-Espliguero R, Kaski JC. Neopterin and cardiovascular disease: growing evidence for a role in patient risk stratification: *Clinical Chemistry*, 2009.
318. Leng SX, Tian X, Matteini A, et al. IL-6-independent association of elevated serum neopterin levels with prevalent frailty in community-dwelling older adults. *Age and Ageing* 2011;40(4):475-81.
319. Lee J, Taneja V, Vassallo R. Cigarette smoking and inflammation: cellular and molecular mechanisms. *Journal of dental research* 2012;91(2):142-49.
320. Albert MA, Danielson E, Rifai N, et al. Effect of statin therapy on C-reactive protein levels: the pravastatin inflammation/CRP evaluation (PRINCE): a randomized trial and cohort study. *Jama* 2001;286(1):64-70.
321. Bates T, Connaughton V, Watts G. Non-adherence to statin therapy: a major challenge for preventive cardiology. *Expert opinion on pharmacotherapy* 2009;10(18):2973-85.
322. Vonbank A, Agewall S, Kjeldsen KP, et al. Comprehensive efforts to increase adherence to statin therapy. *European heart journal* 2017;38(32):2473-79.
323. Cruickshanks KJ, Wiley TL, Tweed TS, et al. Prevalence of hearing loss in older adults in Beaver Dam, Wisconsin: The epidemiology of hearing loss study. *American journal of epidemiology* 1998;148(9):879-86.

List of References

324. Lee J, Dhar S, Abel R, et al. Behavioral hearing thresholds between 0.125 and 20 kHz using depth-compensated ear simulator calibration. *Ear and hearing* 2012;33(3):315.
325. Schmuziger N, Probst R, Smurzynski J. Test-retest reliability of pure-tone thresholds from 0.5 to 16 kHz using Sennheiser HDA 200 and Etymotic Research ER-2 earphones. *Ear and hearing* 2004;25(2):127-32.
326. Quaranta N, Debole S, Di Girolamo S. Effect of ageing on otoacoustic emissions and efferent suppression in humans: efectos de la edad en las emisiones otoacústicas y (EN LA) supresión eferente en humanos. *Audiology* 2001;40(6):308-12.
327. Keppler H, Dhooge I, Corthals P, et al. The effects of aging on evoked otoacoustic emissions and efferent suppression of transient evoked otoacoustic emissions. *Clinical Neurophysiology* 2010;121(3):359-65.
328. Stenklev NC, Laukli E. Transient evoked otoacoustic emissions in the elderly: Emisiones otoacústicas evocadas transitorias en el anciano. *International Journal of Audiology* 2003;42(3):132-39.
329. Uchida Y, Ando F, Shimokata H, et al. The effects of aging on distortion-product otoacoustic emissions in adults with normal hearing. *Ear and hearing* 2008;29(2):176-84.
330. . *Seminars in Hearing*: Copyright© 1992 by Thieme Medical Publishers, Inc.
331. Kemp DT. Otoacoustic emissions, their origin in cochlear function, and use. *British Medical Bulletin* 2002;63(1):223-41.
332. Jang S-k, Kim J-h, Lee Y. Effect of relative handgrip strength on cardiovascular disease among Korean adults aged 45 years and older: Results from the Korean Longitudinal Study of Aging (2006–2016). *Archives of Gerontology and Geriatrics* 2020;86:103937.
333. Horvath S. DNA methylation age of human tissues and cell types. *Genome biology* 2013;14(10):3156.
334. Levine ME, Lu AT, Quach A, et al. An epigenetic biomarker of aging for lifespan and healthspan. *Aging* 2018;10(4):573.
335. Horvath S, Raj K. DNA methylation-based biomarkers and the epigenetic clock theory of ageing. *Nature Reviews Genetics* 2018;19(6):371.
336. Chaudhuri J, Bains Y, Guha S, et al. The role of advanced glycation end products in aging and metabolic diseases: bridging association and causality. *Cell metabolism* 2018;28(3):337-52.
337. Semba RD, Nicklett EJ, Ferrucci L. Does accumulation of advanced glycation end products contribute to the aging phenotype? *Journals of Gerontology Series A: Biomedical Sciences and Medical Sciences* 2010;65(9):963-75.
338. Connelly MA, Otvos JD, Shalurova I, et al. GlycA, a novel biomarker of systemic inflammation and cardiovascular disease risk. *Journal of translational medicine* 2017;15(1):219.
339. Duprez DA, Otvos J, Sanchez OA, et al. Comparison of the predictive value of GlycA and other biomarkers of inflammation for total death, incident cardiovascular events, noncardiovascular and noncancer inflammatory-related events, and total cancer events. *Clinical Chemistry* 2016;62(7):1020-31.

340. Gruppen EG, Riphagen IJ, Connelly MA, et al. GlycA, a pro-inflammatory glycoprotein biomarker, and incident cardiovascular disease: relationship with C-reactive protein and renal function. *PLoS One* 2015;10(9):e0139057.
341. Metsios GS, Stavropoulos-Kalinoglou A, van Zanten JJV, et al. Individualised exercise improves endothelial function in patients with rheumatoid arthritis. *Annals of the Rheumatic Diseases* 2014;73(4):748-51.
342. Manning VL, Hurley MV, Scott DL, et al. Education, self - management, and upper extremity exercise training in people with rheumatoid arthritis: A randomized controlled trial. *Arthritis care & research* 2014;66(2):217-27.
343. Pollock RD, Carter S, Velloso CP, et al. An investigation into the relationship between age and physiological function in highly active older adults. *The Journal of Physiology* 2015;593(3):657-80.
344. Pereira BI, Akbar AN. Convergence of innate and adaptive immunity during human aging. *Frontiers in Immunology* 2016;7:445.
345. Duggal NA, Upton J, Phillips AC, et al. An age - related numerical and functional deficit in CD 19+ CD 24hi CD 38hi B cells is associated with an increase in systemic autoimmunity. *Aging cell* 2013;12(5):873-81.
346. de Araújo AL, Silva LCR, Fernandes JR, et al. Elderly men with moderate and intense training lifestyle present sustained higher antibody responses to influenza vaccine. *Age* 2015;37(6):105.
347. Heubner A, Pfleiderer W, Gunzer G, et al. AN ENZYME-IMMUNOASSAY FOR THE MEASUREMENT OF NEOPTERIN IN URINE AND SERUM SAMPLES. *Biological Chemistry Hoppe-Seyler* 1989;370(5):385-85.
348. Wachter H, Fuchs D, Hausen A, et al. *Neopterin: biochemistry-methods-clinical application*: Walter de Gruyter; 1992.
349. Tomandl J, Tallova J, Tomandlova M, et al. Determination of total oncopterin, neopterin and biopterin in human urine by high performance liquid chromatography with solid phase extraction. *Journal of Separation Science* 2003;26(8):674-78.
350. de Castro MR, Di Marco GS, Arita DY, et al. Urinary neopterin quantification by reverse-phase high-performance liquid ultraviolet chromatography with detection. *Journal of Biochemical and Biophysical Methods* 2004;59(3):275-83.
351. Schroecksadel K, Winkler C, Fuchs D. Method for urinary neopterin measurements by HPLC. *J Biochem Biophys Methods* 2006;66(1-3):99-100.
352. Kneipp K, Wang Y, Kneipp H, et al. Single molecule detection using surface-enhanced Raman scattering (SERS). *Physical review letters* 1997;78(9):1667.
353. Nie S, Emory SR. Probing single molecules and single nanoparticles by surface-enhanced Raman scattering. *Science* 1997;275(5303):1102-06.
354. Stiles PL, Dieringer JA, Shah NC, et al. Surface-Enhanced Raman Spectroscopy. *Annual Review of Analytical Chemistry* 2008;1(1):601-26.
355. Jeanmaire DL, Van Duyne RP. Surface raman spectroelectrochemistry: Part I. Heterocyclic, aromatic, and aliphatic amines adsorbed on the anodized silver electrode. *Journal of Electroanalytical Chemistry and Interfacial Electrochemistry* 1977;84(1):1-20.

List of References

356. Albrecht MG, Creighton JA. Anomalously intense Raman spectra of pyridine at a silver electrode. *J. Am. Chem. Soc* 1977;99(15):5215-17.
357. Willets KA, Duyn RPV. Localized Surface Plasmon Resonance Spectroscopy and Sensing. *Annual Review of Physical Chemistry* 2007;58(1):267-97.
358. Ma K, Yuen JM, Shah NC, et al. In Vivo, Transcutaneous Glucose Sensing Using Surface-Enhanced Spatially Offset Raman Spectroscopy: Multiple Rats, Improved Hypoglycemic Accuracy, Low Incident Power, and Continuous Monitoring for Greater than 17 Days. *Analytical Chemistry* 2011;83(23):9146-52.
359. Zhang D, Haputhanthri R, Ansar SM, et al. Ultrasensitive detection of malondialdehyde with surface-enhanced Raman spectroscopy. *Analytical and Bioanalytical Chemistry* 2010;398(7):3193-201.
360. Zhang K, Liu Y, Wang Y, et al. Quantitative SERS Detection of Dopamine in Cerebrospinal Fluid by Dual-Recognition-Induced Hot Spot Generation. *Acs Applied Materials & Interfaces* 2018;10(18):15388-94.
361. Wu X, Chen X, Gao F, et al. SERS encoded nanoparticle heterodimers for the ultrasensitive detection of folic acid. *Biosensors & Bioelectronics* 2016;75:55-58.
362. Subaihi A, Almanqur L, Muhamadali H, et al. Rapid, Accurate, and Quantitative Detection of Propranolol in Multiple Human Biofluids via Surface-Enhanced Raman Scattering. *Analytical Chemistry* 2016;88(22):10884-92.
363. Kamińska A, Witkowska E, Kowalska A, et al. Highly efficient SERS-based detection of cerebrospinal fluid neopterin as a diagnostic marker of bacterial infection. *Analytical and Bioanalytical Chemistry* 2016;408(16):4319-27.
364. Zhao L, Blackburn J, Brosseau CL. Quantitative Detection of Uric Acid by Electrochemical-Surface Enhanced Raman Spectroscopy Using a Multi layered Au/Ag Substrate. *Analytical Chemistry* 2015;87(1):441-47.
365. Ma L, Zhang Z, Li X. Non-invasive disease diagnosis using surface-enhanced Raman spectroscopy of urine and saliva. *Applied Spectroscopy Reviews* 2019:1-23.
366. Leal LB, Nogueira MS, Canevari RA, et al. Vibration spectroscopy and body biofluids: Literature review for clinical applications. *Photodiagnosis and Photodynamic Therapy* 2018;24:237-44.
367. Baker MJ, Hussain SR, Lovergne L, et al. Developing and understanding biofluid vibrational spectroscopy: a critical review. *Chemical Society Reviews* 2016;45(7):1803-18.
368. Goodacre R, Graham D, Faulds K. Recent developments in quantitative SERS: Moving towards absolute quantification. *TrAC Trends in Analytical Chemistry* 2018;102:359-68.
369. Shiohara A, Wang Y, Liz-Marzán LM. Recent approaches toward creation of hot spots for SERS detection. *Journal of Photochemistry and Photobiology C: Photochemistry Reviews* 2014;21:2-25.
370. Hidi IJ, Jahn M, Weber K, et al. Lab-on-a-Chip-Surface Enhanced Raman Scattering Combined with the Standard Addition Method: Toward the Quantification of Nitroxoline in Spiked Human Urine Samples. *Analytical Chemistry* 2016;88(18):9173-80.
371. Bell SEJ, Mackle JN, Sirimuthu NMS. Quantitative surface-enhanced Raman spectroscopy of dipicolinic acid—towards rapid anthrax endospore detection. *Analyst* 2005;130(4):545-49.

372. Cheung M, Lee WWY, Cowcher DP, et al. SERS of meso-droplets supported on superhydrophobic wires allows exquisitely sensitive detection of dipicolinic acid, an anthrax biomarker, considerably below the infective dose. *Chemical Communications* 2016;52(64):9925-28.
373. Stewart A, Zheng S, McCourt MR, et al. Controlling Assembly of Mixed Thiol Monolayers on Silver Nanoparticles to Tune Their Surface Properties. *ACS Nano* 2012;6(5):3718-26.
374. Shen W, Lin X, Jiang C, et al. Reliable Quantitative SERS Analysis Facilitated by Core-Shell Nanoparticles with Embedded Internal Standards. *Angewandte Chemie International Edition* 2015;54(25):7308-12.
375. Taylor RW, Lee T-C, Scherman OA, et al. Precise subnanometer plasmonic junctions for SERS within gold nanoparticle assemblies using cucurbit [n] uril "glue". *ACS Nano* 2011;5(5):3878-87.
376. Anderson WJ, Nowinska K, Hutter T, et al. Tuning plasmons layer-by-layer for quantitative colloidal sensing with surface-enhanced Raman spectroscopy. *Nanoscale* 2018;10(15):7138-46.
377. Christodoulidis G, Vittorio TJ, Fudim M, et al. Inflammation in coronary artery disease. *Cardiology in review* 2014;22(6):279-88.
378. Leung R, Proitsi P, Simmons A, et al. Inflammatory proteins in plasma are associated with severity of Alzheimer's disease. *PLoS One* 2013;8(6):e64971.
379. Hausen A, Fuchs D, König K, et al. Determination of neopterin in human urine by reversed-phase high-performance liquid chromatography. *Journal of Chromatography B: Biomedical Sciences and Applications* 1982;227(1):61-70.
380. Kamińska A, Szyborski T, Jaroch T, et al. Gold-capped silicon for ultrasensitive SERS-biosensing: Towards human biofluids analysis. *Materials Science and Engineering: C* 2018;84:208-17.
381. Kaminska A, Kowalska AA, Snigurenko D, et al. ZnO oxide films for ultrasensitive, rapid, and label-free detection of neopterin by surface-enhanced Raman spectroscopy. *Analyst* 2015;140(15):5090-8.
382. Xiang Y, Yang H, Guo X, et al. Surface enhanced Raman detection of the colon cancer biomarker cytidine by using magnetized nanoparticles of the type Fe₃O₄/Au/Ag. *Microchimica Acta* 2018;185(3):195.
383. Yang H, Zhao C, Li R, et al. Noninvasive and prospective diagnosis of coronary heart disease with urine using surface-enhanced Raman spectroscopy. *Analyst* 2018;143(10):2235-42.
384. Zou Y, Huang M, Wang K, et al. Urine surface-enhanced Raman spectroscopy for non-invasive diabetic detection based on a portable Raman spectrometer. *Laser Physics Letters* 2016;13(6):065604.
385. Meng J, Tang X, Zhou B, et al. Designing of ordered two-dimensional gold nanoparticles film for cocaine detection in human urine using surface-enhanced Raman spectroscopy. *Talanta* 2017;164:693-99.
386. Han Z, Liu H, Meng J, et al. Portable Kit for Identification and Detection of Drugs in Human Urine Using Surface-Enhanced Raman Spectroscopy. *Analytical Chemistry* 2015;87(18):9500-06.

List of References

387. Alharbi O, Xu Y, Goodacre R. Detection and quantification of the opioid tramadol in urine using surface enhanced Raman scattering. *Analyst* 2015;140(17):5965-70.
388. Alula MT, Yang J. Photochemical decoration of magnetic composites with silver nanostructures for determination of creatinine in urine by surface-enhanced Raman spectroscopy. *Talanta* 2014;130:55-62.
389. Magnusson B. The fitness for purpose of analytical methods: a laboratory guide to method validation and related topics (2014): Eurachem, 2014.
390. Bell SEJ, Charron G, Cortés E, et al. Towards Reliable and Quantitative Surface-Enhanced Raman Scattering (SERS): From Key Parameters to Good Analytical Practice. *Angewandte Chemie International Edition* 2020;59(14):5454-62.
391. Mabbott S, Xu Y, Goodacre R. Objective assessment of SERS thin films: comparison of silver on copper via galvanic displacement with commercially available fabricated substrates. *Analytical Methods* 2017;9(33):4783-89.
392. Villa JEL, Poppi RJ. A portable SERS method for the determination of uric acid using a paper-based substrate and multivariate curve resolution. *Analyst* 2016;141(6):1966-72.
393. Trevisan J, Angelov PP, Scott AD, et al. IRootLab: a free and open-source MATLAB toolbox for vibrational biospectroscopy data analysis. *Bioinformatics* 2013;29(8):1095-97.
394. Prochazka M. Surface-Enhanced Raman Spectroscopy: Bioanalytical, Biomolecular and Medical Applications *Surface-Enhanced Raman Spectroscopy*. 1 ed: Springer International Publishing; 2016 p61-91.
395. Nicol T, Lefeuvre C, Serri O, et al. Assessment of SARS-CoV-2 serological tests for the diagnosis of COVID-19 through the evaluation of three immunoassays: Two automated immunoassays (Euroimmun and Abbott) and one rapid lateral flow immunoassay (NG Biotech). *Journal of Clinical Virology* 2020;129:104511.
396. Kost GJ. Guidelines for point-of-care testing. Improving patient outcomes. *American journal of clinical pathology* 1995;104(4 Suppl 1):S111-27.
397. Vashist SK, Lupton PB, Yeo LY, et al. Emerging technologies for next-generation point-of-care testing. *Trends in biotechnology* 2015;33(11):692-705.
398. St John A, Price CP. Existing and emerging technologies for point-of-care testing. *The Clinical Biochemist Reviews* 2014;35(3):155.
399. Markets Ma. *Point-of-Care Diagnostics Market- Global Forecast to 2021*. <https://www.marketsandmarkets.com/PressReleases/point-of-care-diagnostic.asp> (accessed 21.11.2017).
400. Abe K, Kotera K, Suzuki K, et al. Inkjet-printed paperfluidic immuno-chemical sensing device. *Analytical and Bioanalytical Chemistry* 2010;398(2):885-93.
401. Li C-z, Vandenberg K, Prabhulkar S, et al. Paper based point-of-care testing disc for multiplex whole cell bacteria analysis. *Biosensors and Bioelectronics* 2011;26(11):4342-48.
402. Bahadır EB, Sezgintürk MK. Lateral flow assays: Principles, designs and labels. *TrAC Trends in Analytical Chemistry* 2016;82:286-306.
403. Posthuma-Trumpie GA, Korf J, van Amerongen A. Lateral flow (immuno) assay: its strengths, weaknesses, opportunities and threats. A literature survey. *Analytical and Bioanalytical Chemistry* 2009;393(2):569-82.

404. Hwang J, Lee S, Choo J. Application of a SERS-based lateral flow immunoassay strip for the rapid and sensitive detection of staphylococcal enterotoxin B. *Nanoscale* 2016;8(22):11418-25.
405. Blanco-Covián L, Montes-García V, Girard A, et al. Au@ Ag SERRS tags coupled to a lateral flow immunoassay for the sensitive detection of pneumolysin. *Nanoscale* 2017;9(5):2051-58.
406. Choi S, Hwang J, Lee S, et al. Quantitative analysis of thyroid-stimulating hormone (TSH) using SERS-based lateral flow immunoassay. *Sensors and Actuators B: Chemical* 2017;240:358-64.
407. Wang R, Kim K, Choi N, et al. Highly sensitive detection of high-risk bacterial pathogens using SERS-based lateral flow assay strips. *Sensors and Actuators B: Chemical* 2018;270:72-79.
408. Rong Z, Xiao R, Xing S, et al. SERS-based lateral flow assay for quantitative detection of C-reactive protein as an early bio-indicator of a radiation-induced inflammatory response in nonhuman primates. *Analyst* 2018;143(9):2115-21.
409. Zhang D, Huang L, Liu B, et al. Quantitative and ultrasensitive detection of multiplex cardiac biomarkers in lateral flow assay with core-shell SERS nanotags. *Biosensors and Bioelectronics* 2018;106:204-11.
410. Bai T, Wang M, Cao M, et al. Functionalized Au@ Ag-Au nanoparticles as an optical and SERS dual probe for lateral flow sensing. *Analytical and Bioanalytical Chemistry* 2018;410(9):2291-303.
411. Fu X, Chu Y, Zhao K, et al. Ultrasensitive detection of the β -adrenergic agonist brombuterol by a SERS-based lateral flow immunochromatographic assay using flower-like gold-silver core-shell nanoparticles. *Microchimica Acta* 2017;184(6):1711-19.
412. Shi Q, Huang J, Sun Y, et al. A SERS-based multiple immuno-nanoprobe for ultrasensitive detection of neomycin and quinolone antibiotics via a lateral flow assay. *Microchimica Acta* 2018;185(2):84.
413. Wang X, Choi N, Cheng Z, et al. Simultaneous detection of dual nucleic acids using a SERS-based lateral flow assay biosensor. *Analytical Chemistry* 2017;89(2):1163-69.
414. Liu H-b, Du X-j, Zang Y-X, et al. SERS-based lateral flow strip biosensor for simultaneous detection of listeria monocytogenes and salmonella enterica serotype enteritidis. *Journal of agricultural and food chemistry* 2017;65(47):10290-99.
415. Sánchez-Purrà M, Carré-Camps M, de Puig H, et al. Surface-enhanced raman spectroscopy-based sandwich immunoassays for multiplexed detection of zika and dengue viral biomarkers. *ACS infectious diseases* 2017;3(10):767-76.
416. Khlebtsov BN, Bratashov DN, Byzova NA, et al. SERS-based lateral flow immunoassay of troponin I by using gap-enhanced Raman tags. *Nano Research* 2019;12(2):413-20.
417. Gao X, Zheng P, Kasani S, et al. based surface-enhanced Raman scattering lateral flow strip for detection of neuron-specific enolase in blood plasma. *Analytical Chemistry* 2017;89(18):10104-10.
418. Fu X, Cheng Z, Yu J, et al. A SERS-based lateral flow assay biosensor for highly sensitive detection of HIV-1 DNA. *Biosensors & Bioelectronics* 2016;78:530-37.

List of References

419. Zou L, Ruan F, Huang M, et al. SARS-CoV-2 viral load in upper respiratory specimens of infected patients. *New England Journal of Medicine* 2020;382(12):1177-79.
420. Diao B, Wen K, Chen J, et al. Diagnosis of acute respiratory syndrome coronavirus 2 infection by detection of nucleocapsid protein. *medRxiv* 2020.
421. Lisboa Bastos M, Tavaziva G, Abidi SK, et al. Diagnostic accuracy of serological tests for covid-19: systematic review and meta-analysis. *BMJ* 2020;370:m2516.
422. Krammer F, Simon V. Serology assays to manage COVID-19. *Science* 2020;368(6495):1060.
423. La Marca A, Capuzzo M, Paglia T, et al. Testing for SARS-CoV-2 (COVID-19): a systematic review and clinical guide to molecular and serological in-vitro diagnostic assays. *Reproductive Biomedicine Online* 2020;41(3):483-99.
424. Li Z, Yi Y, Luo X, et al. Development and clinical application of a rapid IgM - IgG combined antibody test for SARS - CoV - 2 infection diagnosis. *Journal of medical virology* 2020.
425. Cassaniti I, Novazzi F, Giardina F, et al. Performance of VivaDiag COVID - 19 IgM/IgG Rapid Test is inadequate for diagnosis of COVID - 19 in acute patients referring to emergency room department. *Journal of medical virology* 2020.
426. Lee Y-L, Liao C-H, Liu P-Y, et al. Dynamics of anti-SARS-Cov-2 IgM and IgG antibodies among COVID-19 patients. *The Journal of Infection* 2020.
427. Shen B, Zheng Y, Zhang X, et al. Clinical evaluation of a rapid colloidal gold immunochromatography assay for SARS-Cov-2 IgM/IgG. *American journal of translational research* 2020;12(4):1348.
428. Döhla M, Boesecke C, Schulte B, et al. Rapid point-of-care testing for SARS-CoV-2 in a community screening setting shows low sensitivity. *Public health* 2020.
429. Hoffman T, Nissen K, Krambrich J, et al. Evaluation of a COVID-19 IgM and IgG rapid test; an efficient tool for assessment of past exposure to SARS-CoV-2. *Infection Ecology & Epidemiology* 2020;10(1):1754538.
430. Imai K, Tabata S, Ikeda M, et al. Clinical evaluation of an immunochromatographic IgM/IgG antibody assay and chest computed tomography for the diagnosis of COVID-19. *Journal of Clinical Virology* 2020:104393.
431. Pan Y, Li X, Yang G, et al. Serological immunochromatographic approach in diagnosis with SARS-CoV-2 infected COVID-19 patients. *Journal of Infection* 2020.
432. Spicuzza L, Montineri A, Manuele R, et al. Reliability and usefulness of a rapid IgM - IgG antibody test for the diagnosis of SARS-CoV-2 infection: A preliminary report. *The Journal of Infection* 2020.
433. Gao Y, Yuan Y, Li TT, et al. Evaluation the auxiliary diagnosis value of antibodies assays for detection of novel coronavirus (SARS-Cov-2) causing an outbreak of pneumonia (COVID-19). *medRxiv* 2020.
434. Demey B, Daher N, François C, et al. Dynamic profile for the detection of anti-SARS-CoV-2 antibodies using four immunochromatographic assays. *Journal of Infection* 2020.
435. Isabel M, Damien G, Benoit K, et al. Evaluation of two automated and three rapid lateral flow immunoassays for the detection of anti-SARS-CoV-2 antibodies. *Journal of Clinical Virology* 2020:104413.

436. Sheridan C. Fast, portable tests come online to curb coronavirus pandemic. *Nature Biotechnology* 2020;38:515-18.
437. Mallapaty S. Will antibody tests for the coronavirus really change everything? *Nature* 2020;580:571-72.
438. Guo T, Fan Y, Chen M, et al. Cardiovascular implications of fatal outcomes of patients with coronavirus disease 2019 (COVID-19). *JAMA cardiology* 2020.
439. Shi S, Qin M, Shen B, et al. Association of cardiac injury with mortality in hospitalized patients with COVID-19 in Wuhan, China. *JAMA cardiology* 2020.
440. Li X, Guan B, Su T, et al. Impact of cardiovascular disease and cardiac injury on in-hospital mortality in patients with COVID-19: a systematic review and meta-analysis. *Heart* 2020.
441. Yao Y, Cao J, Wang Q, et al. D-dimer as a biomarker for disease severity and mortality in COVID-19 patients: a case control study. *Journal of intensive care* 2020;8(1):1-11.
442. Huang C, Wang Y, Li X, et al. Clinical features of patients infected with 2019 novel coronavirus in Wuhan, China. *The Lancet* 2020;395(10223):497-506.
443. Cai Q, Huang D, Yu H, et al. COVID-19: abnormal liver function tests. *Journal of hepatology* 2020.
444. Tang N, Li D, Wang X, et al. Abnormal coagulation parameters are associated with poor prognosis in patients with novel coronavirus pneumonia. *Journal of thrombosis and haemostasis* 2020;18(4):844-47.
445. Zhou J, Lee S, Wang X, et al. Development of a predictive risk model for severe COVID-19 disease using population-based administrative data. *medRxiv* 2020:2020.10.21.20217380.
446. Liang W, Liang H, Ou L, et al. Development and validation of a clinical risk score to predict the occurrence of critical illness in hospitalized patients with COVID-19. *JAMA internal medicine* 2020.
447. Knight SR, Ho A, Pius R, et al. Risk stratification of patients admitted to hospital with covid-19 using the ISARIC WHO Clinical Characterisation Protocol: development and validation of the 4C Mortality Score. *BMJ* 2020;370.
448. Urwin SG, Lendrem BC, Suklan J, et al. FebriDx point-of-care test in patients with suspected COVID-19: a pooled diagnostic accuracy study. *medRxiv* 2020:2020.10.15.20213108.
449. Moore TJ, Moody AS, Payne TD, et al. In Vitro and In Vivo SERS Biosensing for Disease Diagnosis. *Biosensors* 2018;8(2):46.
450. Moody AS, Sharma B. Multi-metal, multi-wavelength surface-enhanced raman spectroscopy detection of neurotransmitters. *ACS chemical neuroscience* 2018;9(6):1380-87.
451. Kong KV, Lam Z, Lau WKO, et al. A Transition Metal Carbonyl Probe for Use in a Highly Specific and Sensitive SERS-Based Assay for Glucose. *Journal of the American Chemical Society* 2013;135(48):18028-31.
452. Guo J, Rong Z, Li Y, et al. Diagnosis of chronic kidney diseases based on surface-enhanced Raman spectroscopy and multivariate analysis. *Laser Physics* 2018;28(7):075603.
453. Li C, Liu Y, Zhou X, et al. A paper-based SERS assay for sensitive duplex cytokine detection towards the atherosclerosis-associated disease diagnosis. *Journal of Materials Chemistry B* 2020.

List of References

454. Carron K, Cox R. Qualitative analysis and the answer box: a perspective on portable Raman spectroscopy: ACS Publications, 2010.
455. Gnyba M, Smulko J, Kwiatkowski A, et al. Portable Raman spectrometer-design rules and applications. *Bulletin of the Polish Academy of Sciences: Technical Sciences* 2011;59(3):325-29.
456. Hajjou M, Qin Y, Bradby S, et al. Assessment of the performance of a handheld Raman device for potential use as a screening tool in evaluating medicines quality. *Journal of pharmaceutical and biomedical analysis* 2013;74:47-55.
457. Zeng F, Mou T, Zhang C, et al. Paper-based SERS analysis with smartphones as Raman spectral analyzers. *Analyst* 2019;144(1):137-42.
458. Restaino SM, White IM. A critical review of flexible and porous SERS sensors for analytical chemistry at the point-of-sample. *Analytica Chimica Acta* 2019;1060:17-29.
459. Wang C, Yu C. Analytical characterization using surface-enhanced Raman scattering (SERS) and microfluidic sampling. *Nanotechnology* 2015;26(9):092001.
460. Zhou Q, Kim T. Review of microfluidic approaches for surface-enhanced Raman scattering. *Sensors and Actuators B: Chemical* 2016;227:504-14.
461. Freeman RG, Grabar KC, Allison KJ, et al. Self-assembled metal colloid monolayers: an approach to SERS substrates. *Science* 1995;267(5204):1629-32.
462. Haddada MB, Blanchard J, Casale S, et al. Optimizing the immobilization of gold nanoparticles on functionalized silicon surfaces: amine-vs thiol-terminated silane. *Gold Bulletin* 2013;46(4):335-41.
463. Nery EW, Kubota LT. Sensing approaches on paper-based devices: a review. *Anal Bioanal Chem* 2013;405(24):7573-95.
464. Lee CH, Tian L, Singamaneni S. Paper-based SERS swab for rapid trace detection on real-world surfaces. *Acs Applied Materials & Interfaces* 2010;2(12):3429-35.
465. Li Y, Zhang K, Zhao J, et al. A three-dimensional silver nanoparticles decorated plasmonic paper strip for SERS detection of low-abundance molecules. *Talanta* 2016;147:493-500.
466. Liao W-J, Roy PK, Chattopadhyay S. An ink-jet printed, surface enhanced Raman scattering paper for food screening. *RSC advances* 2014;4(76):40487-93.
467. Lin S, Lin X, Lou X-T, et al. Rapid fabrication of self-assembled interfacial film decorated filter paper as an excellent surface-enhanced Raman scattering substrate. *Analytical Methods* 2014;6(24):9547-53.
468. Li B, Zhang W, Chen L, et al. A fast and low - cost spray method for prototyping and depositing surface - enhanced Raman scattering arrays on microfluidic paper based device. *Electrophoresis* 2013;34(15):2162-68.
469. Zhang W, Li B, Chen L, et al. Brushing, a simple way to fabricate SERS active paper substrates. *Analytical Methods* 2014;6(7):2066-71.
470. Zhang K, Ji J, Fang X, et al. Carbon nanotube/gold nanoparticle composite-coated membrane as a facile plasmon-enhanced interface for sensitive SERS sensing. *Analyst* 2015;140(1):134-39.

471. Lee CH, Hankus ME, Tian L, et al. Highly sensitive surface enhanced Raman scattering substrates based on filter paper loaded with plasmonic nanostructures. *Analytical Chemistry* 2011;83(23):8953-58.
472. Tran V, Walkenfort B, König M, et al. Rapid, Quantitative, and Ultrasensitive Point-of-Care Testing: A Portable SERS Reader for Lateral Flow Assays in Clinical Chemistry. *Angewandte Chemie International Edition* 2019;58(2):442-46.
473. Yu WW, White IM. Inkjet Printed Surface Enhanced Raman Spectroscopy Array on Cellulose Paper. *Analytical Chemistry* 2010;82(23):9626-30.
474. Zhu Y, Li M, Yu D, et al. A novel paper rag as 'D-SERS' substrate for detection of pesticide residues at various peels. *Talanta* 2014;128:117-24.
475. Sallum LF, Soares FLF, Ardila JA, et al. Optimization of SERS scattering by Ag-NPs-coated filter paper for quantification of nicotinamide in a cosmetic formulation. *Talanta* 2014;118:353-58.
476. Qu L-L, Song Q-X, Li Y-T, et al. Fabrication of bimetallic microfluidic surface-enhanced Raman scattering sensors on paper by screen printing. *Analytica Chimica Acta* 2013;792:86-92.
477. Muniz-Miranda M, Neto N, Sbrana G. Surface studies by SERS and SEM techniques on filters coated with colloidal silver. *Journal of Molecular Structure* 1997;410:205-08.
478. Kim W, Kim Y-H, Park H-K, et al. Facile fabrication of a silver nanoparticle immersed, surface-enhanced Raman scattering imposed paper platform through successive ionic layer absorption and reaction for on-site bioassays. *Acs Applied Materials & Interfaces* 2015;7(50):27910-17.
479. Joshi P, Santhanam V. Paper-based SERS active substrates on demand. *RSC advances* 2016;6(72):68545-52.
480. Fierro-Mercado PM, Hernández-Rivera SP. Highly sensitive filter paper substrate for SERS trace explosives detection. *International Journal of Spectroscopy* 2012;2012.
481. Wang J, Yang L, Liu B, et al. Inkjet-printed silver nanoparticle paper detects airborne species from crystalline explosives and their ultratrace residues in open environment. *Analytical Chemistry* 2014;86(7):3338-45.
482. Bolz A, Panne U, Rurack K, et al. Glass fibre paper-based test strips for sensitive SERS sensing. *Analytical Methods* 2016;8(6):1313-18.
483. Jang W, Byun H, Kim J-H. Rapid preparation of paper-based plasmonic platforms for SERS applications. *Materials Chemistry and Physics* 2020;240:122124.
484. Chen Y, Cheng H, Tram K, et al. A paper-based surface-enhanced resonance Raman spectroscopic (SERRS) immunoassay using magnetic separation and enzyme-catalyzed reaction. *Analyst* 2013;138(9):2624-31.
485. Chamuah N, Hazarika A, Hatiboruah D, et al. SERS on paper: an extremely low cost technique to measure Raman signal. *Journal of Physics D: Applied Physics* 2017;50(48):485601.
486. Polavarapu L, Porta AL, Novikov SM, et al. Pen - on - paper approach toward the design of universal surface enhanced Raman scattering substrates. *Small* 2014;10(15):3065-71.
487. Tian L, Tadepalli S, Farrell ME, et al. Multiplexed charge-selective surface enhanced Raman scattering based on plasmonic calligraphy. *Journal of Materials Chemistry C* 2014;2(27):5438-46.

List of References

488. Qu L-L, Li D-W, Xue J-Q, et al. Batch fabrication of disposable screen printed SERS arrays. *Lab on a Chip* 2012;12(5):876-81.
489. Kim W-S, Shin J-H, Park H-K, et al. A low-cost, monometallic, surface-enhanced Raman scattering-functionalized paper platform for spot-on bioassays. *Sensors and Actuators B: Chemical* 2016;222:1112-18.
490. Lee M, Oh K, Choi H-K, et al. Subnanomolar Sensitivity of Filter Paper-Based SERS Sensor for Pesticide Detection by Hydrophobicity Change of Paper Surface. *ACS Sensors* 2018;3(1):151-59.
491. Wu D, Fang Y. The adsorption behavior of p-hydroxybenzoic acid on a silver-coated filter paper by surface enhanced Raman scattering. *Journal of Colloid and Interface Science* 2003;265(2):234-38.
492. Wu M, Li P, Zhu Q, et al. Functional paper-based SERS substrate for rapid and sensitive detection of Sudan dyes in herbal medicine. *Spectrochimica Acta Part A: Molecular and Biomolecular Spectroscopy* 2018;196:110-16.
493. Weng G, Yang Y, Zhao J, et al. Preparation and SERS performance of Au NP/paper strips based on inkjet printing and seed mediated growth: The effect of silver ions. *Solid State Communications* 2018;272:67-73.
494. Hoppmann EP, Yu WW, White IM. Highly sensitive and flexible inkjet printed SERS sensors on paper. *Methods* 2013;63(3):219-24.
495. Zhang K, Qing J, Gao H, et al. Coupling shell-isolated nanoparticle enhanced Raman spectroscopy with paper chromatography for multi-components on-site analysis. *Talanta* 2017;162:52-56.
496. Weatherston JD, Seguban RKO, Hunt D, et al. Low-Cost and Simple Fabrication of Nanoplasmonic Paper for Coupled Chromatography Separation and Surface Enhanced Raman Detection. *ACS Sensors* 2018;3(4):852-57.
497. Berger AG, Restaino SM, White IM. Vertical-flow paper SERS system for therapeutic drug monitoring of flucytosine in serum. *Analytica Chimica Acta* 2017;949:59-66.
498. Shende C, Brouillette C, Farquharson S. Detection of codeine and fentanyl in saliva, blood plasma and whole blood in 5-minutes using a SERS flow-separation strip. *Analyst* 2019;144(18):5449-54.
499. Li D, Lv DY, Zhu QX, et al. Chromatographic separation and detection of contaminants from whole milk powder using a chitosan-modified silver nanoparticles surface-enhanced Raman scattering device. *Food chemistry* 2017;224:382-89.
500. Villa JEL, Santos DPd, Poppi RJ. Fabrication of gold nanoparticle-coated paper and its use as a sensitive substrate for quantitative SERS analysis. *Microchimica Acta* 2016;183(10):2745-52.
501. She P, Chu Y, Liu C, et al. A competitive immunoassay for ultrasensitive detection of Hg²⁺ in water, human serum and urine samples using immunochromatographic test based on surface-enhanced Raman scattering. *Analytica Chimica Acta* 2016;906:139-47.
502. Yu WW, Hoppmann EP. Functionalized paper SERS (P-SERS) substrates for selective targeting of analytes in complex samples. In: Cullum BM, McLamore ES (eds.) *Smart Biomedical and Physiological Sensor Technology Xii*; 2015.

503. Xie Y, Chang H, Zhao K, et al. A novel immunochromatographic assay (ICA) based on surface-enhanced Raman scattering for the sensitive and quantitative determination of clenbuterol. *Analytical Methods* 2015;7(2):513-20.
504. Li M, Yang H, Li S, et al. An ultrasensitive competitive immunochromatographic assay (ICA) based on surface-enhanced Raman scattering (SERS) for direct detection of 3-amino-5-methylmorpholino-2-oxazolidinone (AMOZ) in tissue and urine samples. *Sensors and Actuators B: Chemical* 2015;211:551-58.
505. Il-Hoon C, Das M, Bhandari P, et al. High performance immunochromatographic assay combined with surface enhanced Raman spectroscopy. *Sensors and Actuators B: Chemical* 2015;213:209-14.
506. Hughes J, Izake EL, Lott WB, et al. Ultra sensitive label free surface enhanced Raman spectroscopy method for the detection of biomolecules. *Talanta* 2014;130:20-25.
507. Lim WY, Goh C-H, Thevarajah TM, et al. Using SERS-based microfluidic paper-based device (μ PAD) for calibration-free quantitative measurement of AMI cardiac biomarkers. *Biosensors and Bioelectronics* 2020;147:111792.
508. Fukushima T, Shiota T. Pterins in human urine. *Journal of Biological Chemistry* 1972;247(14):4549-56.
509. Sakurai A, GOTO M. Neopterin: isolation from human urine. *The Journal of Biochemistry* 1967;61(1):142-45.
510. Kealey DHPJ. *Analytical Chemistry*. Oxford: BIOS Scientific Publishers Ltd; 2002.
511. Bouatra S, Aziat F, Mandal R, et al. The human urine metabolome. *PLoS One* 2013;8(9):e73076.
512. Buettner D, Skemp S. Blue zones: Lessons from the world's longest lived. *American journal of lifestyle medicine* 2016;10(5):318-21.
513. Poulain M, Herm A, Pes G. The Blue Zones: areas of exceptional longevity around the world. *Vienna Yearbook of Population Research* 2013:87-108.
514. Shaw AC, Goldstein DR, Montgomery RR. Age-dependent dysregulation of innate immunity. *Nature Reviews Immunology* 2013;13(12):875-87.
515. Akiyama H, Barger S, Barnum S, et al. Inflammation and Alzheimer's disease. *Neurobiol Aging* 2000;21.
516. Strindhall J, Nilsson B-O, Löfgren S, et al. No Immune Risk Profile among individuals who reach 100 years of age: findings from the Swedish NONA immune longitudinal study. *Experimental gerontology* 2007;42(8):753-61.
517. Glyde H, Cameron S, Dillon H, et al. The effects of hearing impairment and aging on spatial processing. *Ear and hearing* 2013;34(1):15-28.
518. Bourien J, Tang Y, Batrel C, et al. Contribution of auditory nerve fibers to compound action potential of the auditory nerve. *Journal of neurophysiology* 2014;112(5):1025-39.
519. Kujawa SG, Liberman MC. Synaptopathy in the noise-exposed and aging cochlea: Primary neural degeneration in acquired sensorineural hearing loss. *Hearing Research* 2015;330:191-99.

List of References

520. Liberman MC. Noise-induced and age-related hearing loss: new perspectives and potential therapies. *F1000Research* 2017;6.
521. Lobarinas E, Salvi R, Ding D. Insensitivity of the audiogram to carboplatin induced inner hair cell loss in chinchillas. *Hearing Research* 2013;302:113-20.
522. Furman AC, Kujawa SG, Liberman MC. Noise-induced cochlear neuropathy is selective for fibers with low spontaneous rates. *Journal of neurophysiology* 2013.
523. Schmiedt R, Mills J, Boettcher F. Age-related loss of activity of auditory-nerve fibers. *Journal of neurophysiology* 1996;76(4):2799-803.
524. Alvord LS. Cochlear dysfunction in "normal-hearing" patients with history of noise exposure. *Ear and hearing* 1983;4(5):247-50.
525. Dubno JR, Dirks DD, Morgan DE. Effects of age and mild hearing loss on speech recognition in noise. *The Journal of the Acoustical Society of America* 1984;76(1):87-96.
526. Rajan R, Cainer KE. Ageing without hearing loss or cognitive impairment causes a decrease in speech intelligibility only in informational maskers. *Neuroscience* 2008;154(2):784-95.
527. Viana LM, O'Malley JT, Burgess BJ, et al. Cochlear neuropathy in human presbycusis: Confocal analysis of hidden hearing loss in post-mortem tissue. *Hearing Research* 2015;327:78-88.
528. Wu P, Liberman L, Bennett K, et al. Primary neural degeneration in the human cochlea: evidence for hidden hearing loss in the aging ear. *Neuroscience* 2019;407:8-20.
529. Garcia-Valles R, Gomez-Cabrera MC, Rodriguez-Mañas L, et al. Life-long spontaneous exercise does not prolong lifespan but improves health span in mice. *Longevity & healthspan* 2013;2(1):14.
530. Calder PC, Ahluwalia N, Brouns F, et al. Dietary factors and low-grade inflammation in relation to overweight and obesity. *British Journal of Nutrition* 2011;106(S3):S1-S78.
531. Schwingshackl L, Hoffmann G. Mediterranean dietary pattern, inflammation and endothelial function: a systematic review and meta-analysis of intervention trials. *Nutrition, Metabolism and Cardiovascular Diseases* 2014;24(9):929-39.
532. Chrysohoou C, Panagiotakos DB, Pitsavos C, et al. Adherence to the Mediterranean diet attenuates inflammation and coagulation process in healthy adults: The ATTICA Study. *Journal of the American College of Cardiology* 2004;44(1):152-58.
533. Gleeson M, Bishop NC, Stensel DJ, et al. The anti-inflammatory effects of exercise: mechanisms and implications for the prevention and treatment of disease. *Nature Reviews Immunology* 2011;11(9):607-15.
534. Woods J, Ceddia M, Wolters B, et al. Effects of 6 months of moderate aerobic exercise training on immune function in the elderly. *Mechanisms of ageing and development* 1999;109(1):1-19.
535. Woods J, Ceddia M, Zack M, et al. Exercise training increases the naïve to memory T cell ratio in old mice. *Brain Behav Immun* 2003;17(5):384-92.
536. Kohut M, Lee W, Martin A, et al. The exercise-induced enhancement of influenza immunity is mediated in part by improvements in psychosocial factors in older adults. *Brain Behav Immun* 2005;19(4):357-66.

537. Leveille SG, Gray S, LaCroix AZ, et al. Physical inactivity and smoking increase risk for serious infections in older women. *Journal of the American Geriatrics Society* 2000;48(12):1582-88.
538. Lynch HE, Goldberg GL, Chidgey A, et al. Thymic involution and immune reconstitution. *Trends in Immunology* 2009;30(7):366-73.
539. Wallace DL, Bérard M, Soares MV, et al. Prolonged exposure of naïve CD8+ T cells to interleukin - 7 or interleukin - 15 stimulates proliferation without differentiation or loss of telomere length. *Immunology* 2006;119(2):243-53.
540. Barbour KA, Blumenthal JA. Exercise training and depression in older adults. *Neurobiology of aging* 2005;26(1):119-23.
541. Kohut ML, Senchina DS. Reversing age-associated immunosenescence via exercise. *Exerc Immunol Rev* 2004;10(6):41.
542. Kohut M, McCann D, Russell D, et al. Aerobic exercise, but not flexibility/resistance exercise, reduces serum IL-18, CRP, and IL-6 independent of β -blockers, BMI, and psychosocial factors in older adults. *Brain Behav Immun* 2006;20(3):201-09.
543. Simpson RJ, Lowder TW, Spielmann G, et al. Exercise and the aging immune system. *Ageing research reviews* 2012;11(3):404-20.
544. Brand Y, Setz C, Levano S, et al. Simvastatin protects auditory hair cells from gentamicin-induced toxicity and activates Akt signaling in vitro. *BMC neuroscience* 2011;12(1):1-10.
545. Syka J, Ouda L, Nachtigal P, et al. Atorvastatin slows down the deterioration of inner ear function with age in mice. *Neuroscience Letters* 2007;411(2):112-16.
546. Park J, Kim S, Park K, et al. Pravastatin attenuates noise-induced cochlear injury in mice. *Neuroscience* 2012;208:123-32.
547. Richter C-P, Young H, Richter SV, et al. Fluvastatin protects cochleae from damage by high-level noise. *Scientific Reports* 2018;8(1):1-12.
548. Fernandez K, Spielbauer KK, Rusheen A, et al. Lovastatin protects against cisplatin-induced hearing loss in mice. *Hearing Research* 2020;389:107905.
549. Warner HR, Ingram D, Miller RA, et al. Program for testing biological interventions to promote healthy aging. *Mechanisms of ageing and development* 2000;115(3):199-207.
550. Strong R, Miller RA, Astle CM, et al. Nordihydroguaiaretic acid and aspirin increase lifespan of genetically heterogeneous male mice. *Ageing cell* 2008;7(5):641-50.
551. Pearson JD, Morrell CH, Gordon - Salant S, et al. Gender differences in a longitudinal study of age - associated hearing loss. *The Journal of the Acoustical Society of America* 1995;97(2):1196-205.
552. Helzner E, Cauley J, Pratt S, et al. Race and sex differences in age-related hearing loss: The health, aging and body composition study. *Noise and Health* 2006;8(30).
553. Stenberg A, Wang H, Sahlin L, et al. Estrogen receptors α and β in the inner ear of the 'Turner mouse' and an estrogen receptor β knockout mouse. *Hearing Research* 2002;166(1-2):1-8.
554. Hultcrantz M, Simonoska R, Stenberg A. Estrogen and hearing: a summary of recent investigations. *Acta Oto-Laryngologica* 2006;126(1):10-14.

List of References

555. Yan J, Greer JM, Hull R, et al. The effect of ageing on human lymphocyte subsets: comparison of males and females. *Immunity & Ageing* 2010;7(1):4.
556. Park T, Lee S, Seong GH, et al. Highly sensitive signal detection of duplex dye-labelled DNA oligonucleotides in a PDMS microfluidic chip: confocal surface-enhanced Raman spectroscopic study. *Lab on a Chip* 2005;5(4):437-42.
557. Chou I-H, Benford M, Beier HT, et al. Nanofluidic biosensing for β -amyloid detection using surface enhanced Raman spectroscopy. *Nano letters* 2008;8(6):1729-35.
558. Yang X, Shi C, Wheeler D, et al. High-sensitivity molecular sensing using hollow-core photonic crystal fiber and surface-enhanced Raman scattering. *JOSA A* 2010;27(5):977-84.
559. Hoppmann EP, Wei WY, White IM. Inkjet-printed fluidic paper devices for chemical and biological analytics using surface enhanced Raman spectroscopy. *IEEE Journal of Selected Topics in Quantum Electronics* 2014;20(3):195-204.
560. Eshkeiti A, Narakathu BB, Reddy A, et al. Detection of heavy metal compounds using a novel inkjet printed surface enhanced Raman spectroscopy (SERS) substrate. *Sensors and Actuators B: Chemical* 2012;171:705-11.
561. Lee H-H, Chou K-S, Huang K-C. Inkjet printing of nanosized silver colloids. *Nanotechnology* 2005;16(10):2436.
562. Abbas A, Brimer A, Slocik JM, et al. Multifunctional analytical platform on a paper strip: separation, preconcentration, and subattomolar detection. *Analytical Chemistry* 2013;85(8):3977-83.
563. Ngo YH, Then WL, Shen W, et al. Gold nanoparticles paper as a SERS bio-diagnostic platform. *Journal of Colloid and Interface Science* 2013;409:59-65.
564. Cheng Y, Wang M, Borghs G, et al. Gold nanoparticle dimers for plasmon sensing. *Langmuir* 2011;27(12):7884-91.
565. Busson MP, Rolly B, Stout B, et al. Optical and topological characterization of gold nanoparticle dimers linked by a single DNA double strand. *Nano letters* 2011;11(11):5060-65.
566. Indrasekara ASD, Paladini BJ, Naczynski DJ, et al. Dimeric Gold Nanoparticle Assemblies as Tags for SERS - Based Cancer Detection. *Advanced healthcare materials* 2013;2(10):1370-76.
567. Locke A, Belsare S, Deutz NE, et al. Aptamer-switching optical bioassay for citrulline detection at the point-of-care. *Journal of Biomedical Optics* 2019;24(12):127002.
568. Locke A, Deutz N, Coté G. *Development of a paper-based vertical flow SERS assay for citrulline detection using aptamer-conjugated gold nanoparticles*: SPIE; 2018.
569. Hu S-W, Qiao S, Pan J-B, et al. A paper-based SERS test strip for quantitative detection of Mucin-1 in whole blood. *Talanta* 2018;179:9-14.
570. Marks H, Mabbott S, Jackson GW, et al. SERS active colloidal nanoparticles for the detection of small blood biomarkers using aptamers. In: Parak WJ, Osinski M, Liang XJ (eds.) *Colloidal Nanoparticles for Biomedical Applications X*; 2015.
571. Tombelli S, Minunni M, Mascini M. Aptamers-based assays for diagnostics, environmental and food analysis. *Biomolecular engineering* 2007;24(2):191-200.

572. Ellington AD, Szostak JW. In vitro selection of RNA molecules that bind specific ligands. *Nature* 1990;346(6287):818-22.
573. Jayasena SD. Aptamers: an emerging class of molecules that rival antibodies in diagnostics: Oxford University Press, 1999.
574. Sefah K, Shangguan D, Xiong X, et al. Development of DNA aptamers using Cell-SELEX. *Nat Protoc* 2010;5(6):1169-85.
575. Heistermann M, Higham JP. Urinary neopterin, a non-invasive marker of mammalian cellular immune activation, is highly stable under field conditions. *Scientific Reports* 2015;5:16308.
576. Müller MM, Curtius H-C, Herold M, et al. Neopterin in clinical practice. *Clinica Chimica Acta* 1991;201(1-2):1-16.
577. Laich A, Neurauter G, Wirleitner B, et al. Degradation of serum neopterin during daylight exposure. *Clinica Chimica Acta* 2002;322(1-2):175-78.
578. Anestis SF, Breakey AA, Beuerlein MM, et al. Specific gravity as an alternative to creatinine for estimating urine concentration in captive and wild chimpanzee (*Pan troglodytes*) samples. *American Journal of Primatology: Official Journal of the American Society of Primatologists* 2009;71(2):130-35.